Collaborative Distributed Beamforming for Cooperative Spectrum-Sharing Systems

Ali Afana

A Thesis
in
The Department
of
Electrical and Computer Engineering

Presented in Partial Fulfillment of the Requirements
for the Degree of Doctor of Philosophy at
Concordia University
Montréal, Québec, Canada

July, 2014

CONCORDIA UNIVERSITY
SCHOOL OF GRADUATE STUDIES

This is to certify that the thesis prepared

By: Ali Afana

Entitled: Collaborative Distributed Beamforming for Cooperative Spectrum-Sharing Systems

and submitted in partial fulfillment of the requirements for the degree of

Doctor of Philosophy (Ph.D.)

complies with the regulations of the University and meets the accepted standards with respect to originality and quality.

Signed by the final examining committee:

Prof. Maria Elektorowicz — Chair

Prof. Saeed Gazor — External Examiner

Prof. A. Ben Hamza — External to Program

Prof. M. Reza Soleymani — Examiner

Prof. Yousef R. Shayan — Examiner

Prof. Ali Ghrayeb — Thesis Supervisor

Approved by

Prof. William E. Lynch
Chair of Department or Graduate Program Director

Prof. Robin Drew
Dean of Faculty

Abstract

Collaborative Distributed Beamforming for Cooperative Spectrum-Sharing Systems

Ali Afana, PhD.

Concordia University, 2014

The scarcity of bandwidth has always been the main obstacle for providing reliable high date-rate wireless links, which are in great demand to accommodate nowadays and immediate future wireless applications. In addition, recent reports have showed inefficient usage and under-utilization of the available bandwidth. Cognitive radio (CR) has recently emerged as a promising solution to enhance the spectrum utilization, where it offers the ability for unlicensed users to access the licensed spectrum opportunistically. On one hand, by allowing opportunistic spectrum access, the overall spectrum utilization can be improved. On the other hand, transmission from cognitive nodes can cause severe interference to the licensed users of the spectrum. This requires cognitive radio networks (CRNs) to consider two essential design targets, namely, maximizing the spectrum utilization and minimizing the interference caused to the primary users (PUs). Such interference can be reduced through proper resource allocation, power control or other degrees of freedom techniques such as *beamforming*.

In this thesis, we aim to use joint distributed beamforming and cooperative relaying in spectrum-sharing systems in an effort to enhance the spectrum efficiency and improve the performance of the secondary system. We investigate a one-way cooperative spectrum-sharing system in the presence of one PU and multiple PUs. We study two relaying schemes, namely, decode-and-forward (DF) and amplify-and-forward (AF) relaying in conjunction with distributed optimal beamforming. We employ zero forcing beamforming (ZFB) as a sub-optimal scheme, and compare both approaches through simulations. For both schemes, we derive closed-form expressions and asymptotic expressions for the outage probability and bit error rate (BER) over independent and identically distributed Rayleigh fading channels for binary phase shift keying (BPSK) and M-ary quadrature amplitude modulation (M-QAM)

schemes. Numerical results show the effectiveness of the combination of the cooperative diversity and distributed beamforming in compensating for the loss in the secondary system's performance due to the primary user's co-channel interference (CCI).

To further improve the spectrum efficiency, we employ distributed beamforming in two-way AF cooperative spectrum-sharing systems in the presence of multiple PUs. For this system, we investigate the transmission protocols over two, three and four time-slots. Our results show that the three time-slot protocol outperforms the two time-slot and four time-slot protocols in certain scenarios where it offers a good compromise between bandwidth efficiency and system performance.

We extend the two-way relaying system to the DF scheme, where two practical two-way relaying strategies are investigated, namely, DF-XORing (bit-wise level) and DF-superposition (symbol-wise level). For each relaying strategy, we derive general optimal beamforming vectors and sup-optimal ZFB vectors at the relays. Employing ZFB, we present an analytical framework of the secondary system considering the effect of the primary-secondary mutual CCIs. Our results show that, when the received signals at the relays are weighted equally, the DF-XOR always outperforms both DF-superposition and AF relaying.

In the last part of the thesis, we consider a limited feedback system model by assuming partial channel state information (CSI) of the interference channel between the secondary relays and primary receiver. In particular, the CSI feedback is limited only to the quantized channel direction information (CDI). To investigate the effect of the quantized CDI on the secondary system's performance, we derive closed-form expressions for the outage probability and the BER considering the mutual secondary-primary CCI. In the simulation results, we compare the system performance of the limited feedback with the perfect CSI. Our results show that the performance improves as the number of feedback bits increases.

To my dearest parents, for their support and encouragement

and

my family, my wife Islam and our adorable kids Tasnim and Mohamed, for their patience.

Acknowledgments

First and foremost, all praise and thanks are due to Allah (God) for giving me the power to believe in my passion and pursue my dreams. I could never have finished this thesis without the faith I have in Him and depending on Him.

I would like to express my gratitude and thanks to my supervisor Prof. Ali Ghrayeb for his role as a great advisor and all the support he provided me both technically and socially. His support and insightful advices were crucial to my academic success and my development as a researcher. Both on the personal and technical levels, I could easily say that Prof. Ali has a great impact on me and I hope that I will adhere to all the technical and ethical values I have learned from as a supervisor and a teacher.

I am also thankful to Prof. Yousef Shayan, Prof. Reza Soleymani, Prof. A. Ben Hamza, and Prof. Saeed Gazor for serving on my thesis committee and for providing constructive comments that made this thesis better.

I was fortunate to collaborate and discuss research with brilliant researchers at INRS, Quebec University. Thanks to Prof. Sofiene Affes, Dr. Vahid Asghari, and Dr. Salama Ikki. I acknowledge their fruitful discussions.

I am sincerely thankful to Qatar National Research Fund, a member of Qatar Foundation, and Concordia Graduate Student Support Program (GSSP) for funding my PhD's studies. I would like also to thank Hani Qaddomi Scholarship Foundation (HQSF) for funding my master's studies.

Finally, I would like to express my greatest and deepest appreciation to my family. Thanks to my mother and father whose endless love and sincere prayers have always been with me. Special thanks to Islam, my wife and best friend, for all the tremendous love and all the support at all the times she gives to me. Thank you Islam for being a steadfast source of encouragement and inspiration to me. It is no exaggeration to say that without your sacrifice and infinite patience, this thesis would never have existed. Thanks to my brothers and my

sisters for the constant encouragement they always give to me. Thanks also to my father-in-law and mother-in-law for their continuous support as my parents. Last but not least, thanks to our kids, Tasnim and Mohamed, for being so cute and filling our life with joy and hope.

Contents

List of Figures xv
List of Symbols xvii
List of Acronyms xix

1 Introduction **1**
1.1 Cognitive Radio 1
1.2 Beamforming in Cooperative CR Systems 2
1.3 Motivation 2
1.4 Thesis Contributions 3
1.5 Thesis Organization 5

2 Background and Literature Review **7**
2.1 Cognitive Radio 7
2.1.1 Cognitive Cycle 7
2.1.2 Spectrum Sharing 9
2.2 Cooperative Communications 10
2.2.1 Decode-and-Forward Relaying 11
2.2.2 Amplify-and-Forward Relaying 12
2.3 Two-Way Relaying 12
2.3.1 Four Time-Slot Scheme 12
2.3.2 Three Time-Slot Scheme 13
2.3.3 Two Time-Slot Scheme 14
2.4 Cooperative Spectrum-Sharing Systems 14
2.5 Beamforming 15
2.5.1 Transmit and Receive Beamforming 15

2.5.2 Beamforming in Cognitive Radio Networks . . . 16
2.5.3 Related Works . . . 18
2.6 Conclusions . . . 20

3 One-Way Relaying Spectrum-Sharing Systems with Distributed Beamforming 21

3.1 Introduction . . . 21
3.2 System Model and Problem Formulation . . . 23
3.2.1 System Model . . . 23
3.2.2 Channel Model . . . 24
3.2.3 Mathematical Model and Size of Set $\mathcal{C}$ . . . 25
3.3 Optimal Beamforming Weights Design . . . 27
3.4 Performance Analysis of the SDF scheme . . . 29
3.4.1 End-to-End Received SINR Statistics . . . 29
3.4.2 Outage Probability Analysis . . . 31
3.4.3 Bit Error Rate Analysis . . . 33
3.5 Performance Analysis of the AF scheme . . . 36
3.5.1 End-to-End Statistical Analysis of γ_{eq}^{AF} . . . 37
3.5.2 MGF of $\gamma_{eq_2}^{AF}$ . . . 39
3.5.3 Outage Probability Analysis . . . 41
3.5.4 Bit Error Rate Analysis . . . 42
3.6 Numerical Results and Discussions . . . 42
3.6.1 SDF Scheme . . . 43
3.6.2 AF Scheme . . . 46
3.7 Multi-PUs with CCI . . . 48
3.7.1 System Model . . . 48
3.7.2 Transmission Protocol . . . 50
3.7.3 Mathematical Model and Size of $\mathcal{C}$ . . . 51
3.7.4 Sub-Optimal ZFB Weights Design . . . 52
3.7.5 End-to-End SINR statistics . . . 53

3.7.6 Outage Probability . . . 54
3.7.7 E2E BER . . . 54
3.7.8 Simulation Results and Discussion . . . 56
3.8 Conclusion . . . 59

4 Two-Way AF Relaying Spectrum-Sharing Systems with Collaborative Beamforming 60

4.1 Introduction . . . 60
4.2 System and Channel Models . . . 64
4.3 Transmission Protocols . . . 66
4.3.1 2-TS protocol . . . 66
4.3.2 3-TS protocol . . . 67
4.4 ZFB Weights Design . . . 68
4.4.1 2-TS protocol . . . 68
4.4.2 3-TS protocol . . . 70
4.5 End-to-end SNR analysis . . . 71
4.5.1 First Order Statistics of $\gamma_{eq}^{2\text{-TS}}$ . . . 71
4.5.2 First Order Statistics of $\gamma_{eq}^{3\text{-TS}}$ . . . 72
4.6 Outage Probability Analysis . . . 73
4.6.1 2-TS protocol . . . 73
4.6.2 3-TS protocol . . . 76
4.6.3 Asymptotic outage probability . . . 77
4.7 Average Error Probability Analysis . . . 78
4.7.1 2-TS protocol . . . 78
4.7.2 3-TS protocol . . . 81
4.7.3 Asymptotic average bit error probability . . . 83
4.7.4 Power allocation at the relays . . . 84
4.8 Numerical Results and Discussion . . . 85
4.8.1 Effects of ZFB, number of relays and number of PUs on the performance 86
4.8.2 Comparison between 2-TS and 3-TS . . . 88

4.8.3 Comparison between the sub-optimal ZFB beamforming scheme and the optimal beamforming scheme . . . 91
4.8.4 Relays positioning . . . 94
4.9 Conclusion . . . 95

5 Two-Way DF Relay Cognitive Networks under Primary-Secondary Mutual Interference and Beamforming 96
5.1 Introduction . . . 96
5.2 System and Channel Models . . . 97
5.2.1 System Model . . . 97
5.2.2 Transmission Model . . . 99
5.2.3 XOR Relaying . . . 100
5.2.4 Superposition Relaying . . . 100
5.2.5 Mathematical Model and Size of $\mathcal{C}$ . . . 101
5.3 Optimal Beamforming Weights Design . . . 102
5.3.1 XOR Relaying . . . 104
5.3.2 Superposition Relaying . . . 104
5.4 Performance Analysis . . . 105
5.4.1 Statistics of the Total Received SINR . . . 105
5.4.2 Outage Probability . . . 107
5.4.3 E2E BER . . . 107
5.4.4 Achievable Sum-Rate . . . 109
5.5 Numerical Results and Discussion . . . 109
5.5.1 Fixed Power Allocation Parameters . . . 110
5.5.2 Optimal Power Allocation Parameters . . . 115
5.6 Conclusion . . . 116

6 Distributed Beamforming with Limited Feedback 117
6.1 Introduction . . . 117
6.2 System and Channel Models . . . 119
6.2.1 Quantized CSI Feedback Model . . . 120

6.2.2 Transmission Protocol . . . 120
6.2.3 Mathematical Model and Size of $\mathcal{C}$ . . . 121
6.2.4 ZFB Weights Design . . . 122
6.3 Performance Analysis . . . 122
6.3.1 End-to-End SINR statistics . . . 122
6.3.2 Outage Probability . . . 125
6.3.3 E2E BER . . . 125
6.4 Numerical Results and Discussion . . . 127
6.5 Conclusion . . . 128

7 Conclusions and Future Work **129**
7.1 Conclusions . . . 129
7.2 Future Work . . . 131

A Proofs of Chapter 3 **145**
A.1 Proof of Lemma 3.2.1 . . . 145
A.2 Proof of Theorem 3.4.2 . . . 147
A.3 Proof of Lemma 3.5.2 . . . 147
A.4 Proof of Theorem 3.5.3 . . . 148
A.5 Proof of Theorem 3.5.4 . . . 150

B Proofs of Chapter 5 **151**
B.1 Proof of Lemma 5.2.1 . . . 151
B.2 Proof of Lemma 5.4.1 . . . 152
B.3 Proof of Corollary 5.4.2 . . . 153
B.4 Proof of Theorem 5.4.3 . . . 154
B.5 Proof of Theorem 5.4.5 . . . 155

List of Figures

2.1 Spectrum utilization, measurements from DARPA XG. 8
2.2 Cognitive cycle [1]. 8
2.3 (a) Underlay approach, (b) Overlay approach for spectrum sharing [10]. . . 10
2.4 Comparison of different cooperative schemes. 11
2.5 Comparison of different cooperative network coding schemes. 13
2.6 Convergence of the SINR balancing technique versus the iteration number [29]. 18

3.1 System model. 24
3.2 Geometric explanation of $\mathbf{v}_{opt}$ 28
3.3 PDF of the End-to-End received SNR at SD, $f^{AF}_{\gamma_{eq_2}}(\gamma)$ for different values of potential relays in the AF-ZFB scheme for the second case. 40
3.4 Outage probability of SDF-ZFB vs. Q(dB) for L=7 and R_{min}= 0.5 bits/s/Hz. 43
3.5 Outage probability of SDF-ZFB vs. the number of relays for $Q = -3, 0, 3$dB and $R_{min} = 0.2, 0.5$ bits/s/Hz. 44
3.6 Average BER of the SDF-ZFB vs. Q for L=7 at R_{min} = 0.5 bit/s/Hz and BPSK scheme. 45
3.7 Average SER of M_q-QAM for the SDF-ZFB vs. Q for L=7 at $R_{min} = 0.2, 0.5$ bit/s/Hz. 45
3.8 Comparison between the outage probabilities of SDF-ZFB and the opportunistic SDF presented in [16] for L=5, 6 at R_{min}= 0.5 bits/s/Hz. 46
3.9 Outage Probability of AF-ZFB vs. P_s for different number of relays L=4, 5, 6 at R_{min}=0.5 bits/s/Hz in the first case (non-cognitive). 47
3.10 Outage probability of AF-ZFB vs. Q for L=4, 6, 8 and R_{min}=1 bits/s/Hz in the second case (cognitive). 48

3.11 Average BER of AF-ZFB vs. Q(dB) for L=4, 6, 8 at R_{min} = 0.5 bits/s/Hz and $\gamma_r = 7$ dB. 49
3.12 Spectrum-Sharing System with multiple-PUs. 49
3.13 Outage probability vs. Q (dB) for L=8 and $M = N = 2$. 56
3.14 Outage probability vs. d for L=10 and $M = N = 1$. 57
3.15 BER vs. Q (dB) for L= 8 and $M = N = 2$. 58
3.16 BER vs. L for $M = N = 1, 2$. 58

4.1 Spectrum-sharing system with two-way AF relaying. 63
4.2 Outage probability vs. Q_1 (dB) for the 2-TS protocol for L_s= 6, 8, 10 and M=1, 2 86
4.3 Outage Probability vs. Q_1 (dB) for the 3-TS protocol for L_s= 6, 8, 10 and M=2,3 87
4.4 Average bit error probability vs. Q (dB) for the 2-TS protocol forL_s=6, 8, 10 and M=1, 2. 87
4.5 Average bit error probability vs. Q (dB) for the 3-TS protocol for L_s=6, 8, 10 and M=2, 3. 88
4.6 Outage probability vs. Q (dB) for the 2-TS, 3-TS and 4-TS protocols, with L_s=8 and M=4. 89
4.7 Average bit error probability vs. Q (dB) for the 2-TS with (QPSK) 3-TS with (8-PSK) and 4-TS with (16-PSK) protocols, L_s=8 and M= 4. 90
4.8 Asymptotic average bit error probability vs. Q_2 (dB) for the 2-TS and 3-TS protocols, L_s=10 and M= 2,3 using BPSK. 91
4.9 Power allocation parameter α vs. Q_2 (dB) for the 3-TS protocol, L_s=6 and M= 3. and $P_r = 10$ dB 92
4.10 Average sum rate comparison between the proposed ZFB scheme and the optimal beamforming scheme, with L_s=4 and M=1,2. 92
4.11 Outage probability vs. d_{S_1} of 2-TS and 3-TS protocols, L_s=7 and M=4. . . 93
4.12 Average error probability vs. d_{S_1} of 2-TS and 3-TS protocols, L_s=6 and M=4. 94

5.1 Spectrum-sharing system with two-way DF relaying. 98

5.2 Geometric explanation of v_{opt_j}. 104
5.3 PDF of the end-to-end received SIR at S_j, $f_{\gamma^*_{s_j}}(\gamma)$. 106
5.4 Outage probability vs. Q (dB) for $M = N = 2, 3, L = 10$ and different P_{int} values. 110
5.5 Asymptotic outage probability vs. P_{s_j} (dB) for $M = N = 2, 3, L = 6$ and fixed P_{int}. 111
5.6 Outage performance comparison employing ZFB and optimal beamforming vectors for $M = N = 2, L = 8$ and fixed P_{int}. 112
5.7 E2E BER vs. Q (dB) for $L = 6, M = N = 2$ and different P_{int} values. . . . 113
5.8 E2E BER vs. L for $M = N = 1, 2$ at fixed P_{int}. 113
5.9 Achievable Sum-Rates vs. Q (dB) for $L = 6, M = N = 2$ and different CCI values. 114
5.10 Achievable Sum-Rates vs. Q (dB) for $L = 6, M = N = 2$ with fixed P_{int} and different $\lambda_{s_j,p}$ values. 114
5.11 E2E BER vs. Q (dB) for $L = 6, 8, M = N = 2$ and different P_{int} values at fixed and optimal α_j values. 115

6.1 Spectrum-Sharing System with Dual-hop Relaying. 119
6.2 $F_{\gamma_{d|\mathcal{C}}}(x)$ vs. x for L=5 and $M = 1$ and different values of B. 125
6.3 Outage probability vs. P_s (dB) for different values of B. 127
6.4 BER vs. P_s (dB) for different values of B. 128

List of Symbols

$\mathbf{x}$	vector $\mathbf{x}$
$\mathbf{X}$	matrix $\mathbf{X}$
$\mathbf{w_{zf}}$	zero-forcing beamforming vector
$(\mathbf{x})^T$	transpose of vector $\mathbf{x}$
$(\mathbf{x})^H$	conjugate Transpose of vector $\mathbf{x}$
$(\mathbf{x})^*$	complex conjugate of vector $\mathbf{x}$
$\|\mathbf{x}\|$	euclidean norm for vector $\mathbf{x}$
min	minimization
max	maximization
$\mathrm{E}\,(a)$	expectation of random variable a
$\log(a)$	natural logarithm of a
$\mathrm{Diag}\,(\mathbf{a})$	makes a diagonal matrix whose diagonal elements are entries of vector $\mathbf{a}$
$(\mathbf{X})^\dagger$	Pseudo-inverse of matrix $\mathbf{X}$
$\|\,\mathcal{C}\,\|$	cardinality of a set $\mathcal{C}$
Pr(a)	Probability of event a
$\Gamma(\cdot,\cdot)$	Upper incomplete Gamma function
$\gamma(\cdot,\cdot)$	Lower incomplete Gamma function
$W(\cdot,\cdot,)$	Whittaker function
$Q(x)$	Q-function
$G^{\cdot,\cdot}_{\cdot,\cdot}\left(\cdot\middle\vert{}^{\cdot}_{\cdot}\right)$	Meijer G-function
$\delta(x)$	Dirac delta function
${}_2F_1(\cdot,\cdot;\cdot;\cdot)$	Gauss hypergeometric function
$K(x)$	Modified Bessel function
$F_x(x)$	Cumulative distribution function
$f_x(x)$	Probability density function
$\phi_x(x)$	moment generation function

R_i	ith secondary relay
L	number of available secondary relays
M	number of PUs
L_s	number of selected potential relays
N	number of primary receivers
h_{s,r_i}	channel coefficient from the secondary source to the ith relay
$h_{r_i,d}$	channel coefficient from the ith relay to the secondary destination
$h_{s,p}$	channel coefficient from the secondary source to the primary receiver
P_{out}	Outage probability
P_e	Probability of average error
P_{int}	transmit power of the primary user
P_s	maximum available transmit power of the secondary source
P_r	total transmit power of the secondary relays
P_{off}	probability of a relay being inactive
Q	peak interference threshold
$\mathcal{CN}$	complex Gaussian random variable
γ_{s_j}	total received SNR or SINR at transceiver S_j
$\gamma_{s_j\|\mathcal{C}}$	received SNR or SINR at transceiver S_j given a set $\mathcal{C}$
$i.i.d.$	independent identical distribution
n_i	thermal noise for terminal i
σ_i^2	variance of noise level at node i
$\mathbf{v}_{opt}$	optimal beamforming vector
λ_x	channel coefficient parameter
$\triangleq$	equivalent in distribution
χ_k^2	Chi-square random variable with k degrees of freedom
$\beta(\cdot,\cdot)$	Beta random variable

List of Acronyms

AF	Amplify-and-forward
AWGN	Additive white Gaussian noise
BER	Bit error rate
BPSK	Binary phase shift keying
CCI	Co-channel interference
CDI	Channel direction information
CDF	Cumulative distribution function
CR	Cognitive Radio
CRN	Cognitive radio network
CSI	Channel state information
CSCG	Circularly symmetric complex Gaussian
DF	Decode-and-forward
E2E	End-to-end
FCC	Federal Communications Commission
i.i.d.	Independent and identically distributed
IEEE	Institute of Electrical and Electronics Engineers
LTE	Long-Term Evolution
MAC	Multiple access channel

M-QAM	M-ary quadrature amplitude modulation
MGF	Moment Generation Function
MIMO	Multiple-input/ multiple-output
MISO	Multiple-input/ single-output
MRT	Maximum ratio transmission
NC	Network coding
OFDM	Orthogonal frequency division multiplexing
PBS	Primary base station
PDF	Probability density function
PU	Primary user
PU-TXs	Primary transmitters
PU-RXs	Primary receivers
QoS	Quality of Service
RVQ	Random vector quantization
SBS	Secondary base station
SDF	Selective DF
SDP	Semi-definite programming
SER	Symbol error rate
SINR	Signal-to-interference-plus-noise ratio
SIMO	Single-input multiple-output
SNR	Signal-to-noise ratio

SU	Secondary user
TDD	Time division duplex
TDBC	Time division broadcast
TS	Time slot
2-TS	Two time-slot protocol
3-TS	Three time-slot protocol
TWRC	Two-way relay channel
ZFB	Zero-forcing beamforming

Chapter 1

Introduction

1.1 Cognitive Radio

The rapid demand for providing high throughputs in wireless communications that support new applications such as video-streaming, cellular phones and high-speed Internet etc. makes wireless communications a challenging field. For instance, cellular systems have experienced a tremendous growth over the last decade, and this translates to requiring more frequency spectrum to accommodate this unprecedented increase in the number of subscribed users. However, spectrum is very scarce, and, if available, it is very expensive. At the same time, the allocated spectrum has been shown to be severely under-utilized. This scarcity and under-utilization of the spectrum usage necessitate exploiting the available spectrum opportunistically. Cognitive radio (CR), as an emerging solution, offers the cognitive (secondary) users (SUs) the ability to access the licensed spectrum in an opportunistic manner. More specifically, the CR techniques allow SUs to sense the unused spectrum and share it without bad interference with other users (Spectrum sensing), to manage the best available spectrum to fulfill the user communication demands (Spectrum management), to maintain certain required quality of service (QoS) during switching to better spectrum (Spectrum mobility) and to provide a fair spectrum sharing among all coexisting users (Spectrum sharing) [1].

By allowing opportunistic spectrum access, the overall spectrum utilization can be improved. On the other side, transmission from cognitive nodes can cause bad interference to the licensed (primary) users (PUs) of the spectrum. This requires spectrum-sharing systems to consider two essential design methods, namely, maximizing the spectrum utilization and minimizing the interference caused to PUs [2]. Since the PUs have a higher priority

of using the spectrum, a basic challenge is to guarantee the QoS of the PUs and the SUs simultaneously [3]. Such interference can be reduced through suitable resource allocation, power control or other degrees of freedom technique such as *beamforming* at the secondary transmitters.

1.2 Beamforming in Cooperative CR Systems

Beamforming is a technology used to alleviate the inflicted interference in spectrum-sharing systems [4], [5]. It enables simultaneous transmission by the PUs and SUs without interference. However, beamforming needs multiple antennas to be deployed by the unit to be realized which is prohibited in the first CR based IEEE standard (IEEE 802.22) where a single antenna is used at each secondary node [6]. Foe example, the underutilized television bands between 54 and 862 MHz prohibit the use of multiple transmit antennas at the user side. Moreover, single-antenna receivers are quite common due to the size and cost limitations of mobile terminals, hence, creating a virtual antenna array via cooperative relaying becomes a necessity so that beamforming is performed in a distributed fashion.

Cooperative relaying emerged as a powerful solution for improving the performance of single-antenna communication nodes. This is achieved by making use of intermediate relay nodes, which are used to assist transmission from the source to the destination. In [7], two basic relaying protocols are introduced where the relay decides either to amplify-and-forward (AF) or decode-and-forward (DF) according to the received signal-to-noise ratio (SNR). Cooperative relaying schemes are adopted in spectrum-sharing systems in order to increase the capacity, the reliability and the coverage of the secondary system.

1.3 Motivation

The proposed work is important in various ways. It certainly addresses a timely topic (cognitive radio systems), which is expected to play a major role in many of the future wireless communication systems. In fact, this technology is expected to revolutionize how wireless communication networks will be implemented or deployed in the future, with a focus on ad-

dressing the problem of spectrum under-utilization. Very recently, Qualcomm has proposed to extend the benefits of Long-Term Evolution (LTE) Advanced to unlicensed spectrum around 5 GHz band, which will offer unpredictable QoS and will be ideal for local area access, and opportunistic use for mobile broadband.

Combination between cooperative relaying and distributed beamforming seems to be a good solution in spectrum-sharing systems. However, such systems have critical challenges that must be addressed in order to get the benefits from this combination. The main challenges include: how to optimize the beamformers in a distributed manner, and how to obtain the interference channel state information (CSI) between the secondary transmitters and the primary receivers.

Some work has been done in this area, but most of this work has focused on adjusting the transmit power of the secondary transmitters to mitigate the interference inflicted on the PUs. Other works have used optimal transmit beamforming techniques in multiple antenna systems to cancel the inflicted interference. In their work, complex iterative algorithms are developed to get the optimal beamformers since most of these techniques suffer from non-convex and non-linear optimization problems. In light of this, we believe that simpler and more practically implementable distributed beamforming techniques are still lacking in the literature.

The main objectives of this thesis are to 1) combine distributed beamforming and cooperative techniques for spectrum sharing systems; 2) develop low complexity distributed beamforming techniques with various system objectives; and 3) develop analytical frameworks for the developed techniques.

1.4 Thesis Contributions

The contributions of this thesis can be summarized as follows.

- We investigate a one-way cooperative spectrum-sharing system in the presence of a PU. We study two basic relaying strategies, namely, DF and AF relaying in conjunction with distributed optimal beamforming. However, given the complexity of the performance analysis with optimal beamforming, we use zero forcing beamforming (ZFB), and com-

pare both approaches through simulations. For both schemes, we derive closed-form expressions for the outage probability and bit error rate (BER) over independent and identically distributed Rayleigh fading channels for binary phase shift keying (BPSK) and M-ary quadrature amplitude modulation (M-QAM) schemes. We also extend the DF scheme for multiple PUs system model and generalize the ZFB approach. Numerical results demonstrate the efficacy of the proposed scheme in improving the outage and BER performance of the secondary system while limiting the interference to the primary system. In addition, the results show the effectiveness of the combination of the cooperative diversity and distributed beamforming in compensating for the loss in the secondary system's performance due to the primary user's co-channel interference (CCI).

- To further improve the spectrum efficiency, we employ distributed beamforming in two-way AF cooperative spectrum-sharing systems. For this system, we investigate the transmission protocols over two, three and four time-slots. To study and compare the performance tradeoffs between the two transmission protocols, for both of them, we derive closed-form expressions for the user outage probability and the average error probability. To get more insights, we derive the asymptotic expressions of the outage and error probabilities. We also compare both protocols with the four time-slot protocol in simulations. Our results show that the three time-slot protocol outperforms the two time-slot protocol and four time-slot protocol in certain scenarios where it offers a good compromise between bandwidth efficiency and system performance.

- We extend the two-way relaying system to the DF scheme, where two practical two-way relaying strategies are investigated, namely, DF-XORing and DF-superposition. The former is based on bit-wise level XORing of the detected signals at the relays, whereas the latter is based on symbol-wise level addition at the relays. For each relaying strategy, we derive general optimal beamforming vectors at the relays to keep the interference inflicted on the primary receivers to a predefined threshold. Employing ZFB as a special case, we present an analytical framework of the secondary system considering the effect of the primary-secondary mutual CCIs. The simulation results

show that, when the received signals at the relays are weighted equally, the DF-XOR always outperforms both DF-superposition and AF relaying.

- In the last part of the thesis, we consider the same one-way system model but assuming partial CSI of the interference channel between the secondary relays and the primary receiver. In particular, the CSI feedback is limited only to the quantized channel direction information (CDI). In this context, we derive an upper bound for the secondary relays transmit power that meets the PU interference constraint. We also derive the statistics of the end-to-end signal-to-interference-and-noise ratio (SINR) employing the ZFB with limited feedback. To investigate the effect of the quantized CSI on the secondary system performance, we derive closed-form expressions for the outage probability and the BER assuming that the secondary receivers (relays and destination) are affected by the PU's CCI.

1.5 Thesis Organization

The rest of the thesis is organized as follows:

In Chapter 2, we present some relevant background on the fundamentals of cooperative CR systems. We begin by introducing the CR concept, where we focus on spectrum-sharing scenario. We also present briefly the various types of cooperative communication schemes. Then, beamforming techniques in conventional and CR systems are described. In the last part of this chapter, we provide the related works to this research in the literature.

In Chapter 3, cooperative one-way relaying spectrum-sharing system is investigated, where two basic AF and DF relaying schemes are employed in conjunction with distributed optimal beamforming. We devise the ZFB as a special case in two scenarios, when one PU exists and when multiple PUs exist. To analyze the proposed techniques, we derive closed-form expressions for outage probability and BER using BPSK and M-QAM schemes. We also present some numerical results to show the effectiveness of using distributed beamforming with cooperative diversity in compensating for the loss in secondary system's performance due to PUs's CCI in spectrum-sharing systems

In Chapter 4, we shift our focus to two-way relaying to further improve the spectral

efficiency. We investigate two and three time-slot transmission protocols. For both of them, we derive the exact and asymptotic expressions in order to get valuable insights about few key parameters that affect the system performance. Then, we present some numerical results, where we compare the performance tradeoffs between the two transmission protocols and the four time-slot protocol. We conclude that the three time-slot protocol outperforms other protocols in certain scenarios.

In Chapter 5, we extend our study to two-way DF relaying scheme, where DF-XORing and DF-superposition relaying strategies are investigated. For both strategies, we derive optimal beamforming vectors employed at the secondary relays. Then, we analyze the secondary system's performance using ZFB as a sub-optimal scheme for mathematical tractability. We also present the simulation results to compare the performance of both strategies with AF relaying scheme considering the mutual CCI between primary and secondary system.

In Chapter 6, we investigate a more practical cooperative spectrum-sharing system assuming a quantized CSI of the interference channel between the secondary relays and the PUs. We derive an upper bound for the relays' transmit power providing the partial CSI availability. Then, to investigate the impact of the quantized CSI on the secondary system's performance, we analyze the outage and error probabilities for different numbers of feedback bits. We also compare the limited CSI feedback performance with the perfect CSI performance in the numerical results.

In Chapter 7, we present a brief summery of our investigation and some important conclusions. We also suggest some potential topics for future research.

Chapter 2

Background and Literature Review

In this chapter, a brief background pertaining to the main topics of this thesis is given, including cognitive radio, beamforming and cooperative relaying. It also summarizes recent works that relate to the problems studied in this thesis.

2.1 Cognitive Radio

The existence of many wireless applications, especially in the region of 1-10 GHz, has tremendously reduced spectrum availability. Moreover, according to Federal Communications Commission (FCC), it was shown that the actual spectrum usage varies between 15% and 85% based on location and time variations as shown in Fig. 2.1. Although the fixed spectrum assignment policy worked well to a large extent in the last decade, it has been challenged more recently, owing to the exponential growth in the demand for more throughput to accommodate more users and bandwidth-hungry applications. So the scarcity and under-utilization of the spectrum have urged the researchers and agencies to search for new ways to exploit the limited spectrum resources. With two primary objectives in mind, ubiquitous coverage and more efficient utilization of the radio spectrum, CR is proposed as an emerging solution that provides the capability to use or share the spectrum in an opportunistic manner [9], [10]. In the following sections, we elaborate on various aspects of CR.

2.1.1 Cognitive Cycle

The cognitive cycle normally consists of a number operations, which is given in Fig. 2.2. As shown in the figure, there are three main steps, including spectrum sensing, spectrum anal-

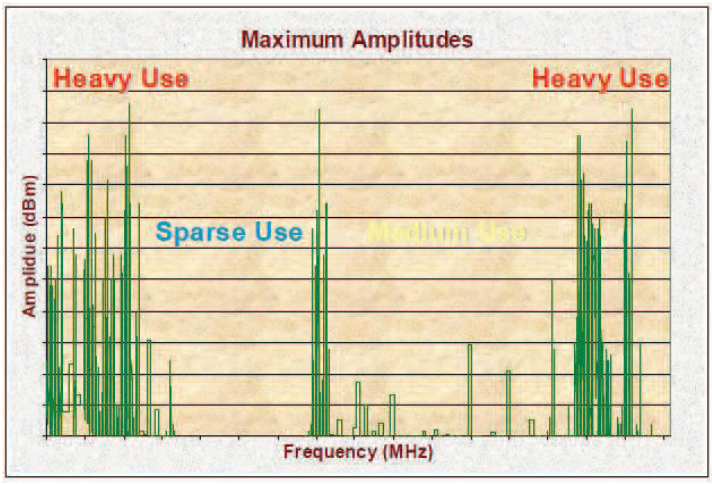

Figure 2.1: Spectrum utilization, measurements from DARPA XG.

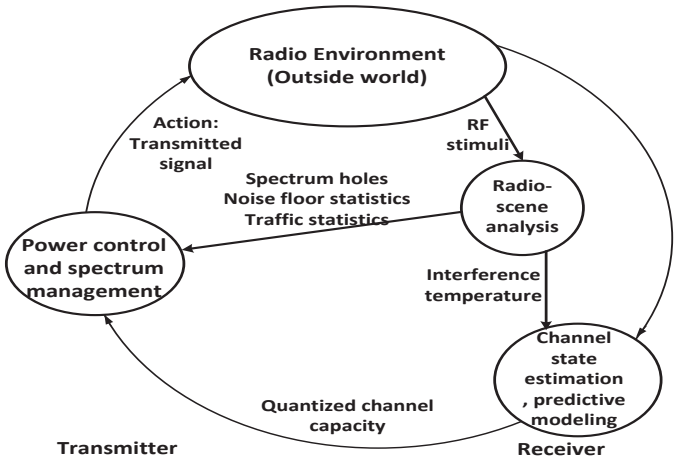

Figure 2.2: Cognitive cycle [1].

ysis, and spectrum decision. In spectrum sensing, a cognitive radio monitors the unoccupied spectrum bands, captures their information, and then detects the spectrum holes. In spectrum analysis, the characteristics of the detected spectrum holes through spectrum sensing are then estimated. Whereas in spectrum decision, cognitive radio determines the transmission mode, the data rate, and the bandwidth of the transmission. Then, according to the spectrum characteristics and user requirements, the appropriate spectrum band is chosen. Once the operating spectrum band is determined, the communication can be performed over this spectrum band. However, because the radio environment changes over time and space, the cognitive radio should keep track of the changes of the radio environment. If the current spectrum band in use becomes unavailable, search for another available spectrum band is performed to provide a continuous transmission.

2.1.2 Spectrum Sharing

In cognitive radio networks (CRNs), spectrum sharing is considered as one of the main challenges in open spectrum usage. Spectrum sharing is similar to the generic multiple access channel (MAC) problems in traditional wireless systems. However, substantially different challenges exist for spectrum sharing in the context of CRNs. The fundamental challenge is how to protect the PUs from the inflected interference from the SUs. Two main approaches of spectrum sharing are identified as shown in Fig. 2.3. One is the underlay approach which operates over ultra-wide bandwidths with strict restrictions on transmitted power levels and the other is the overlay approach based on giving higher priority for primary users through the use of spectrum sensing and adaptive allocation.

While the underlay approach allows multiple systems to be deployed in overlapping locations and spectrum, in the overlay approach, the CR users try to access the available spectrum without causing interference to the primary users. Referring to the above-mentioned spectrum sharing structures, the CR users need to efficiently exploit and share the spectrum without causing harmful interference to the licensed users. To address the interference problem, the CR should be designed to co-exist with the licensed users without creating harmful interference to the latter. Several techniques have been proposed in the literature to solve this problem including using power control, transmit beamforming, receive beamforming, orthog-

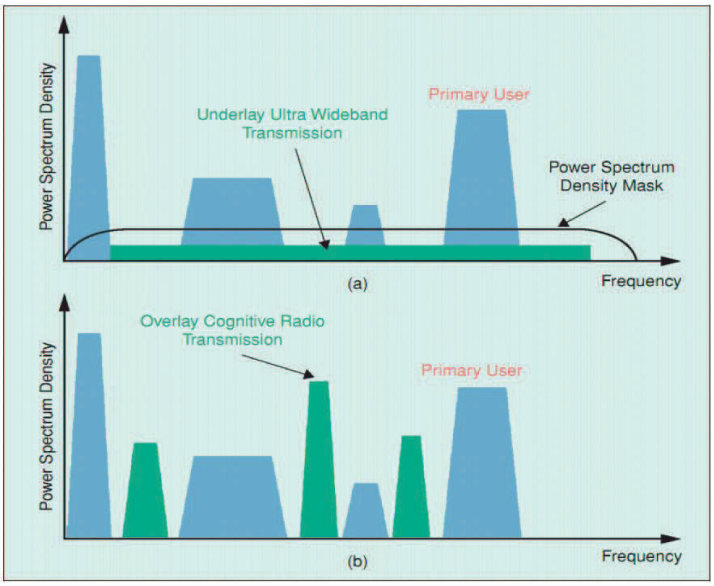

Figure 2.3: (a) Underlay approach, (b) Overlay approach for spectrum sharing [10].

onal frequency division multiplexing (OFDM), frequency selection, and space-time coding, to name a few. In this thesis, beamforming and power control techniques in spectrum-sharing systems will be considered.

2.2 Cooperative Communications

To alleviate the deleterious effect of fading, one may use transmit diversity, which is achieved by deploying multiple antennas at the transmitter. However, this is not always possible in many wireless devices due to the size and/or power limitations. Cooperative communication is proposed to enable single antenna nodes in a multi-user network to cooperate and generate a virtual multiple-antenna transmitter that allows them to achieve transmit diversity. In cooperative networks, wireless nodes are assumed to transmit their own data while acting as cooperative agents (relays) for other nodes, which is a win-win situation because this improves the overall performance. There are several cooperative signaling methods in the literature, among which are DF and AF schemes [11], which we review next.

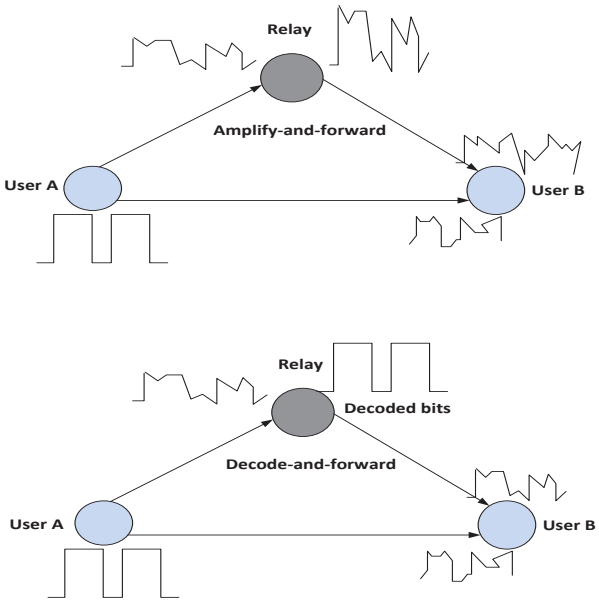

Figure 2.4: Comparison of different cooperative schemes.

2.2.1 Decode-and-Forward Relaying

In this scheme, a cooperative user attempts to detect the partners bits and then retransmits the detected bits to destination as shown in Fig 2.4. Those partners are usually assigned by the transmitter [12]. The main advantage of this scheme is its adaptability to the channel conditions. However, there is a possibility that the detection by the relay node is unsuccessful, in which case, cooperation leads to error propagation and this affects the detection probability at the final destination. In addition, the receiver needs to know the error characteristics of the inter-user channel for optimal detection. To circumvent error propagation, a hybrid decode-and-forward method is proposed where users cooperate when the received SNR is above a certain threshold to guarantee a certain detection reliability. Otherwise, no cooperation takes place [7].

2.2.2 Amplify-and-Forward Relaying

AF is simpler than DF relaying in the sense that it receives a noisy corrupted version of the signal transmitted by its partner and the node, amplifies and retransmits this noisy version to the destination. The destination then combines the received signals from the original source node (if there is a direct link) and the relaying node and makes the final decision on the received bits as shown in Fig 2.4. Although the noise is amplified by this type of cooperation, the destination receives two independently faded versions of the signal and hence a better detection probability can be achieved [7].

In AF, it is assumed that the receiver knows the inter-user channel coefficients to do optimal detection, so there must be a mechanism of channel estimation employed to achieve reliable channel. Another potential challenge is the dealing with analog values in sampling, amplifying, and retransmitting which is not that easy. Nevertheless, AF is a simple scheme that is extensively analyzed, and thus has been very useful in furthering our understanding of cooperative communication systems.

2.3 Two-Way Relaying

The concept of network coding (NC) can be easily explained with the two-way relay channel (TWRC). TWRC is a three-node network in which two end nodes (transceivers) want to communicate via a relay node. For practical reasons, half-duplex communication is often imposed in TWRC networks. With the half-duplex constraint, a node cannot transmit and receive at the same time. In the following, we revisit various relaying schemes that involve different numbers of time slots for two transceivers to exchange information.

2.3.1 Four Time-Slot Scheme

To avoid interference, a total of four time slots are needed to exchange data between a pair of transceivers without the use of NC as illustrated in Fig 2.5. In the first time slot (TS_1), transceiver A transmits its signal S_1 to relay R; in the second time slot (TS_2), relay R forwards S_1 to transceiver B; in the third time slot (TS_3), transceiver B transmits its signal S_2 to R;

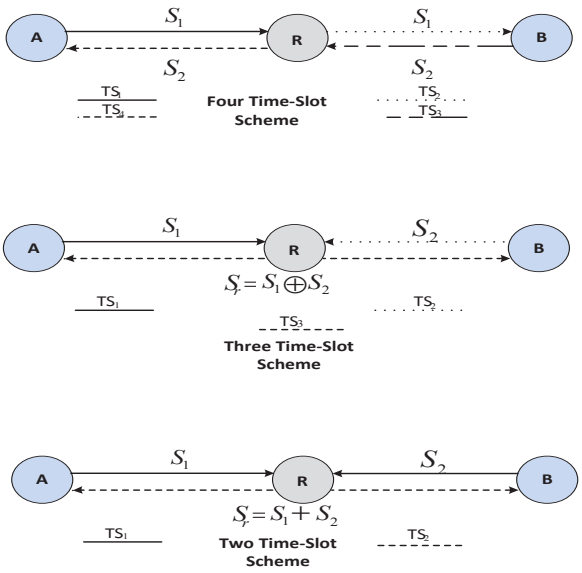

Figure 2.5: Comparison of different cooperative network coding schemes.

and in the fourth time slot (TS_4), R forwards S_2 to transceiver A.

2.3.2 Three Time-Slot Scheme

A direct way of applying NC can decrease the number of time slots to three. By decreasing the number of time slots from four to three, a three time-slot scheme has a throughput improvement of 33% over the four time-slot scheme. Fig. 2.5 clarifies the idea of the three time-slot scheme. In TS_1, transceiver A transmits its signal S_1 to R, and in TS_2, transceiver B transmits its signal S_2 to R. After receiving S_1 and S_2, in TS_3, R adds them exclusively and forms a network-coded signal S_r as follows:

$$S_r = S_1 \oplus S_2, \tag{2.1}$$

where $\oplus$ denotes the XOR symbol over S_1 and S_2. Then, R retransmits S_r to both transceivers. It is noted that NC is performed by the relay after having received of the two signals in different time slots in order to avoid interference.

2.3.3 Two Time-Slot Scheme

Two time-slot scheme further decreases the number of time slots to two and hence yields the best throughput improvement. It allows both transceivers to transmit simultaneously to R in TS_1 as illustrated in Fig. 2.5. In TS_2, R receives the added two signals received from transceivers A and B ($S_r = S_1 + S_2$) and rebroadcasts S_r back to both transceivers.

2.4 Cooperative Spectrum-Sharing Systems

Recently, cooperative relaying schemes have been adopted in spectrum-sharing systems where the inflicted interference at the PUs is limited by only controlling the transmit power of the secondary transmitters. Both DF and AF schemes are employed in order to increase the reliability and the coverage of the secondary systems. Also, different selection methods are applied such as opportunistic and partial relay selection [13]- [16].

In [13], the author proposed a new two-phase protocol based on a DF relaying scheme in a spectrum-sharing system in order to access the spectrum. In their work, the outage probability was investigated for both primary and secondary systems. The end-to-end performance of cooperative relaying in spectrum-sharing systems with QoS requirements was studied in [14] where the authors investigated the BER and outage probability performance for a DF relaying system. All these works considered only a single relay. The authors in [15] investigated the outage probability for a multi-relay system with best relay selection based on spectrum sharing constraints. Later, in [16], the exact outage performance of the opportunistic selective DF relaying scheme in the CRNs was derived subject to the certain transmit power limits. The capacity of the reactive and proactive DF scheme in CRNs was investigated in [17] under peak power interference constraints while [18] considered the average interference constraint.

Little works considered AF relaying systems in the CRNs. In [19], the achievable rates of the secondary and primary systems were analyzed for a two-phase AF system in a spectrum-sharing environment. The performance of an AF relaying system with partial relay selection under both the peak and the average interference constraints was investigated in [20]. All the

previous works considered either the received peak or average power interference constraints or both of them to limit the interference to PUs.

2.5 Beamforming

Beamforming is a powerful technique to transmit, receive, or relay signals of interest in a spatially exclusive way in the presence of interference and noise. Receive beamforming is a definitive yet dynamically developing area that has extensive theoretical research and practical applications to communications, radar, and microphone array speech/audio processing etc. [21]. Transmit beamforming is a relatively new and continuously developing research field. In transmit and receive beamforming, the beamforming vector is matched to a single directional vector of interest and its aim is to insure that the inner product of the beamforming weight vector and the vector of interest is strong, while the inner product of the beamforming weight vector and all other non-desirable vectors is weak (to mitigate interference).

Network beamforming is a quickly emerging field that ties with the general area of cooperative relaying networks [7]. The fundamental concept of network beamforming is to exploit the relay nodes as a virtual antenna array that retransmit processed weighted signals from the source to the destination [22], thereby making use of cooperation diversity. Relay processing types are classified into two simple settings, the AF protocol and the DF protocol where a distributed network beamformer uses an adaptive complex-valued weighting of the received signal. An attractive feature of network beamforming is that it can be expressed as a certain combination of receive and transmit beamforming schemes. However, the main difference between the concept of network beamforming and the conventional concepts of transmit and receive beamforming is that there is no exchange information between the relays about their received signals, so that beamforming is performed in a distributed manner.

2.5.1 Transmit and Receive Beamforming

In the uplink strategy, each user can be viewed as a transmit antenna and the same receiver architecture can be used at the basestation to separate each users data (receive beamforming).

The antenna weights of all beamformers can be explained as linear multiuser receivers. In the downlink case, a similar strategy can be used when the basestation broadcasts independent data streams to different mobile users (transmit beamforming). The downlink problem is more complicated than the uplink one since the beamformers must be optimized jointly in the first case. However, by exploiting an interesting duality between the uplink and the downlink, each downlink problem is turned into a virtual uplink problem and, in other words, each receive beamforming strategy in the uplink has a corresponding transmit beamforming strategy in the downlink [23]- [34]. There is a large number of optimization problems that are formulated in the literature to optimize the beamforming vectors, and due to the limited space, we present only the optimization problem formulation for the SINR balancing in the downlink conventional systems (a basestation with N antennas serving K mobile terminals). It can be expressed as:

$$\begin{aligned} &\max_{\mathbf{W},\mathbf{p}} \min_{1\leq k\leq K} \frac{\mathrm{SINR}_k(\mathbf{W},\mathbf{p})}{\gamma_k} \\ &\text{subject to} \, ||\mathbf{p}||_1 \leq P_{max}, \\ &||\mathbf{w}_i||_2 = 1,\, i = 1, ..., K, \end{aligned} \tag{2.2}$$

where $\mathbf{W} = [\mathbf{w}_1, ..., \mathbf{w}_N]$ is the beamforming matrix, $\mathbf{p}$ is the transmit power vector, γ_k is the target SINR for the k^{th} user, and P_{max} is the basestation maximum transmit power.
This form of optimization problem is solved by exploiting the special structure of eigensytem characteristics which is proved in [28]. In the following subsection, we extend the above-mentioned optimization problem to a CR system, where an additional interference constraint is imposed.

2.5.2 Beamforming in Cognitive Radio Networks

Consider a CRN composing of a secondary basestation (SBS) with N transmit antennas, L PUs and K SUs. All the PUs and SUs are single antenna users. The signal transmitted by the SBS is given by: $\mathbf{x}(n) = \mathbf{W}\,\mathbf{s}(n)$, where $\mathbf{s}(n) = [s_1(n), ..., s_k(n)$
$..., s_K(n)]^T$, $s_k(n)$ is the symbol intended for the k^{th} SU, $\mathbf{W} = [\sqrt{p_1}\mathbf{w}_1, ..., \sqrt{p_k}\mathbf{w}_K]$, and $||\mathbf{w}_k||_2 = 1$. Here, $\mathbf{w}_k$ is the k^{th} transmit beamforming weight vector and p_k is the corresponding allocated power for k^{th} SU. The varaince of the symbol $s(n)$ is assumed to be unity.

The received signal at the k^{th} SU can be written as

$$y_k(n) = \mathbf{h}_k^H \mathbf{x}(n) + \eta_k(n), \tag{2.3}$$

where the signal is distorted by complex channel vector $\mathbf{h}_k = [h_{1k}, ..., h_{N_t k}]^H$ between the SBS and the k^{th} SU. We assume that $\eta_k(n)$ is a zero-mean additive white Gaussian noise (AWGN) with variance σ_k^2. The available total power at the SBS is determined by P_{max}. The interference power leakage to the l^{th} PU due to the k^{th} SU transmission is given by

$$\epsilon_{l,k} = p_k ||\mathbf{g}_l^H \mathbf{w}_k||_2^2, \tag{2.4}$$

where $\mathbf{g}_l = [g_{1l}, ..., g_{N_t l}]^H$ is the channel vector from SBS to the l^{th} PU. The SINR of the k^{th} SU can be written as

$$\text{SINR}_k^{DL} = \frac{p_k \mathbf{w}_k^H \mathbf{R}_k \mathbf{w}_k}{\sum_{i=1, i\neq k}^{K} p_i \mathbf{w}_i^H \mathbf{R}_k \mathbf{w}_i + \sigma_k^2}, \quad \forall k, \tag{2.5}$$

where $\mathbf{R}_k = \mathbf{h}_k \mathbf{h}_k^H$. The problem formulation which always guarantees feasibility is based on SINR balancing with extra PU interference leakage constraints. It can be written as

$$\begin{aligned} &\max_{\mathbf{W},\mathbf{p}} \min_{1\leq k\leq K} \frac{SINR_k(\mathbf{W}, \mathbf{p})}{\gamma_k} \\ &\text{subject to } \mathbf{1}^T \mathbf{p} \leq P_{max}, \\ &p_k ||\mathbf{g}_l^H \mathbf{w}_k||_2^2 \leq P_{n,l},\ k = 1, ..., K,\ l = 1, ..., L \end{aligned} \tag{2.6}$$

where γ_k is the target SINR for k^{th} SU, $P_{n,l}$ is the interference limit on the l^{th} PU due to the transmission of each SU, $\mathbf{p} = [p_1, ..., p_K]^T$ and $\mathbf{1} = [1, 1, ..., 1]$. The principle of uplink-downlink duality is used to balance the SINR of the SUs while satisfying the constraints. The beamformer designed in the virtual uplink mode can be used in the downlink mode to achieve the same SINR values by selecting suitable downlink power allocations [28] and considering the level of interference that will leak to PUs. Those and other types of problems are extensively studied in the literature and solved in many different ways such as standard interior points methods and iterative optimal algorithms [29].

In Fig 2.6, the convergence of the SINR balancing technique versus the number of iterations is plotted. It shows how fast the convergence of the algorithm by using an iterative uplink-downlink duality technique. However, most of these algorithms suffer from high complexity and implementation difficulties.

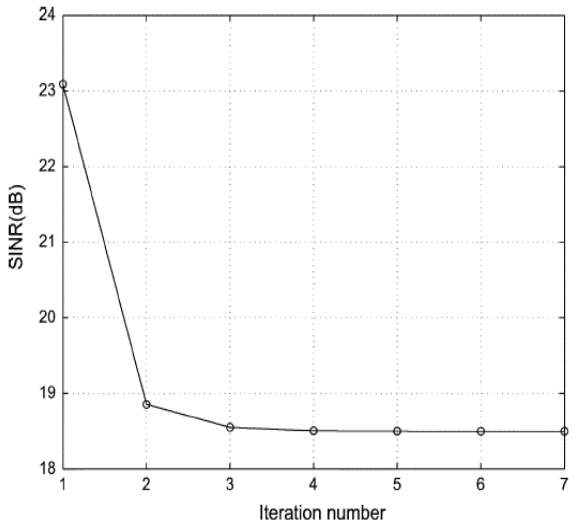

Figure 2.6: Convergence of the SINR balancing technique versus the iteration number [29].

2.5.3 Related Works

In [39], authors exploited multi-antennas (spatial diversity) in the downlink problem to improve the channel capacity between SUs, while putting constraints on the PU interference power and the SU transmit power. In [39], convex optimization techniques were used to design iterative algorithms that achieve the optimal capacity of the secondary system. In [40], joint beamforming and scheduling schemes were investigated for CRNs. An efficient transmit beamforming technique combined with user selection criteria was proposed to maximize the downlink throughput and satisfy the SINR constraint while limiting the interference to the existing PU. The authors in [41] designed robust CRN beamformers that match specific target SU SINRs. This approach gets the beamformer weights and corresponding power allocations through reaching the required SINR for each SU within the given available power while guaranteeing that the interference leakage to PUs is below specific thresholds.

While the previous works considered perfect CSI, robust cognitive beamforming was used in [4] in the case of imperfect CSI between secondary and primary users. Standard interior point optimization algorithms were performed to find the optimal solutions. In [5], iterative sub-optimal optimization algorithms were developed to design the optimal weight beamform-

ers for the SUs and rates were assigned to them in a distributed manner to maximize the smallest weighted rate among the SUs. An SINR balancing optimization problem in [42] is developed in a different approach over CRNs where it optimizes the worst SU SINR while ensuring conditions on the total transmit power of the secondary network base-station and the PU interference constraints. The technique given in [42] is a direct extension of the SINR balancing technique of [28] for traditional fixed spectrum systems, that is, the uplink and downlink power allocation algorithms have been modified in [42] to explicitly include the PU interference constraint. However, all the above-mentioned algorithms and tools are developed for a non-cooperative networks.

Combination between the cooperative diversity and distributed beamforming in CRNs leads to higher gains in the received SNR and hence better system performance. Recently, in [43], a fair transmit beamforming algorithm that maximizes the overall minimum throughput of a relay-assisted CR system while guaranteeing certain QoS requirements to the primary system was developed. The authors in [43] used iterative convex optimization tools to derive the optimal beamformers weights for the secondary base-station with a multi-antenna system that helps a pair of PUs to communicate with each other. A cooperative relaying scheme was proposed in [44] for an underlay CRN where the relays used their beam-steering capability to improve the target SINR at the secondary terminals while keeping the interference and the noise leakage to the PUs below a tolerable threshold. Similar work was done in [45] for a multipoint-to-multipoint CRN where the relays were used in a dual-hop AF cooperative relaying scheme. The authors in [45] developed an iterative algorithm that jointly optimizes the sources transmit powers and the relays' beamforming weights to maximize the worst SINR at the destinations while satisfying the sources and relays total transmit power constraints as well as the sources individual power constraints and further guaranteeing that the interference powers from the CRN on the existing PUs are below predefined thresholds. In [46], suboptimal scheme was used in an overlay model.

All these works assumed one-way cooperative relaying. Recently, the authors in [47] obtained the optimal beamforming coefficients in a cognitive two-way relaying system using iterative semidefinite programming and bisection search methods.

2.6 Conclusions

We have presented a brief background related to the main topics investigated in this thesis. We conclude that the use of cooperative relaying in spectrum-sharing systems is a new promising topic and is studied extensively nowadays. Reviewing the literature in depth shows that it is still lacking in depth investigation of the combination between cooperative relaying and distributed beamforming in spectrum-sharing systems. Unlike CR systems, a lot of work was done on the use of beamforming in conventional cooperative wireless systems. Moreover, most of the beamforming work in spectrum-sharing systems was performed for multiple antenna systems where the optimal beamformers were optimized via different iterative algorithms and standard interior points optimization tools. Nevertheless, those tools and algorithms were developed to transfer the non-convex problems into convex ones to obtain the optimal beamformers which made them very complicated.

Combination of cooperative relaying and distributed beamforming to enhance the secondary system performance seems to be a good solution. It is a challenging task to incorporate distributed beamforming in cooperative spectrum-sharing systems. Two main challenges exist, the first one is how to obtain the optimal beamformers in a distributed fashion and the second one is how to investigate the secondary system with the difficulty of obtaining the perfect CSI at transmitters. Such challenges will be tackled in the next chapters.

Chapter 3

One-Way Relaying Spectrum-Sharing Systems with Distributed Beamforming

3.1 Introduction

In this chapter, we combine cooperative dual-hop relaying and distributed beamforming with the objective of improving the secondary system's performance and limiting the interference inflicted at the primary system. Recently, there have been a few articles on relaying schemes in CRNs where the inflicted interference at the PUs is limited by controlling the transmit power of the secondary transmitters [14]- [17]. The end-to-end performance of cooperative relaying in spectrum-sharing systems with QoS requirements was studied in [14] where the authors investigated the BER and outage probability performance for DF relaying. This work considered only a single relay. The authors in [15] investigated the outage probability for a multi-relay system with best relay selection based on spectrum sharing constraints. Later, in [16], the exact outage performance of opportunistic selection decode-and-forward (SDF) relaying in CRNs was derived subject to maximum transmit power limits. Recently, the capacity of reactive and proactive DF relaying in CRNs was investigated in [17] under peak power interference constraints. All these works considered either the received peak or average power interference constraints or both of them to limit the interference to PUs.

Other works exploited beamforming to mitigate interference to PUs [43], [45], [46]. In [43], convex optimization tools were used to find the sub-optimal beamformers in relay assisted CRNs. In [45], an iterative alternating optimization-based algorithm was developed to obtain the optimal beamforming weights in order to maximize the worst signal to interference noise

ratio in multiuser CRNs. However, these algorithms and tools suffer from high computational complexity. ZFB is considered as a simple sub-optimal approach that can be practically implemented. In [46], a ZFB approach in a single relay with a collocated multi-antenna system was applied to improve the primary system performance in an overlay CR scenario. In this work, upper bounds for the outage and error probabilities were derived.

Motivated by the potential of combining cooperative diversity and beamforming, we adopt in this chapter distributed beamforming in a dual-hop relaying spectrum-sharing system [48]-[51]. Beamforming is done such that the received SNR at the secondary destination is maximized subject to a non-zero interference constraint (predefined threshold) at the primary receiver. This method of beamforming is general and encompasses ZFB as a special case. For tractability reasons, we apply distributed ZFB in conjunction with SDF and AF relaying in a spectrum sharing environment where the secondary source communicates with its destination in the presence of a PU. We limit the inflicted interference at the PU from both the secondary source and relays. A peak power interference constraint is imposed on the source's transmission in the broadcasting phase while a distributed ZFB is applied to null the interference to the PU in the the relaying phase.

To analyze the secondary performance under the impact of the PU's CCI, we derive the cumulative distribution functions (CDFs) and probability density functions (PDFs) of the received SINRs in the SDF scheme. For the AF scheme, the CDF and the moment generating function (MGF) of the end-to-end (E2E) equivalent SNR are derived. Making use of these statistics, we derive closed-form expressions for the outage probability and the BER of the proposed spectrum-sharing system and confirm the results numerically and by simulations for different values of interference temperatures Q, number of relays and PU's CCI interference values.

In addition, asymptotic analysis of both metrics is performed in order to investigate the achievable diversity order of the proposed system, and to gain some insight on the impact of key parameters on the overall performance. Two scenarios are considered: 1) when a fixed interference constraint is imposed, which leads to an error floor; and 2) when the interference threshold scales with the secondary transmit power, which leads to a diversity gain in the low secondary transmit power regime. We also compare the performance of the proposed

schemes to the opportunistic SDF scheme presented in [15] and [16] for strict levels of the reflected interference at the PUs. We demonstrate that the proposed schemes outperform those in [15] and [16] for low to medium values of Q, which is the range of interest in cognitive radio networks.

As a generalized model, we extend the previous system model assuming that multiple PUs coexist with the secondary system. Considering this, we obtain a generalized beamforming vector and perform a comprehensive analysis. We investigate the effect of the number of the PUs on the secondary performance and the impact of the beamforming to compensate the gain loss due to the existence of those PUs [49].[1]

The rest of this chapter is organized as follows. Section 3.2 describes the system model. Section 3.3 represents the optimal beamforming weights design. The system performance of the SDF scheme is analyzed in Section 3.4 while the performance of the AF scheme is analyzed in Section 3.5. Numerical results are given in Section 3.6. Multi-PUs with CCI system model is explained in Section 3.7. Finally, Section 3.8 concludes the chapter.

3.2 System Model and Problem Formulation

3.2.1 System Model

Consider a relay-assisted spectrum-sharing system shown in Fig. 3.1 where each SU and PU is equipped with a single antenna. Specifically, our system model consists of a secondary source (SS), a secondary destination (SD) and a set of secondary relays R_i, $\forall i = 1, 2, ..., L$. There is no direct link between the source and destination, and they communicate only via potential relays $L_s \leq L$ that relay the source's message. A primary system coexists in the same area with the secondary system. The SUs are allowed to share the same frequency spectrum with the PU as long as the interference to the PU is limited to a predefined threshold. Both systems transmit simultaneously in an underlay manner. The transmission protocol consists of two orthogonal time slots and is divided into two phases as shown in Fig. 3.1.

[1] Hereafter, for simplicity, we refer to our system models as SDF-ZFB for the selection DF relaying scheme with ZFB applied, and AF-ZFB for the AF relaying scheme with ZFB applied.

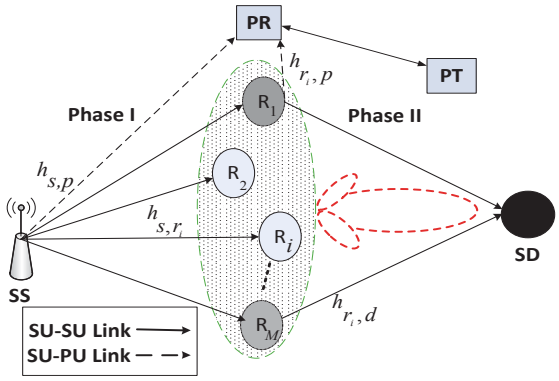

Figure 3.1: System model.

In the first phase, based on the interference CSI between SS and PU, SS adjusts its transmit power under a predefined threshold Q and broadcasts its message to the relays. Any data transmitted from SS resulting in an interference level higher than Q, which is the maximum tolerable interference power level at PU, is not allowed. Hence, a peak power constraint is imposed on the interference received at PU. In the second phase of the SDF scheme, the potential relays, which are selected during the first-hop transmission, become members of the potential relays set $\mathcal{C}$ where ZFB is applied to null the interference from $\mathcal{C}$ to PU. Meanwhile in the AF scheme, all L_s potential relays participate in the beamforming process. By applying ZFB, the set of potential relays are able to always transmit without interfering with the PU.

3.2.2 Channel Model

All channel coefficients are assumed to be independent Rayleigh fading. Let $h_{a,b}$ denote the channel coefficient between nodes a and b, which is modeled as a zero mean, circularly symmetric complex Gaussian (CSCG) random variable with variance $\lambda_{a,b}$. n_a denotes additive white Gaussian noise which is also modeled as a zero mean, CSCG random variable with variance σ^2. Let h_{s,r_i} denote the channel coefficient between the source's transmit antenna and the receive antenna of the ith relay and $h_{r_i,d}$ represent the channel coefficient between the

ith relay and SD and their channel power gains are $|h_{s,r_i}|^2$ and $|h_{r_i,d}|^2$, which are exponentially distributed with parameter λ_{s,r_i} and $\lambda_{r_i,d}$, respectively. Denote $h_{s,p}$ as the interference channel coefficient between SS and PU and its channel power gain $|h_{s,p}|^2$, which is also exponentially distributed with parameter $\lambda_{s,p}$. Let $h_{r_i,p}$, g_{m,r_i} and $g_{m,d}$ represent the interference channel coefficients between the ith relay and PU, and between the PU and both the ith relay and SD with their channel power gains $|h_{r_i,p}|^2, |g_{m,r_i}|^2$ and $|g_{m,d}|^2$ are also exponentially distributed with parameters $\lambda_{r_i,p}$, λ_{m,r_i} and $\lambda_{m,d}$, respectively. Let the ZFB vector be $\mathbf{w}_{\mathbf{zf}}^T = [w_1, w_2, ..., w_{L_s}]$. Also let $\mathbf{h}_{\mathbf{rd}}^T = [h_{r_1,d}, ..., h_{r_{L_s},d}]$, and $\mathbf{h}_{\mathbf{rp}}^T = [h_{r_1,p}, ..., h_{r_{L_s},p}]$ be the channel vectors between the relays and both SD and PU, respectively.

It is assumed that SS has perfect knowledge of the interference channel between itself and the PU, i.e., h_{sp}. We also assume that each selected relay R_i has perfect knowledge about its interference channel $h_{r_i,p}$ to the PU and then it shares this channel information with the SD to design the ZFB process at the second-hop transmission. It is worth mentioning that the availability of this interference channel information can be acquired through a spectrum-band manager that mediates between the primary and secondary users [52]. It is also assumed that SD has perfect knowledge of the channel coefficients between the selected relays and itself, i.e., (R_i - SD), which can be obtained via traditional channel estimation [53]. In our scheme, the ZFB weights associated with the selected relays are designed at the SD by exploiting the aforementioned channel information. Then, each weight is sent back to the selected relay via a low data-rate feedback link, and that is applicable in slow fading environments [54].[2]

3.2.3 Mathematical Model and Size of Set $\mathcal{C}$

In the underlay approach of this model, the SU can utilize the PU's spectrum as long as the interference it generates at the PUs remains below Q, which is the maximum tolerable

[2]We acknowledge that obtaining the interference channel between the primary and secondary users is a challenging problem in practice. However, the level of interference caused on the PU can be estimated by the fact that SS can hear the uplink signal of the PU. Feeding back the interference CSI to the SS may be carried out directly by the licensee or indirectly through a band manager, which mediates between the two parties (top of page 6 of [52]). To this end, several protocols have been proposed in [25], [52], which allow secondary and primary users to collaborate and exchange information such that the interference channel gains can be directly fed-back from the primary receiver to the secondary network.

interference level at which the PU can still maintain reliable communication [55]. Hence, the SS's power P is constrained as $P = \min\left\{\frac{Q}{|h_{s,p}|^2}, P_s\right\}$ where P_s is the maximum transmission power of SS [15]. In our model, we also assume that the PU imposes CCI at the secondary relays and SD. To this end, the received SINR $\hat{\gamma}_{s,r_i}$ at the ith relay is given as:

$$\hat{\gamma}_{s,r_i} = \min\left\{\frac{Q}{|h_{s,p}|^2}, P_s\right\}\frac{|h_{s,r_i}|^2}{P_{int}|g_{m,r_i}|^2 + \sigma^2}, \tag{3.1}$$

where P_{int} is the PU's transmit power.

Lemma 3.2.1. *The CDF of $\hat{\gamma}_{s,r_i}$, i.e., $F_{\hat{\gamma}_{s,r_i}}(\gamma)$ is given as*

$$\begin{aligned} F_{\hat{\gamma}_{s,r_i}}(\gamma) &= 1 - F_{h_{s,p}}(\vartheta) - \frac{Q\lambda_{s,p}\lambda_{m,r_i}e^{-\lambda_{s,p}\vartheta + \frac{\lambda_{m,r_i}\sigma^2}{P_{int}}}}{\lambda_{s,r_i}P_{int}\gamma} \times \left(-e^{\frac{Q\lambda_{s,p}}{\lambda_{s,r_i}\gamma}\left(\frac{\lambda_{m,r_i}}{P_{int}} + \frac{\lambda_{s,r_i}\gamma}{Q}\right)}\right. \\ &\times \left. Ei\left[-\left(\sigma^2 + \frac{Q\lambda_{s,p}}{\gamma\lambda_{s,r_i}}\right)\left(\frac{\lambda_{m,r_i}}{P_{int}} + \frac{\lambda_{s,r_i}\gamma}{Q}\right)\right]\right) \\ &+ F_{h_{s,p}}(\vartheta)\left(1 - \frac{e^{-\frac{\sigma^2\lambda_{s,p}\gamma}{P_s}}P_s}{P_{int}\lambda_{s,p}\gamma + P_s\lambda_{m,r_i}}\right), \end{aligned} \tag{3.2}$$

where $\vartheta = \frac{Q}{P_s}$, $F_{h_{s,p}}(\vartheta) = 1 - e^{-\lambda_{s,p}\vartheta}$and $Ei[.]$ is the exponential integral defined in [56].

Proof. See Appendix A.1. □

For AWGN only, i.e. $P_{int} = 0$, the CDF of the received SNR at the ith relay γ_{s,r_i} is given as

$$F_{\gamma_{s,r_i}}(\gamma) = 1 - e^{\frac{-\lambda_{s,p}\gamma}{\gamma_s}} + \frac{\gamma e^{-\frac{\frac{\lambda_{s,r_i}Q}{\sigma^2} + \lambda_{s,p}\gamma}{\gamma_s}}}{\frac{\lambda_{s,r_i}Q}{\lambda_{s,p}} + \gamma}, \tag{3.3}$$

where $\gamma_s = \frac{P_s}{\sigma^2}$.

We define $\mathcal{C}$ to be the set of relays which have their received instantaneous SINRs exceeding a certain threshold in the first time slot. This translates to the fact that the mutual information between SS and each relay is above a specified target value. In this case, the potential ith relay is only required to meet the following constraint given as [7]

$$\Pr\left[R_i \in \mathcal{C}\right] = \Pr\left[\frac{1}{2}\log_2(1 + \gamma^*_{s,r_i}) \geq R_{min}\right], i = 1, 2, ..., L, \tag{3.4}$$

where the coefficient $\frac{1}{2}$ comes from the dual-hop transmission in two time slots, γ^*_{s,r_i} represents either γ_{s,r_i} or $\hat{\gamma}_{s,r_i}$ and R_{min} denotes the minimum target rate below which outage occurs. According to (3.3), we can obtain

$$\Pr\left[R_i \in \mathcal{C}\right] \;=\; 1 - F_{\gamma^*_{s,r_i}}(\gamma_{min}), \tag{3.5}$$

where $\gamma_{min} = 2^{2R_{min}} - 1$ is the SINR threshold.

Without loss of generality, for all sub-channels being symmetrical, i.e., $\lambda_{s,r_i} = \lambda_{s,r}\,\forall\, i$, then $\Pr\left[R_i \in \mathcal{C}\right]$ is exactly the same for all i. Let $\Pr\left[R_i \in \mathcal{C}\right] = q$, and denote the cardinality of the set $\mathcal{C}$ as $|\mathcal{C}|$, then according to the Binomial Law, $\Pr\left[|\mathcal{C}| = L_s\right]$ becomes

$$\Pr\left[|\mathcal{C}| = L_s\right] = \binom{L}{L_s} q^{L_s}(1-q)^{L-L_s}. \tag{3.6}$$

3.3 Optimal Beamforming Weights Design

Our aim is to maximize the received power at the destination in order to maximize the mutual information of the secondary system while limiting the interference to the PU receiver to a tolerable level. Mathematically, the problem formulation for finding the optimal weight vector is described as follows.

$$\begin{aligned} \max_{\mathbf{v}_{opt}, P_r} \quad & |\mathbf{h}_{\mathbf{rd}}^H \mathbf{v}_{opt}|^2 \\ \text{s.t.:} \quad & |\mathbf{h}_{\mathbf{rp}}^H \mathbf{v}_{opt}|^2 \le Q/P_r, \\ & \|\mathbf{v}_{opt}\|^2 = 1, P_r \le P_v. \end{aligned} \tag{3.7}$$

To solve the above problem, we first find the optimal beamforming vector $\mathbf{v}_{opt}$, and then the transmit power of the relays $P_r \le P_v$, is found such that the interference constraint is satisfied, where P_v is the total available power at the relays. We decompose $\mathbf{v}_{opt}$ as a linear combination of two orthonormal vectors, namely, $\mathbf{v}_{opt} = \alpha_v \mathbf{w}_{\mathbf{zf}} + \beta_v \mathbf{w}_{\mathbf{o}}$, where α_v and β_v are complex valued weights with $|\alpha_v|^2 + |\beta_v|^2 = 1$ to keep $\|\mathbf{v}_{opt}\|^2 = 1$.

For the zero-interference constraint case, i.e., $Q = 0$, the optimal beamforming vector is the ZFB vector, i.e., $\mathbf{v}_{opt} = \mathbf{w}_{\mathbf{zf}}$. According to the ZFB principles, $\mathbf{w}_{\mathbf{zf}}$ is chosen to lie in the orthogonal space of $\mathbf{h}_{\mathbf{rp}}^H$ such that $|\mathbf{h}_{\mathbf{rp}}^H \mathbf{w}_{\mathbf{zf}}| = 0$ and $|\mathbf{h}_{\mathbf{rd}}^H \mathbf{w}_{\mathbf{zf}}|$ is maximized. By

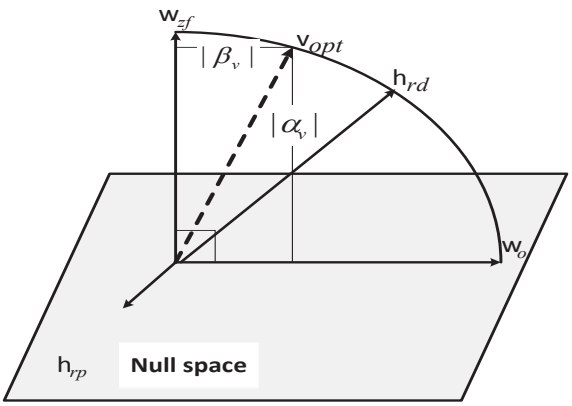

Figure 3.2: Geometric explanation of $\mathbf{v}_{opt}$

applying a standard Lagrangian multiplier method, the weight vector that satisfies the above optimization method is given as

$$\mathbf{w_{zf}} = \frac{\mathbf{T}^{\perp}\mathbf{h_{rd}}}{\|\mathbf{T}^{\perp}\mathbf{h_{rd}}\|}, \tag{3.8}$$

where $\mathbf{T}^{\perp} = \left(\mathbf{I} - \mathbf{h_{rp}}(\mathbf{h_{rp}^{\dagger}}\mathbf{h_{rp}})^{-\mathbf{1}}\mathbf{h_{rp}^{\dagger}}\right)$ is the projection idempotent matrix with rank $(L_s - 1)$.

For the non-zero interference constraint, the secondary relays can increase their transmit power in their own direction, i.e., $\mathbf{h_{rd}}$ while the interference to the PU is constrained to a predefined threshold. Generally, in this case, the beamforming vector is not in the null space of $\mathbf{h_{rp}}$ and since $\mathbf{w_{zf}^H w_o} = 0$, we have

$$\mathbf{w_o} = \frac{\mathbf{h_{rd}} - \mathbf{w_{zf}^H h_{rd} w_{zf}}}{\sqrt{1 - |\mathbf{w_{zf}^H h_{rd}}|^2}}. \tag{3.9}$$

By finding $\mathbf{w_{zf}}$ and $\mathbf{w_o}$, the optimal weights are derived as $\alpha_v = \frac{\mathbf{w_{zf}^H h_{rd}}}{|\mathbf{w_{zf}^H h_{rd}}|}\sqrt{1-\beta_v^2}$, $|\beta_v| \leq \sqrt{\frac{Q}{P_r|\mathbf{h_{rp}}|^2}}$, and $P_r = \frac{Q}{|\mathbf{h_{rp}}|^2}$. To elaborate, a geometric explanation of $\mathbf{v}_{opt}$ is given in Fig. 3.2 where by rotating $\mathbf{v}_{opt}$ from the ZFB vector $\mathbf{w_{zf}}$ toward the maximum ratio transmission (MRT) beamformer $\mathbf{h_{rd}}$, the secondary relays can maximize the SNR received at the secondary destination at the expense of increasing the interference to the PU while still respecting a predefined threshold Q. In the case of MRT, $\mathbf{v}_{opt} = \mathbf{h_{rd}}$, and therefore the interference constraint becomes irrelevant (non-cognitive case).

Although the optimal scheme yields the maximum SNR at the secondary receiver, it is not commonly used due to its intractability, both in terms of design complexity and performance analysis. As an alternative, ZFB is widely used for its simplicity and low complexity, which

is attributed to the fact that designing the ZFB vector involves only a projection of the interference channel vector onto the null space without the extra complexity of computing α_v and β_v. Moreover, as we will demonstrate later, simulation results suggest that there is a little difference in performance between ZFB (given by (3.8)) and the non-zero interference constraint with α_v and β_v. Motivated by this, for the analysis part, we only consider $\mathbf{w_{zf}}$ because it enables us to obtain closed-form expressions and get insights on the asymptotic performance of the underlying system, which will not be possible otherwise.[3]

3.4 Performance Analysis of the SDF scheme

In this section, we investigate the SDF relaying protocol employed jointly with ZFB. We consider the SDF scheme where only a set of potential relays who have strong channel conditions to the source and perfectly decode the source's message participate in the second phase. In the first phase, when SS broadcasts a signal x_s to the L relays, the received signal at the ith relay is given as

$$y_r = \sqrt{P} h_{s,r_i} x_s + \sqrt{P_{int}}\ g_{m,r_i} x_p + n_r, \tag{3.10}$$

where n_r denotes the noise at each R_i with variance σ^2 and x_p is the PU's signal. For the second phase, when the potential relays forward the SS's signal after applying ZFB, the received signal at the SD is given as

$$y_d = \sqrt{P_r} \mathbf{h_{rd}^H} \mathbf{w_{zf}} x_s + \sqrt{P_{int}}\ g_{m,d} x_p + n_d, \tag{3.11}$$

where x_s is the decoded symbol with $\mathrm{E}\left[|x_s|^2\right] = \left[|x_p|^2\right] = 1$, and n_d denotes the noise at SD with variance σ^2.

3.4.1 End-to-End Received SINR Statistics

We substitute (3.8) into (3.11) to get the conditional received SINR as

$$\hat{\gamma}_{eq|\mathcal{C}}^{DF} = \frac{P_r ||\mathbf{T}^{\perp} \mathbf{h_{r,d}}||^{\mathbf{2}}}{P_{int}|g_{m,d}|^2 + \sigma^2}. \tag{3.12}$$

[3]To be able to apply ZFB, we consider the general assumption that the number of relays must be greater than or equal to the number of primary receivers plus the secondary destination, hence $L_s \geq 2$.

To analyze the system, we need to obtain the PDF and CDF of $\hat{\gamma}_{eq|\mathcal{C}}^{DF}$. Let $X = P_r||\mathbf{T}^{\perp}\mathbf{h_{r,d}}||^2$ and $Y = P_{int}|g_{m,d}|^2$. Now we have the following *Lemma*.

Lemma 3.4.1. *Let each entry of* $\mathbf{h_{rd}}$ *be i.i.d.* $\mathcal{CN} \sim (0,1)$*, then* $\left\|\mathbf{T}^{\perp}\mathbf{h_{rd}}\right\|^2$ *is a chi-square random variable with* $2(L_s-1)$ *degrees of freedom [57, Theorem 2, Ch.1] with CDF is given as*

$$F_{X|\mathcal{C}}(\gamma) = 1 - \frac{1}{(L_s-2)!}\Gamma\left(L_s - 1, \frac{\gamma}{\gamma_r}\right), \ \gamma \geq 0, \tag{3.13}$$

where $\gamma_r = \frac{P_r}{\sigma^2}$ and $\Gamma(.,.)$ is the upper incomplete Gamma function defined in [56]. Accordingly, the PDF of $f_{\gamma_{eq|\mathcal{C}}}^{DF}(\gamma)$ is given as

$$f_{X|\mathcal{C}}(\gamma) = \frac{(\gamma)^{L_s-2}e^{-\frac{\gamma}{\gamma_r}}}{(L_s-2)!(\gamma_r)^{L_s-1}}, \ \gamma \geq 0, \ L_s \geq 2. \tag{3.14}$$

Incorporating (3.14) and the PDF of the exponential random variable Y into the integral of [58, Eq. 6.60], and using [56, (3.326.2)], the PDF of $\hat{\gamma}_{eq}^{DF}$ conditional on $\mathcal{C}$ is given as

$$f_{\hat{\gamma}_{eq|\mathcal{C}}^{DF}}(\gamma) \ = \ \frac{\zeta\gamma^{\varphi-1}}{\left(\frac{\gamma}{P_r} + \frac{\lambda_{m,d}}{P_{int}}\right)^{\varphi+1}}, \tag{3.15}$$

where $\zeta = \frac{\lambda_{m,d}}{\Gamma(\varphi)P_{int}(P_r)^{\varphi}}$ and $\varphi = L_s - 1$. Finally, the unconditional PDF of the total received SINR, denoted by γ_{tot}, is written as

$$\begin{aligned} f_{\gamma_{tot}^{DF}}(\gamma) \ &= \ \sum_{L_s=0}^{1}\binom{L}{L_s}q^{L-L_s}(1-q)^{L_s}\delta(\gamma) \\ &+ \ \sum_{L_s=2}^{L}\binom{L}{L_s}q^{L-L_s}(1-q)^{L_s}\frac{\zeta\gamma^{L_s-2}}{\left(\frac{\gamma}{P_r} + \frac{\lambda_{m,d}}{P_{int}}\right)^{L_s}}, \end{aligned} \tag{3.16}$$

where $\delta(\,.\,)$ is the Dirac function that refers to the received SINR when the relays are inactive. To compute $F_{\gamma_{tot}^{DF}}(\gamma)$, we integrate (3.16) which, with the help of [56, 3.194.1], results in

$$\begin{aligned} F_{\gamma_{tot}^{DF}}(\gamma) \ &= \ \sum_{L_s=0}^{1}\binom{L}{L_s}q^{L-L_s}(1-q)^{L_s} + \sum_{L_s=2}^{L}\binom{L}{L_s}q^{L-L_s}(1-q)^{L_s} \\ &\times \ \xi\gamma^{\varphi}\,{}_2F_1\left(L_s, \varphi; L_s; -\frac{P_{int}\gamma}{\lambda_{m,d}P_r}\right), \end{aligned} \tag{3.17}$$

where $\xi = \frac{(P_r)\lambda_{m,d}^{\varphi+2}}{\Gamma(\varphi+1)P_{int}^{\varphi+1}}$ and ${}_2F_1(\cdot)$ is a Gauss-hypergeometric function defined in [56, Eq. 9.11].

3.4.2 Outage Probability Analysis

In this section, we analyze the secondary outage performance. To this end, the mutual information at SD, I_{DF}, can be written as [7]

$$I_{DF} = \frac{1}{2}\log_2\left(1 + \sum_{i\in\mathcal{C}} \gamma_i\right), \tag{3.18}$$

where γ_i represents the received SNR for each relay-destination link. An outage event occurs when I_{DF} falls below a certain target rate. For a given rate R_{min}, the outage probability, P_{out}, can be rewritten using the total probability theorem as

$$P_{out}^{DF} = \sum_{L_s=0}^{L} \Pr(|\mathcal{C}| = L_s)\Pr(I_{DF} < R_{min} | \, |\mathcal{C}| = L_s). \tag{3.19}$$

There exist two exclusive outage events for the secondary system with distributed ZFB. Event A: failing to apply ZFB when $L_s < 2$,[4] and Event B: failing to achieve the target rate when $L_s \geq 2$. The probability of event A is

$$\Pr(\text{A}) = \sum_{L_s=0}^{1} \binom{L}{L_s} q^{L_s}(1-q)^{L-L_s}, \tag{3.20}$$

and the probability of event B is

$$\begin{aligned} \Pr(\text{B}) &= \Pr(I_{DF} < R_{min} | \, |\mathcal{C}| = L_s) \\ &= \Pr\left[\frac{1}{2}\log_2(1+\hat{\gamma}_{eq|\mathcal{C}}^{DF}) < R_{min}\right] = F_{\hat{\gamma}_{eq|\mathcal{C}}^{DF}}(\gamma_{min}), \end{aligned} \tag{3.21}$$

where $\gamma_{min} = 2^{2R_{min}} - 1$.

Then, from (3.17), the outage probability is simply given by

$$P_{out}^{DF} = F_{\gamma_{tot}^{DF}}(\gamma_{min}). \tag{3.22}$$

For the case of $P_{int} = 0$, the outage probability for the AWGN scenario is given as

$$P_{out}^{DF} = 1 - \sum_{L_s=2}^{L} \binom{L}{L_s} q^{L_s}(1-q)^{L-L_s} \left(\frac{\Gamma(L_s - 1, \frac{\gamma_{min}}{\gamma_r})}{(L_s-2)!}\right). \tag{3.23}$$

Diversity Gain: To gain some insight about the achievable diversity order, we investigate two cases. The first case is when a fixed power constraint is imposed, i.e., Q is fixed and the

[4] In this case, the system can limit the interference following the same approach used in the first phase. This case was studied in [59].

second case is when a proportional interference constraint is imposed, i.e., $Q = aP_s$.

In the first case, i.e., when $Q \to \infty$ and $P_s \ll Q$, (18) reduces to

$$\begin{aligned} P_{out}^{high} &\approx \sum_{L_s=0}^{L} \binom{L}{L_s} \left(1 - e^{-\frac{\gamma_{min}\lambda_{s,p}}{\gamma_s}}\right)^{L-L_s} \\ &\times \left(e^{-\frac{\gamma_{min}\lambda_{s,p}}{\gamma_s}}\right)^{L_s} \left(\frac{\gamma(L_s - 1, \frac{\gamma_{min}}{\gamma_r})}{(L_s - 2)!}\right). \end{aligned} \tag{3.24}$$

It is interesting to observe from (3.24) that the outage probability results in a non-zero constant value. This means that P_{out} saturates when the SU transmit power exceeds the PU threshold. This suggests that the outage probability saturates due to the restriction of Q, leading to a diversity order of zero.

Mathematically, the asymptotic diversity order d with respect to Q is given by

$$\begin{aligned} d &= \lim_{Q\to\infty} - \frac{\log\ (P_{out}^{high})}{\log\ (Q)} \\ &= \lim_{Q\to\infty} - \frac{\log(K)}{\log\ (Q)} = 0, \end{aligned} \tag{3.25}$$

where K is a non-zero constant. Noting that $\lambda_{r,p}, \gamma_s, L_s, \gamma_{min}$ are all constants and using (3.24), we arrive at (3.25). Hence, the diversity order is zero in this case.

For the second case, that is, for low to medium values of Q, we assume that Q scales with the maximum power level P_s, i.e., $Q = aP_s$, which effectively neglects the effect of the interference constraint by allowing a large transmit power. The objective here is to examine the achievable diversity for this range of Q. To this end, we first represent (3.3) in the following form to ease the expansion at high SNRs

$$\begin{aligned} F_{\gamma_{s,r_i}}(\gamma) &= \left(1 - e^{-\frac{Q\lambda_{s,r_i}}{P_s}}\right)\left(1 - e^{-\frac{\sigma^2\gamma\lambda_{s,p}}{P_s}}\right) \\ &+ e^{-\frac{Q\lambda_{s,r_i}}{P_s}} \left(1 - \frac{Q\lambda_{s,r_i} e^{-\frac{\sigma^2\gamma\lambda_{s,p}}{P_s}}}{\lambda_{s,p}\sigma^2\gamma + Q\lambda_{s,r_i}}\right). \end{aligned} \tag{3.26}$$

For sufficiently high SNR, i.e., as $P_s \to \infty$, using Taylor series expansion, (3.26) can asymptotically be expressed as

$$F_{\gamma_{s,r_i}}(\gamma) \approx \frac{\sigma^2\gamma\lambda_{s,p}}{P_s} + e^{-\frac{\lambda_{s,r_i}Q}{P_s}} \frac{\sigma^2\gamma\lambda_{s,p}}{Q\lambda_{s,r_i}}. \tag{3.27}$$

Substituting $Q = aP_s$ and $\gamma = \gamma_{min}$ into (3.27), the approximate outage probability expression is given as

$$\begin{aligned} P_{out}^{high} &\approx \sum_{L_s=0}^{L} \binom{L}{L_s} \left(1 - \psi \frac{1}{P_s}\right)^{L_s} \left(\psi \frac{1}{P_s}\right)^{L-L_s} \\ &\times \left(\frac{\gamma(L_s - 1, \frac{\gamma_{min}}{\gamma_r})}{(L_s - 2)!}\right). \\ &\approx G_a \left(\frac{1}{P_s}\right)^{L-1}, \end{aligned} \tag{3.28}$$

where $\psi = \sigma^2 \lambda_{s,p} \gamma_{min} + e^{-a\lambda_{s,r_i}} \frac{\sigma^2 \lambda_{s,p} \gamma_{min}}{a\lambda_{s,r_i}}$ and $G_a = \sum_{L_s=0}^{L} \binom{L}{L_s} \psi^L \left(\frac{\gamma(L_s-1, \frac{\gamma_{min}}{\gamma_r})}{(L_s-2)!}\right)$. Note that (3.28) suggests that the diversity gain is achieved with order $d = L - 1$ in this case.

3.4.3 Bit Error Rate Analysis

We analyze the BER performance due to the errors occurring at SD assuming that all participating relays have accurately decoded and regenerated the message. As such, the BER analysis follows similar lines like those of the outage probability. In particular, the error probability at SD can be written as

$$P_e^{DF} = \sum_{L_s=0}^{L} \Pr(|\mathcal{C}| = L_s) \Pr(P_e | |\mathcal{C}| = L_s), \tag{3.29}$$

where $\Pr(P_e||\mathcal{C}| = L_s)$ is the error probability conditioned on $|\mathcal{C}| = L_s$. The symbol error rate (SER) could be evaluated using the following identity

$$P_{SER}^{DF} = \frac{a\sqrt{b}}{2\sqrt{\pi}} \int_0^\infty \frac{e^{-bu}}{\sqrt{u}} F_{\gamma_{tot}^{DF}}(u) du, \tag{3.30}$$

where (a,b) depends on the modulation scheme.

Theorem 3.4.2. *A closed-form expression for the BER for the SDF-ZFB with the effect of the CCI of the PU is given by*

$$\begin{aligned} P_e^{DF} &= \frac{1}{2} \sum_{L_s=0}^{1} \binom{L}{L_s} q^{L-L_s} (1-q)^{L_s} + \epsilon\, \varpi \sum_{L_s=2}^{L} \binom{L}{L_s} q^{L-L_s} (1-q)^{L_s} \\ &\times \Sigma^{\nu} G_{2,3}^{3,1} \left(-\frac{\nu\, b\, \lambda_{m,d} P_r}{P_{int}} \middle|_{0, \frac{1}{2}, -\frac{1}{2}}^{\frac{1}{2} - \varphi, \frac{1}{2}} \right), \end{aligned} \tag{3.31}$$

where $\Sigma = \left(\frac{\lambda_{m,d}P_r}{P_{int}}\right)$, $\varpi = \frac{a\sqrt{b}}{2\sqrt{\pi}}\frac{\lambda_{m,d}}{P_{int}\Gamma(\varphi)P_r^{\varphi}}$, $\nu = \varphi + \frac{3}{2}$, $\epsilon = \frac{\varphi P_{int}}{\Gamma(L_s)P_r}$ and $(a,b) = (1,1)$ for BPSK.

Proof. See Appendix A.2. □

In the following, we analyze the BER using BPSK and the SER using M_q-QAM for the AWGN scenario, where M_q is the constellation size.

BER of BPSK

This probability could be evaluated by averaging the error probability P_e over the PDF in (3.14). Since P_e depends on the modulation scheme, many expressions can be used. In the case of BPSK, $P_e = Q\left(\sqrt{2\gamma_{eq|\mathcal{C}}^{DF}}\right)$ where $Q(.)$ denotes the $Q-$function defined as $Q(.) = \frac{1}{\sqrt{2\pi}}\int_x^{\infty} e^{-x^2/2}dx$. After averaging this expression over the PDF in (3.14), $\Pr(P_e||\mathcal{C}| = L_s)$ can be calculated as [60, Eq. 14-4-15]

$$\Pr(P_e||\mathcal{C}| = L_s) = [\frac{1}{2}(1-\mu)]^{L_s-1}\sum_{k=0}^{L_s-2}\binom{L_s-2+k}{k}[\frac{1}{2}(1+\mu)]^k, \tag{3.32}$$

where $\mu = \sqrt{\frac{\gamma_r}{1+\gamma_r}}$ and $L_s \geq 2$.
Now substituting (3.32) into (3.29), P_e^{DF} can be obtained as

$$\begin{aligned} P_{e_{BPSK}}^{DF} &= \frac{1}{2}\sum_{L_s=0}^{1}\binom{L}{L_s}q^{L_s}(1-q)^{L-L_s} + \sum_{L_s=2}^{L}\binom{L}{L_s}q^{L_s}(1-q)^{L-L_s} \\ &\times [\frac{1}{2}(1-\mu)]^{L_s-1}\sum_{k=0}^{L_s-2}\binom{L_s-2+k}{k}[\frac{1}{2}(1+\mu)]^k, \end{aligned} \tag{3.33}$$

where the first term in the expression appears when the number of selected relays is less than two, hence, we do not have any transmission in the second phase. It is worth noting that the PDF of the received SNR at SD in the non-transmission case (the relay keeps silent) is $\delta(x)$, where $\delta(\cdot)$ is the delta function.

Diversity Gain: Similar to the outage probability case, to analyze the asymptotic behavior of (3.33), we let $Q \to \infty$ while $P_s \ll Q$. The resulting expression can be expressed

as

$$\begin{aligned} P_e^{high} &\approx \sum_{L_s=0}^{L} \binom{L}{L_s} \left(1 - e^{-\frac{\gamma_{min}\lambda_{s,p}}{\gamma_s}}\right)^{L-L_s} \\ &\times \left(e^{-\frac{\gamma_{min}\lambda_{s,p}}{\gamma_s}}\right)^{L_s} [\frac{1}{2}(1-\mu)]^{L_s-1} \\ &\times \sum_{k=0}^{L_s-2} \binom{L_s-2+k}{k} [\frac{1}{2}(1+\mu)]^k. \end{aligned} \tag{3.34}$$

Mathematically, noting that all $\lambda_{r,p}, \gamma_s, L_s, \gamma_{min}$ are constants, the asymptotic diversity order d with respect to Q is given by

$$\begin{aligned} d &= \lim_{Q\to\infty} -\frac{\log\ (P_e^{high})}{\log\ (Q)} \\ &= \lim_{Q\to\infty} -\frac{\log(K)}{\log\ (Q)} = 0, \end{aligned} \tag{3.35}$$

which suggests that the diversity order is zero.

SER of M_q-QAM: For a square M_q-QAM modulation signal ($M_q = 2^k$ with even k), since it can be considered as two independent $\sqrt{k}$-pulse amplitude modulation (PAM) signals, its conditional average SER can be written as

$$\begin{aligned} P_{e_{M_q-QAM}^{DF}} &= \underbrace{\int_0^\infty 4DQ\left(\sqrt{\frac{3}{M_q-1}z} f_{\gamma_{eq|\mathcal{C}}^{DF}}(z)\right) dz}_{I_1} \\ &- \underbrace{\int_0^\infty 4D^2Q^2\left(\sqrt{\frac{3}{M_q-1}z} f_{\gamma_{eq|\mathcal{C}}^{DF}}(z)\right) dz}_{I_2} \end{aligned} \tag{3.36}$$

where $D = \left(1 - \frac{1}{\sqrt{M_q}}\right)$. For the first integral I_1, we have

$$\begin{aligned} I_1 &= \frac{2a\sqrt{b}}{\sqrt{\pi}} \int_0^\infty \frac{e^{-bz}}{\sqrt{z}} F_{\gamma_{eq|\mathcal{C}}^{DF}}(z) dz \\ &= \frac{2a\sqrt{b}}{\sqrt{\pi}} \int_0^\infty \frac{e^{-bz}}{\sqrt{z}} \frac{\gamma(L_s-1, \frac{z}{\gamma_r})}{(L_s-2)!} dz, \end{aligned} \tag{3.37}$$

where $a = 1 - \frac{1}{\sqrt{M_q}}$ and $b = \frac{3}{2(M_q-1)}$ for M_q-QAM. Using [56, 6.455.2], I_1 results in

$$I_1 = \frac{2a\sqrt{b}}{\sqrt{\pi}} \frac{\Gamma(L_s-\frac{1}{2})(\frac{1}{\gamma_r})^{L_s-1}}{(L_s-1)!(\frac{1}{\gamma_r}+b)^{L_s-\frac{1}{2}}} {}_2F_1\left(1, L_s-\frac{1}{2}; L_s; \frac{1}{\gamma_r(\frac{1}{\gamma_r}+b)}\right). \tag{3.38}$$

For the second integral I_2, we use [61, Eq. 39] as

$$\begin{aligned} I_2 &= \frac{1}{6}a^2\left[3\int_0^{\infty} e^{-\frac{6}{M_q-1}z} f^{DF}_{\gamma_{eq|\mathcal{C}}}(z)dz + \int_0^{\infty} e^{-\frac{3}{M_q-1}z} f^{DF}_{\gamma_{eq|\mathcal{C}}}(z)dz\right] \\ &= \frac{1}{6}a^2\left[\frac{3}{\gamma_r^{L_s-1}}\left(\frac{6}{M_q-1}+\frac{1}{\gamma_r}\right)^{-L_s+1} + \frac{1}{\gamma_r^{L_s-1}}\left(\frac{3}{M_q-1}+\frac{1}{\gamma_r}\right)^{-L_s+1}\right]. \end{aligned} \tag{3.39}$$

By adding (3.38) and (3.39) and following the same steps as in (3.29), we get a closed-form expression for the SER of M_q-QAM. We note that, in many previous works, I_2 is omitted which may cause a significant error to the SER at low SNRs. In contrast, our closed-form expression gives more accurate results.

3.5 Performance Analysis of the AF scheme

In this section, we consider the AF scheme where a set of relays L_s simply weight and forward the received signals in the second phase. The AF relaying scheme is beneficial in our system model because it is desired to reduce the complexity in CRN. In the proposed setup, in the first phase, the SS broadcasts its signal to all L relays, then the received signal at the ith relay is given in (3.10). When the potential relays $L_s = L$ participate in the second phase, the received $L_s \times 1$ vector at the relays can be written in a vector form as[5]

$$\mathbf{y_r} = \sqrt{P}\mathbf{h_{sr}}x_s + \mathbf{n_r}, \tag{3.40}$$

where $\mathbf{h_{sr}}$ is the $L_s \times 1$ source- relays channel vector and $\mathbf{n_r}$ is the relays' noise vector with its elements having variance σ^2. In the second phase, the potential relays amplify and forward the received signals to the destination. To allow concurrent transmission of the secondary relays and PU, we first apply the $L_s \times 1$ ZFB vector denoted by $\mathbf{w_{zf}}$ and then the weighted signals are forwarded to SD. The received signal at SD is given as

$$y_d = \sqrt{P}A_r\mathbf{h}^H_{\mathbf{rd}}\mathrm{Diag}(\mathbf{w_{zf}})\mathbf{h_{sr}}x_s + A_rB_r\mathbf{h}^H_{\mathbf{rd}}\mathrm{Diag}(\mathbf{w_{zf}})\mathbf{n_r} + n_d, \tag{3.41}$$

[5]In the AF scheme, we do the performance analysis while assuming AWGN because it is mathematically tractable. As for the case with interference, we provide only simulation results because the performance analysis is complex.

where A_r is the normalization constant designed to ensure that the total transmit power at the relays is constrained and it is given by (assuming each R_i knows perfectly h_{s,r_i}) [35]

$$A_r = \sqrt{\frac{P_r}{\mathbf{w_{zf}^H}(P\mathbf{h_{sr}}\mathbf{h_{sr}^H} + \sigma^2\mathbf{I})\mathbf{w_{zf}}}}. \tag{3.42}$$

Then the total received SNR at SD is given as

$$\gamma_{eq}^{AF} = \frac{PA_r^2|\mathbf{h_{rd}^H}\mathrm{Diag}(\mathbf{w_{zf}})\mathbf{h_{sr}}|^2}{A_r^2|\mathbf{h_{rd}^H}\mathbf{w_{zf}}|^2\sigma^2 + \sigma^2}. \tag{3.43}$$

Now substituting (3.8) and (3.42) into (3.43), and after simple manipulations, the equivalent SNR at SD can be written in the general form of $\gamma_{eq} = \frac{\gamma_1\gamma_2}{\gamma_1+\gamma_2+1}$ as:

$$\gamma_{eq}^{AF} = \frac{\frac{P}{\sigma^2}\left\|\mathbf{h_{sr}}\right\|^2\gamma_r\left\|\mathbf{T}^{\perp}\mathbf{h_{rd}}\right\|^2}{\frac{P}{\sigma^2}\left\|\mathbf{h_{sr}}\right\|^2 + \gamma_r\left\|\mathbf{T}^{\perp}\mathbf{h_{rd}}\right\|^2 + 1}. \tag{3.44}$$

Considering the peak power constraint on the PU, we express γ_{eq}^{AF} as

$$\gamma_{eq}^{AF} = \begin{cases} \frac{\gamma_s\|\mathbf{h_{sr}}\|^2\gamma_r\left\|\mathbf{T}^{\perp}\mathbf{h_{rd}}\right\|^2}{\gamma_s\|\mathbf{h_{sr}}\|^2+\gamma_r\left\|\mathbf{T}^{\perp}\mathbf{h_{rd}}\right\|^2+1}, & P_s < \frac{Q}{|h_{s,p}|^2} \\ \frac{\gamma_q\frac{\|\mathbf{h_{sr}}\|^2}{|h_{s,p}|^2}\gamma_r\left\|\mathbf{T}^{\perp}\mathbf{h_{rd}}\right\|^2}{\gamma_q\frac{\|\mathbf{h_{sr}}\|^2}{|h_{s,p}|^2}+\gamma_r\left\|\mathbf{T}^{\perp}\mathbf{h_{rd}}\right\|^2+1}, & P_s \geq \frac{Q}{|h_{s,p}|^2} \end{cases} \tag{3.45}$$

where $\gamma_q = \frac{Q}{\sigma^2}$.

3.5.1 End-to-End Statistical Analysis of γ_{eq}^{AF}

We first present the statistics of the new random variables. Then, we derive the CDFs and PDFs of both cases of γ_{eq}^{AF} which will be used in the derivation of the performance metrics. We focus on the analysis of the second case $\left(P_s \geq \frac{Q}{|h_{s,p}|^2}\right)$ as it is more effective and restrictive than the first case $\left(P_s < \frac{Q}{|h_{s,p}|^2}\right)$. It determines the effect of the peak power constraint in the first phase on the performance of the secondary system while the system in the first case becomes a non-cognitive one.

Let $\gamma_1 = \gamma_s\left\|\mathbf{h_{sr}}\right\|^2$, $\gamma_2 = \gamma_r\left\|\mathbf{T}^{\perp}\mathbf{h_{rd}}\right\|^2$, and $\gamma_3 = \gamma_q\frac{\|\mathbf{h_{sr}}\|^2}{|h_{s,p}|^2}$. We first need to find the CDFs and PDFs for all γ_1, γ_2 and γ_3. The CDF and PDF of γ_2 are given in (3.13) and (3.14), respectively, and in the following we derive the PDFs and CDFs of γ_1 and γ_3.

Lemma 3.5.1 ((PDF and CDF of γ_1)). *Let each entry of* $\mathbf{h_{sr}}$ *be i.i.d.* $\mathcal{CN} \sim (0,1)$, *i.e.,* $\|\mathbf{h_{sr}}\|^2$ *is a chi-square random variable with* $2L_s$ *degrees of freedom. Then the PDF and CDF* γ_1 *are given by*

$$f_{\gamma_1}(\gamma) = \frac{(\gamma)^{L_s-1}e^{-\frac{\gamma}{\gamma_s}}}{(L_s-1)!(\gamma_s)^{L_s}},\ \gamma \geq 0, \tag{3.46}$$

and

$$F_{\gamma_1}(\gamma) = 1 - \frac{1}{(L_s-1)!}\Gamma\left(L_s, \frac{\gamma}{\gamma_s}\right). \tag{3.47}$$

Proof. See [62, Chapter 9]. □

Lemma 3.5.2 ((PDF and CDF of γ_3)). *Given that* $\|\mathbf{h_{sr}}\|^2$ *is a chi-square random variable with* $2L_s$ *degrees of freedom (Lemma 3), and* $|h_{s,p}|^2$ *is an exponential random variable, then the PDF and CDF of* $\gamma_3 = \gamma_q \frac{\|\mathbf{h_{sr}}\|^2}{|h_{s,p}|^2}$ *are given by:*

$$f_{\gamma_3}(\gamma) = \frac{\lambda_{s,p}L_s}{(\gamma_q)^{L_s}} \frac{(\gamma)^{L_s-1}}{(\frac{\gamma}{\gamma_q}+\lambda_{s,p})^{L_s+1}}, \tag{3.48}$$

and

$$F_{\gamma_3}(\gamma) = \left(\frac{\gamma}{\gamma_q\lambda_{s,p}}\right)^{L_s} {}_2F_1(L_s+1, L_s; L_s+1; -\frac{\gamma}{\gamma_q\lambda_{s,p}}), \tag{3.49}$$

where ${}_2F_1(\ ,\ ;\ ;\ )$ is the Gauss hypergeometric function defined in [56].

Proof. See Appendix A.3. □

To proceed, we compute the statistics of γ_{eq}^{AF} defined by

$$\gamma_{eq}^{AF} = \frac{\gamma_1\gamma_2}{\gamma_1+\gamma_2}, \tag{3.50}$$

which can be considered as a tractable tight upper bound to the actual equivalent E2E SNR. To this end, γ_{eq}^{AF} in (3.45) can be rewritten as

$$\gamma_{eq}^{AF} = \begin{cases} \gamma_{eq_1}^{AF}, & P_s < \frac{Q}{|h_{s,p}|^2} \\ \gamma_{eq_2}^{AF}, & P_s \geq \frac{Q}{|h_{s,p}|^2} \end{cases} \tag{3.51}$$

where $\gamma_{eq_1}^{AF} = \frac{\gamma_s\|\mathbf{h_{sr}}\|^2\gamma_r\left\|\mathbf{T}^{\perp}\mathbf{h_{rd}}\right\|^2}{\gamma_s\|\mathbf{h_{sr}}\|^2+\gamma_r\left\|\mathbf{T}^{\perp}\mathbf{h_{rd}}\right\|^2}$ and $\gamma_{eq_2}^{AF} = \frac{\gamma_q\frac{\|\mathbf{h_{sr}}\|^2}{|h_{s,p}|^2}\gamma_r\left\|\mathbf{T}^{\perp}\mathbf{h_{rd}}\right\|^2}{\gamma_q\frac{\|\mathbf{h_{sr}}\|^2}{|h_{s,p}|^2}+\gamma_r\left\|\mathbf{T}^{\perp}\mathbf{h_{rd}}\right\|^2}$.

Theorem 3.5.3 ((CDF of $\gamma_{eq_1}^{AF}$)). *The CDF of the tight upper bounded $\gamma_{eq_1}^{AF}$ is given by*

$$\begin{aligned} F_{eq_1}^{AF}(\gamma) &= 1 - b_o\, e^{(-\frac{\gamma}{\gamma_s})} e^{(-\frac{\gamma}{\gamma_r})} \sum_{n=0}^{Ls-2} \sum_{k=0}^{Ls-1} \sum_{v=0}^{k} \binom{L_s-2}{n} \\ &\times \frac{1}{k!}\binom{k}{v} 2(\gamma_r)^{\frac{n-v+1}{2}} (\frac{1}{\gamma_s})^{k+\frac{n-v+1}{2}} (\gamma)^{k+L_s-1} \\ &\times K_{n-v+1}\left(2\sqrt{\frac{\gamma^2}{\gamma_s\gamma_r}}\right), \end{aligned} \tag{3.52}$$

where $b_o = \frac{1}{(L_s-2)!\gamma_r^{L_s-1}}$.

Proof. See Appendix A.4. □

Theorem 3.5.4 ((CDF of $\gamma_{eq_2}^{AF}$)). *The CDF of the tight upper bounded $\gamma_{eq_2}^{AF}$ is given by*

$$\begin{aligned} F_{\gamma_{eq_2}}^{AF}(\gamma) &= 1 - d\, e^{(-c\gamma)} \sum_{n=0}^{Ls-1} \sum_{k=0}^{Ls-2} \sum_{v=0}^{k} \frac{1}{k!}\binom{k}{v}\binom{L_s-1}{n} \\ &\times (c)^{k+\frac{n-v}{2}} \Gamma(L_s-n+v)(\gamma)^{L_s-1+k} \\ &\times (\gamma+\lambda_{s,p}\gamma_q)^{\frac{n-v}{2}-L_s} e^{\left(\frac{c\gamma^2}{2(\gamma+\lambda_{s,p}\gamma_q)}\right)} \\ &\times W_{\frac{n-v}{2}-L_s,\frac{-n+v-1}{2}}\left(\frac{c\gamma^2}{(\gamma+\lambda_{s,p}\gamma_q)}\right), \end{aligned} \tag{3.53}$$

where $d = \frac{\lambda_{s,p}}{\gamma_q}$, $c = 1/\gamma_r$ and $W_{.,.}(.)$ is the Whittaker function defined in [56]. It is worth noting that the Whittaker function is implemented in many mathematical softwares such as Matlab and Mathematica.

Proof. See Appendix A.5. □

By differentiating $F_{\gamma_{eq_2}}^{AF}(\gamma)$ with respect to γ, we get the PDF of $\gamma_{eq_2}^{AF}$ which is evaluated numerically and plotted in Fig. 3.3 for various values of L_s.

3.5.2 MGF of $\gamma_{eq_2}^{AF}$

In order to obtain the average BER for the AF scheme in the second case, the MGF based approach in [62] is used in this paper. Let $\gamma_{eq_2}^{-1} = \gamma_3^{-1} + \gamma_2^{-1} = X_1 + X_2$ where $X_1 = \gamma_3^{-1}$ and $X_2 = \gamma_2^{-1}$. As $\gamma_{eq_2}^{-1}$ is the sum of two independent random variables, the MGF of $\gamma_{eq_2}^{-1}$ results

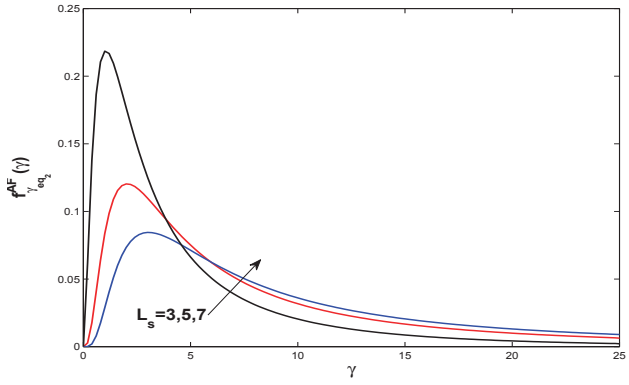

Figure 3.3: PDF of the End-to-End received SNR at SD, $f_{\gamma_{eq_2}}^{AF}(\gamma)$ for different values of potential relays in the AF-ZFB scheme for the second case.

simply from the product of the two MGFs of X_1 and X_2. The MGF of random variable X is defined as

$$\phi_X(s) = \mathrm{E}_X\left\{\exp(-sX)\right\} = \int_0^\infty e^{-sz} f_X(z) dz. \tag{3.54}$$

First, we need to find the PDFs of X_1 and X_2. For the PDF of X_1, we follow the same mathematical approach applied in (A.12), which after some mathematical manipulations, is obtained as

$$f_{X_1}(z) = \frac{\lambda_{s,p} L_s}{(\gamma_q)^{L_s}} \frac{1}{(\lambda_{s,p} z + \frac{1}{\gamma_q})^{L_s+1}}. \tag{3.55}$$

The PDF of X_2 is the PDF of the inverse chi-square random variable which leads to the following expression

$$f_{X_2}(z) = \frac{e^{\frac{-1}{\gamma_r z}}}{(\gamma_r)^{L_s-1}(L_s-2)! z^{L_s}}. \tag{3.56}$$

Substituting (3.55) into (3.54), and using [56, 3.382.4], the MGF of X_1 is

$$\phi_{X_1}(s) = \frac{L_s}{(\lambda_{s,p})^{L_s}(\gamma_q)^{L_s}} s^{L_s} e^{\frac{s}{\gamma_q \lambda_{s,p}}} \Gamma(-L_s, \frac{s}{\gamma_q \lambda_{s,p}}). \tag{3.57}$$

Similarly, substituting (3.56) into (3.54), and using [56, 3.471.9], the MGF of X_2 is

$$\phi_{X_2}(s) = \frac{2}{(\gamma_r)^{L_s-1}(L_s-2)!} \left(\frac{s}{\gamma_r}\right)^{\frac{L_s-1}{2}} K_{L_s-1}\left(2\sqrt{\frac{s}{\gamma_r}}\right), \tag{3.58}$$

where $K_v(.)$ is the modified Bessel function defined in [56].

Now, we can easily compute the MGF of $\gamma_{eq_2}^{-1}$ as the product of $\phi_{X_1}(s)$ and $\phi_{X_2}(s)$ which is

given as

$$\begin{aligned}\phi_{\gamma_{eq2}^{-1}}(s) &= \frac{2L_s}{(\lambda_{s,p})^{L_s}(\gamma_q)^{L_s}(\gamma_r)^{\frac{L_s-1}{2}}(L_s-2)!}s^{\frac{3s-1}{2}}e^{\frac{s}{\gamma_q\lambda_{s,p}}} \\ &\times \Gamma(-L_s,\frac{s}{\gamma_q\lambda_{s,p}})K_{L_s-1}\left(2\sqrt{\frac{s}{\gamma_r}}\right). \end{aligned} \tag{3.59}$$

We can make use of the following formula to find the MGF of $\gamma_{eq_2}^{AF}$ utilizing the MGF $\gamma_{eq_2}^{-1}$ [64, Eq. 18]

$$\phi_{\gamma_{eq_2}^{AF}}(s) = 1 - 2\sqrt{s}\int_0^\infty J_1(2\beta\sqrt{s})\phi_{\gamma_{eq}^{-1}}(\beta^2)d\beta, \tag{3.60}$$

where $J_1(.)$ is the Bessel function of the first kind [56]. Although this formula seems to be difficult, we can still use it to study the performance of the BER based on the relationship that exists between the MGF and symbol error rate [62].

3.5.3 Outage Probability Analysis

In traditional systems, outage occurs when the received SNR at the destination falls below a pre-determined threshold. However, in spectrum-sharing systems, besides the previous reason, outage occurs when the interference constraint imposed on the secondary transmitters (to limit the inflicted interference on primary users) is not satisfied. Therefore, outage in such systems cannot be avoided. To this end, the mutual information at SD, I_{AF}, can be written as [7]

$$I_{AF} = \frac{1}{2}\log_2(1+\gamma_{eq}^{AF}), \tag{3.61}$$

where γ_{eq}^{AF} represents the E2E received SNR at SD. An outage event occurs when I_{AF} falls below a certain target rate. For a given rate R_{min}, the outage probability, P_{out}^{AF}, can be rewritten as

$$P_{out}^{AF} = \Pr(I_{AF} < R_{min}) = F_{eq}^{AF}(\gamma_{min}). \tag{3.62}$$

The corresponding total outage probability for the first case $\left(P_s < \frac{Q}{|h_{s,p}|^2}\right)$ can be computed by substituting (3.52) into (3.62), yielding

$$P_{out_1}^{AF} = F_{eq_1}^{AF}(\gamma_{min}), \tag{3.63}$$

and the corresponding total outage probability for the second case $\left(P_s \geq \frac{Q}{|h_{s,p}|^2}\right)$ can be computed by substituting (3.53) into (3.62), and is given as

$$P_{out_2}^{AF} = F_{\gamma_{eq_2}}^{AF}(\gamma_{min}). \tag{3.64}$$

3.5.4 Bit Error Rate Analysis

Exploiting the MGF-based form, the average BER is given by [62]

$$P_e = \frac{1}{\pi}\int_0^{\pi/2} \phi_{\gamma_{eq}}\left(\frac{1}{\sin^2\varphi}\right) d\varphi. \tag{3.65}$$

Substituting (3.60) into (3.65) and after some manipulations, the formula of the BER becomes

$$P_e = \frac{1}{2} - \frac{2}{\pi}\int_0^{\infty} \phi_{\gamma_{eq}^{-1}}(\beta^2)\int_0^{\pi/2}\left(\sqrt{\frac{1}{\sin^2\varphi}}J_1\left(2\beta\sqrt{\frac{1}{\sin^2\varphi}}\right)\right) d\varphi d\beta. \tag{3.66}$$

The inner integral of (3.66) can be solved by using change of variables and equation [63, eq. 2.12.4.15] which leads to the value $\frac{\sin(2\beta)}{2\beta}$. So the BER can be evaluated according to the following formula

$$P_e = \frac{1}{2} - \frac{2}{\pi}\int_0^{\infty} \phi_{\gamma_{eq}^{-1}}(\beta^2)\frac{\sin(2\beta)}{2\beta} d\beta, \tag{3.67}$$

where $\phi_{\gamma_{eq}^{-1}}$ is the MGF of the inverse SNR given in (3.59).

Regarding the diversity gain in the AF scheme, in the literature, there were many articles that analyzed the diversity gain especially in traditional and spectrum-sharing systems. Since it is similar to the analysis of the asymptotic behavior of the DF scheme with the same conclusion, we opted for not including it here as it will be a repetition otherwise [46].

3.6 Numerical Results and Discussions

In this section, we investigate the performance of the derived results numerically and through simulations. For the outage probability analysis, without loss of generality, we assume that $\lambda_{s,p} = \lambda_{s,r_i} = \lambda_{r_i,p} = 1$ and $\lambda_{m,r_i} = \lambda_{m,d} = 1$. We also assume that the maximum transmit powers for the SS and the secondary relays are $P_r = 5$dB and $P_s = 7$dB, respectively.

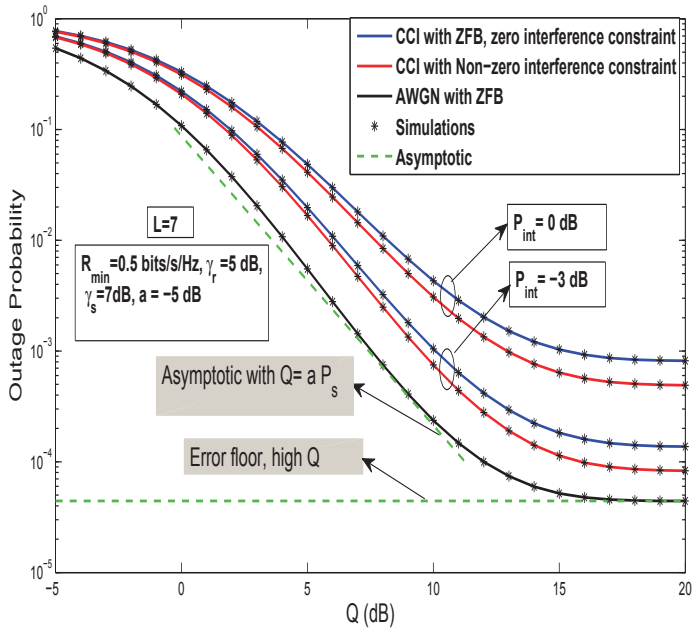

Figure 3.4: Outage probability of SDF-ZFB vs. Q(dB) for L=7 and R_{min}= 0.5 bits/s/Hz.

3.6.1 SDF Scheme

Fig. 3.4 shows the outage performance of the SDF-ZFB system versus the peak interference level Q at PU for $L = 7$ and $R_{min} = 0.5$ bits/s/Hz. Clearly, the higher the tolerable interference level, the better the outage performance. The figure also shows that the outage performance saturates at high values of Q which is a result of the limitation on the maximum transmit power of the secondary transmitters. It is obvious that the outage performance with the effect of the CCI from the PU becomes worse than its performance without CCI at the same transmit power and number of relays. The figure also shows the outage performance when a non-zero interference constraint beamforming vector is employed (simulation only). It shows that there is a little difference between the system performance in this case and ZFB due to the loose Q. This appears at high values of Q which is not in the range of operation in cognitive networks.

In Fig. 3.5, we simulate the outage probability versus the number of potential relays for $Q = -3, 0, 3$ dB and $R_{min} = 0.2, 0.5$ bits/s/Hz. It is clear that by increasing the number of relays that participate in the second phase, the outage performance improves as compared

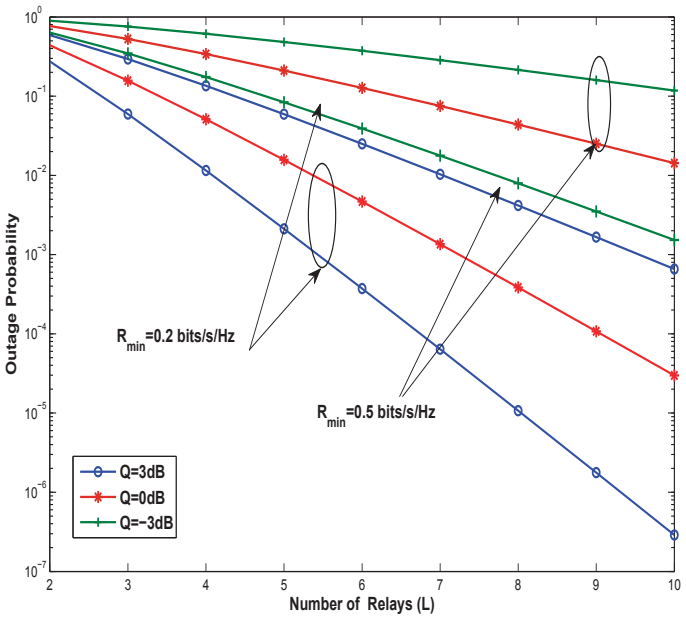

Figure 3.5: Outage probability of SDF-ZFB vs. the number of relays for $Q = -3, 0, 3$dB and $R_{min} = 0.2, 0.5$ bits/s/Hz.

to the non-beamforming SDF case. This is attributed to the fact that applying ZFB acts as an opportunistic relaying in the second phase and it only needs one time slot to transmit as compared to the time division multiple access (TDMA) schemes that need M time slots.

Fig. 3.6 illustrates the average BER performance versus Q for L= 7 and R_{min} = 0.5 bits/s/Hz. It is obvious that for low to moderate Q values, the BER improves substantially as the number of potential relays increases and Q becomes less strict. It saturates to a good BER performance for high Q values since the secondary source and the relays transmit at a fixed transmit power as well as maintaining the QoS at the PU. The asymptotic behavior when Q scales with P_s, i.e., $Q = aP_s$ gives a diversity gain with $L-1$ which emphasizes that the diversity is achieved only in the low transmit power regimes. Moreover, for low value of $P_{int} = -3$ dB, the BER performance with CCI is close to the performance with AWGN only which can happen in practical systems when the PU signal is a Gaussian codeword for instance.

Fig. 3.7 plots the average SER of the SDF scheme versus Q employing M_q-QAM modulation scheme. We use BPSK, 4-QAM and 16-QAM. Clearly, BPSK gives better performance,

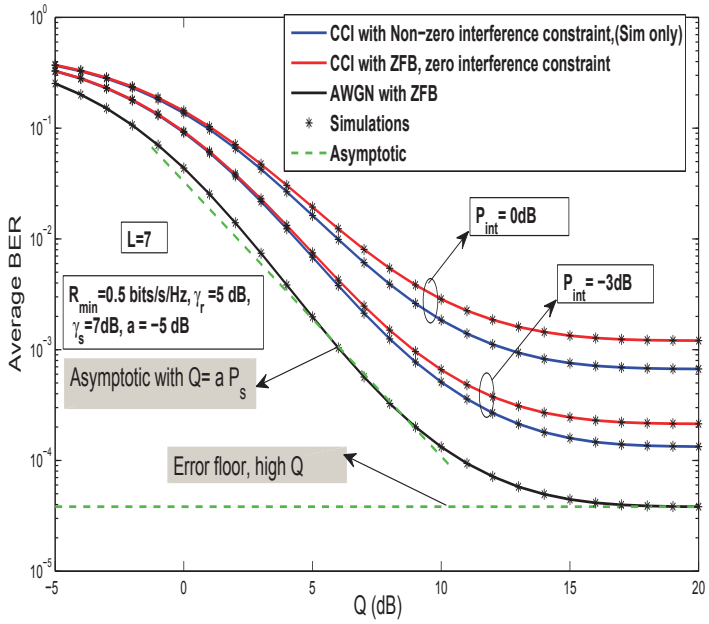

Figure 3.6: Average BER of the SDF-ZFB vs. Q for L=7 at $R_{min} = 0.5$ bit/s/Hz and BPSK scheme.

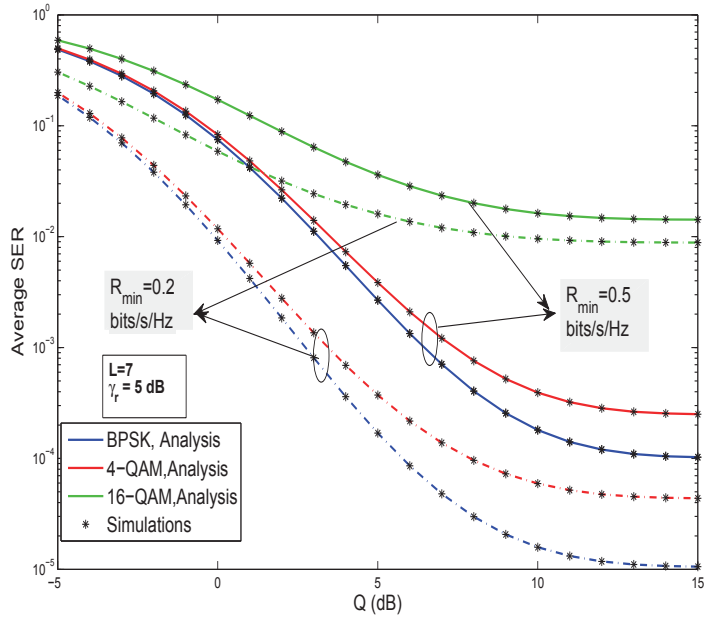

Figure 3.7: Average SER of M_q-QAM for the SDF-ZFB vs. Q for L=7 at $R_{min} = 0.2, 0.5$ bit/s/Hz.

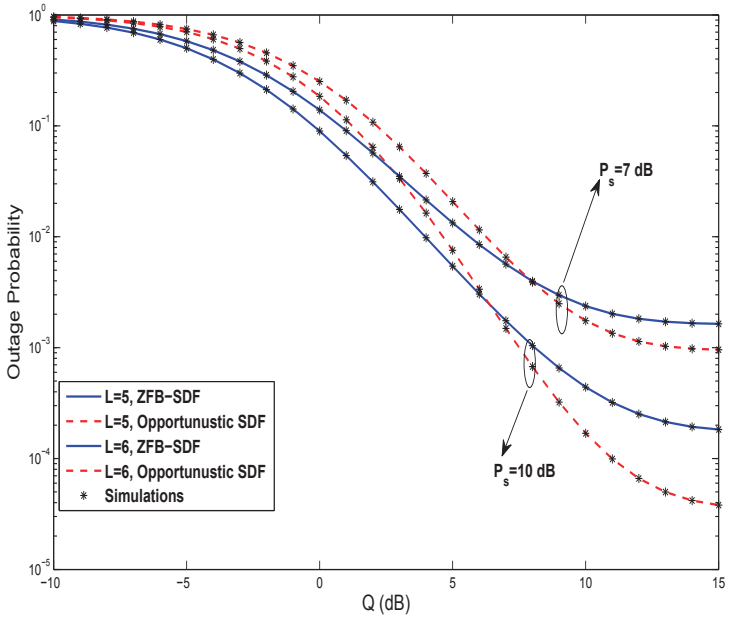

Figure 3.8: Comparison between the outage probabilities of SDF-ZFB and the opportunistic SDF presented in [16] for L=5, 6 at R_{min}= 0.5 bits/s/Hz.

however, the 4-QAM and 16-QAM offer better throughput.

Comparison between the outage performances of our system SDF-ZFB and the opportunistic-SDF without the direct path used in [15] and [16] is simulated in Fig. 3.8. In the figure, we examine the outage probability versus different values of Q with $L = 5, 6$ and maximum transmit power of the secondary transmitters $P_s = 7, 10$ dB at $R_{min} = 0.5$ bits/s/Hz. Our proposed system outperforms the system in [15] and [16] for strict values of Q which is great news as it is more acceptable and practical in cognitive radio systems. For very loose values of Q, the system in [15] and [16] outperforms our proposed system performance. The reason is, at high Q values, their system is described as a non-cognitive system without any interference constraint which is not tolerable in spectrum sharing environments.

3.6.2 AF Scheme

With the same assumptions as in the SDF scheme, we study the performance of the proposed AF scheme through numerical evaluation and simulations. Fig. 3.9 shows the outage

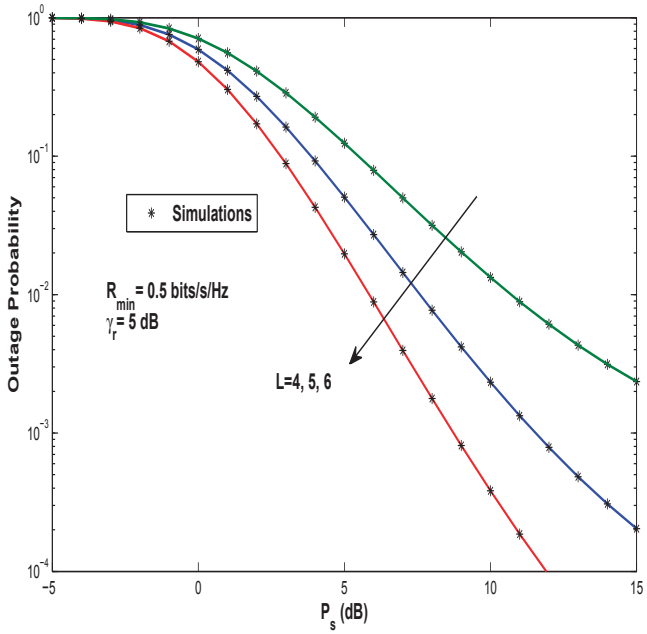

Figure 3.9: Outage Probability of AF-ZFB vs. P_s for different number of relays L=4, 5, 6 at R_{min}=0.5 bits/s/Hz in the first case (non-cognitive).

performance of AF-ZFB for the first case versus the maximum transmit power of the SS for $L = 4, 5, 6$ and $R_{min} = 0.5$ bits/s/Hz at $\gamma_r = 5$ dB. The behavior of the system in this case is the same as the non-cognitive system as it is now free from the interference constraint, and hence, its performance is better than the cognitive ones.

Fig. 3.10 shows the outage performance of AF-ZFB for the second case versus Q for $L = 4, 6, 8$ and $R_{min} = 0.5, 1$ bits/s/Hz. It can be seen that as the values of Q become less restrict, the outage performance improves substantially. Moreover, by increasing the number of potential relays with ZFB, we observe significant improvements in the outage performance. It is translated to the effect of the combined cooperative diversity and beamforming on enhancing the total received SNR and the mutual information. We also simulate the outage performance considering the PU's CCI in both ZFB and non-zero interference constraint cases. The figure shows that an error floor occurs in the CCI case due to the presence of interference. In the case of AWGN, however, there is no such saturation since there is also no limitation on the maximum transmit power of SS.

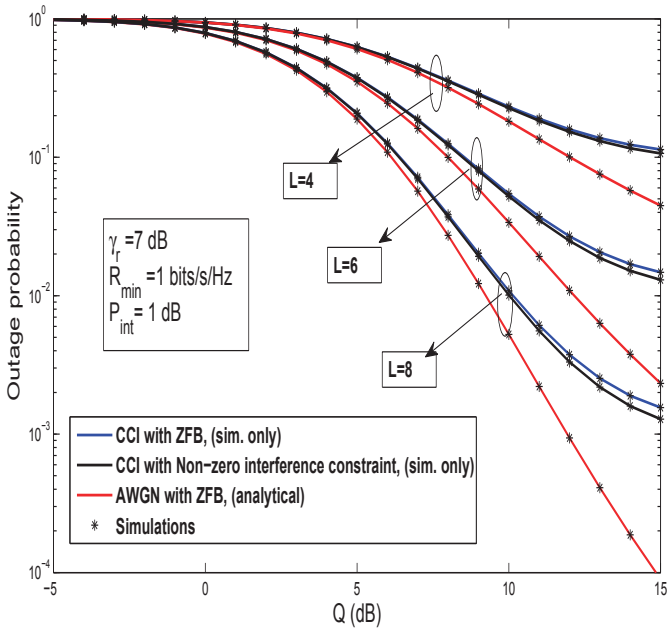

Figure 3.10: Outage probability of AF-ZFB vs. Q for L=4, 6, 8 and R_{min}=1 bits/s/Hz in the second case (cognitive).

Fig. 3.11 illustrates the average BER performance for the second case versus the interference threshold Q for L= 6, 8, 10 and $\gamma_r = 3, 7$ dB at $R_{min} = 1$ bits/s/Hz. It is obvious that the BER improves substantially as the number of potential relays increases and Q becomes looser. The same interpretation as in Fig. 11 still holds.

3.7 Multi-PUs with CCI

3.7.1 System Model

We consider a dual-hop relaying system that is composed of a pair of secondary source SS and destination SD and a set of L DF secondary relays denoted by R_i for $i = 1, ..., L$ coexisting in the same spectrum band with a primary system which consists of a cluster of M primary transmitters (PU-TXs)- N primary receivers (PU-RXs) pairs as shown in Fig. 3.12. All nodes are equipped with one antenna. Due to the severe impairments such as multipath effects, there is no direct link between the source and destination and thus the source can only send

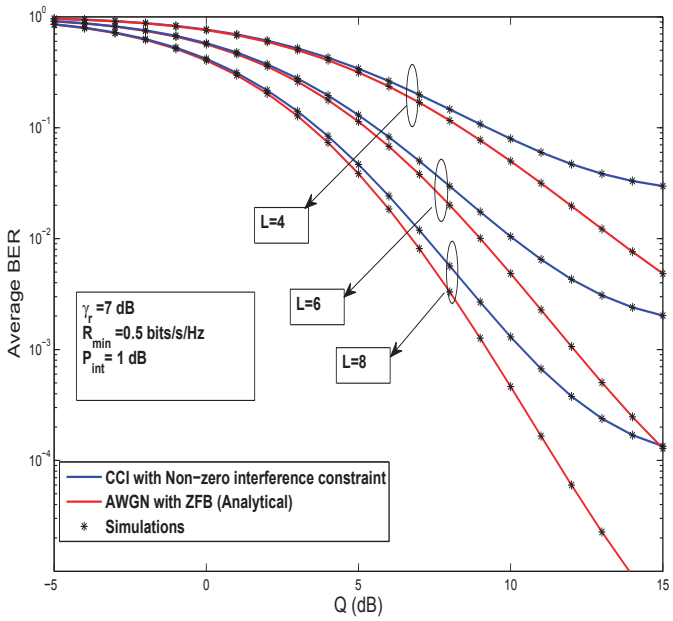

Figure 3.11: Average BER of AF-ZFB vs. Q(dB) for L=4, 6, 8 at $R_{min} = 0.5$ bits/s/Hz and $\gamma_r = 7$ dB.

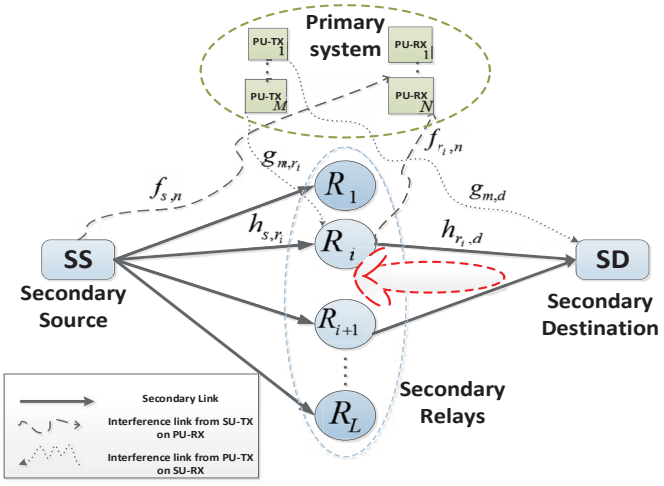

Figure 3.12: Spectrum-Sharing System with multiple-PUs.

messages via secondary relay nodes over two time-slot.

In the first time-slot, based on the CSI from S to the nth PU-RX, which suffers the most interference caused by SS (the strongest interference channel), SS adjusts its transmit power under predefined threshold Q and broadcasts its message to all relays. In the second time-slot, ZFB is applied to null the interference from the selected potential relays L_s (which decided to participate) to the PU-RXs so that the relays are always able to transmit without interfering with the PU-RXs. The ZFB processing vector, namely $\mathbf{w_{zf}}$, is optimized so as to maximize the received SNR at the secondary destination, while nulling the inflicted interference to the existing PU-RXs.

All channel coefficients are assumed to be independent Rayleigh flat fading such that $|h_{s,r_i}|^2, |f_{s,n}|^2, |f_{r_i,n}|^2, |g_{m,d}|^2$ and $|g_{m,r_i}|^2$ are exponential distributed random variables with parameters $\lambda_{sr_i}, \lambda_{sn}, \lambda_{r_in}, \lambda_{md}$ and λ_{mr_i} respectively. All the noises are assumed to be additive white complex Gaussian with zero-mean and variance σ^2. Let the ZFB vector $\mathbf{w}_{\mathbf{zf}}^T = [w_1, w_2, ..., w_{L_s}]$ used to direct the signal to SD. Let $\mathbf{h}_{r,d}^T = [h_{r_1,d}, ..., h_{r_{L_s},d}]$ be the channel vector between the potential relays and SD. Let $\mathbf{F}_{\mathbf{rp}}^T = [\mathbf{f_{r,p_1}}, ..., \mathbf{f_{r,p_N}}]$ be the channel matrix between the potential relays and all N PU-RXs where $\mathbf{f_{r,p_n}} = [f_{r_1,n}, ..., f_{r_{L_s},n}]$.

3.7.2 Transmission Protocol

In this dual-hop system, the communication process occurs over two time-slots. In the first time-slot, SS broadcasts its signal to all L relays, then the received signal at the ith relay is given as

$$y_{r_i} = \sqrt{P} h_{s,r_i} x_s + \sum_{m=1}^{M} \sqrt{P_{int}}\, g_{m,r_i} \hat{x}_{im} + n_{i1}, \tag{3.68}$$

where P is the source's transmit power, P_{int} is interference power from PU-TXs, x_s is the information symbol of SS, $\hat{x}_{im}$ is the mth PU-TX interfering symbol at the ith relay and n_{i1} denotes the noise at the ith relay in the first time-slot. We assume that the transmitted symbols are equiprobable with unit energy.

In the second time-slot, the decoding set $\mathcal{C}$, which consists of the relays that can correctly decode x_s by using cyclic redundancy codes, transmits the decoded signals to the destination simultaneously by using beamforming. In particular, each relay weights the decoded signal

and forwards it to the destination. Thus the received signal at SD is given by

$$y_d = \sqrt{P_r}\mathbf{h}_{r,d}^H \hat{\mathbf{x}}_s + \sum_{m=1}^{M} \sqrt{P_{int}}\, g_{m,d}\hat{x}_{md} + n_2, \tag{3.69}$$

where $\hat{\mathbf{x}}_s = \mathbf{w_{zf}} x_s$ is the weighted vector, $\hat{x}_{md}$ is the mth PU-TX interfering symbol at D and n_2 is the noise at SD in the second time-slot. Therefore, the corresponding total received SINR at SD given $\mathcal{C}$, denoted $\gamma_{d|\mathcal{C}}$, is given as

$$\gamma_{d|\mathcal{C}} = \frac{P_r|\mathbf{h}_{r,d}^H \mathbf{w_{zf}}|^2}{\sum_{m=1}^{M} P_{int}\,|g_{m,d}|^2 + \sigma^2}. \tag{3.70}$$

3.7.3 Mathematical Model and Size of $\mathcal{C}$

In the underlay approach of this model, source's power P is constrained as $P = \min\left\{\frac{Q}{|f_{s,n}|^2}, P_s\right\}$ where P_s is the maximum transmission power of S. So the received SINR, γ_{s,r_i} at the ith relay is given as

$$\gamma_{s,r_i} = \frac{\min\left\{\frac{Q}{|f_{s,n}|^2}, P_s\right\}|h_{s,r_i}|^2}{\sum_{m=1}^{M} P_{int}|g_{m,r_i}|^2 + \sigma^2}. \tag{3.71}$$

Next, we derive the CDF of $\gamma_{s,r_i} = \frac{U}{P_{int}V+\sigma^2}$, where $U = \min\left\{\frac{Q}{|f_{s,n}|^2}, P_s\right\}|h_{s,r_i}|^2$ and $V = \sum_{m=1}^{M}|g_{m,r_i}|^2$. By using the definition of CDF of γ_{s,r_i}, we find

$$F_{\gamma_{s,r_i}}(x) = \int_0^\infty \Pr(U < (P_{int}\,y + \sigma^2)x) f_V(y) dy. \tag{3.72}$$

Since V is the sum of M exponential random variables with parameter λ_{m,r_i}, it presents a chi-square random variable with $2M$ degrees of freedom and its PDF is given by

$$f_V(y) = \frac{\lambda_{m,r_i}^M y^{M-1} e^{-\lambda_{m,r_i} y}}{\Gamma(M)}. \tag{3.73}$$

The CDF of U is obtained with the help of (3.3) as,

$$F_U(x) = 1 + e^{-\frac{\lambda_{sr_i} x}{P_s}}\left(\frac{e^{-\frac{\lambda_{sn} Q}{P_s}}}{\frac{\lambda_{sn} Q}{\lambda_{sr_i} x} + 1} - 1\right). \tag{3.74}$$

Substituting (3.73) and (3.74) into (3.72), and after several algebraic manipulations, (3.72) is equivalently expressed as

$$\begin{aligned} F_{\gamma_{s,r_i}}(x) &= 1 + \psi e^{-\frac{\lambda_{sr_i}\sigma^2 x}{P_s}} \int_0^\infty y^{M-1} e^{-(\frac{\lambda_{sr_i}\sigma^2 x}{P_s} + \lambda_{mr_i})y} \\ &\times \left[(e^{-\frac{\lambda_{sn} Q}{P_s}} - 1) - \frac{\frac{\lambda_{sn} Q}{\lambda_{sr_i}} e^{-\frac{\lambda_{sn} Q}{P_s}}}{x P_{int}\, y + \sigma^2 x + \frac{\lambda_{sn} Q}{\lambda_{sr_i}}}\right] dy. \end{aligned} \tag{3.75}$$

where $\psi = \frac{\lambda_{mr_i}^M}{\Gamma(M)}$. After easy simplifications, and with the help of [56, Eqs. (3.351.3), (3.353.5)], the CDF of γ_{s,r_i} is derived as

$$F_{\gamma_{s,r_i}}(x) = 1 + \psi e^{-\frac{\lambda_{sr_i}\sigma^2 x}{P_s}} \left[\frac{(e^{-\frac{\lambda_{sn}Q}{P_s}} - 1)\kappa!}{\frac{\lambda_{sr_i}P_{int}x}{P_s} + \lambda_{mr_i}} - (\frac{\lambda_{sn}Qe^{-\frac{\lambda_{sn}Q}{P_s}}}{\lambda_{sr_i}}) \left((-1)^{\kappa-1}\beta^{\kappa}e^{\beta\mu}Ei[-\beta\mu] + \sum_{k=1}^{\kappa}\Gamma(k)(-\beta)^{\kappa-k}\mu^{-k} \right) \right], \tag{3.76}$$

where $\kappa = M-1$, $\beta = \frac{\sigma^2}{P_{int}} + \frac{\lambda_{sn}Q}{\lambda_{sr_i}P_{int}x}$, $\mu = \lambda_{mr_i} + \frac{\lambda_{sr_i}P_{int}x}{P_s}$ and $Ei[\,.\,]$ is the exponential integral defined in [56].

As in (3.6), the probability $\Pr[|\mathcal{C}| = L_s]$ in this case becomes

$$\Pr[|\mathcal{C}| = L_s] = \binom{L}{L_s} P_{\text{off}}^{L-L_s}(1 - P_{\text{off}})^{L_s}, \tag{3.77}$$

where P_{off} denotes the probability that the relay does not decode correctly the received signal and keeps silent in the second time-slot. Then P_{off} is computed as

$$P_{\text{off}} = F_{\gamma_{s,r_i}}(\gamma_{th}), \tag{3.78}$$

where $F_{\gamma_{s,r_i}}(\gamma_{th})$ is substituted from (3.76) and $\gamma_{th} = 2^{2R_{min}} - 1$ is the SINR threshold.

3.7.4 Sub-Optimal ZFB Weights Design

To be able to apply ZFB, the general assumption $L_s > N$ is considered. According to the ZFB principles, the transmit weight vector $\mathbf{w_{zf}}$, is chosen to lie in the orthogonal space of $\mathbf{F_{rp}^H}$ such that $|\mathbf{f_{r,p_i}^H w_{zf}}| = 0\ \forall i = 1, ..., N$ and $|\mathbf{h_{r,d}^H w_{zf}}|$ is maximized. So the problem formulation for finding the optimal weight vector is introduced as.

$$\begin{aligned} \max_{\mathbf{w_{zf}}} \quad & |\mathbf{h_{r,d}^H w_{zf}}|^2 \\ \text{s.t.:} \quad & |\mathbf{f_{r,p_n}^H w_{zf}}| = 0, \quad \forall n = 1, ..., N \\ & \|\mathbf{w_{zf}}\| = 1. \end{aligned} \tag{3.79}$$

By applying a standard Lagrangian multiplier method, the weight vector that satisfies the above optimization method is given as

$$\mathbf{w_{zf}} = \frac{\mathbf{\Xi}^{\perp}\mathbf{h}_{r,d}}{\|\mathbf{\Xi}^{\perp}\mathbf{h}_{r,d}\|}, \tag{3.80}$$

where $\mathbf{\Xi}^{\perp} = \left(\mathbf{I} - \mathbf{F_{rp}}(\mathbf{F_{rp}^H F_{rp}})^{-1}\mathbf{F_{rp}^H} \right)$ is the projection idempotent matrix with rank $(L_s - N)$.

3.7.5 End-to-End SINR statistics

Now, after finding $\mathbf{w_{zf}}$, we substitute (3.80) into (3.70) to get

$$\gamma_{d|\mathcal{C}} = \frac{P_r||\mathbf{\Xi}^{\perp}\mathbf{h_{r,d}}||^{\mathbf{2}}}{\sum_{m=1}^{M} P_{int}|g_{m,d}|^2 + \sigma^2}, \tag{3.81}$$

To analyze the system performance, we firstly need to obtain the CDF of $\gamma_{d|\mathcal{C}}$. Let $U_1 = P_r||\mathbf{\Xi}^{\perp}\mathbf{h_{r,d}}||^{\mathbf{2}}$ and $V_1 = \sum_{m=1}^{M}|g_{m,d}|^2$, by following the same previous approach, we need the CDF of $U_1$and the PDF of V_1 which can obtained from (3.13) and (3.73), respectively. We find the conditional CDF of $\gamma_{d|\mathcal{C}}$

$$F_{\gamma_{d|\mathcal{C}}}(x) = \int_0^{\infty} \frac{\psi_1 \gamma\left(\tau, \frac{(P_{int}\, y+\sigma^2)x}{P_r}\right) y^{\kappa} e^{-\lambda_{md} y}}{\Gamma(L_s - N - 1)} dy, \tag{3.82}$$

where $\psi_1 = \frac{\lambda_{md}^M}{\Gamma(M)}$ and $\tau = L_s - N$. By representing the incomplete Gamma function into another form utilizing the identities [56, Eqs. (8.352.1), (1.11)], and after several mathematical manipulations, the integral in (3.82) is expressed as

$$\begin{aligned} F_{\gamma_{d|\mathcal{C}}}(x) &= 1 - \psi_1 e^{-\frac{\sigma^2 x}{P_r}} \sum_{i=0}^{L_s-N-1} \sum_{j=0}^{i} \binom{j}{i} P_{int}^{j} (\sigma^2)^{i-j} x^i \\ &\times \int_0^{\infty} y^{M-1+j} e^{-(\lambda_{md} + \frac{P_{int}x}{P_r})y} dy. \end{aligned} \tag{3.83}$$

With the help of [56, (3.3351.3)], the CDF of $\gamma_{d|\mathcal{C}}$ is given as

$$F_{\gamma_{d|\mathcal{C}}}(x) = 1 - \psi_1 \sum_{i=0}^{L_s-N-1} \sum_{j=0}^{i} \binom{j}{i} P_{int}^{j} (\sigma^2)^{i-j} e^{-\frac{\sigma^2 x}{P_r}} \frac{(M-1+j)! x^i}{(\lambda_{md} + \frac{P_{int}x}{P_r})^{M+j}}. \tag{3.84}$$

To compute the unconditional CDF denoted as $F_{\gamma_d}(\gamma)$, we use the total probability theorem to get

$$\begin{aligned} F_{\gamma_d}(x) &= \sum_{L_s=0}^{N} \binom{L}{L_s} P_{\text{off}}^{L-L_s} (1 - P_{\text{off}})^{L_s} \\ &+ \sum_{L_s=N+1}^{L} \binom{L}{L_s} P_{\text{off}}^{L-L_s} (1 - P_{\text{off}})^{L_s} F_{\gamma_{d|\mathcal{C}}}(x), \end{aligned} \tag{3.85}$$

where $F_{\gamma_{d|\mathcal{C}}}(x)$ is substituted from (3.84). In the subsequent section, we make use of $F_{\gamma_d}(x)$ to derive closed-form expressions for the outage and E2E BER performance.

3.7.6 Outage Probability

By using (3.85), the outage probability of the secondary system in a closed-form can be written as

$$P_{out} = F_{\gamma_d}(\gamma_{th}). \tag{3.86}$$

3.7.7 E2E BER

This probability could be evaluated using the following identity

$$P_e = \frac{a\sqrt{b}}{2\sqrt{\pi}} \left(A \underbrace{\int_0^\infty \frac{e^{-bx}}{\sqrt{x}} dx}_{I_1} + B \underbrace{\int_0^\infty \frac{e^{-bx}}{\sqrt{x}} F_{\gamma_{d|\mathcal{C}}}(x) dx}_{I_2} \right) \tag{3.87}$$

where $A = \sum_{L_s=0}^{N} \binom{L}{L_s} P_{\text{off}}^{L-L_s} (1-P_{\text{off}})^{L_s}$ and $B = \sum_{L_s=N+1}^{L} \binom{L}{L_s} P_{\text{off}}^{L-L_s} (1-P_{\text{off}})^{L_s}$. We consider BPSK for which $(a, b) = (1, 1)$. I_1 is evaluated with the help of [56, (3.361.2)]. Next, to compute I_2, we represent the integrands of I_2 in terms of Meijer's G-functions using [65, Eqs. 10, 11], which are given, respectively, as

$$\left(\lambda_{md} + \frac{P_{int} x}{P_r}\right)^{-\nu} = \eta x^{-\nu} G_{1,1}^{1,1}\left(\frac{P_{int}\, x}{\lambda_{md} P_r}\Big|_{\nu}^{1}\right), \tag{3.88}$$

where $\eta = \frac{(\frac{P_{int}}{P_r})^{-(M+j)}}{\Gamma(M+j)}$ and $\nu = (M+j)$.

$$e^{-(b+\frac{\sigma^2}{P_r})x} = G_{0,1}^{1,0}\left(\left(b + \frac{\sigma^2}{P_r}\right) x\Big|_{0}^{-}\right). \tag{3.89}$$

Thus, I_2 yields as

$$\begin{aligned} I_2 &= 0.5 - \eta\, \Phi \int_0^\infty x^{-M-j+i-\frac{1}{2}} G_{1,1}^{1,1}\left(\frac{P_{int}\, x}{\lambda_{md} P_r}\Big|_{M+j}^{1}\right) \\ &\times G_{0,1}^{1,0}\left(\left(b + \frac{\sigma^2}{P_r}\right) x\Big|_{0}^{-}\right) dx, \end{aligned} \tag{3.90}$$

where $\Phi = \frac{\lambda_{md}^M}{\Gamma(M)} \sum_{i=0}^{L_s-N-1} \sum_{j=0}^{i} \binom{j}{i} P_{int}^j (\sigma^2)^{i-j} (M-1+j)!$. Exploiting that the integral of the product of a power term and two Meijer's G-function [65, Eq. 21], I_2 results in

$$\begin{aligned} I_2 &= 0.5 - \frac{\eta\, \Phi}{\Gamma(M+j)} \left(\frac{P_{int}}{P_r}\right)^{-(M+j)} \left(\frac{\sigma^2}{P_r} + b\right)^{-\alpha} \\ &\times G_{2,1}^{1,2}\left(\frac{P_{int}}{bP_r + \lambda_{md}\sigma^2}\Big|_{M+j}^{1,1-\alpha}\right), \end{aligned} \tag{3.91}$$

where $\alpha = i - M - j + 0.5$. By incorporating the results of I_1 and I_2 into (3.87), a closed-form expression for the unconditional E2E BER at D is given as

$$\begin{aligned} P_e &= 0.5A + B\left(0.5 - \frac{\eta\,\Phi}{\Gamma(M+j)}\left(\frac{P_{int}}{P_r}\right)^{-(M+j)}\right. \\ &\times \left.\left(\frac{\sigma^2}{P_r}+1\right)^{-\alpha} G_{2,1}^{1,2}\left(\frac{P_{int}}{P_r+\lambda_{md}\sigma^2}\Big|_{M+j}^{1,1-\alpha}\right)\right). \end{aligned} \tag{3.92}$$

Diversity Gain: To gain some insight about the achieved diversity order and understand the impact of the interference threshold on the BER performance, we derive the asymptotic expression when a fixed power constraint is imposed. We consider the scenario where $Q \to \infty$ and $P_s \ll Q$. According to [66, Eqs. (5.1.7) and (5.1.20)], we have $\lim_{x\to\infty} e^x Ei(-x) = 0$. It is also known that $\lim_{x\to\infty} xe^{-x} = 0$. Using these formulas, for $Q \to \infty$, the CDF in (3.84) is approximated as

$$\tilde{F}_{\gamma_{s,r_i}}(x) \approx 1 - \psi\frac{\kappa! e^{-\frac{\lambda_{sr_i}\sigma^2 x}{P_s}}}{\frac{\lambda_{sr_i}P_{int}\,x}{P_s} + \lambda_{mr_i}}. \tag{3.93}$$

Substituting (3.93) into (3.78), we get

$$\tilde{P}_{\text{off}} \approx \tilde{F}_{\gamma_{s,r_i}}(\gamma_{th}). \tag{3.94}$$

and then incorporating (3.94) into (3.92), we get an approximate expression for the asymptotic BER performance.

$$\tilde{P}_e \approx 0.5\tilde{A} + \tilde{B}I_2 \tag{3.95}$$

where $\tilde{A} = \sum_{L_s=0}^{N}\binom{L}{L_s}\tilde{P}_{\text{off}}^{L-L_s}(1-\tilde{P}_{\text{off}})^{L_s}$, $\tilde{B} = \sum_{L_s=N+1}^{L}\binom{L}{L_s}\tilde{P}_{\text{off}}^{L-L_s}(1-\tilde{P}_{\text{off}})^{L_s}$ and I_2 is the result of (3.91). It is interesting to observe from (3.95) that the approximate BER expression is independent of the interference threshold Q and results in a non-zero constant value. This means that $\tilde{P}_e$ saturates when the SD transmit power exceeds the PU-RX threshold, leading to a diversity order of zero.

Mathematically, the asymptotic diversity order d with respect to Q is given by

$$\begin{aligned} d &= \lim_{Q\to\infty} -\frac{\log\ (\tilde{P}_e)}{\log\ (Q)} \\ &= \lim_{Q\to\infty} -\frac{\log(K)}{\log\ (Q)} = 0 \end{aligned} \tag{3.96}$$

where K is a non-zero constant. Noting that $P_s, P_{int}, P_r, L, M, \gamma_{th}, \lambda_{md}, \lambda_{sr_i}$ are all constants and using (3.95), we reach to (3.96). Hence, the diversity order is zero in this case.

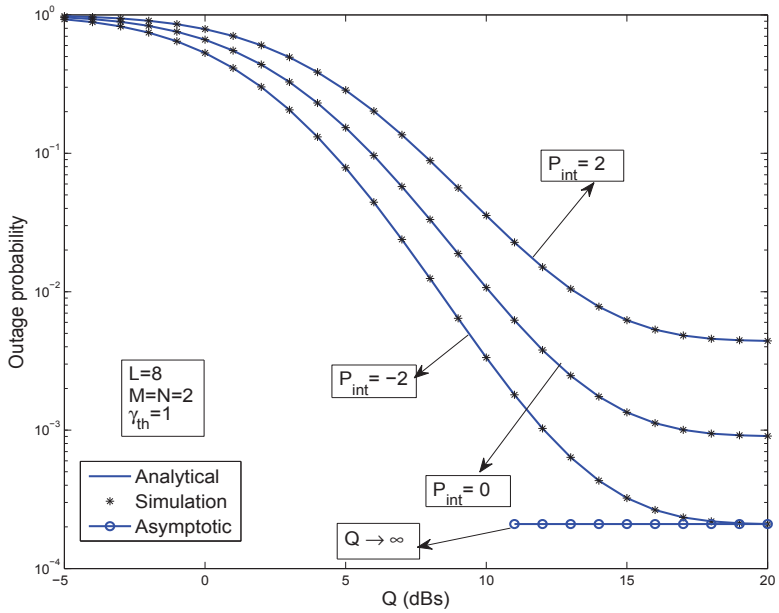

Figure 3.13: Outage probability vs. Q (dB) for L=8 and $M = N = 2$.

3.7.8 Simulation Results and Discussion

In this section, we present numerical results to validate our derived expressions in Section IV. Without loss of generality, we assume that the relays are located on a straight line vertical to the distance between the source and destination. The distance between them equals one. We further assume that the primary system forms a cluster where PU-TXs are closely located to each others and as all PU-RXs. Unless otherwise stated, we also assume that $\lambda_{sn} = \lambda_{r_i n} = 1$, $\lambda_{sr_i} = \lambda_{r_i d} = 1, \forall i$ and $\lambda_{mr_i} = \lambda_{md} = 1, \forall i$. we fix the value of $\gamma_{th} = 1$ dB, $P_s = 20$ dB.

Fig. 3.13 shows the outage performance versus Q for $L = 8$, $M = N = 2$ under different values of $P_{int} = -2, 0, 2$dB. As observed from the figure, as the value of Q increases, the outage performance improves substantially. Also, the figure shows the impact of co-channel interference on the outage performance. As P_{int} increases, it degrades the system performance significantly. However, a compensation of this loss in performance is gained by the use of beamforming process. A floor in the outage performance curve is noticed which is due to the interference level constraint.

Fig. 3.14 illustrates the outage probability for different locations of the PU-TX and dif-

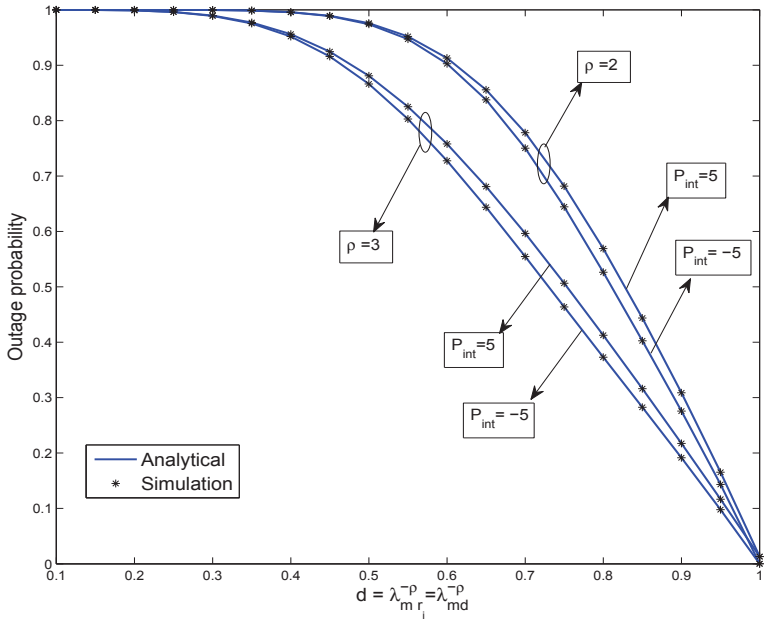

Figure 3.14: Outage probability vs. d for L=10 and $M = N = 1$.

ferent P_{int} values with $M = N = 1$, and $Q = 20$. It is assumed that $\lambda_{mr_i} = \lambda_{md} = d^{-\rho}$, where ρ is the path loss exponent and d is the distance between PU-TX and secondary receiver. It is observed that the outage performance is better for the lower PU-TX transmit power P_{int} and higher path loss exponent ρ. That happens because when PU-TX locates closer to the secondary receivers, the outage performance of the secondary system becomes worse.

Fig. 3.15 illustrates the BER performance versus Q for L= 8 and $M = N = 2$. Similar observation is obtained as in Fig. 3.13. It is seen that as Q increases, the BER performance improves. While the performance deteriorates when P_{int} increases. In addition, it is observed from the figure that BER curve saturates in high Q region and an error floor occurs which results in zero-diversity. This error flooring is due to the limitations on the secondary transmit powers and co-channel interferences.

Fig. 3.16 shows the BER performance versus the number of available relays L under different number of PU-TXs-RXs with $P_{int} = 0, Q = 2$ dB. It is obvious that the BER performance improves substantially as the number of relays increases. This is attributed to the combined cooperative diversity and beamforming which enhances the total received SINR at the secondary destination. Clearly, as the number of existing PU-TXs increases from one

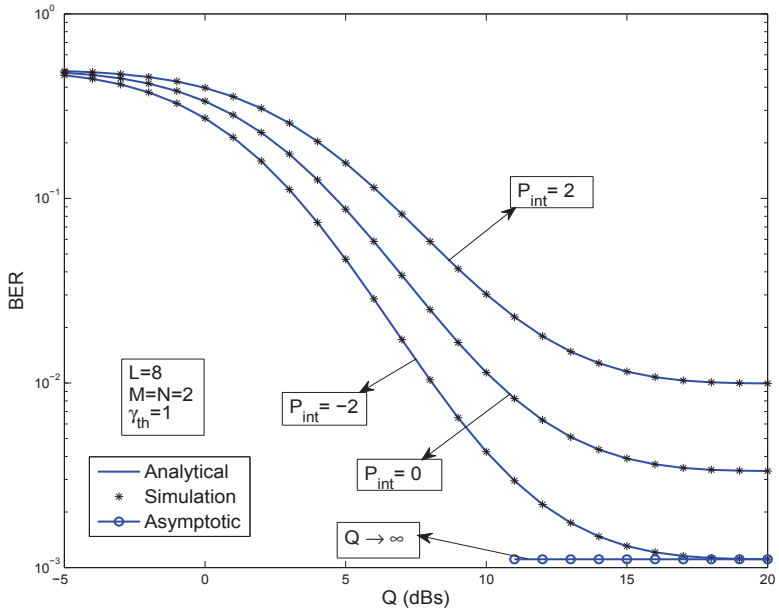

Figure 3.15: BER vs. Q (dB) for L= 8 and $M = N = 2$.

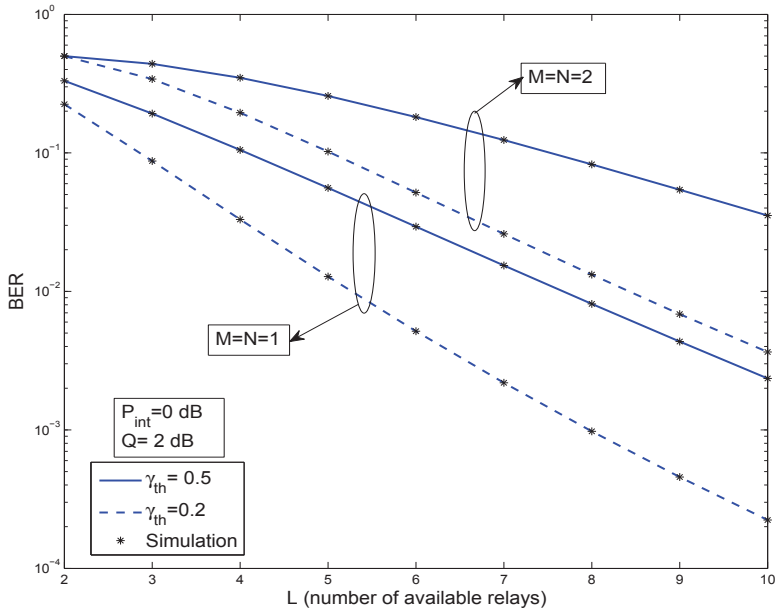

Figure 3.16: BER vs. L for $M = N = 1, 2$.

to two, the BER performance becomes worse as this will increase the sum of the CCIs that severely affects the received signals at secondary receivers. In addition, the figure shows that

the BER performance is better when the SINR threshold γ_{th} is less strict.

3.8 Conclusion

We considered cooperative relaying and distributed beamforming for spectrum sharing systems with the objective of improving the performance of the secondary system while respecting the interference constraint imposed by the PU. We considered both DF and AF relaying. The optimal beamforming weights were derived to maximize the received SNR at the secondary destination while the interference to the PU is kept to a predefined threshold. Given the high complexity of using optimal beamforming in the analysis, we adopted ZFB instead. In addition, we extended the ZFB approach to a multiple PUs system. With this, we analyzed the performance of the secondary system by deriving the outage probability and BER. We verified our analytical results through simulations which showed the benefits of our proposed system in improving the secondary system performance by compensating the performance loss due to the PUs' CCI. The results showed that distributed ZFB improves the outage probability and BER performance by increasing number of participating relays compared to non-beamforming selection relaying schemes. The results also demonstrated the deteriorating impact of the PU's strict interference threshold and CCI. The results also showed that our proposed SDF-ZFB system outperforms the opportunistic SDF system performance for strict values of the interference constraint.

Chapter 4

Two-Way AF Relaying Spectrum-Sharing Systems with Collaborative Beamforming

4.1 Introduction

While Chapter 3 investigates the one-way relaying in spectrum-sharing systems, this chapter is concerned with the two-way relaying to further improve the spectrum efficiency. Two-way relaying achieves higher bandwidth efficiency than one-way relaying. Both techniques have been extensively studied in the traditional non-cognitive radio sense. The authors in [67]- [69] and references therein considered threshold-based relaying strategies for two-way DF (digital network coding) cooperative communication networks in an effort to mitigate the impact of error propagation, resulting in preserving the diversity order of the system. In [70]- [72], two-way AF (analog network coding) cooperative relaying networks were investigated where the performance of two, three and four time-slot transmission protocols were compared and analyzed.

A common conclusion shared by all mentioned published papers is that the two time-slot (2-TS) transmission protocol offers an improved spectral efficiency as compared to the three time-slot (3-TS) transmission strategy. However, such conclusion ignores the fact that, for the 2-TS protocol, the number of degrees of freedom decreases, and at the same time, the level of interference at the relays increases. This motivates us to study the tradeoff between the two schemes in terms of bandwidth efficiency, relay power consumption, and interference cancellation (or equivalently, QoS at the transmitters) in spectrum-sharing systems.

While cooperative one-way relaying systems in CRNs have been heavily studied, two-

way relaying in spectrum-sharing environments received little attention [73], [74]. Recently, in [73], outage probability expressions for both primary and secondary systems were derived in a cooperative two-way DF relaying system where a SU helps two primary transceivers to communicate with each other. In [74], the outage performance of a two-way AF relaying system in a spectrum sharing environment was investigated. However, in [73] and [74], an overlay spectrum-sharing scenario is assumed.

Applying beamforming in cooperative CRNs has recently received considerable interest [45]- [47]. The authors in [47] obtained the optimal beamforming coefficients in a cognitive two-way relaying system using iterative semidefinite programming (SDP) and bisection search methods with the objective of minimizing the interference at the PU with SUs SINR constraints. The problem of sum-rate maximization under constraints on interference on a primary receiver for multi-antenna cognitive two-way relay network was investigated in [75]. In that paper, the authors provided a structure of the optimal relay beamformer and proposed projection-based suboptimal beamforming schemes such as zero-forcing reception-orthogonally projected zero-forcing transmission. This scheme suffers from high computational complexity and implementation difficulties. We remark that all previous works considered only one primary user that coexists with the secondary users. Recently, in [76], the authors proposed a transceiver design for an overlay cognitive two-way relay network where a secondary multi-antenna relay helps two PUs to communicate between themselves. Optimal precoders using SDP methods were found with the aim of maximizing the achievable transmission rate of the SU while maintaining the rate requirements of the PUs for different relay strategies.

Motivated by the great potential of combining two-way relaying and beamforming, we use in this chapter collaborative distributed ZFB in two-way AF relaying in a spectrum sharing environment [77]- [78]. In particular, we consider a spectrum-sharing system comprising two secondary sources communicating with each other in two or three consecutive time slots, a number of secondary AF relays and a number of PUs. The available relays that receive the signals (from the sources) are used for relaying in the second time-slot or in the third time-slot according to the adopted transmission protocol. Specifically, the selected relays employ distributed ZFB to null the inflicted interference on the PUs in the relaying phase in

addition to improve the performance of the secondary system. We also limit the interference from the secondary sources by imposing peak constraints on the their transmit powers in the broadcasting phase. Based on the aforementioned facts, comparing the 2-TS and 3-TS-based distributed beamforming techniques in spectrum-sharing systems is important because the 3-TS protocol offers certain advantages, which can result in improved performance of two-way network beamforming as compared to the 2-TS protocol. These advantages include the additional degrees of freedom in suppressing the interference. While such a comparison may include the four time-slot protocol, in this paper, we restrict our investigation to the 2-TS and 3-TS protocols as these two competing protocols are more feasible among the two-way network beamforming techniques. To study and compare the performance tradeoffs between the two transmission protocols, we derive the CDF and the MGF of the end-to-end equivalent SNR in both protocols. Exploiting these statistics, the outage probability and the average error probability are derived. It is shown that the ZFB approach has the potential of improving the secondary performance and limiting the interference in a simple practical manner compared to other complex approaches.

In this Chapter, we derive closed-form expressions for the outage and average error probabilities for the two transmission protocols (2-TS and 3-TS) and confirm the results numerically as well as by simulations for different values of interference temperatures Q, different number of relays and different number of PUs. We also derive the diversity order of the proposed system by analyzing the asymptotic behavior of the secondary system performance at high SNRs (high values of Q). We show that the diversity order is $(L_s - M)$ which indicates that the diversity order increases linearly with increasing the number of secondary relays L_s and decreases with increasing the number of primary receivers M. The beamforming weights at the secondary relays are optimized to maximize the received SNR at the secondary receivers subject to nulling the interference inflicted on the existing primary users. From the closed-form solutions of the beamforming weight vectors, we propose a distributed scheme that requires little cooperation between the two transceivers and the relays, which leads to a reduced overhead. Compared to [47] where optimal beamforming weights are obtained via iterative and semidefinite relaxation methods, our proposed scheme exploits ZFB as a sub-optimal approach to obtain the beamforming weights using a standard linear optimization

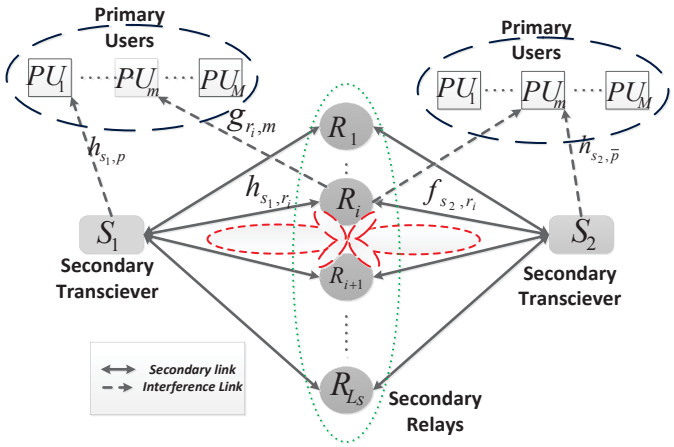

Figure 4.1: Spectrum-sharing system with two-way AF relaying.

method. Moreover, we consider a more general assumption by considering multiple existing PUs where [47] considers only one PU.

Comparison between the performance of the 2-TS and 3-TS based ZFB techniques is evaluated and discussed. It is demonstrated that the 3-TS protocol outperforms the 2-TS protocol in terms of performance in certain practical scenarios. We show that this occurs when the two transceivers transmit at different powers as the 3-TS will allocate more power to the received signal transmitted from the transceiver with higher power. The advantage of the 2-TS protocol, however, is that it achieves higher bandwidth efficiency. Moreover, comparison between the sum-rate performances of the optimal beamforming scheme and the adopted sub-optimal ZFB scheme is simulated and discussed in the numerical results. It is demonstrated that the adopted sub-optimal scheme presents a good performance with less complexity and therefore offers a good compromise between complexity and performance.

The rest of this chapter is organized as follows. Section 4.2 describes the system model. The transmission protocols are presented in Section 4.3. ZFB weight design is described in Section 4.4. Section 4.5 introduces the end-to-end SNR analysis. The outage probability analysis of the 2-TS and 3-TS protocols is analyzed in Section 4.6 while the average error probability analysis is analyzed in Section 4.7. Numerical results and discussions are given in Section 4.8. Section 4.9 concludes the chapter.

4.2 System and Channel Models

We consider a two-way relaying system that is composed of two secondary transceivers S_j, $j = 1, 2$ and a set of L_s AF secondary relays denoted by R_i for $i = 1, ..., L_s$ coexisting in the same spectrum band with M PUs as shown in Fig. 4.1. All nodes are equipped with one antenna. The two sources wish to communicate with each other in a half-duplex way. There is no direct link between the sources and thus they can only exchange messages via relay nodes. The SUs are allowed to share the same frequency spectrum with the PUs as long as the interference to the PUs is limited to a predefined threshold. Both systems transmit simultaneously in an underlay manner.

We consider in this work two transmission protocols, the first protocol is the 2-TS scheme, and the second protocol is the 3-TS scheme [70]. In 2-TS, in the first time-slot (TS_1), based on the interference CSI from S_1 to the pth PU, which suffers the most interference caused by S_1, S_1 adjusts its transmit power under predefined threshold Q_1 [1] and broadcasts its message to all relays. Simultaneously, in TS_1, based on the interference CSI from S_2 to the $\bar{p}$th PU, which suffers the most interference caused by S_2 (the pth and $\bar{p}$th PUs could be different or the same), S_2 adjusts its transmit power under predefined threshold Q_2 and broadcasts its message to all relays. In the second time-slot (TS_2), ZFB is applied to null the interference from the reliable relays L_s (that are allowed to participate) to the PUs so that the relays are always able to transmit without interfering with the PUs.

Similarly, in TS_1 of the 3-TS protocol, S_1 adjusts its transmit power under a predefined threshold Q_1 and broadcasts its message to all relays. In TS_2, S_2 also transmits its message to all relays under a tolerable threshold Q_2. In the third time-slot (TS_3), ZFB is applied to null the interference from the reliable relays L_s to the PUs. Two ZFB weight vectors, namely $\mathbf{w_{zf_1}}$ and $\mathbf{w_{zf_2}}$, are optimized so as to maximize the received SNRs at S_1 and S_2, respectively, while nulling the inflicted interference to the existing PUs.

All channel coefficients are assumed to be independent Rayleigh flat fading and quasi-static, so that the channel gains remain unchanged during the transmission period. Let h_{s_1,r_i},

[1] When the PUs are affected from the interference of both transceivers simultaneously, Q_1 and Q_2 could be optimized to maximize the SU performance such that QoS at the PUs is ensured.

f_{s_2,r_i} denote the channel coefficients from the sources S_1 and S_2 to the ith relay, respectively, which are modeled as zero mean, CSCG random variables with variance λ_{s_1,r_i},λ_{s_2,r_i}. Denote $h_{s_1,p}$ and $h_{s_2,\bar{p}}$ as the interference channel coefficients from S_1 and S_2 to the pth and $\bar{p}$th PUs, and their channel power gains are $|h_{s_1,p}|^2$ and $|h_{s_2,\bar{p}}|^2$, which are exponentially distributed with parameter $\lambda_{s_1,p}$ and $\lambda_{s_2,\bar{p}}$, respectively. Let the ZFB matrix in the 2-TS protocol be $\mathbf{w}_{\mathbf{zf}}^T = [w_1, w_2, ..., w_{L_s}]$. Also, let the ZFB vectors in the 3-TS protocol be $\mathbf{w}_{\mathbf{zf_1}}^T = [w_{11}, w_{12}, ..., w_{1L_s}]$ used to direct the signal to S_1 and $\mathbf{w}_{\mathbf{zf_2}}^T = [w_{21}, w_{22}, ..., w_{2L_s}]$ used to direct the signal to S_2. Let $\mathbf{h}^T = [h_{r_1,s}, ..., h_{r_{L_s},s}]$ and $\mathbf{f}^T = [f_{r_1,s}, ..., f_{r_{L_s},s}]$ be the channel vectors between the relays and S_1 and S_2, respectively. Let $\mathbf{G}_{\mathbf{rp}}^T = [\mathbf{g}_{\mathbf{r,p_1}}, ..., \mathbf{g}_{\mathbf{r,p_M}}]$ be the channel matrix between the relays and all M PUs where $\mathbf{g}_{\mathbf{r,p_m}} = [g_{r_1,p_m}, ..., g_{r_{L_s},p_m}]$. It is assumed that S_1 and S_2 have perfect knowledge of their interference channel power gains, which can be acquired through a spectrum-band manager that mediates between the primary and secondary users [46], [55], [74], [75]. It is also assumed that the ith relay knows the CSI for the links $(R_i - S_j)$. In the underlying system model, full knowledge of the CSI $\mathbf{h}$ and $\mathbf{f}$ is assumed at S_1 and S_2 [71]. In practice, this CSI can be obtained by the traditional channel training, estimation, and feedback mechanisms as in [53]. Also, the transceivers are assumed to have full knowledge of the interference between L_s and PUs, i.e., $\mathbf{G}_{\mathbf{rp}}$. We acknowledge that obtaining the interference might be a challenging problem in practice. To this end, several protocols have been proposed in [76]- [79], which allow secondary and primary users to collaborate and exchange information such that the interference channel gains can be directly fed-back from the primary receiver to the secondary network. In practice, for a primary licensee that allows the secondary to access the spectrum band, presumably for a fee, certain cooperation between the primary and secondary networks can be expected [52]. Exploiting the knowledge of the CSI at the transceivers, $\mathbf{w}_{\mathbf{zf_1}}$ and $\mathbf{w}_{\mathbf{zf_2}}$ are designed at S_1 and S_2 and sent back to the relays by only one of the transceivers via low date-rate feedback links, and that is applicable in slow fading environments [54], [72]. We argue later that each relay (exploiting the knowledge of the CSI between itself and both transceivers) can calculate its own optimal beamforming weight based only on the information that are broadcasted to all relays by the two transceivers.[2]

[2]It is also assumed that the interference from the primary transmitter is treated as AWGN, which accounts for the worst case scenario, but leads to tractable upper-bounds on the performance of the secondary

4.3 Transmission Protocols

4.3.1 2-TS protocol

In this scheme, the sources communicate with each other over two time-slots. In the first time slot, S_1 and S_2 broadcast their signals to the relays simultaneously. The received signal at the ith relay in TS_1 can be written as

$$y_{r_i}^1 = \sqrt{P_1} h_{s_1,r_i} x_{s_1} + \sqrt{P_2} f_{s_2,r_i} x_{s_2} + n_{i1}, \tag{4.1}$$

where P_1 and P_2 are the S_1 and S_2 transmit powers, respectively, x_{s_1} and x_{s_2} are the information symbols of S_1 and S_2 with $\mathrm{E}[|x_{s_1}|^2]$=$\mathrm{E}[|x_{s_2}|^2] = 1$ and n_{i1} denotes the zero-mean CSCG noise at the ith relay with variance σ^2 in TS_1.

In the second time slot, the relays that received the signal reliably weight the received signals and forward them to the two sources. The weighted transmitted signal in a vector form is

$$\mathbf{x_R} = \mathrm{Diag}(\mathbf{w_{zf}})\mathbf{y_r^1}, \tag{4.2}$$

where $\mathbf{y_r^1}$ is the relays received signals in a vector form. The received signal at S_2 is given as

$$y_{S_2}^2 = \sqrt{P_1} B_r \mathbf{f}^\dagger \mathrm{Diag}(\mathbf{w_{zf}})\mathbf{h} x_{s_1} + \sqrt{P_2} B_r \mathbf{f}^\dagger \mathrm{Diag}(\mathbf{w_{zf}})\mathbf{f} x_{s_2} + B_r \mathbf{f}^\dagger \mathrm{Diag}(\mathbf{w_{zf}})\mathbf{n_1} + n_{s_2}, \tag{4.3}$$

where n_{s_2} denotes the zero-mean CSCG noise at S_2 with variance σ^2, and B_r is the normalization constant designed to ensure that the total transmit power at the relays is constrained, and they are given as [70]

$$B_r = \sqrt{\frac{P_r}{P_1 \left\|\mathbf{W_{zf}}\mathbf{h}\right\|^2 + P_2 \left\|\mathbf{W_{zf}}\mathbf{f}\right\|^2 + \mathrm{Trace}\left(\mathbf{W_{zf}}\mathbf{W_{zf}^\dagger}\right)\sigma^2}}, \tag{4.4}$$

system [79], and is justified in the following cases: 1) the interference is represented in terms of AWGN when the primary transmitter's signal is generated by random Gaussian codebooks [7], [79]; and 2) as a practical scenario, consider a heterogeneous network in which the primary transmitter is a macro base station and the secondary receiver could be a femto base station. When both base stations are far away from each other, which is mostly the case, they do not impose interference on each other [80]. It is worth noting that this assumption is widely used in the literature (see for example [46], [74], [79]).

where $\mathbf{W_{zf}} = \text{Diag}(\mathbf{w_{zf}})$ and P_r is the total transmit power at the relays.

As the two transceivers have perfect knowledge of $\mathbf{h}$, $\mathbf{f}$ and $\mathbf{G_{rp}}$ [71], the transceivers can use this knowledge to determine the self-interference signal. Note that the second term in (4.3) depends on the signal transmitted by S_2 during the first time slot. Also, the weight vector $\mathbf{w_{zf}}$ is calculated at this transceiver [54], [72]. Furthermore, B_r is known at both transceivers. Therefore, the second term in (4.3) is known at S_2. Hence, this self-interference term can be removed and the received signal at S_2 becomes

$$y_{S_2}^2 = \sqrt{P_1} B_r \mathbf{f}^\dagger \text{Diag}(\mathbf{w_{zf}}) \mathbf{h} x_{s_1} + B_r \mathbf{f}^\dagger \text{Diag}(\mathbf{w_{zf}}) \mathbf{n_1} + n_{s_2}. \tag{4.5}$$

The combined received SNR at S_2 in the 2-TS protocol is given as

$$\gamma_{eq}^{\text{2-TS}} = \frac{P_1 B_r^2 ||\mathbf{f}^\dagger \text{Diag}(\mathbf{w_{zf}}) \mathbf{h}||^2}{B_r^2 ||\mathbf{f}^\dagger \text{Diag}(\mathbf{w_{zf}})||^2 \sigma^2 + \sigma^2}. \tag{4.6}$$

Similarly, the total received SNR at S_1 is obtained with the notations interchanged. Hereafter, since the analysis is the same for S_1 and S_2, we consider only S_2.

4.3.2 3-TS protocol

As mentioned above, the communication process occurs over three time-slots. In TS_1, S_1 broadcasts its signal x_{s_1} to all relays, then the received signal at the ith relay is given as

$$y_{r_i}^1 = \sqrt{P_1} h_{s_1, r_i} x_{s_1} + n_{i1}, \tag{4.7}$$

In TS_2, S_2 broadcasts its signal x_{s_2} to all relays, then the received signal at the ith relay is

$$y_{r_i}^2 = \sqrt{P_2} f_{s_2, r_i} x_{s_2} + n_{i2}, \tag{4.8}$$

where n_{i2} denotes zero-mean CSCG noise at the ith relay with variance σ^2 during TS_2. In TS_3, the relays that received the signal reliably combine linearly the weighted received signals from TS_1 and TS_2 and forward the sum to both transceivers, e.g., the ith relay forwards $(w_{i,2} y_{r_i}^1 + w_{i,1} y_{r_i}^2)$ to both S_1 and S_2. As such the received signal at S_2 in a vector form

$$\begin{aligned} y_{S_2}^3 &= \sqrt{P_2} \bar{B}_r \sqrt{(1-\alpha)} \mathbf{f}^H \text{Diag}(\mathbf{w_{zf1}}) \mathbf{f} x_{s_2} + \sqrt{P_1} \bar{B}_r \sqrt{\alpha} \mathbf{f}^H \text{Diag}(\mathbf{w_{zf2}}) \mathbf{h} x_{s_1} \\ &+ \bar{B}_r \sqrt{\alpha} \mathbf{f}^H \text{Diag}(\mathbf{w_{zf2}}) \mathbf{n_1} + \bar{B}_r \sqrt{(1-\alpha)} \mathbf{f}^H \text{Diag}(\mathbf{w_{zf1}}) \mathbf{n_2} + n_{s_2}, \end{aligned} \tag{4.9}$$

where $\bar{B}_r$ is the normalization constant designed to ensure that the total transmit power at the relays is constrained and they are given as [70]

$$\bar{B}_r = \sqrt{\frac{P_r}{\text{Trace}\left((1-\alpha)(\mathbf{w_{zf1}}\mathbf{h}^H\mathbf{h}\mathbf{w}_{\mathbf{zf1}}^H)\right) + \text{Trace}\left(\alpha(\mathbf{w_{zf2}}\mathbf{f}^H\mathbf{f}\mathbf{w}_{\mathbf{zf2}}^H)\right) + \sigma^2}}, \tag{4.10}$$

and α is the power allocation parameter used to allocate the available power at the relays with $0 < \alpha < 1$.[3] As S_1 and S_2 know the CSI and their transmitted signal, the self-interference term (first term) can be perfectly subtracted before further processing of the received signals.[4]

$$\begin{aligned} y_{S_2}^3 &= \sqrt{P_1}\bar{B}_r\sqrt{\alpha}\mathbf{f}^H\text{Diag}(\mathbf{w_{zf2}})\mathbf{h}x_{s_1} \\ &+ \bar{B}_r\sqrt{\alpha}\mathbf{f}^H\text{Diag}(\mathbf{w_{zf2}})\mathbf{n_2} + n_{s_2}. \end{aligned} \tag{4.11}$$

Then the total received SNR at S_2 in the 3-TS protocol is given as

$$\gamma_{eq}^{\text{3-TS}} = \frac{P_1\bar{B}_r^2\alpha||\mathbf{f}^H\text{Diag}(\mathbf{w_{zf2}})\mathbf{h}||^2}{\bar{B}_r^2\alpha||\mathbf{f}^H\mathbf{w_{zf2}}||^2\sigma^2 + \sigma^2}. \tag{4.12}$$

4.4 ZFB Weights Design

Our objective here is to maximize the received SNRs at the two transceivers in order to enhance the performance of the secondary system while limiting the interference reflected on the PUs. To be able to apply ZFB, the general assumption that the number of relays must be greater than the number of primary receivers is considered, hence, $L_s > M$.

4.4.1 2-TS protocol

According to the ZFB principles, the transmit weight vectors $\mathbf{w_{zf_1}}$, $\mathbf{w_{zf_2}}$ are chosen to lie in the orthogonal space of $\mathbf{G}_{\mathbf{rp}}^H$ such that $|\mathbf{g}_{\mathbf{r,p_i}}^H\mathbf{w_{zf_1}}| = 0$ and $|\mathbf{g}_{\mathbf{r,p_i}}^H\mathbf{w_{zf_2}}| = 0$, $\forall i = 1, .., M$

[3] α is chosen to satisfy the minimum average error probability at the two secondary receivers. Since the optimization problem is very complicated to get an optimal solution in closed-form, it can be solved numerically. When α is optimized, the secondary system performance should perform better than when it is fixed (more details in the section VII).

[4] $\mathbf{w_{zf1}}$ is designed to direct the signal to S_1 as will be explained in the next section. The term $|\mathbf{f}^H\text{Diag}(\mathbf{w_{zf1}})|^2$ results in a negligible gain. This is verified through simulations.

and $|\mathbf{h}^H\mathbf{w}_{\mathbf{zf_1}}|$, $|\mathbf{f}^H\mathbf{w}_{\mathbf{zf_2}}|$ are maximized. So the problem formulation for finding the optimal weight vectors is divided into two parts as follows.

$$\begin{aligned} \max_{\mathbf{w}_{\mathbf{zf_1}}} \quad & |\mathbf{h}^H\mathbf{w}_{\mathbf{zf_1}}| \\ \text{s.t.:} \quad & |\mathbf{g}_{\mathbf{r,p_i}}^H\mathbf{w}_{\mathbf{zf_1}}| = 0, \quad \forall i = 1,..,M \\ & \|\mathbf{w}_{\mathbf{zf_1}}\| = 1. \end{aligned} \tag{4.13}$$

$$\begin{aligned} \max_{\mathbf{w}_{\mathbf{zf_2}}} \quad & |\mathbf{f}^H\mathbf{w}_{\mathbf{zf_2}}| \\ \text{s.t.:} \quad & |\mathbf{g}_{\mathbf{r,p_i}}^H\mathbf{w}_{\mathbf{zf_2}}| = 0, \quad \forall i = 1,..,M \\ & \|\mathbf{w}_{\mathbf{zf_2}}\| = 1. \end{aligned} \tag{4.14}$$

By applying a standard Lagrangian multiplier method, the weight vectors that satisfy the above optimization methods are given as

$$\mathbf{w}_{\mathbf{zf_1}} = \frac{\mathbf{\Xi}^{\perp}\mathbf{h}}{\|\mathbf{\Xi}^{\perp}\mathbf{h}\|}, \tag{4.15}$$

and

$$\mathbf{w}_{\mathbf{zf_2}} = \frac{\mathbf{\Xi}^{\perp}\mathbf{f}}{\|\mathbf{\Xi}^{\perp}\mathbf{f}\|}, \tag{4.16}$$

where $\mathbf{\Xi}^{\perp} = \left(\mathbf{I} - \mathbf{G_{rp}}(\mathbf{G_{rp}^{\dagger}}\mathbf{G_{rp}})^{-\mathbf{1}}\mathbf{G_{rp}^{\dagger}}\right)$ is the projection idempotent matrix with rank $(L_s - M)$. The rank of the matrix is approved from the following Lemma in the projection matrix theory [82].

Lemma 1: Let $\mathbf{G}$ be an $n \times k$ matrix with full column rank k, $k < n$, then the nonzero matrix $\mathbf{G}(\mathbf{G}^{\dagger}\mathbf{G})^{-\mathbf{1}}\mathbf{G}^{\dagger}$ is an idempotent symmetric matrix and its orthogonal projection matrix is $\mathbf{I} - \mathbf{G}(\mathbf{G}^{\dagger}\mathbf{G})^{-\mathbf{1}}\mathbf{G}^{\dagger}$ with rank $(n-k)$ [82, Theorems 4.21, 4.22].

It can be observed from the rank of the matrix that the cooperative ZBF beamformer becomes effective only when $L_s > M$. Otherwise, the interference from secondary relays to primary receivers cannot be mitigated. The case when $L_s \leq M$ can be handled using conventional schemes by limiting the interference via transmit power control methods, e.g., [73], [74].

In the 2-TS protocol, since each relay knows the CSI of the channels between itself and both secondary sources and between itself and the primary receivers, the ZFB vector $\mathbf{w}_{\mathbf{zf}}$ is made up by the diagonal of the product of the two ZFB vectors $\mathbf{w}_{\mathbf{zf_1}}$ (used to direct the

signal to S_1) and $\mathbf{w_{zf_2}}$ (used to direct the signal to S_2) which is represented as [36]- [37] and references therein

$$\mathbf{w_{zf}} = \text{Diag}(\mathbf{w_{zf_1}}\mathbf{w_{zf_2}}^T). \tag{4.17}$$

Proof. Let $\mathbf{H_{UL}} = [\mathbf{h}, \mathbf{f}]$ with dimension space $L_s \times 2$, and $\mathbf{H_{DL}} = [\mathbf{f}, \mathbf{h}]^T$ with dimension space $2 \times L_s$. First, construct the subspace $\mathbf{\Xi}^\perp$ such as $\mathbf{\Xi}^\perp = \left(\mathbf{I} - \mathbf{G_{rp}}(\mathbf{G_{rp}}^\dagger\mathbf{G_{rp}})^{-1}\mathbf{G_{rp}}^\dagger\right)$ with $L_s \times L_s$ dimension. Second, project the CR channels to the space $\mathbf{\Xi}^\perp$, utilizing that $\mathbf{\Xi}^\perp$ is idempotent matrix matrix, i.e., $\mathbf{\Xi}^\perp = (\mathbf{\Xi}^\perp)^2$, then $\mathbf{H_{DL}}\mathbf{\Xi}^\perp\mathbf{H_{UL}} = \mathbf{H_{DL}}\mathbf{\Xi}^\perp\mathbf{\Xi}^\perp\mathbf{H_{UL}}$. Third, perform ZFB to the CRs within the subspace orthogonal to the PU channel with the power constraint $\mathbf{W_{zf}} = (\mathbf{H_{DL}}\mathbf{\Xi}^\perp)^T \begin{bmatrix} \frac{1}{\|\mathbf{\Xi}^\perp\mathbf{h}\|} & 0 \\ 0 & \frac{1}{\|\mathbf{\Xi}^\perp\mathbf{f}\|} \end{bmatrix} (\mathbf{\Xi}^\perp\mathbf{H_{UL}})^T$. This results in $\mathbf{W_{zf}}$= Diag $(\mathbf{w_{zf_1}}\mathbf{w_{zf_2}}^T)$ and $\mathbf{w_{zf}} = \text{Diag}(\mathbf{W_{zf}})$. □

It is worth noting that the weights matrix is diagonal, which guarantees that the relays transmit only their own received signal and there is no data exchange among the relays. Thus, the algorithm works in a distributed manner.

4.4.2 3-TS protocol

The ZFB vectors in 3-TS protocol are simply chosen to be $\mathbf{w_{zf_1}}$ and $\mathbf{w_{zf_2}}$ given by (4.15) and (4.16) in the first and second time-slot, respectively. In the third time-slot, the weighted received signals are combined linearly with certain power allocation values as described previously.

Remark: By having a closer look at the closed-form solutions of the optimal weight vectors in (4.15) and (4.16), we propose a distributed implementation instead of the centralized one mentioned before. From (4.15) and (4.16), to design $\mathbf{w_{zf_1}}$ and $\mathbf{w_{zf_2}}$ at the relays, each relay needs the global constants $\frac{1}{\|\mathbf{\Xi}^\perp\mathbf{h}\|}$ and $\frac{1}{\|\mathbf{\Xi}^\perp\mathbf{f}\|}$ and also the interference matrix, i.e. $\mathbf{\Xi}^\perp$, which are broadcasted by either S_1 or S_2. Upon receiving the broadcast messages from S_1 or S_2, each ith relay node determines the optimal w_{1i} and w_{2i} weights from its local information of h_{r_i,s_1} and f_{r_i,s_2}. As such, the beamforming computation is calculated in a distributed manner.

4.5 End-to-end SNR analysis

4.5.1 First Order Statistics of $\gamma_{eq}^{\text{2-TS}}$

In this model, the secondary source can utilize the PU's spectrum as long as the interference it generates at the PUs remains below the interference threshold Q_j, $\forall j = 1, 2$. For that reason, P_j is constrained as $P_j = \min\left\{\frac{Q_j}{|h_{s_j,p}|^2}, P_{s_j}\right\}$ where P_{s_j} is the maximum transmission power of S_j.

So the received SNR γ_{s_j,r_i} at the ith relay is given as

$$\gamma_{s_j,r_i} = \begin{cases} \frac{P_{s_j}|f_{s_j,r_i}|^2}{\sigma^2}, & P_{s_j} < \frac{Q_j}{|h_{s_j,p}|^2} \\ \frac{Q_j|f_{s_j,r_i}|^2}{\sigma^2|h_{s_j,p}|^2}, & P_{s_j} \geq \frac{Q_j}{|h_{s_j,p}|^2} \end{cases}, \tag{4.18}$$

where σ^2 is the noise variance at each relay. We focus on the analysis of the second case $\left(P_{s_j} \geq \frac{Q_j}{|h_{s_j,p}|^2}\right)$ as it is more effective and restrictive than the first case $\left(P_{s_j} < \frac{Q_j}{|h_{s_j,p}|^2}\right)$. It determines the effect of the peak power constraint in the first time-slot on the performance of the secondary system while the system in the first case becomes a non-cognitive system. So the transmit powers P_1 and P_2 are constrained as $P_1 \leq \frac{Q_1}{|h_{s_1,p}|^2}$ and $P_2 \leq \frac{Q_2}{|h_{s_2,p}|^2}$.

Substituting (4.4), and (4.17) into (4.6), and after simple manipulations, the equivalent SNR at S_2 can be written in the general form of $\gamma_{eq}^{\text{2-TS}} = \frac{\gamma_{1,2TS}\ \gamma_{3,2TS}}{\gamma_{1,2TS}+\gamma_{2,2TS}+\gamma_{3,2TS}+1}$ as:

$$\gamma_{eq}^{\text{2-TS}} = \frac{\frac{P_1}{\sigma^2}\left\|\boldsymbol{\Xi}^{\perp}\mathbf{h}\right\|^2 \frac{P_r}{\sigma^2}\left\|\boldsymbol{\Xi}^{\perp}\mathbf{f}\right\|^2}{\frac{P_1}{\sigma^2}\left\|\boldsymbol{\Xi}^{\perp}\mathbf{h}\right\|^2 + \frac{P_2}{\sigma^2}\left\|\boldsymbol{\Xi}^{\perp}\mathbf{f}\right\|^2 + \frac{P_r}{\sigma^2}\left\|\boldsymbol{\Xi}^{\perp}\mathbf{f}\right\|^2 + 1}. \tag{4.19}$$

Considering the peak constraint on the received power at the most affected primary user, we substitute P_1 and P_2 into (4.19). Then $\gamma_{eq}^{\text{2-TS}}$ becomes

$$\gamma_{eq}^{\text{2-TS}} = \frac{\gamma_{q_1}\frac{\left\|\boldsymbol{\Xi}^{\perp}\mathbf{h}\right\|^2}{|h_{s_1,p}|^2}\gamma_r\left\|\boldsymbol{\Xi}^{\perp}\mathbf{f}\right\|^2}{\gamma_{q_1}\frac{\left\|\boldsymbol{\Xi}^{\perp}\mathbf{h}\right\|^2}{|h_{s_1,p}|^2} + \gamma_{q_2}\frac{\left\|\boldsymbol{\Xi}^{\perp}\mathbf{f}\right\|^2}{|h_{s_2,p}|^2} + \gamma_r\left\|\boldsymbol{\Xi}^{\perp}\mathbf{f}\right\|^2 + 1}, \tag{4.20}$$

where $\gamma_r = \frac{P_r}{\sigma^2}$, $\gamma_{q_1} = \frac{Q_1}{\sigma^2}$ and $\gamma_{q_2} = \frac{Q_2}{\sigma^2}$.

We first find the statistics of the new random variables defined above. Then, we compute the CDF and MGF of $\gamma_{eq}^{\text{2-TS}}$, which will be used in the the derivation of the performance metrics. To continue, let $\gamma_{1,2TS} = \gamma_{q_1}\frac{\left\|\boldsymbol{\Xi}^{\perp}\mathbf{h}\right\|^2}{|h_{s_1,p}|^2}$, $\gamma_{2,2TS} = \gamma_{q_2}\frac{\left\|\boldsymbol{\Xi}^{\perp}\mathbf{f}\right\|^2}{|h_{s_2,p}|^2}$and $\gamma_{3,2TS} = \gamma_r\left\|\boldsymbol{\Xi}^{\perp}\mathbf{f}\right\|^2$.

Lemma 4.5.1 ((PDFs of $\gamma_{1,2TS}$ and $\gamma_{2,2TS}$)). *Let each entry of* $\mathbf{h}$ *and* $\mathbf{f}$ *be i.i.d.* $\mathcal{CN} \sim (0,1)$, *then* $\left\|\mathbf{\Xi}^{\perp}\mathbf{h}\right\|^2$ *and* $\left\|\mathbf{\Xi}^{\perp}\mathbf{f}\right\|^2$ *are chi squared random variables with* $2(L_s - M)$ *degrees of freedom. Given that* $|h_{s_1,p}|^2$ *and* $|h_{s_2,\bar{p}}|^2$ *are exponential random variables, the PDFs of* $f_{\gamma_{1,2TS}}(\gamma)$ *and* $f_{\gamma_{2,2TS}}(\gamma)$ *are given respectively by:*

$$f_{\gamma_{i,2TS}}(\gamma) = \frac{\lambda_{s_i,p}(L_s - M + 1)\gamma^{L_s-M}}{\gamma_{q_i}^{L_s-M}(\frac{\gamma}{\gamma_{q_i}} + \lambda_{s_i,p})^{L_s-M+2}}, \quad \forall i = 1, 2. \tag{4.21}$$

Lemma 4.5.2 ((CDF of $\gamma_{3,2TS}$)). *Let each entry of* $\mathbf{f}$ *be i.i.d.* $\mathcal{CN} \sim (0,1)$, *then* $\left\|\mathbf{\Xi}^{\perp}\mathbf{f}\right\|^2$ *is a chi squared random variable with* $2(L_s - M)$ *degrees of freedom [57, Theorem 2 Ch.1]. The CDF of* $\gamma_{3,2TS}$ *can be expressed as*

$$F_{\gamma_{3,2TS}}(\gamma) = 1 - \frac{\Gamma\left(L_s - M, \frac{\gamma}{\gamma_r}\right)}{(L_s - M - 1)!}, \ \gamma \geq 0. \tag{4.22}$$

4.5.2 First Order Statistics of $\gamma_{eq}^{\text{3-TS}}$

Substituting (4.10), (4.15) and (4.16) into (4.12), and after simple manipulations, the equivalent SNR at S_2 can be written in the general form of $\gamma_{eq}^{\text{3-TS}} = \frac{\gamma_{1,3TS}\ \gamma_{3,3TS}}{\gamma_{1,3TS}+\gamma_{2,3TS}+\gamma_{3,3TS}+1}$ as:

$$\gamma_{eq}^{\text{3-TS}} = \frac{\frac{P_1}{\sigma^2}\left\|\mathbf{h}\right\|^2 \alpha\frac{P_r}{\sigma^2}\left\|\mathbf{\Xi}^{\perp}\mathbf{f}\right\|^2}{\frac{P_1}{\sigma^2}\left\|\mathbf{h}\right\|^2 + \frac{P_2}{\sigma^2}\left\|\mathbf{f}\right\|^2 + \alpha\frac{P_r}{\sigma^2}\left\|\mathbf{\Xi}^{\perp}\mathbf{f}\right\|^2 + 1}. \tag{4.23}$$

Again, considering the peak constraint on the received power at the most affected primary user, $\gamma_{eq}^{\text{3-TS}}$ becomes

$$\gamma_{eq}^{\text{3-TS}} = \frac{\gamma_{q_1}\frac{\|\mathbf{h}\|^2}{|h_{s_1,p}|^2}\gamma_{r_1}\left\|\mathbf{\Xi}^{\perp}\mathbf{f}\right\|^2}{\gamma_{q_1}\frac{\|\mathbf{h}\|^2}{|h_{s_1,p}|^2} + \gamma_{q_2}\frac{\|\mathbf{f}\|^2}{|h_{s_2,p}|^2} + \gamma_{r_1}\left\|\mathbf{\Xi}^{\perp}\mathbf{f}\right\|^2 + 1}, \tag{4.24}$$

where $\gamma_{r_1} = \frac{\alpha P_r}{\sigma^2}$.

Remark: We notice in (4.23) that the 3-TS protocol results in a different received SNRs at S_1 and S_2, depending on the power allocation parameter α. However, for the 2-TS protocol, equal power allocation is used since the sum of the two signals at the relay(s) is weighted by the same vector. This gives an advantage to the 3-TS protocol since it benefits from allocating different transmit powers to the sources.

To proceed, let $\gamma_{1,3TS} = \gamma_{q_1}\frac{\|\mathbf{h}\|^2}{|h_{s_1,p}|^2}$, $\gamma_{2,3TS} = \gamma_{q_2}\frac{\|\mathbf{f}\|^2}{|h_{s_2,p}|^2}$ and $\gamma_{3,3TS} = \gamma_{r_1}\left\|\mathbf{\Xi}^{\perp}\mathbf{f}\right\|^2$.

Lemma 4.5.3 ((PDFs of $\gamma_{1,3TS}$ and $\gamma_{2,3TS}$)). *Let each entry of* $\mathbf{h}$ *and* $\mathbf{f}$ *be i.i.d.* $\mathcal{CN} \sim (0,1)$, *then* $\|\mathbf{h}\|^2$ *and* $\|\mathbf{f}\|^2$ *are chi squared random variables with* $2L_s$ *degrees of freedom, Given that* $|h_{s_1,p}|^2$ *and* $|h_{s_2,p}|^2$ *are exponential random variables, the PDFs of* $f_{\gamma_{1,3TS}}(\gamma)$ *and* $f_{\gamma_{2,3TS}}(\gamma)$ *are given respectively by:*

$$f_{\gamma_{i,3TS}}(\gamma) = \frac{\lambda_{s_i,p} L_s (\gamma)^{L_s-1}}{(\gamma_{q_i})^{L_s} (\frac{\gamma}{\gamma_{q_i}} + \lambda_{s_i,p})^{L_s+1}}, \quad i = 1, 2. \tag{4.25}$$

According to **Lemma** 4.5.3, the CDF of $\gamma_{3,3TS}$ is

$$F_{\gamma_{3,3TS}}(\gamma) = 1 - \frac{\Gamma\left(L_s - M, \frac{\gamma}{\gamma_{r_1}}\right)}{(L_s - M - 1)!}, \ \gamma \geq 0. \tag{4.26}$$

In the subsequent sections, we consider the statistics of the random variable γ_{eq}^{iTS} defined by $\gamma_{eq}^{iTS} = \frac{\gamma_{1,iTS} \ \gamma_{3,iTS}}{\gamma_{1,iTS}+\gamma_{2,iTS}+\gamma_{3,iTS}}$, $i = 2, 3$, which can be considered as a tractable tight upper bound to the actual equivalent SNR.

4.6 Outage Probability Analysis

In this section, we derive the outage probability for both 2-TS and 3-TS. As previously mentioned, the interference CSI between S_1 and the pth PU, i.e., $h_{s_1,p}$ is unknown at S_2, and $h_{s_2,\bar{p}}$ is also unknown at S_1. Due to this randomness, the end-to-end received SNR at each transceiver in (4.20) and (4.24) is still a random variable and there is no guarantee of zero-outage.

4.6.1 2-TS protocol

An outage event occurs when $\gamma_{eq}^{\text{2-TS}}$ falls below a certain threshold γ_{th}, which can be characterized mathematically as follows.

$$P_{out}^{\text{2-TS}} = \Pr(\gamma_{eq}^{\text{2-TS}} < \gamma_{th}) = F_{\gamma_{eq}^{\text{2-TS}}}(\gamma_{th}). \tag{4.27}$$

Theorem 4.6.1. *A closed-form expression for the outage probability in the 2-TS protocol for a two-way AF relaying in spectrum-sharing system is given by*

$$\begin{aligned} P_{out}^{2\text{-}TS} &= 1-\hat{b}\sum_{m=0}^{L_s-M-1}\sum_{k=0}^{m}\sum_{r=0}^{k}\frac{(\gamma_{th})^{k-r}}{m!}\binom{m}{k}\binom{k}{r}\hat{a}^{\frac{r}{2}}e^{-\frac{\gamma_{th}}{\gamma_r}}\frac{2^{\frac{-2L_s+2M-2-r}{2}}}{\sqrt{2\pi}}\sqrt{\frac{\hat{a}\gamma_{th}}{\gamma_r}}\left(\frac{\gamma_{th}}{\gamma_r}\right)^{m-\frac{3r}{2}} \\ &\times \sum_{p=0}^{L_s-M}\binom{L_s-M}{p}\gamma_{th}^{L_s-M-p}\sum_{s=0}^{N}\frac{1}{s!}\left(\frac{-\gamma_{th}^2}{\gamma_r}+\frac{\gamma_{th}\hat{a}}{\gamma_r}\right)^{s}\frac{2^{L_s-M+1}(\gamma_{th}+a)^{\mu}}{2\pi\Gamma(L_s-M+2)} \\ &\times G_{6,4}^{2,6}\left(\frac{4\gamma_r^2(\gamma_{th}+\hat{a})^2}{(\hat{a}\gamma_{th})^2}\middle|_{\Delta(2,(L_s+1)-\alpha_o),\Delta(1,1-a_r)}^{\Delta(2,1-\alpha_o),\Delta(1,1-b_r)}\right), \end{aligned} \tag{4.28}$$

where $\hat{a}=\lambda_{s_2,p}\gamma_{q_2}$, $\hat{b}=(L_s-M+1)\Gamma(r+L_s-M+1)$, $a_r=(\frac{1}{4}-\frac{1}{4}(-2L_s+2M-2-r),\ \frac{3}{4}-\frac{1}{4}(-2L_s+2M-2-r))$, $b_r=(\frac{1}{2}+\frac{1}{4}(1-r),\ \frac{1}{2}-\frac{1}{4}(1-r),\ \frac{1}{4}(1-r),\ \frac{-1}{4}(1-r))$, $\mu_o=p-k+\frac{3r}{2}-s-L_s+M-\frac{3}{2}$, $\alpha_o=\mu_o+L_s-M+2$, $\Delta(i,a)=\frac{a}{i},\frac{a+1}{i},...,\frac{a-i+1}{i}$ and $G_{.,.}^{.,.}\left(.\middle|.\right)$ is the Meijer's G-function defined in [56].

Proof. To derive the outage probability of $\gamma_{eq}^{2\text{-TS}}$, conditioned on $\gamma_{1,2TS}$ and $\gamma_{2,2TS}$, we first express the CDF of $\gamma_{eq}^{2\text{-TS}}$ as

$$F_{\gamma_{eq}^{2\text{-TS}}}(\gamma_{th})=\int_0^{\infty}\Pr\left(\gamma_{3,2TS}<\frac{\gamma_{th}(y+z)}{y-\gamma_{th}}\right)f_{\gamma_{1,2TS}}(y)f_{\gamma_{2,2TS}}(z)dydz. \tag{4.29}$$

Using variable change, $w=y-\gamma_{th}$, and after some algebraic manipulations, we have

$$\begin{aligned} F_{\gamma_{eq}^{2\text{-TS}}}(\gamma_{th}) &= 1-\int_0^{\infty}\Pr\left(\gamma_{3,2TS}\geq\frac{\gamma_{th}(w+\gamma_{th}+z)}{w}\right) \\ &\times f_{\gamma_{1,2TS}}(w+\gamma_{th})f_{\gamma_{2,2TS}}(z)dwdz. \end{aligned} \tag{4.30}$$

Substituting in the complementary of the CDF of $\gamma_{3,2TS}$ and the PDF of $\gamma_{1,2TS}$ from (4.22) and (4.21), respectively, we obtain

$$\bar{F}_{\gamma_{3,2TS}}(\gamma)=\frac{1}{(L_s-M-1)!}\Gamma\left(L_s-M,\frac{\gamma_{th}(w+\gamma_{th}+z)}{\gamma_r w}\right), \tag{4.31}$$

where $\bar{F}_{\gamma_{3,2TS}}(\gamma)$ denotes the complementary of the CDF of $\gamma_{3,2TS}$. Before proceeding in the derivation, (4.31) is expressed in another mathematical form using [56, Eq. 8.352.2] and [56, Eq. 1.111] as follows.

$$\begin{aligned} \bar{F}_{\gamma_{3,2TS}}(\gamma) &= e^{-\frac{\gamma_{th}(w+\gamma_{th}+z)}{\gamma_r w}}\sum_{m=0}^{Ls-M-1}\sum_{k=0}^{m}\sum_{r=0}^{k}\frac{1}{m!}\binom{m}{k}\binom{k}{r} \\ &\times \left(\frac{\gamma_{th}}{\gamma_r}\right)^{m-k+r}\left(\frac{\gamma_{th}^2}{w\gamma_r}\right)^{k-r}\left(\frac{z}{w}\right)^{r}. \end{aligned} \tag{4.32}$$

Then substituting (4.32) into (4.30) and after some mathematical manipulations, we have

$$\begin{aligned} F_{\gamma_{eq}^{\text{2-TS}}}(\gamma_{th}) &= 1 - \sum_{m=0}^{Ls-M-1} \sum_{k=0}^{m} \sum_{r=0}^{k} \frac{1}{m!} \left(\frac{\gamma_{th}}{\gamma_r}\right)^{m-k} \binom{m}{k} \\ &\times \binom{k}{r} e^{-\frac{\gamma_{th}}{\gamma_r}} \int_0^{\infty} \left(\frac{\gamma_{th}^2}{w\gamma_r}\right)^{k-r} f_{\gamma_{1,2TS}}(w+\gamma_{th}) \\ &\times \underbrace{\left(\int_0^{\infty} \left(\frac{\gamma_{th} z}{w\gamma_r}\right)^{r} e^{-\frac{z\gamma_{th}}{w\gamma_r}} f_{\gamma_{2,2TS}}(z) dz\right)}_{I_1} dw. \end{aligned} \tag{4.33}$$

The inner integral I_1 can be solved using the variable change, $u = z + \lambda_{s_2,p}\gamma_{q_2}$, leading to

$$I_1 = \int_{\lambda_{s_2,p}\gamma_{q_2}}^{\infty} \hat{a}\ L_s \left(\frac{\gamma_{th}}{w\gamma_r}\right)^{r} e^{-\frac{\gamma_{th}}{w\gamma_r}(u-\hat{a})} \frac{(u-\hat{a})^{r+L_s-M}}{(u)^{L_s-M+2}} du, \tag{4.34}$$

Using [56, eq. 3.383.4], I_1 results in

$$I_1 = \hat{a}^{\frac{r}{2}}\ \hat{b} \left(\frac{\gamma_{th}}{w\gamma_r}\right)^{-r/2} e^{\frac{\hat{a}\gamma_{th}}{2w\gamma_r}} W_{\frac{-2L_s+2M-2-r}{2}, \frac{1-r}{2}} \left(\frac{\hat{a}\gamma_{th}}{w\gamma_r}\right), \tag{4.35}$$

where $W_{.,.}(.)$ is the Whittaker function [56].

Returning to the main expression in (4.33), after substituting the results in (4.35) with further simplifications, we obtain

$$\begin{aligned} F_{\gamma_{eq}^{\text{2-TS}}}(\gamma_{th}) &= 1 - \sum_{m=0}^{Ls-M-1} \sum_{k=0}^{m} \sum_{r=0}^{k} \frac{(\gamma_{th})^{k-r}}{m!} \binom{m}{k} \binom{k}{r} \hat{b} e^{-\frac{\gamma_{th}}{\gamma_r}} \left(\frac{\gamma_{th}}{\gamma_{r_1}}\right)^{m-\frac{3r}{2}} \hat{a}^{\frac{r}{2}} \\ &\times \underbrace{\int_0^{\infty} \left(\frac{1}{w}\right)^{k-\frac{3r}{2}} e^{-\frac{\gamma_{th}^2}{w\gamma_r} + \frac{\hat{a}\gamma_{th}}{2w\gamma_r}} W_{\frac{-2L_s+2M-2-r}{2}, \frac{1-r}{2}} \left(\frac{\hat{a}\gamma_{th}}{w\gamma_r}\right) f_{\gamma_{1,2TS}}(w+\gamma_{th}) dw}_{I_2} \end{aligned} \tag{4.36}$$

To the best of our knowledge, the integral I_2 in (4.36) has no closed-form solution. To solve I_2, we first represent the exponential term using Taylor series representation [56, eq. 1.211.1], apply the binomial theorem [56, eq. 1.11.1] for the term $(w+\gamma_{th})^{Ls-M}$ and express the Whittaker function in terms of Meijer's G-function using [56, eq. 9.34.9] and [56, eq.

9.31.2], which after many manipulations results in

$$
\begin{aligned}
F_{\gamma_{eq}^{2\text{-TS}}}(\gamma_{th}) &= 1 - \sum_{m=0}^{Ls-M-1} \sum_{k=0}^{m} \sum_{r=0}^{k} \frac{(\gamma_{th})^{k-r}}{m!} \binom{m}{k} \binom{k}{r} \\
&\times \hat{b}\, \hat{a}^{\frac{r}{2}} e^{-\frac{\gamma_{th}}{\gamma_r}} \frac{2^{\frac{-2Ls+2M-2-r}{2}}}{\sqrt{2\pi}} \sqrt{\frac{\hat{a}\gamma_{th}}{\gamma_r}} \left(\frac{\gamma_{th}}{\gamma_r}\right)^{m-\frac{3r}{2}} \\
&\times \sum_{p=0}^{Ls-M} \binom{Ls-M}{p} \gamma_{th}^{Ls-M-p} \sum_{s=0}^{N} \frac{1}{s!} \left(\frac{-\gamma_{th}^2}{\gamma_r} + \frac{\gamma_{th}\hat{a}}{\gamma_r}\right)^s \\
&\times \underbrace{\int_0^{\infty} \left(\frac{w^{p-k+\frac{3r}{2}-s-1/2}}{(w+\gamma_{th}+\hat{a})^{Ls-M+2}} \left(G_{4,2}^{0,4} \left(\frac{4\gamma_r^2 w^2}{(\hat{a}\gamma_{th})^2} \Big|_{1-a_r}^{1-b_r} \right) \right) \right) dw}_{I_3}. \qquad (4.37)
\end{aligned}
$$

The integral I_3 in (4.37) is solved using [63, eq. 2.24.2.4, vol. 3], then after few simplifications, *the outage probability in the 2-TS protocol* is expressed as in (4.28), thus completing the proof. □

We remark that the Taylor series in the outage expression is expressed in the form of a finite sum where only six terms are needed in the summation over index s to obtain the accuracy to the degree of seven decimals as will be explained in the numerical results.

4.6.2 3-TS protocol

Similarly, for this scheme, an outage event occurs when $\gamma_{eq}^{3\text{-TS}}$ falls below a certain threshold γ_{th}. As such, $P_{out}^{3\text{-TS}}$ can be expressed as

$$
P_{out}^{3\text{-TS}} = \Pr(\gamma_{eq}^{3\text{-TS}} < \gamma_{th}) = F_{\gamma_{eq}^{3\text{-TS}}}(\gamma_{th}). \qquad (4.38)
$$

Theorem 4.6.2. *A closed-form expression for the outage probability in the 3-TS protocol for a two-way AF relaying based distributed ZFB in spectrum-sharing system is given by*

$$
\begin{aligned}
P_{out}^{3\text{-}TS} &= 1 - b \sum_{m=0}^{Ls-M-1} \sum_{k=0}^{m} \sum_{r=0}^{k} \frac{(\gamma_{th})^{k-r}}{m!} \binom{m}{k} \binom{k}{r} a^{\frac{r+1}{2}} e^{-\frac{\gamma_{th}}{\gamma_{r_1}}} \frac{2^{\frac{-2Ls-r}{2}}}{\sqrt{2\pi}} \left(\frac{\gamma_{th}}{\gamma_{r_1}}\right)^{m-\frac{3r+1}{2}} \\
&\times \sum_{p=0}^{Ls-1} \binom{Ls-1}{p} \gamma_{th}^{Ls-1-p} \sum_{s=0}^{N} \frac{1}{s!} \left(\frac{-\gamma_{th}^2 + \gamma_{th} a}{\gamma_{r_1}}\right)^s \frac{2^{Ls}(\gamma_{th}+a)^{\mu_1}}{2\pi\Gamma(Ls+1)} \\
&\times G_{6,4}^{2,6} \left(\frac{4\gamma_{r_1}^2 (\gamma_{th}+a)^2}{(a\gamma_{th})^2} \Big|_{\Delta(2,(Ls+1)-\alpha_1),\Delta(1,1-a_{r_1})}^{\Delta(2,1-\alpha_1),\Delta(1,1-b_{r_1})} \right), \qquad (4.39)
\end{aligned}
$$

where $\mu_1 = p - k + \frac{3r}{2} - s - L_s - \frac{1}{2}$ and $\alpha_1 = \mu_1 + L_s + 1$, $a_{r_1} = (\frac{1}{4} - \frac{1}{4}(-2L_s - r), \frac{3}{4} - \frac{1}{4}(-2L_s - r))$, $b_{r_1} = (\frac{1}{2} + \frac{1}{4}(1-r), \frac{1}{2} - \frac{1}{4}(1-r), \frac{1}{4}(1-r), \frac{-1}{4}(1-r))$.

Proof. To derive the outage probability expression in the 3-TS protocol, we follow the same steps as performed in the case of the 2-TS protocol. This yields the expression in (4.39). Although we have multiple summations, all of them are finite and easy to compute numerically. □

4.6.3 Asymptotic outage probability

Although the expressions in (4.28) and (4.39) enable numerical evaluation of the exact system outage performance, they do not provide useful insights on the effect of key parameters (e.g., the number of secondary relays, the number of PUs, etc.) that influence the system performance. To get more insights, we now introduce asymptotic outage probability expressions, i.e., $\gamma_{q_i} \to \infty$, for the 2-TS and 3-TS transmission protocols. The obtained asymptotic expressions are useful in analyzing the average error probability at high SNR in the next section.

Corollary 4.6.3. *The asymptotic outage probability at the secondary source in the 2-TS and 3-TS protocols for a two-way AF relaying based distributed ZFB in spectrum-sharing system is given by*

$$P_{out_\infty}^{\tau\text{-}TS} \approx \left(\frac{(L_s - M + 1)\gamma_{th}^{L_s - M + 1}}{\lambda_{s_i,p}^{L_s - M + 1}} + \frac{c\ \gamma_{th}^{L_s - M}}{\Gamma(L_s - M + 1)} \right) \left(\frac{1}{\gamma_{q_i}} \right)^{L_s - M} + o(\gamma_{th}^2), \tag{4.40}$$

where $\tau = 2, 3, i = 1, 2$, respectively, $c = (\alpha\gamma_r)^{L_s - M + 2}$ where $\alpha = 1$ for 2-TS and $o(\gamma_{th}^2)$ stands for higher-order terms.

Proof. The technique developed in [81] can be used to find asymptotic behavior of $P_{out}^{\tau\text{-TS}}$ at high SNR. First, we find the approximate CDFs of the total received SNR at S_j, $\gamma_{eq}^{\tau - TS}$. Recalling (4.20) and (4.24), we make use of the infinite series representation of the incomplete

Gamma function as in [56, Eq. 8.354.2]

$$\Gamma(\theta, x) = \Gamma(\theta) - \sum_{n=0}^{\infty} \frac{(-1)^n x^{\theta+n}}{n!(\theta+n)}. \tag{4.41}$$

which leads to

$$\Gamma(\theta, x) \overset{x\to 0}{\approx} \Gamma(\theta) - \frac{x}{\theta}. \tag{4.42}$$

Therefore, using the mutual independence between h_{s_1,r_i}, f_{s_2,r_i} $(i = 1, ..., L_s)$, $h_{s_1,p}, h_{s_2,p}$ and $g_{r_i,p_m}, (m = 1, ..., M)$ and by using Taylor's series, the approximate CDF of $\gamma_{eq}^{\tau-TS}$, denoted by $F_{\gamma_{eq_\infty}}^{\tau\text{-TS}}(\gamma)$, can be written as

$$F_{\gamma_{eq_\infty}}^{\tau\text{-TS}}(\gamma) \approx \left(\frac{\gamma^{L_s-M+1}}{\lambda_{s_i,p}^{L_s-M+1}} + \frac{c\,\gamma^{L_s-M}}{\Gamma(L_s-M+1)}\right)\left(\frac{1}{\gamma_{q_i}}\right)^{L_s-M} + o(\gamma). \tag{4.43}$$

Finally, by computing $F_{\gamma_{eq_\infty}}^{\tau\text{-TS}}(\gamma)_{|\gamma=\gamma_{th}}$, we get (4.40), thus completes the proof. □

It can be observed from (4.40) that the diversity order is $L_s - M$. This means that the diversity gain increases linearly with the number of the secondary relays. Furthermore, as the number of the primary receivers increases, the outage probability increases. Meanwhile, as the value of Q increases, the outage probability decreases.

4.7 Average Error Probability Analysis

In this section, we derive expressions for the end-to-end of average error probability performance for both 2-TS and 3-TS.

4.7.1 2-TS protocol

Theorem 4.7.1. *A closed-form expression for the average error probability in the 2-TS protocol for a two-way AF relaying based distributed ZFB in spectrum-sharing system is given by*

$$P_e^{2\text{-}TS} = \frac{1}{2} - \frac{1}{2\sqrt{\pi}}\bar{\delta}\sum_{m=0}^{M-L_s-2}\frac{1}{c^m m!}\left(\frac{1}{A}\right)^{v+\frac{3}{4}} G_{4,4}^{4,1}\left(\frac{b^2}{A}\Big|_{L_s-M,0,0,-L_s+M}^{-v-\frac{1}{4},0,\frac{1}{2},-v+\frac{1}{4}}\right), \tag{4.44}$$

where $\bar{\delta} = \delta(M - L_s - 2)!, \delta = \frac{4(L_s-M+1)\gamma_r^{-(L_s-M)}}{c^{L_s-M+1}(\Gamma(L_s-M))^2}, v = 2L_s - 2M + m + \frac{3}{4}$, $A = 1$ (for BPSK), $c = \lambda_{s_1,p}\gamma_{q_1}$ and $b = \frac{2}{\sqrt{\gamma_r}}$.

Proof. In order to obtain the average error probability for the secondary system, the MGF based approach will be used in this paper. Let $(\gamma_{eq}^{\text{2-TS}})^{-1} = \gamma_{1,2TS}^{-1} + \frac{\gamma_{2,2TS}}{\gamma_{1,2TS}\ \gamma_{3,2TS}} + \gamma_{3,2TS}^{-1} = X_1 + X_2 + X_3$ where $X_1 = \gamma_{1,2TS}^{-1}$, $X_2 = \frac{\gamma_{2,2TS}}{\gamma_{1,2TS}\ \gamma_{3,2TS}}$ and $X_3 = \gamma_{3,2TS}^{-1}$. As $(\gamma_{eq}^{2TS})^{-1}$ is the sum of three independent random variables, the MGF of the $(\gamma_{eq}^{\text{2-TS}})^{-1}$, denoted by $\phi_{(\gamma_{eq}^{\text{2-TS}})^{-1}}(s)$, results simply from the product of the three MGFs of X_1, X_2 and X_3, denoted as $\phi_{X_1}(s)$, $\phi_{X_2}(s)$ and $\phi_{X_3}(s)$, respectively. The MGF of random variable X with PDF $f_X(x)$ is defined as

$$\phi_X(s) = \int_0^\infty e^{-sx} f_X(x) dx, \tag{4.45}$$

We first need to find the PDFs of X_1, X_2 and X_3. For the PDF of X_1, we derive it in the same way we did in (4.25), which after a few mathematical manipulations, is obtained as

$$f_{X_1}(x) = \frac{\lambda_{s_1,p}(L_s - M + 1)}{(\gamma_{q_1})^{L_s-M+1}(\lambda_{s_1,p}x + \frac{1}{\gamma_{q_1}})^{L_s-M+2}}. \tag{4.46}$$

Without loss of generality, we assume here that both of the sources have the same maximum transmission powers, i.e., $P_{s_1} = P_{s_2}$. Considering that $X_2 = \frac{1}{\gamma_r \left\| \Xi^{\perp} \mathbf{h} \right\|^2}$, which is an inverse chi-square random variable with $2(L_s - M)$ degrees of freedom, the PDF of X_2 is given as

$$f_{X_2}(x) = \frac{e^{\frac{-1}{\gamma_r x}}}{(\gamma_r)^{L_s-M}(L_s - M - 1)! x^{L_s-M+1}}. \tag{4.47}$$

Similarly, the PDF of X_3 is the PDF of the inverse chi-square random variable, which also leads to the following expression

$$f_{X_3}(x) = \frac{e^{\frac{-1}{\gamma_r x}}}{(\gamma_r)^{L_s-M}(L_s - M - 1)! x^{L_s-M+1}}. \tag{4.48}$$

Substituting (4.46) into (4.45), and using [56, 3.382.4], the MGF for X_1 is

$$\phi_{X_1}(s) = \frac{L_s - M + 1}{c^{L_s-M+1}} s^{L_s-M+1} e^{\frac{s}{c}} \Gamma\left(-L_s + M - 1, \frac{s}{c}\right). \tag{4.49}$$

Similarly, substituting (4.47) and (4.48) into (4.45), and using [56, 3.471.9], the MGFs for X_2 and X_3 are

$$\phi_{X_j}(s) = \frac{2(\gamma_r)^{-(L_s-M)}}{\Gamma(L_s - M)} (\gamma_r s)^{\frac{L_s-M}{2}} K_{L_s-M}\left(2\sqrt{\frac{s}{\gamma_r}}\right), \forall\ j = 2, 3, \tag{4.50}$$

where $K_v(.)$ is the modified Bessel function [56].

Now, we can easily find the MGF of $(\gamma_{eq}^{\text{2-TS}})^{-1}$ as the product of $\phi_{X_1}(s)$, $\phi_{X_2}(s)$ and $\phi_{X_3}(s)$, which is given as

$$\phi_{(\gamma_{eq}^{\text{2-TS}})^{-1}}(s) = \delta s^{2L_s-2M+1} e^{\frac{s}{c}} \Gamma\left(-L_s+M-1, \frac{s}{c}\right) \left(K_{L_s-M}\left(2\sqrt{\frac{s}{\gamma_r}}\right)\right)^2. \quad (4.51)$$

By representing the incomplete Gama function into another mathematical form using [56, 3.352.2], (4.51) simplifies to

$$\phi_{(\gamma_{eq}^{\text{2-TS}})^{-1}}(s) = \delta(M-L_s-2)! \sum_{m=0}^{M-L_s-2} \frac{1}{c^m m!} s^{2L_s-2M+1+m} \left(K_{L_s-M}\left(2\sqrt{\frac{s}{\gamma_r}}\right)\right)^2 \quad (4.52)$$

We utilize the following formula to compute the MGF of the $\gamma_{eq}^{\text{2-TS}}$ exploiting the MGF of $(\gamma_{eq}^{\text{2-TS}})^{-1}$ [64, Eq. 18]

$$\phi_{\gamma_{eq}^{\text{2-TS}}}(s) = 1 - 2\sqrt{s}\int_0^\infty J_1(2\beta\sqrt{s})\phi_{(\gamma_{eq}^{\text{2-TS}})^{-1}}(\beta^2)d\beta, \quad (4.53)$$

where $J_1(.)$ is the Bessel function of the first kind [56]. Despite seeming difficult, this formula can still be used to study the performance of the average error probability based on the relationship that exists between the MGF and the symbol error rate [62]. Utilizing the MGF-based form, the average error probability of coherent binary signaling is given by [62, Eq. 9.15]

$$P_e^{\text{2-TS}} = \frac{1}{\pi}\int_0^{\pi/2} \phi_{\gamma_{eq}^{\text{2-TS}}}\left(\frac{A}{\sin^2\varphi}\right) d\varphi, \quad (4.54)$$

where $A = 1$ for BPSK. Substituting (4.53) into (4.54) and after some manipulations, the formula of the error probability becomes

$$P_e^{\text{2-TS}} = \frac{1}{2} - \frac{2}{\pi}\int_0^\infty \phi_{(\gamma_{eq}^{\text{2-TS}})^{-1}}(\beta^2)\int_0^{\frac{\pi}{2}} \sqrt{\frac{A}{\sin^2\varphi}} J_1\left(\sqrt{\frac{4\beta^2 A}{\sin^2\varphi}}\right) d\varphi d\beta. \quad (4.55)$$

The inner integral of (4.55) can be solved by using the variable change and equation [63, eq. 2.12.4.15] which results in the value $\frac{\sin(2\beta\sqrt{A})}{2\beta}$. So the error probability can be evaluated according to the following formula

$$P_e^{\text{2-TS}} = \frac{1}{2} - \frac{2}{\pi}\underbrace{\int_0^\infty \phi_{(\gamma_{eq}^{\text{2-TS}})^{-1}}(\beta^2)\frac{\sin(2\beta\sqrt{A})}{2\beta}d\beta}_{I_4}, \quad (4.56)$$

where $\phi_{(\gamma_{eq}^{2\text{-TS}})^{-1}}$ is the MGF of the inverse SNR given in (4.52).

We put I_4 in the following format

$$I_4(\nu,\mu,a_1,\lambda_1,\lambda_2,b_1,b_2)=\int_0^{\infty} s^{\nu}J_{\mu}(a\sqrt{s})K_{\lambda_1}(b_1\sqrt{s})K_{\lambda_2}(b_2\sqrt{s})ds. \tag{4.57}$$

To continue, we make use of the identity

$$\sin(2\beta\sqrt{A})=\sqrt{\pi\beta\sqrt{A}}\;J_{\frac{1}{2}}(\sqrt{4\beta^2\sqrt{A}}). \tag{4.58}$$

By incorporating (4.52) and (4.58) into (4.56), the format of I_4 in (4.56) becomes as in (4.57), that is,

$$I_4=\int_0^{\infty}\delta(M-L_s-2)!\frac{\sqrt{\pi\sqrt{A}}}{2}\sum_{m=0}^{M-L_s-2}\frac{1}{c^m m!}\beta^{2(z)}\;J_{\frac{1}{2}}(\sqrt{4\beta^2\sqrt{A}})\left(K_{L_s-M}\left(2\sqrt{\frac{\beta^2}{\gamma_r}}\right)\right)^2 d\beta. \tag{4.59}$$

where $z=2L_s-2M+m+\frac{3}{4}$. By solving I_4 in (4.59) using [83], *a closed-form expression for the BER in the 2-TS protocol* is shown as in (4.44). This completes the proof. □

4.7.2 3-TS protocol

Following the same steps used in the 2-TS protocol, the MGF based approach is used to obtain the average error probability expression in the 3-TS protocol. Let $(\gamma_{eq}^{3\text{-TS}})^{-1}=\gamma_{1,3TS}^{-1}+\frac{\gamma_{2,3TS}}{\gamma_{1,3TS}\,\gamma_{3,3TS}}+\gamma_{3,3TS}^{-1}=Y_1+Y_2+Y_3$ where $Y_1=\gamma_{1,2TS}^{-1}$, $Y_2=\frac{\gamma_{2,2TS}}{\gamma_{1,2TS}\,\gamma_{3,2TS}}$ and $Y_3=\gamma_{3,2TS}^{-1}$. As $(\gamma_{eq}^{3\text{-TS}})^{-1}$ is the sum of three independent random variables, the MGF of the $(\gamma_{eq}^{3\text{-TS}})^{-1}$, denoted by $\phi_{(\gamma_{eq}^{3\text{-TS}})^{-1}}(s)$, is $\phi_{(\gamma_{eq}^{3\text{-TS}})^{-1}}(s)=Y_1\times Y_2\times Y_3$.

For the PDF of Y_1, we derive it in the same way as applied in (4.46), which after a few mathematical manipulations, is obtained as

$$f_{Y_1}(x)=\frac{\lambda_{s_1,p}L_s}{(\gamma_{q_1})^{L_s}(\lambda_{s_1,p}x+\frac{1}{\gamma_{q_1}})^{L_s+1}}. \tag{4.60}$$

Considering the same maximum power constraints, $Y_2=\frac{\|\mathbf{f}\|^2}{\gamma_{r_1}\left\|\mathbf{\Xi}^{\perp}\mathbf{f}\right\|^2\|\mathbf{h}\|^2}$, which is a ratio between a chi-square random variable and a product of two chi-square random variables. The PDF of Y_2 is obtained using [84, eq. 22] which after few mathematical manipulations

results in

$$f_{Y_2}(x) = \left(\frac{1}{\gamma_{r_1}}\right)^{\frac{(2L_s-M-1)}{2}} \frac{x^{\frac{-(2L_s-M+1)}{2}}}{(\Gamma(L_s))^2\Gamma(L_s-M)} \times G_{2,1}^{1,2}\left(\gamma_{r_1}x\Big|_{(4L_s-M-1)/2}^{(1+M)/2,(1-M)/2}\right). \quad (4.61)$$

The PDF of Y_3 is the same as the one in (4.48). Substituting (4.60) into (4.45), and using [56, 3.382.4], the MGF for Y_1 is

$$\phi_{Y_1}(s) = \frac{L_s}{c^{L_s}} s^{L_s} e^{\frac{s}{c}} \Gamma(L_s, \frac{s}{c}). \quad (4.62)$$

Similarly, substituting (4.61) into (4.45) and representing the exponential part in terms of Meiger's G-function using [65, eq. 11] as $e^{-sx} = G_{0,1}^{1,0}\left(sx\Big|_{0}^{-}\right)$, $\phi_{Y_2}(s)$ is expressed as

$$\phi_{Y_2}(s) = \int_0^\infty (\gamma_{r_1})^{-(\frac{2L_s-M-1}{2})} \frac{x^{\frac{-(2L_s-M+1)}{2}}}{(\Gamma(L_s))^2\Gamma(L_s-M)} \times G_{2,1}^{1,2}\left(\gamma_{r_1}x\Big|_{(4L_s-M-1)/2}^{(1+M)/2,(1-M)/2}\right) G_{0,1}^{1,0}\left(sx\Big|_{0}^{-}\right) dx. \quad (4.63)$$

Knowing that the integral of the product of two Meijer's G-functions and a power term results also in a Meijer's G-function [65, eq. 21], $\phi_{Y_2}(s)$ simplifies to

$$\phi_{Y_2}(s) = \frac{1}{(\Gamma(L_s))^2\Gamma(L_s-M)} G_{1,3}^{3,1}\left(\frac{s}{\gamma_{r_1}}\Big|_{0,L_s-M,L_s}^{1-L_s}\right). \quad (4.64)$$

The MGF for Y_3 is the same as the one in (4.50). We can now easily find the MGF $\phi_{(\gamma_{eq}^{3\text{-TS}})^{-1}}$ as

$$\phi_{(\gamma_{eq}^{3\text{-TS}})^{-1}}(s) = \delta_1 s^{\frac{3L_s-M}{2}} e^{\frac{s}{c}} \Gamma(L_s, \frac{s}{c}) K_{L_s-M}\left(2\sqrt{\frac{s}{\gamma_{r_1}}}\right) \times G_{1,3}^{3,1}\left(\frac{s}{\gamma_{r_1}}\Big|_{0,L_s-M,L_s}^{1-L_s}\right), \quad (4.65)$$

where $\delta_1 = \frac{2L_s(\gamma_{r_1})^{-\frac{L_s-M}{2}}}{c^{L_s}(\Gamma(L_s))^2}$.

Again, utilizing the relationship that exists between the MGF and symbol error rate [62], the average error probability in the 3-TS protocol can be evaluated according to the following formula

$$P_e^{3\text{-TS}} = \frac{1}{2} - \frac{2}{\pi}\int_0^\infty \phi_{(\gamma_{eq}^{3TS})^{-1}}(\beta^2)\frac{\sin(2\beta\sqrt{A})}{2\beta}d\beta, \quad (4.66)$$

where $\phi_{(\gamma_{eq}^{3\text{-TS}})^{-1}}$ is the MGF of the inverse SNR given in (4.65). Unfortunately, the integral in (4.66) is difficult to evaluate. Therefore, we tackle it using the Gauss-Laguerre quadrature numerical integration as follows [66]:

$$P_e^{3\text{-TS}} \approx \frac{1}{2} - \frac{2}{\pi}\sum_{j=1}^{J} w_j f(A, x_j), \tag{4.67}$$

where J is the number of interpolation points, x_j are the jth zeros of the Laguerre polynomial $L_n(x)$, w_j are the associated weights given by

$$w_j = \frac{(n!)^2 x_j}{(n+1)^2 L_{n+1}(x_j)^2} \tag{4.68}$$

and

$$f(A, x_j) = e^x \phi_{(\gamma_{eq}^{3TS})^{-1}}(x^2)\frac{\sin(2x\sqrt{A})}{2x}. \tag{4.69}$$

The approximate BER expression in (4.67) gives high accuracy results, which will be clear in the subsequent numerical results section.

Remark: Using $\phi_{(\gamma_{eq}^{2\text{-TS}})^{-1}}(s)$ and $\phi_{(\gamma_{eq}^{3\text{-TS}})^{-1}}(s)$ derived in (4.51) and (4.65) respectively, and with the help of the formula in (4.53), the average error probability can be evaluated for different modulation schemes such as M-ary phase shift keying (M-PSK) and M-QAM [62]. For example, the average SER for M-PSK can be obtained as [56, Eq. 9.15]

$$P_e^{\tau\text{-TS}} = \frac{1}{\pi}\int_0^{(\mathrm{M}-1)\pi/\mathrm{M}} \phi_{\gamma_{eq}^{\tau\text{-TS}}}\left(\frac{A}{\sin^2\varphi}\right) d\varphi, \tag{4.70}$$

where $A = \sin^2(\frac{\pi}{\mathrm{M}})$ and $\tau = 2, 3$. Furthermore, (4.55) can be upper bounded by a simple form as in [56, Eq. 9.27]

$$P_e^{\tau\text{-TS}} \leq (1 - 1/\mathrm{M})\phi_{\gamma_{eq}^{\tau\text{-TS}}}(A) \tag{4.71}$$

The equivalent average bit error probability for M-ary PSK assuming Gray coding is well approximated as [60, (5.2.62)]

$$P_b^{\tau\text{-TS}} \approx \frac{P_e^{\tau\text{-TS}}}{\log_2 \mathrm{M}}. \tag{4.72}$$

4.7.3 Asymptotic average bit error probability

To gain key insights, we consider the average bit error probability at high SNR.

Corollary 4.7.2. *The asymptotic average bit error probability at the secondary source S_j in the 2-TS and 3-TS protocols for a two-way AF relaying based distributed ZFB in spectrum-sharing system is obtained by*

$$P_e^{\tau\text{-}TS} \approx \frac{a\sqrt{b}}{2\sqrt{\pi}} \left(\frac{\Gamma(L_s - M + \frac{3}{2})}{c\ \lambda_{s_i,p}^{L_s-M+1} b^{L_s-M+\frac{3}{2}}} + \frac{c\ \Gamma(L_s - M + \frac{1}{2})}{\Gamma(L_s - M + 1) b^{L_s-M+\frac{1}{2}}} \right) \left(\frac{1}{\gamma_{q_i}} \right)^{L_s-M}, \tag{4.73}$$

where $\tau = 2, 3, i = 1, 2$, $c = (\alpha\gamma_r)^{L_s-M+2}$ where $\alpha = 1$ for 2-TS and (a, b) values depend on the modulation scheme.

Proof. The asymptotic error probability can be given through

$$P_{e_\infty}^{\tau\text{-TS}} \approx \frac{a\sqrt{b}}{2\sqrt{\pi}} \int_0^\infty \frac{e^{-bu}}{\sqrt{u}} F_{\gamma_{eq_\infty}}^{\tau\text{-TS}}(u) du. \tag{4.74}$$

where $F_{\gamma_{eq_\infty}}^{\tau\text{-TS}}(u)$ is the approximate CDF as $\gamma_{q_i} \to \infty$. Utilizing (4.43) combined with Corollary 4.6.3 and after doing the integration, we get (4.73). This concludes the proof. □

Similar to the asymptotic outage probability case, (4.73) suggests the same diversity gain $L_s - M$ with similar conclusions. It is worth noting that this diversity gain is achieved in the regime where there is a constraint on Q, not on P_{s_j}. However, if P_{s_j} is limited, an error floor will occur and hence the diversity gain approaches zero at high SNRs.

4.7.4 Power allocation at the relays

In this section, the design of the power allocation parameter α at the secondary relays is investigated. The objective is to pick α such that the minimum average error probability at the two secondary receivers is achieved. Specifically, α is chosen according to the optimization problem:

$$\begin{aligned} \alpha_{opt} = \arg \min_{\alpha} \left(P_e^{3\text{-TS},S_2}(\alpha) + P_e^{3\text{-TS},S_1}(\alpha) \right) \\ \text{subject to } 0 < \alpha < 1 \end{aligned} \tag{4.75}$$

where $P_e^{3\text{-TS},S_2}$ and $P_e^{3\text{-TS},S_1}$ are the average error probability at S_2 and S_1, respectively and can be obtained from (4.56). Obtaining a closed-form expression for the solution to (4.75) is not easy. As an alternative, it can be solved numerically as we will show later. Obviously

the sum average error probability is minimized when α_{opt} is used, and this yields better performance compared to the case when α is fixed.

To get more insight on the impact of α, we exploit the asymptotic error expression in (4.73) to find the behavior of α if different transmit powers from the sources are assumed.

Corollary 4.7.3. *For the 3-TS protocol, the power allocation parameter which minimizes the sum of of the average error probability at both transceivers at high SNR is given by*

$$\alpha = \left(\frac{(\gamma_{q_1})^{L_s-M}\Gamma(L_s-M+\frac{3}{2})P_r^{L_s-m+2}}{\lambda_{s_2,p}^{L_s-M+1}\Gamma(L_s-M+\frac{1}{2})(\gamma_{q_2})^{L_s-M}+\lambda_{s_1,p}^{L_s-M+1}\Gamma(L_s-M+\frac{1}{2})(\gamma_{q_1})^{L_s-M}P_r^{L_s-m+2}} \right)^{\frac{1}{L_s-M+1}} \tag{4.76}$$

Proof. By suming the average error probability at both transceivers from (4.73) and taking the derivative with respect to α and then solve for α, we get (4.76). □

We observe that for a fixed total transmit power at the transceivers and relays, α gradually increases with Q_1, suggesting that more power is allocated for the transceiver with a higher transmit power. We stress here the fact that the value of α in (4.76) is not the exact solution to (4.75). However, (4.76) gives a good indication on the impact of the power allocation on the system performance in the 3-TS protocol, as shown in Fig. 8.

4.8 Numerical Results and Discussion

In this section, we investigate the performance of the derived results through numerical examples and simulations. Unless otherwise stated, the distance between the sources equals d. Let d_{S_j,R_i}denote the distance from S_j to the ith relay, and hence, $d_{S_1,R_i} = d - d_{S_2,R_i}$. We assume that the relays are located on a straight line vertical to the distance between the two sources, however, the results and conclusions of this paper extend to any setting. Furthermore, the path loss exponents is set to four. The channel mean power for the links from PUs to the secondary nodes is defined by the locations, as $\lambda_{r_i,p} = (\sqrt{d_x^2+d_y^2})^{-4}$, where (d_x, d_y) are the coordinates of the PUs. We also assume that $\lambda_{s_1,p} = \lambda_{s_2,\bar{p}} = 1$. It is also assumed that the range of the power transmission of S_1 and S_2 is limited according to the peak power constraints that were mentioned in the system model.

4.8.1 Effects of ZFB, number of relays and number of PUs on the performance

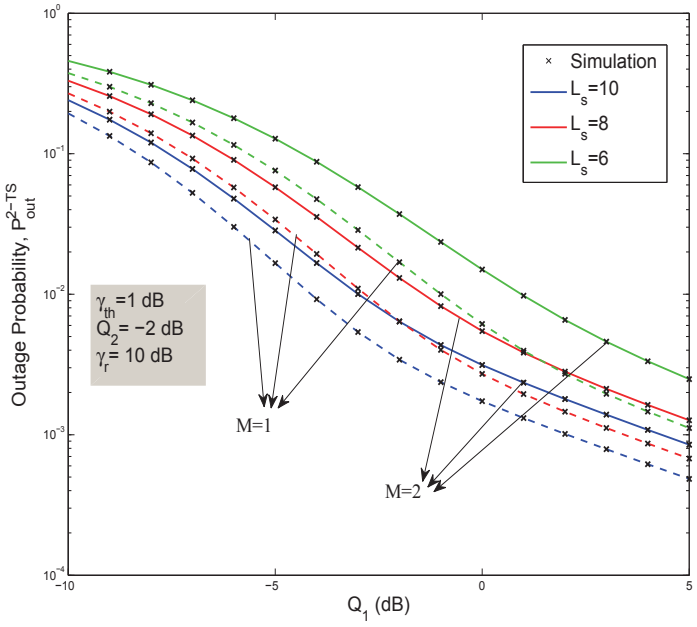

Figure 4.2: Outage probability vs. Q_1 (dB) for the 2-TS protocol for L_s= 6, 8, 10 and M=1, 2

Figs. 4.2 and 4.3 show the outage performance of S_2 versus Q_1 for $L_s = 6, 8, 10$, $M = 1, 2$ at $\gamma_{th} = 1$ dB, $\gamma_{q_2} = -2$ dB, $\gamma_r = 10$ dB and $\gamma_{r_1} = 5$ dB. As observed from the figures, as the value of Q_1 increases, the outage performance improves substantially. Moreover, by increasing the number of relays with ZFB, we observe significant improvements in the outage performance. This is attributed to the combined cooperative diversity and beamforming which enhances the total received SNR at the receiver. Clearly, as the number of existing PUs increases from one to two, the outage performance becomes worse because the secondary sources have to adapt their transmit powers according to the most affected PU.

Figs. 4.4 and 4.5 illustrate the average bit error probability performance versus $Q_1 = Q_2 = Q$ for L_s= 6, 8, 10 and $M = 1, 2, 3$, $\gamma_r = \gamma_{r_1} = 5$ dB at $\gamma_{th} = 1$dB. It is obvious that the average bit error probability performance improves substantially as the number of relays increases and Q becomes looser. With beamforming and increasing the number of relays, the

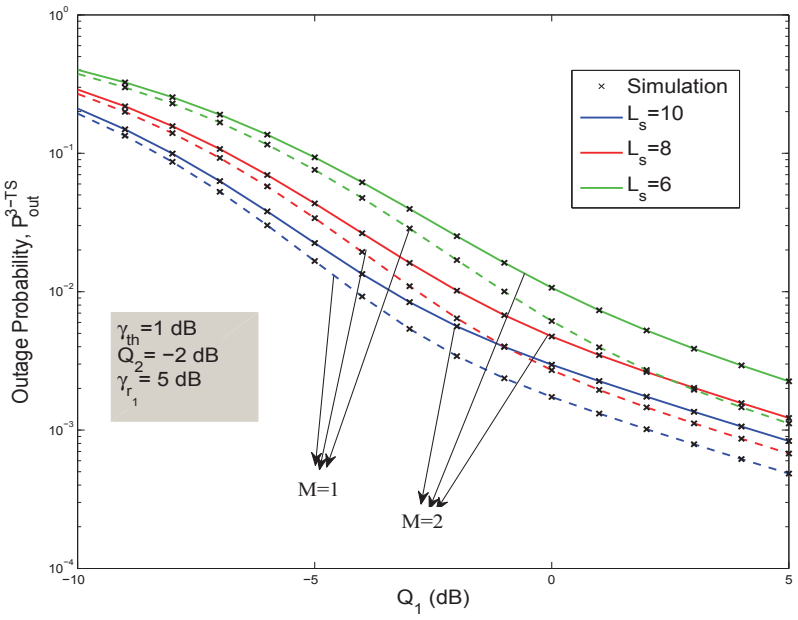

Figure 4.3: Outage Probability vs. Q_1 (dB) for the 3-TS protocol for L_s= 6, 8, 10 and M=2,3

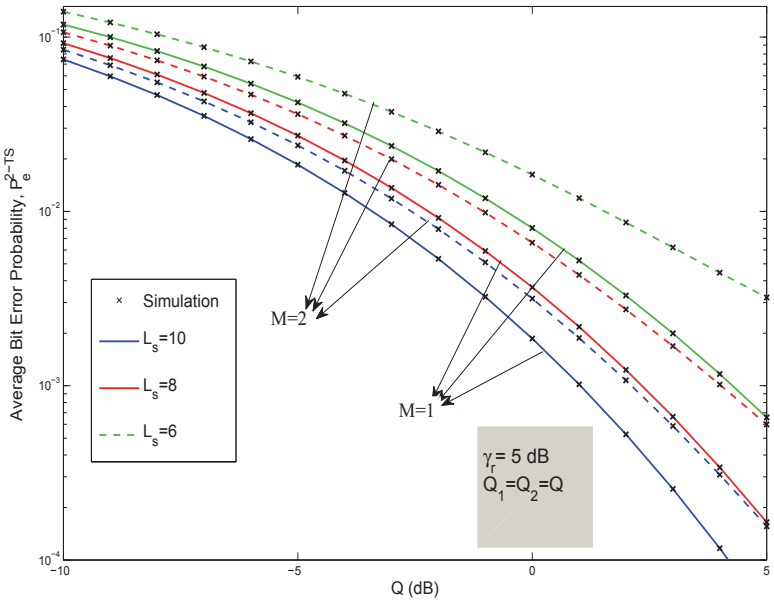

Figure 4.4: Average bit error probability vs. Q (dB) for the 2-TS protocol forL_s=6, 8, 10 and M=1, 2.

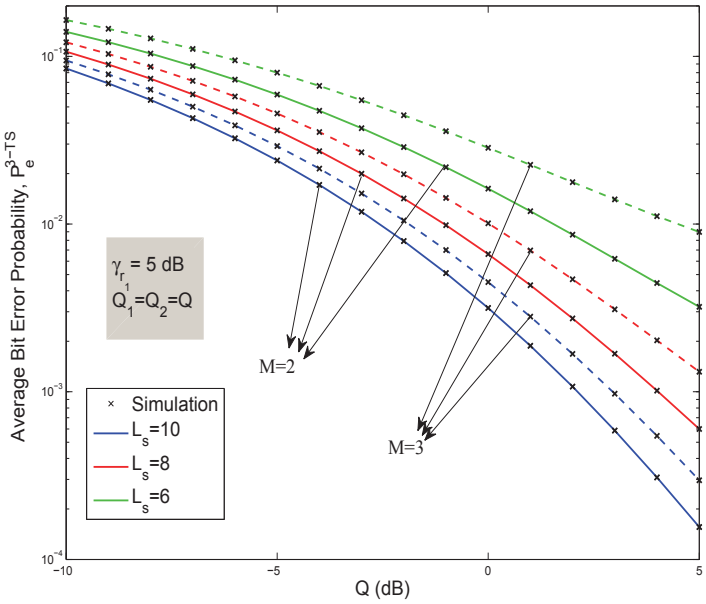

Figure 4.5: Average bit error probability vs. Q (dB) for the 3-TS protocol for L_s=6, 8, 10 and M=2, 3.

gain becomes more. The larger the number of existing PUs, the worse the error probability, as expected.

4.8.2 Comparison between 2-TS and 3-TS

For fair comparison, we fix the total transmit power at the relays, i.e. P_r and the total available power at both transceivers, i.e., $P_{s_1} + P_{s_2}$. Hence, for 4-TS protocol, we use $P_r/2$ in the second and fourth time-slot to keep the total power the same.

In Fig. 4.6, the outage probability for the 2-TS, 3-TS and 4-TS protocols is investigated. We use $\gamma_{r_1} = 0.5\gamma_r$, $L_s = 7, 8$, $M = 4$ at two different SNR thresholds $\gamma_{th} = 1, 3$ dB. It can be readily seen that the outage performance in the 3-TS protocol performs better than that of the 2-TS and 4-TS protocols for the same values of L_s, M and γ_{th}. This offers a good trade-off between the system performance and bandwidth efficiency. It is also clear from the figure that as γ_{th} goes from one to three, the curves shift up implying worse performance.

For a fair comparison in the average bit error probability curves, we use two different

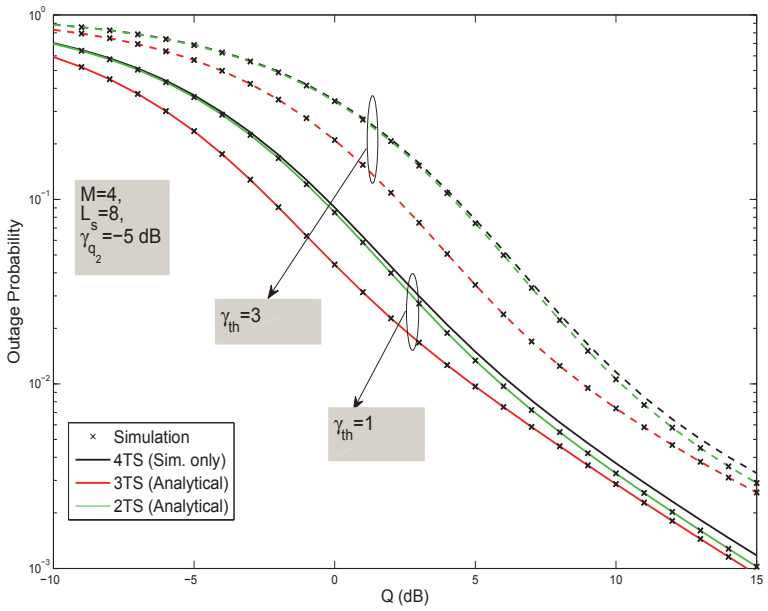

Figure 4.6: Outage probability vs. Q (dB) for the 2-TS, 3-TS and 4-TS protocols, with L_s=8 and M=4.

modulation schemes to maintain the same spectral efficiency. We use quadrature phase shift keying (QPSK), 8-PSK and 16-PSK modulation schemes for the 2-TS, 3-TS and 4-TS transmission protocols, respectively.

Fig. 4.7 shows a plot for the average bit error probability versus Q_2 of both 2-TS, 3-TS and 4-TS for varying values of Q_1, $L_s = 6, 8$ and $M = 4$. The analytical results are based on (4.72). For the 3-TS protocol, we use the optimum values of α according to (4.75) obtained only by simulations which minimize the average error probability at both transceivers. We notice that when the values of Q_2 increases from 0 to 10, the 3-TS protocol performs better than the 2-TS protocol when $Q_1 = 1.8Q_2$ and also when $Q_1 = 0.5Q_2$. This is due to the reason that, in 3-TS, the different transmit powers at transceivers S_1 and S_2 lead to a different power weightining at the relays. The transceiver with a higher transmit power will be weighted more at the relay than the transceiver with a lower transmit power. This is not the case in the 2-TS and 4-TS where the received signals from both transceivers are weighted equally and thus can not make use of the different transmit power to improve the system performance [70]. This highlights a good advantage that the 3-TS is effective when

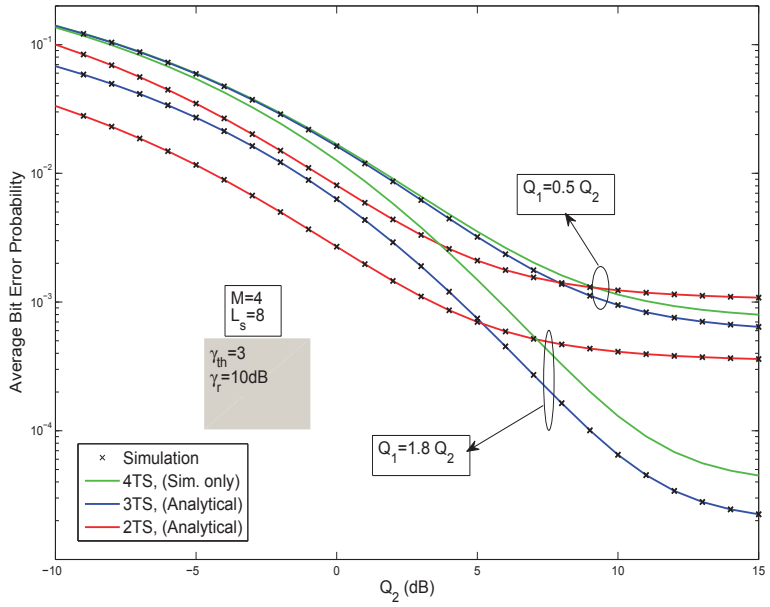

Figure 4.7: Average bit error probability vs. Q (dB) for the 2-TS with (QPSK) 3-TS with (8-PSK) and 4-TS with (16-PSK) protocols, L_s=8 and M= 4.

the transmit powers at the transceivers are different. This is a practical scenario since in underly cognitive radio networks, the transceivers powers vary, depending on the interference constraints.

Fig. 4.8 shows the asymptotic average bit error probability performance of the 2-TS and 3-TS protocol versus Q assuming $\gamma_r = 10$, $L_s = 10$, $M = 2, 3$ at $\gamma_{th} = 1$ dBs. We see a good match between the asymptotic results based on (4.73) and the simulation results. Observations and conclusions similar to the ones made for the other figures hold for this figure. Based on the analytical results in (4.73), it is obvious that the diversity gain of both schemes at the given parameters is same.

In Fig. 4.9, we plot the optimal values of α for the 3-TS protocol as function of Q_2 for different values of Q_1. As explained in the analytical section, the value of α increases or decreases with Q_1. The signal broadcasted by the transceiver with a higher transmit power will be weighted more at the relays than the signal broadcasted by the transceiver with lower transmit power. Meanwhile, in the 2-TS protocol, the received signals at the relays are weighted equally. Note that the curves are not matching at high values of Q_2 because one

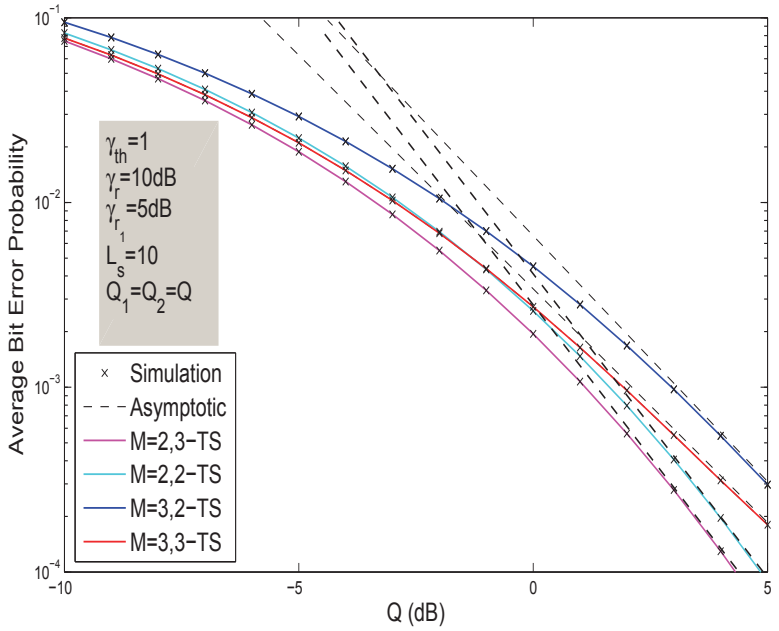

Figure 4.8: Asymptotic average bit error probability vs. Q_2 (dB) for the 2-TS and 3-TS protocols, L_s=10 and M= 2,3 using BPSK.

curve results from simulations whereas the other is obtained analytically at high values of Q_2. However, they have the same trend.

4.8.3 Comparison between the sub-optimal ZFB beamforming scheme and the optimal beamforming scheme

In Fig. 4.10, the performance of the achievable sum-rate for the 2-TS and 3-TS protocols employing the ZFB scheme is compared (the achievable sum-rate curve is generated by simulations, where over 50,000 channel realizations were generated and averaged) with the one that employed optimal beamforming scheme, e.g., [75]. The optimization problem for the system in [75] is to maximize the sum-rate of both transceivers subject to power constraints. The system is a two-way multi-antenna relay channel that transmits over two time-slots. For comparison, we assume that the total power available at the relay/s is the same, the number of antennas in [75] is equal to the number of relays $L_s = 4$ in our system and $M = 1, 2$. It is observed that there is a 1-dB gap between the performance of the adopted ZFB scheme and

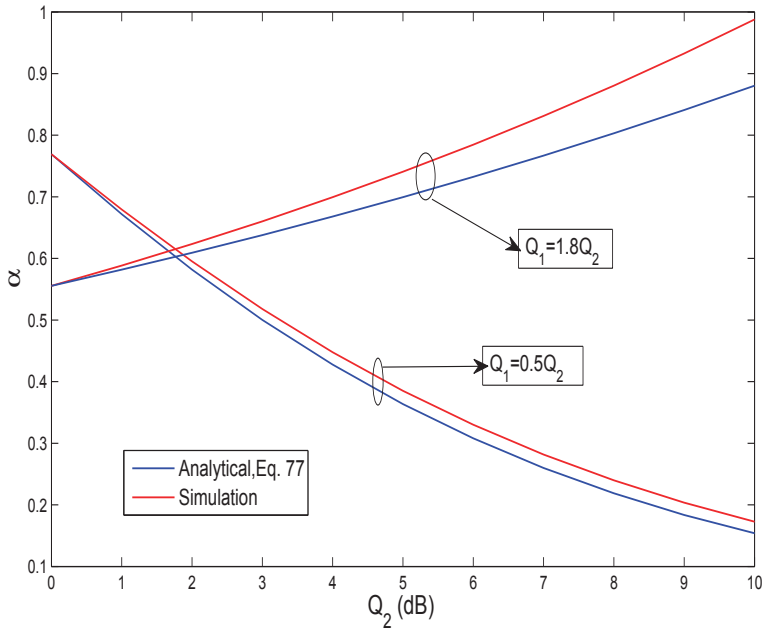

Figure 4.9: Power allocation parameter α vs. Q_2 (dB) for the 3-TS protocol, L_s=6 and M= 3. and $P_r = 10$ dB

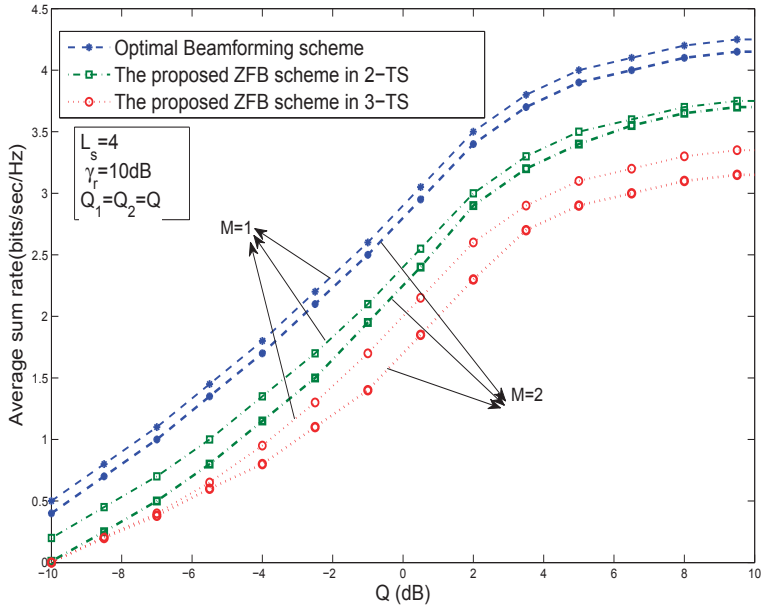

Figure 4.10: Average sum rate comparison between the proposed ZFB scheme and the optimal beamforming scheme, with L_s=4 and M=1,2.

the optimal beamforming scheme. However, our proposed scheme offers a good performance at lower complexity in addition to being practically implementable if compared to the optimal scheme. The figure also clarifies that 2-TS is better than the 3-TS protocol in terms of bandwidth efficiency, which is expected. Although adding one more time-slot in the 3-TS protocol enhances the performance in terms of outage and error probabilities, the bandwidth efficiency of 2-TS protocol is still better.

To compare the complexity between the proposed scheme and the optimal scheme, we note that the ZFB vector has a small fixed complexity, requiring only one matrix inversion $\mathbf{\Xi}^{\perp}$ and one matrix multiplication to obtain the beamforming weights. However, in the optimal scheme in [75], an iterative numerical optimization technique is used which converges within 20-30 iterations. Within each of these iterations, a number of matrix multiplications, matrix inversions, and vector 2-norm calculations for each user are needed to find the solution. So the computational complexity of the two schemes is not comparable.

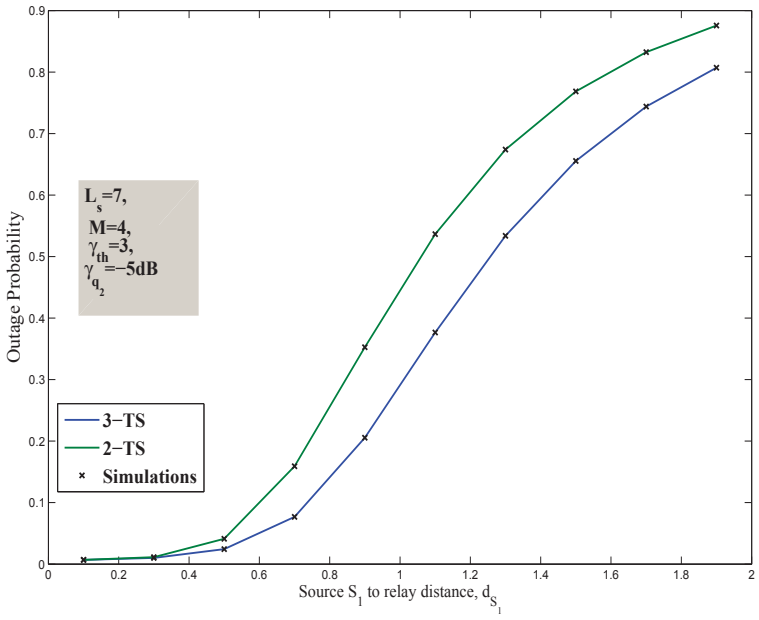

Figure 4.11: Outage probability vs. d_{S_1} of 2-TS and 3-TS protocols, L_s=7 and M=4.

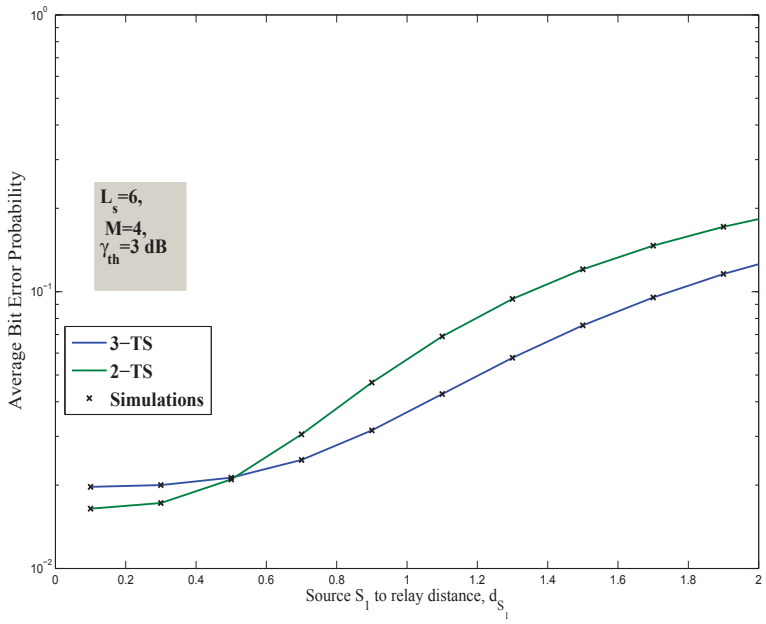

Figure 4.12: Average error probability vs. d_{S_1} of 2-TS and 3-TS protocols, L_s=6 and M=4.

4.8.4 Relays positioning

We can consider different relay positions by suitably scaling the average transmit SNR at the secondary transceivers and relays. In particular, if d_{S_1} is the distance between source S_1 and the ith relay, and d_{S_2} the distance between source S_2 and the ith relay, then the average transmit SNRs, which consider the relay positions, can be written as

$$\bar{\gamma_{q_1}} = \frac{\gamma_{q_1}}{d_{S_1}^n}, \bar{\gamma_{q_2}} = \frac{\gamma_{q_2}}{d_{S_2}^n}, \bar{\gamma_r} = \frac{\gamma_r}{d_{S_2}^n}, \bar{\gamma_{r_1}} = \frac{\gamma_{r_1}}{d_{S_2}^n}, \tag{4.77}$$

where n is the path loss exponent.

For comparison, we fix the distance between sources S_1 and S_2, denoted by d, such that $d = d_{S_1} + d_{S_2}$.

Fig. 4.11 illustrates the outage performance in the 2-TS and 3-TS protocols versus d_{S_1} for $L_s = 7$, $M = 4$ at $\gamma_{th} = 3$ dB and $n = 3$. Both of the protocols performs better in the low d_{S_1} values and becomes worse for higher values. So the best range for d_{S_1} is $d_{S_1} < 0.4$. The figure also shows that the 3-TS protocol performs better than 2-TS protocol as the distance becomes higher.

In Fig. 4.12, the average error probability performance versus d_{S_1} for $L_s = 6$, $M = 4$ at

$\gamma_{th} = 3$ dB and $n = 3$ for both 2-TS and 3-TS protocols is evaluated. For low values of d_{S_1}, the 2-TS protocol outperform the 3-TS protocol but for moderate to higher values of d_{S_1}, the 3-TS protocol performs better. This happens due to the same reasons mentioned before.

4.9 Conclusion

We investigated a cooperative two-way AF relaying system model in a spectrum sharing environment. The proposed system limits the interference to the primary users using a distributed ZFB approach and peak interference power constraints. The beamforming weights were optimized to maximize the received SNR at both secondary transceivers and to null the interference inflicted on the primary users. We considered two transmission protocols over two time-slots and three time-slots. It is often expected that the three time-slot protocol is subordinate to the two time-slot protocol due to the loss in the data rate. Such a comparison, however, ignores the fact the 3-TS protocol benefits from one additional degree of freedom per relay. To clarify the potential advantages of 3-TS and 2-TS transmission protocols and study the performance tradeoffs of both of them in spectrum sharing systems, we investigated the performance of the secondary system by deriving closed-form expressions for the outage and average error probabilities. We compared the performances of the two protocols in terms of outage probability, average error probability and average sum-rate. When compared to the performance of the optimal beamforming scheme, the adopted sub-optimal ZFB scheme performance is somehow close to the optimality in terms of average sum-rate performance. Our numerical results showed that the distributed ZFB method enhances the outage and error probability performances by increasing number of participating relays in addition to limiting interference to PUs. In addition, our results showed that the 3-TS protocol outperforms the 2-TS protocol in certain scenarios, which was clear in the outage and error probabilities performance. As a result, the 3-TS protocol offers a good compromise between bandwidth efficiency and system performance. As an extension, adaptive 2-TS/3-TS system could be adopted to enhance both bandwidth and performance.

Chapter 5

Two-Way DF Relay Cognitive Networks under Primary-Secondary Mutual Interference and Beamforming

5.1 Introduction

In Chapter 4, two-way AF relaying in spectrum-sharing systems was studied to further improve the spectrum efficiency and enhance the secondary system performance. In this chapter, we adopt collaborative distributed beamforming in two-way DF selective relay CR network. We consider a three TS underlay spectrum-sharing two-way relay network comprising two secondary transceivers communicating with each other via a number of secondary DF relays in the presence a number of PUs. In the first and second TSs, the first and second transceivers broadcast their signals to all available relays, respectively. In the third TS, only the relays that receive the signals (from both transceivers) reliably are used for relaying and beamforming. Specifically, the selected relays combine the two received signals using physical layer network coding (XORing or superposition) and employ distributed beamforming to keep the reflected interference at the PU-RXs to a predefined threshold in addition to improving the performance of the secondary system.

In this chapter, we aim to address three main issues: 1) which two-way relaying strategy should be chosen to achieve two-way communication between the two transceivers; 2) how to design the optimal beamforming weights at the secondary relays in order to maximize the received SNRs at the destinations while the interference to the PU-RXs is constrained to a tolerable threshold; and 3) how to allocate the power at the relays in an efficient way. To

this end, we consider two-way relaying strategies: DF-XOR and DF-superposition [85]- [87]. For each relaying strategy, we adopt the sub-optimal ZFB vectors as a special case of optimal beamforming for tractability at the secondary relays. To analyze the system performance and compare between the relaying strategies, we present an analytical framework for each relaying strategy under the effect of the PU-TXs' CCIs. In particular, we derive closed-form expressions for the E2E outage probability, BER and achievable sum-rates. To get more insight, we derive asymptotic expressions of the outage and BER performance at high SNRs. We also compare the proposed relaying strategies with the three time-slot AF relaying strategy reported in Chapter 4. The analytical and simulation results show that DF-XOR outperforms DF-superposition and AF when fixed power allocation is used at the relays. However, when optimal power allocation is used at the relays, DF-superposition performs similar to DF-XOR while the former outperforms AF. This is attributed to the different weighting of the received signals at the relays where the transceiver with a higher transmit power is weighted with a higher weight as compared to the one with a lower transmit power. The results also demonstrate the efficacy of combining beamforming and cooperative diversity for compensating for the secondary performance loss due to the CCI.

The rest of this chapter is organized as follows. Section 5.2 describes the system and channel models. Optimal beamfrming and ZFB weight design is described in Section 5.3. Section 5.4 introduces the end-to-end performance analysis. Numerical results are presented in Section 5.5. Section 5.6 concludes the chapter.

5.2 System and Channel Models

5.2.1 System Model

We consider a two-way relaying system that is composed of two secondary transceivers S_j, $j = 1, 2$ and a set of L DF secondary relays denoted by R_i for $i = 1, 2, ..., L$ coexisting in the same spectrum band with a primary system consisting of a cluster of M PU-TXs- N PU-RXs pairs as shown in Fig. 5.1. All nodes are equipped with one antenna. The two SUs wish to exchange information through the secondary relays. It is assumed that there is no direct link

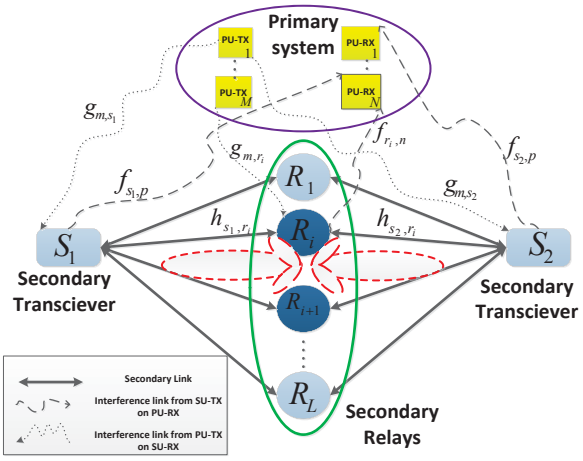

Figure 5.1: Spectrum-sharing system with two-way DF relaying.

between the two SUs. The relay nodes operate in the half-duplex mode and they use the time division broadcast (TDBC) protocol during three time-slots $(\mathrm{TS}_i), i = 1, 2, 3$ [71]. In TS_1, based on the interference CSI from S_1 to the nth PU-RX, which suffers the most interference caused by S_1 (the strongest interference channel), S_1 adjusts its transmit power under a predefined threshold Q_1 and broadcasts its message to all relays.[1] Similarly, in TS_2, based on the interference CSI from S_2 to the $\bar{n}$th PU-RX, which suffers the most interference caused by S_2 (the nth and $\bar{n}$th PU-RXs could be different or the same), S_2 adjusts its transmit power under a predefined threshold Q_2 and broadcasts its message to all relays. In TS_3, distributed beamforming employing ZFB is applied to null the interference from the selected potential relays L_s (that are eligible to participate) to the N PU-RXs so that the relays are always able to transmit without interfering with the PU-RXs.[2]

All channel coefficients are assumed to be independent Rayleigh flat fading such that $|h_{s_j,r_i}|^2, |f_{s_j,p}|^2, |f_{r_i,n}|^2, |g_{m,s_j}|^2$, $|g_{m,r_i,1}|^2$ and $|g_{m,r_i,2}|^2$ are exponential distributed random variables with parameters $\lambda_{s_j,r_i}, \lambda_{s_j,p}, \lambda_{r_i,n}, \lambda_{m,s_j}$, $\lambda_{m,r_i,1}$ and $\lambda_{m,r_i,2}$ respectively. Let the ZFB vectors $\mathbf{w}_{\mathbf{zf_1}}^T = [w_{11}, w_{12}, ..., w_{1L_s}]$ used to direct the signal to S_1 and $\mathbf{w}_{\mathbf{zf_2}}^T = [w_{21}, w_{22}, ..., w_{2L_s}]$ used to direct the signal to S_2 and $\mathbf{W_{zf}}$ is $L_s \times L_s$ ZFB processing matrix. Let $\mathbf{h}_{r,s_j}^T =$

[1]It is assumed that S_1 and S_2 have perfect knowledge of their interference channel power gains, which can be acquired through a spectrum-band manager that mediates between the primary and secondary users [46], [74], [88]

$[h_{r_1,s_j},...,h_{r_{L_s},s_j}]$ be the channel vectors between the potential relays and S_j, $j=1,2$. Let $\mathbf{F}_{\mathbf{rp}}^T = [\mathbf{f}_{\mathbf{r},\mathbf{p_1}},...,\mathbf{f}_{\mathbf{r},\mathbf{p_N}}]$ be the channel matrix between the relays and all N PU-RXs where $\mathbf{f}_{\mathbf{r},\mathbf{p_n}} = [f_{r_1,n},...,f_{r_{L_s},n}]$.

In the underlying system model, we assume that the transceivers acting as transmitters do not have any CSI, however, it is assumed that each transceiver as a receiver knows the channels from the other transmitter to the relays and its own receiving channels. In other words, each S_j knows $\mathbf{h}_{\mathbf{r},\mathbf{s_j}}$, $j=1,2$ [71]. In practice, this CSI can be obtained by traditional channel training, estimation, and feed-back mechanisms (see for example [53] and references therein.) Also, the transceivers are assumed to have full knowledge of the interference between L_s and PUs, i.e., $\mathbf{F}_{\mathbf{rp}}$. Exploiting the knowledge of the CSI at the transceivers, $\mathbf{w}_{\mathbf{zf_1}}$ and $\mathbf{w}_{\mathbf{zf_2}}$ are designed at S_1 and S_2 and sent back to the relays by only one of the transceivers via low date-rate feedback links, and that is applicable in slow fading environments [54], [72].

5.2.2 Transmission Model

As mentioned earlier, the communication process occurs over three time-slots. In the first time slot, TS_1, S_1 transmits and in the second time slot, TS_2, S_2 transmits. As such, when S_j for $j=1,2$ transmit, the received signal at the ith relay is given as

$$y_{r_{i,j}} = \sqrt{P_j} h_{s_j,r_i} x_{s_j} + \sum_{m=1}^{M} \sqrt{P_{int}}\, g_{m,r_i,j}\, \hat{x}_{im,j} + n_{i,j}, \tag{5.1}$$

where P_j is the transmit power of S_j , P_{int} is the interference power inflicted from the PU-TX, x_{s_j} is the information symbol of S_j, $\hat{x}_{im,j}$ is the mth PU-TX interfering symbol at the ith relay and $n_{i,j}$ denotes the noise at the ith relay in the jth TS. We assume that the transmitted symbols are equiprobable with unit energy. As the secondary relays adopt DF relaying, they need to decode the signals in TS_1 and TS_2. Upon receiving both signals, the set of relays, that can correctly decode both of x_{s_1} and x_{s_2} by using cyclic redundancy codes, is referred as the decoding set $\mathcal{C}$. Each relay in $\mathcal{C}$ performs certain processing and then forwards simultaneously the combined signal in the third time-slot to both transceivers. In

[2] As we will see late, we derive the optimal beamforming weights where optimality is in the sense of maximizing the SNRs at the destinations. However, we use ZFB in the analysis for tractability. Note that, ZFB is a special case of the derived optimal weights.

this work, we consider on DF-XOR and DF-Superposition in our analysis and compare their performances with performance of three time-slot AF relaying.

5.2.3 XOR Relaying

In this strategy, each relay combines the received signals from TS_1 and TS_2 by adding the decoded bit sequences using exclusive-OR addition. Let $\mathbf{b_{s_j}}$ denote the decoded bit sequence from x_{s_j}, for $j = 1, 2$. By applying the XOR operation ($\oplus$), the combined bit sequence results in $\mathbf{b_{s_{1,2}}} = \mathbf{b_{s_1}} \oplus \mathbf{b_{s_2}}$. Then the combined bit sequence is encoded, modulated and weighted as $L_s \times 1$ signal $\mathbf{x}_{s_{1,2}} = \mathbf{W_{zf}}\mathbf{b_{s_{1,2}}}$. Thus the received signal at each S_j is given by

$$y_{s_j,3} = \sqrt{P_r}\mathbf{h}^H_{r,s_j}\mathbf{x}_{s_{1,2}} + \sum_{m=1}^{M}\sqrt{P_{int}}\, g_{m,s_j}\hat{x}_{jm,3} + n_{j,3}, \tag{5.2}$$

wher $\hat{x}_{jm,3}$ is the mth PU-TX interfering symbol at S_j and $n_{j,3}$ denotes the noise at each S_j in TS_3. Each S_j can demodulate the received signal and then XOR it with its own transmit bits to obtain the desired data.

Therefore, the corresponding total received SINR at S_j given $\mathcal{C}$, denoted $\gamma^{\oplus}_{s_j|\mathcal{C}}$, is given by

$$\gamma^{\oplus}_{s_j|\mathcal{C}} = \frac{P_r|\mathbf{h}^H_{r,s_j}\mathbf{x}_{s_{1,2}}|^2}{\sum_{m=1}^{M} P_{int}\,|g_{m,s_j}|^2 + \sigma^2}. \tag{5.3}$$

5.2.4 Superposition Relaying

If the secondary relays adopt superposition relaying, each relay weights the received signals (from both sources) and combines them linearly, i.e., $\mathbf{x}_{s_{1,2}} = \sqrt{\alpha_1}\mathbf{w_{zf_1}}x_{s_1} + \sqrt{\alpha_2}\mathbf{w_{zf_2}}x_{s_2}$. Then the received signal at each S_j is given by

$$y_{s_j,3} = \sqrt{P_r}\mathbf{h}^H_{r,s_j}(\sqrt{\alpha_1}\mathbf{w_{zf_1}}x_{s_1} + \sqrt{\alpha_2}\mathbf{w_{zf_2}}x_{s_2}) + \sum_{m=1}^{M}\sqrt{P_{int}}\, g_{m,s_j}\hat{x}_{jm,3} + n_{j,3}, \tag{5.4}$$

where α_1 and α_2 are the power allocation parameters such that $\alpha_1^2 + \alpha_2^2 = 1$. As each S_j has perfect knowledge of x_{s_j}, $\mathbf{w_{zf_j}}$ and $\mathbf{h}^H_{r,s_j}$, it subtracts the self-interference term and therefore the resultant total received SINR at S_j given $\mathcal{C}$, denoted $\gamma^{+}_{s_j|\mathcal{C}}$, is given by

$$\gamma^{+}_{s_j|\mathcal{C}} = \frac{P_r\alpha_j|\mathbf{h}^H_{r,s_j}\mathbf{w_{zf_j}}|^2}{\sum_{m=1}^{M} P_{int}\,|g_{m,s_j}|^2 + \sigma^2}. \tag{5.5}$$

Remark: If the relay does not have any knowledge of the channels between itself and the transceivers, it chooses $\alpha_1 = \alpha_2 = 0.5$. For the case when the ith relay has some channel knowledge about h_{r_i,s_1} and h_{r_i,s_2} (it may learn it during the previous transmission from the transceivers to the ith relay in slow fading environments), α_j may be optimized such that the sum-rate is maximized. This will be explored in the performance analysis section.

5.2.5 Mathematical Model and Size of $\mathcal{C}$

In this underlay model, S_j can utilize the PU's spectrum as long as the interference it generates at the most affected PU-RX remains below the interference threshold Q_j. For that reason, P_j is constrained as $P_j = \min\left\{\frac{Q_j}{\max\limits_{n=1,\ldots,N}|f_{s_j,n}|^2}, P_{s_j}\right\}$ where P_{s_j} where P_{s_j} is the maximum transmission power of S_j, for $j = 1, 2$. So the received SINR at the ith relay in the k time-slot for $k = 1, 2$ is given as

$$\gamma_{s_j,r_i,k} = \frac{\min\left\{\frac{Q_j}{\max\limits_{n=1,\ldots,N}|f_{s_j,n}|^2}, P_{s_j}\right\}|h_{s_j,r_i}|^2}{\sum_{m=1}^{M} P_{int}|g_{m,r_i,k}|^2 + \sigma^2}, \tag{5.6}$$

Lemma 5.2.1. *The CDF expression of the received SINR at the ith secondary relay in the kth time-slot is derived as*

$$\begin{aligned} F_{\gamma_{s_j,r_i,k}}(x) &= 1 - e^{-\frac{\lambda_{s_j,r_i}\sigma^2 x}{P_s}} F_T(\frac{Q_j}{P_s})\left(\frac{\lambda_{s_j,r_i}P_{int}x}{\lambda_{m,r_i,k}P_s}+1\right)^{-M} - \psi\frac{Q_j N\lambda_{s_j,n}}{\lambda_{s_j,r_i}P_{int}\,x}\sum_{n=1}^{N-1}\binom{N-1}{n}(-1)^n \\ &\times\ e^{-\frac{Q_j}{P_s}\lambda_{s_j,n}(n+1)}\left[(-1)^{\kappa-1}\beta^\kappa e^{\beta\mu}Ei[-\beta\mu] + \sum_{a=1}^{\kappa}\Gamma(a)(-\beta)^{\kappa-a}\mu^{-a})\right), \end{aligned} \tag{5.7}$$

where $F_T(\frac{Q_j}{P_s}) = (1 - e^{\frac{\lambda_{s_j,n}Q_j}{P_s}})^N$,$\psi = e^{-\frac{\lambda_{s_j,r_i}\sigma^2 x}{P_s}}\frac{\lambda_{m,r_i,k}^M}{\Gamma(M)}$, $\kappa = M-1$, $\beta = \frac{\sigma^2}{P_{int}} + \frac{(n+1)\lambda_{s_j,n}Q_j}{\lambda_{s_j,r_i}P_{int}\ x}$, $\mu = \lambda_{m,r_i,k} + \frac{\lambda_{s_j,r_i}P_{int}\ x}{P_{s_j}}$ and $Ei[.]$ is the exponential integral defined in [56].

Proof. See Appendix B.1. □

We define $\mathcal{C}$ to be the set of relays which perfectly decode both signals received in TS_1 and TS_2, which implies that there is no outage at these relays. This translates to the fact that the mutual information between each S_j and the ith relay is above a specified target value. In this case, the potential ith relay is only required to meet the decoding constraint

given as [7]

$$\Pr\left[R_i \in \mathcal{C}\right] = \Pr\left[\frac{1}{3}\log_2(1+\gamma_{s_j,r_i,k}) \geq \frac{R_{th}}{2}\right], i = 1,..,L \tag{5.8}$$

where (1/3) is from the message transmission in three time-slots and R_{th} denotes the minimum target rate below which outage occurs. By using the the Binomial distribution, the probability that the size of $\mathcal{C}$ equals L_s, denoted by, $\Pr\left[|\mathcal{C}| = L_s\right]$ becomes

$$\Pr\left[|\mathcal{C}| = L_s\right] = \binom{L}{L_s} P_{\text{off}}^{L-L_s}(1-P_{\text{off}})^{L_s}, \tag{5.9}$$

where P_{off} denotes the probability that the relay does not decode correctly both signals and keeps silent in TS_3. Let P_{o_1} and P_{o_2} be the outage probabilities at any relay for a signal transmitted from S_1 and S_2, respectively, then P_{off} is computed as

$$P_{\text{off}} = 1-(1-P_{o_1})(1-P_{o_2}), \tag{5.10}$$

where P_{o_j} for $j = 1, 2$ can be computed from (5.7) as

$$P_{o_j} \quad = \quad F_{\gamma_{s_j,r_i,k}}(\gamma_{th}), \tag{5.11}$$

where $\gamma_{th} = 2^{\frac{3}{2}R_{th}} - 1$ is the SINR threshold at the ith relay in the kth time-slot.

5.3 Optimal Beamforming Weights Design

Our objective here is to maximize the received SNRs at the two transceivers in order to enhance the performance of the secondary system while limiting the interference to the PU receivers to a tolerable level. Mathematically, the problem formulations for finding the optimal weight vector are described as follows.

$$\begin{aligned} \max_{\mathbf{v}_{opt_1},P_r} \quad & P_v|\mathbf{h}_{\mathbf{r},\mathbf{s_1}}^H \mathbf{v}_{opt_1}|^2 \\ \text{s.t.:} \quad & |\mathbf{f}_{\mathbf{r},\mathbf{p_i}}^H \mathbf{v}_{opt_1}|^2 \leq Q_i/P_r, \ \forall i = 1,...,N \\ & \|\mathbf{v}_{opt_1}\|^2 = 1, P_r \leq P_v. \end{aligned} \tag{5.12}$$

$$\begin{aligned} \max_{\mathbf{v}_{opt_2},P_r} \quad & P_v|\mathbf{h}_{\mathbf{r},\mathbf{s_2}}^H \mathbf{v}_{opt_2}|^2 \\ \text{s.t.:} \quad & |\mathbf{f}_{\mathbf{r},\mathbf{p_i}}^H \mathbf{v}_{opt_2}|^2 \leq Q_i/P_r, \ \forall i = 1,...,N \\ & \|\mathbf{v}_{opt_2}\|^2 = 1, P_r \leq P_v. \end{aligned} \tag{5.13}$$

To solve the above problems, we first find the optimal beamforming vectors $\mathbf{v}_{opt_j}$ for $j = 1, 2$ and then the relays transmit power P_v is found so that the interference constraint is satisfied. We decompose $\mathbf{v}_{opt_j}$ as a linear combination of two orthonormal vectors, namely, $\mathbf{v}_{opt_j} = \alpha_{v_j}\mathbf{w_{zf_j}} + \beta_{v_j}\mathbf{w_{o_j}}$, where α_{v_j} and β_{v_j} are complex valued weights with $|\alpha_{v_j}|^2 + |\beta_{v_j}|^2 = 1$ to keep $\left\|\mathbf{v}_{opt_j}\right\|^2 = 1$.

For the zero-interference constraint case, i.e. $Q_i = 0$ for all $i = 1, ..., N$, the optimal beamforming vectors are the ZFB vectors, i.e., $\mathbf{v}_{opt_j} = \mathbf{w_{zf_j}}$. According to the ZFB principles, $\mathbf{w_{zf_1}}$, $\mathbf{w_{zf_2}}$ are chosen to lie in the orthogonal space of $\mathbf{F}_{\mathbf{rp}}^H$ such that $|\mathbf{f}_{\mathbf{r,p_i}}^H\mathbf{w_{zf_1}}| = 0$ and $|\mathbf{f}_{\mathbf{r,p_i}}^H\mathbf{w_{zf_2}}| = 0$, $\forall i = 1, ..., N$ and $|\mathbf{h}_{r,s_1}^H\mathbf{w_{zf_1}}|$, $|\mathbf{h}_{r,s_2}^H\mathbf{w_{zf_2}}|$ are maximized. By applying a standard Lagrangian multiplier method, the weight vectors that satisfy the above optimization methods are given as

$$\mathbf{w_{zf_1}} = \frac{\mathbf{\Xi}^{\perp}\mathbf{h}_{r,s_1}}{\|\mathbf{\Xi}^{\perp}\mathbf{h}_{r,s_1}\|}, \ \mathbf{w_{zf_2}} = \frac{\mathbf{\Xi}^{\perp}\mathbf{h}_{r,s_2}}{\|\mathbf{\Xi}^{\perp}\mathbf{h}_{r,s_2}\|}, \tag{5.14}$$

where $\mathbf{\Xi}^{\perp} = \left(\mathbf{I} - \mathbf{F_{rp}}(\mathbf{F_{rp}^{\dagger}}\mathbf{F_{rp}})^{-1}\mathbf{F_{rp}^{\dagger}}\right)$ is the projection idempotent matrix with rank $(L_s - N)$. It can be observed from the rank of the matrix that the cooperative ZBF beamformer becomes effective only when $L_s > N$.

For the non-zero interference constraint, the secondary relays can increase their transmit power in their own direction, i.e. $\mathbf{h_{r,s_j}}$. Generally, in this case, the beamforming vector is not in the null space of $\mathbf{F_{rp}}$ and since $\mathbf{w}_{\mathbf{zf_j}}^H\mathbf{w_{o_j}} = 0$, we have

$$\mathbf{w_{o_j}} = \frac{\mathbf{h_{r,s_j}} - \mathbf{w}_{\mathbf{zf_j}}^H\mathbf{h_{r,s_j}}\mathbf{w_{zf_j}}}{\sqrt{1 - |\mathbf{w}_{\mathbf{zf_j}}^H\mathbf{h_{r,s_j}}|^2}}. \tag{5.15}$$

By finding $\mathbf{w_{zf_j}}$ and $\mathbf{w_{o_j}}$, the optimal weights are derived as $|\beta_{v_j}| \leq \sqrt{\frac{Q_i}{P_v||\mathbf{f_{r,p_i}}||^2|\mathbf{f}_{\mathbf{r,p_i}}^H\mathbf{w_{o_j}}|^2}}$, $\alpha_{v_j} = \frac{\mathbf{w}_{\mathbf{zf_j}}^H\mathbf{h_{r,s_j}}}{|\mathbf{w}_{\mathbf{zf_j}}^H\mathbf{h_{r,s_j}}|}\sqrt{1 - \beta_{v_j}^2}$ and $P_v \leq P_r$. To elaborate, a geometric explanation of $\mathbf{v}_{opt_j}$ is given in Fig. 5.2 where by rotating $\mathbf{v}_{opt_j}$ from the ZFB vector $\mathbf{w_{zf_j}}$ toward the MRT beamformer $\frac{\mathbf{h_{r,s_j}}}{||\mathbf{h_{r,s_j}}||}$, the secondary relays can maximize the SNR received at the secondary destination at the expense of increasing the interference to the PU while still respecting a predefined threshold Q_i. In the case of MRT, $\mathbf{v}_{opt_j} = \frac{\mathbf{h_{r,s_j}}}{||\mathbf{h_{r,s_j}}||}$, and therefore the interference becomes inactive (non-cognitive case). In overall, the optimal beamforming vector is given as

$$\mathbf{v}_{opt_j} = \frac{\mathbf{h_{r,s_j}} - \mathbf{w}_{\mathbf{zf_j}}^H\mathbf{h_{r,s_j}}\mathbf{w_{zf_j}}}{\sqrt{1 - |\mathbf{w}_{\mathbf{zf_j}}^H\mathbf{h_{r,s_j}}|^2}} + \frac{\mathbf{\Xi}^{\perp}\mathbf{h}_{r,s_j}}{\left\|\mathbf{\Xi}^{\perp}\mathbf{h}_{r,s_j}\right\|}. \tag{5.16}$$

Motivated by simplicity and low complexity of ZFB, we only consider $\mathbf{w_{zf_j}}$ for $j = 1, 2$

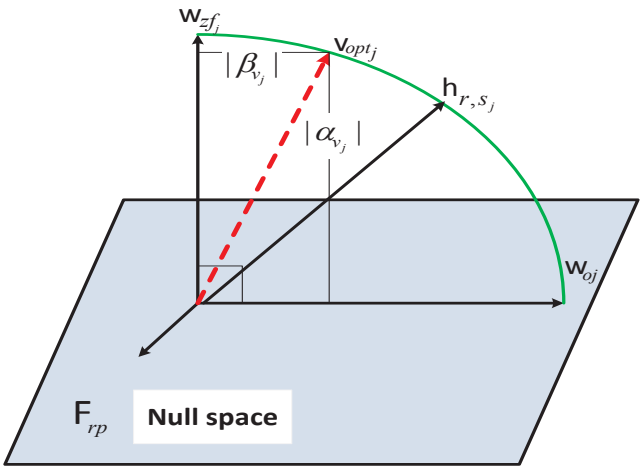

Figure 5.2: Geometric explanation of v_{opt_j}.

because it enables us to obtain closed-form expressions and get insights on the asymptotic performance of the underlying system.

5.3.1 XOR Relaying

Since each relay knows its weight coefficients, the ZFB matrix $\mathbf{W_{zf}}$ is made up by the diagonal of the product of the two ZFB vectors $\mathbf{w_{zf_1}}$ and $\mathbf{w_{zf_2}}$ which is represented as (see [54], [72], [75] and references therein)

$$\mathbf{W_{zf}} = \mathrm{Diag}(\mathbf{w_{zf_1}}\mathbf{w}_{\mathbf{zf_2}}^{T}). \tag{5.17}$$

It is worth noting that the weights matrix is diagonal, which guarantees that the relays transmit only their own received signal and there is no data exchange among the relays. Thus, the algorithm works in a distributed manner.

5.3.2 Superposition Relaying

The ZFB vectors in superposition relaying are simply chosen to be $\mathbf{w_{zf_1}}$ and $\mathbf{w_{zf_2}}$ given by (5.14) in the first and second time-slot, respectively. In the third time-slot, the weighted received signals are combined linearly with certain power allocation values as described previously.

5.4 Performance Analysis

In this section, we examine the performance of the proposed relaying strategies in terms of the outage probability, BER and achievable sum-rates metrics in the presence of CCIs. As we will see, the derived expressions are cumbersome, and therefore, to get more insights, we derive asymptotic expressions for the outage and BER performance.

5.4.1 Statistics of the Total Received SINR

After finding $\mathbf{W_{zf}}$ in the XOR relaying strategy, we substitute (5.17) into (5.3) to get the total received SINR at S_j given $\mathcal{C}$

$$\gamma^{\oplus}_{s_j|\mathcal{C}} = \frac{P_r||\mathbf{\Xi}^{\perp}\mathbf{h_{r,s_j}}||^{\mathbf{2}}}{\sum_{m=1}^{M} P_{int}|g_{m,s_j}|^2 + \sigma^2}. \tag{5.18}$$

Similarly, in superposition relaying, substituting (5.14) into (5.5), the total received SINR at S_j given $\mathcal{C}$ is given by

$$\gamma^{+}_{s_j|\mathcal{C}} = \frac{P_r\alpha_j||\mathbf{\Xi}^{\perp}\mathbf{h_{r,s_j}}||^{\mathbf{2}}}{\sum_{m=1}^{M} P_{int}\,|g_{m,s_j}|^2 + \sigma^2}. \tag{5.19}$$

To analyze the system, we firstly need to obtain the PDF and CDF of the unconditional total received SINR, i.e., $\gamma^{*}_{s_j}$, where $(^*)$ refers to ($^+$ or $^{\oplus}$).

Lemma 5.4.1. *The CDF expression of the total received SINR at S_j is given by substituting the values of $\alpha_j = 1$ for DF-XOR and $0 < \alpha_j < 1$ for superposition relaying in the following expression*

$$\begin{aligned} F_{\gamma^{*}_{s_j}}(x) &= \sum_{L_s=0}^{N} \binom{L}{L_s} P_{off}^{L-L_s}(1-P_{off})^{L_s} + \sum_{L_s=N+1}^{L} \binom{L}{L_s} P_{off}^{L-L_s}(1-P_{off})^{L_s} \\ &\times \left(1 - \frac{\lambda_{m,s_j}^{M}}{\Gamma(M)} \sum_{i=0}^{L_s-N-1} \sum_{k=0}^{i} \binom{k}{i} P_{int}^{k}(\sigma^2)^{i-k} e^{-\frac{\sigma^2 x}{\alpha_j P_r}} \frac{(M-1+k)!\,x^i}{(\lambda_{m,s_j} + \frac{P_{int}x}{\alpha_j P_r})^{M+k}}\right). \end{aligned} \tag{5.20}$$

Proof. See appendix B.2. □

The PDF of $\gamma^{*}_{s_j}$, denoted by, $f_{\gamma^{*}_{s_j}}(\gamma)$ is simply obtained by differentiating (5.20). For an

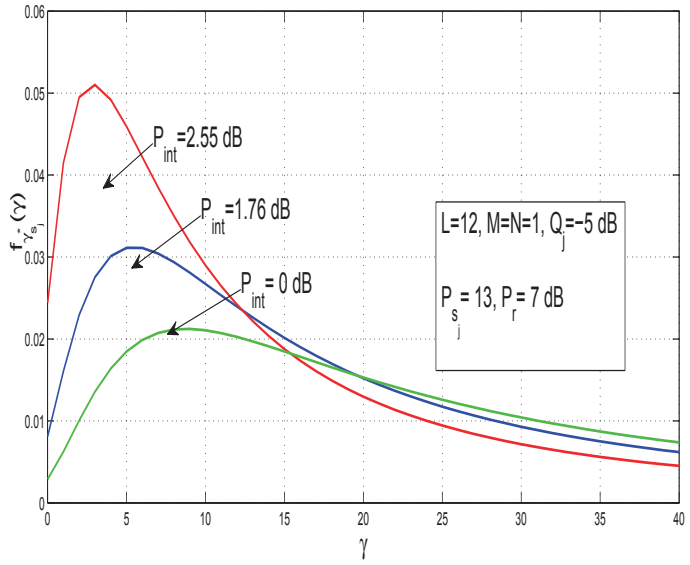

Figure 5.3: PDF of the end-to-end received SIR at S_j, $f_{\gamma^*_{s_j}}(\gamma)$.

interference-limited scenario, i.e., $\sigma^2 = 0$, the PDF is given as

$$f_{\gamma^*_{s_j}}(x) = \sum_{L_s=0}^{N} \binom{L}{L_s} P_{\text{off}}^{L-L_s}(1-P_{\text{off}})^{L_s}\delta(x) + \sum_{L_s=N+1}^{L} \binom{L}{L_s} P_{\text{off}}^{L-L_s}(1-P_{\text{off}})^{L_s} \times \Gamma[L_s-N+M]\left(\frac{\zeta \; x^{L_s-N-1}}{\left(\frac{x}{\alpha_j P_r}+\frac{\lambda_{m,s_j}}{P_{int}}\right)^{L_s-N+M}}\right), \tag{5.21}$$

where $\zeta = \frac{(\lambda_{m,s_j})^M}{\Gamma(\varphi)\Gamma(M)P_{int}^M(\alpha_j P_r)^{\varphi}}$, and $\delta(.)$ is the Dirac function that refers to received SIR when the relays are inactive. It is plotted in Fig. 5.3 for various values of P_{int}. It clarifies the effect of reducing the interference power from PU-TXs on improving the total received SINR at S_j. As P_{int} decreases, the curve shifts towards the right-side, which means that the probability to have a better received SINR for a certain channel condition becomes higher.

In the subsequent sections, we exploit the statistics of the received SINR at both transceivers to investigate the performance of the outage probability, the E2E BER and the achievable sum-rate metrics.

5.4.2 Outage Probability

An outage event occurs when the total received SINR falls below a certain threshold γ_{th} and is expressed as $P_{out_j^*} = \Pr(\gamma_{s_j}^* < \gamma_{th})$. By using (5.20), the user outage probability of S_j in a closed-form can be written as

$$P_{out_j^*} = F_{\gamma_{s_j}^*}(\gamma_{th}). \tag{5.22}$$

To get more insight on the key parameters, e.g., M, N, L etc., we derive an approximate expression for the outage probability that shows the behavior of the system at high SINRs.

Corollary 5.4.2. *An asymptotic outage probability expression is given by substituting the values of $\alpha_j = 1$ for DF-XOR and $0 < \alpha_j < 1$ for superposition relaying in the following expression*

$$P_{out_j^*}^{\infty} = \sum_{L_s=0}^{N} \binom{L}{L_s} \tilde{P}_{off}^{L-L_s}(1-\tilde{P}_{off})^{L_s} + \sum_{L_s=N+1}^{L} \binom{L}{L_s} \tilde{P}_{off}^{L-L_s}(1-\tilde{P}_{off})^{L_s} F_{\gamma_{s_j|\mathcal{C}}^*}(\gamma_{th}) \tag{5.23}$$

where $\tilde{P}_{\text{off}} \overset{P_{s_j}\to\infty}{\approx} \left(\left(\sum_{n=0}^{N-1} \binom{N-1}{n} \frac{(-1)^n}{(n+1)^2} \right) \frac{\lambda_{s_j,r_i} MNP_{int}}{\lambda_{s_j,p}\lambda_{m,r_i,k} Q_j} + \left(1 - e^{-\frac{Q_j}{\lambda_{s_j,p} P_{s_j}}}\right)^N \left(\frac{\lambda_{s_j,r_i} MP_{int}}{\lambda_{m,r_i,k} P_{s_j}} \right) \right) \gamma_{th}$

and $F_{\gamma_{s_j|\mathcal{C}}^*}(\gamma_{th})$ is given in (B.7).

Proof. See appendix B.3. □

As can be observed from (5.23), when the peak interference threshold Q_j is fixed and the maximum transmit power P_{s_j} is constrained, the outage performance exhibits an error-floor at the high SINR. As a conclusion, the diversity order is zero at high SINR and therefore the secondary network is more applicable for low P_{s_j} values.

5.4.3 E2E BER

We analyze the BER performance due to errors occurring at S_j assuming that all participating relays have accurately decoded and regenerated the message. This probability could be evaluated using the following identity

$$P_{err_j^*} = \frac{a\sqrt{b}}{2\sqrt{\pi}} \int_0^{\infty} \frac{e^{-bu}}{\sqrt{u}} F_{\gamma_{s_j}^*}(u) du. \tag{5.24}$$

Since P_{err_j} depends on the modulation scheme, many expressions can be used. For example, BPSK is obtained by setting $(a, b) = (1, 1)$, whereas quadrature phase-shift keying (QPSK) is attained by setting $(a, b) = (2, 1/2)$.

Theorem 5.4.3. *A closed-form expression for a two-way DF relaying strategy with ZFB based is given by substituting the values of $\alpha_j = 1$ and $0 < \alpha_j < 1$ with DF-XOR and superposition relaying, respectively.*

$$P_{err_j^*} = \frac{a}{2}\sum_{L_s=0}^{N}\binom{L}{L_s}P_{off}^{L-L_s}(1-P_{off})^{L_s} + \sum_{L_s=N+1}^{L}\binom{L}{L_s}P_{off}^{L-L_s}(1-P_{off})^{L_s} \times \left(\frac{a}{2} - \frac{\eta\,\Phi}{\Gamma(M+k)}\left(\frac{P_{int}}{\alpha_j P_r}\right)^{-(M+k)}\left(\frac{\sigma^2}{\alpha_j P_r}+b\right)^{-\beta} G_{2,1}^{1,2}\left(\frac{P_{int}}{b\alpha_j P_r + \lambda_{m,s_j}\sigma^2}\middle|_{M+k}^{1,1-\beta}\right)\right), \tag{5.25}$$

where $\eta = \frac{(\frac{P_{int}}{\alpha_j P_r})^{-(M+k)}}{\Gamma(M+k)}$, $\beta = i-M-k+0.5$ and $\Phi = \frac{a\sqrt{b}}{2\sqrt{\pi}}\frac{\lambda_{m,s_j}^M}{\Gamma(M)}\sum_{i=0}^{L_s-N-1}\sum_{k=0}^{i}\binom{k}{i}P_{int}^k(\sigma^2)^{i-k}(M-1+k)!$.

Proof. See Appendix B.4. □

Although the expressions in (5.25) enable numerical evaluation of the exact E2E BER performance, it may not provide useful insights on the effect of key parameters (e.g., the number of secondary relays, the number of PUs, etc.) that influence the system performance. To get more insights, we now introduce an asymptotic BER expression, i.e., $P_{s_j} \to \infty$, for the DF-XOR and DF-Superposition relaying strategies.

Corollary 5.4.4. *An asymptotic BER expression is given by substituting the values of $\alpha_j = 1$ for DF-XOR and $0 < \alpha_j < 1$ for superposition relaying in the following expression*

$$P_{err_j^*}^{\infty} = \frac{a}{2}\sum_{L_s=0}^{N}\binom{L}{L_s}\tilde{P}_{off}^{L-L_s}(1-\tilde{P}_{off})^{L_s} + \sum_{L_s=N+1}^{L}\binom{L}{L_s}\tilde{P}_{off}^{L-L_s}(1-\tilde{P}_{off})^{L_s}\ I_2, \tag{5.26}$$

where I_2 is evaluated in (B.23).

Proof. Similar to the proof of Corollary 1. □

Similar to the asymptotic outage probability case, (5.26) suggests a zero diversity gain with similar conclusions. It is worth noting that diversity gain of $(L - N)$ is achieved in the low Q_j regime. However, if P_{s_j} is limited, an error floor will occur and hence the diversity gain approaches zero at high SINRs [89].

5.4.4 Achievable Sum-Rate

The achievable sum-rate is a substantial performance metric for wireless communications systems because it determines the maximum achievable transmission rate under which the system may adequately function. Specifically, for two-way relaying systems, the achievable sum-rate can be expressed as [70], [71]

$$R_{sum} = \underbrace{\frac{1}{3}\mathrm{E}[\log_2(1+\gamma^*_{s_1})]}_{R_1} + \underbrace{\frac{1}{3}\,\mathrm{E}[\log_2(1+\gamma^*_{s_2})]}_{R_2}. \tag{5.27}$$

Theorem 5.4.5. *A closed-form expression for the unconditional achievable rate at S_j in an interference-limited scenario is given by substituting the values of $\alpha_j = 1$ and $0 < \alpha_j < 1$ for DF-XOR and superposition relaying, respectively.*

$$R_j \;=\; \sum_{L_s=N+1}^{L} \binom{L}{L_s} P_{off}^{L-L_s}(1-P_{off})^{L_s}\psi\, G_{3,3}^{3,2}\left(\frac{P_{int}}{\lambda_{m,s_j}\alpha_j P_r}\middle|_{L_s-N+M,M,M}^{1,M,1+M}\right), \tag{5.28}$$

where $\psi = \frac{\log_2(e)}{3}\frac{(-1)^{-M-1}(\alpha_j P_r)^M}{\Gamma(\varphi)\Gamma(M)P_{int}^M}$. By substituting (5.28) into (5.27), we get a closed form expression of the achievable sum-rate of the system.

Proof. See Appendix B.5. □

It can be seen from (5.28) that when the number of the relays is less than the number of primary receivers, i.e., $L_s < N$, the first term of the sum-rate expression disappears and the reason is that the relays are inactive.

5.5 Numerical Results and Discussion

In this section, we investigate the performance of the derived results through numerical examples and simulations. Unless otherwise stated, let d_{S_j,R_i}denote the distance from S_j to the ith relay, and hence, $d_{S_1,R_i} = 1 - d_{S_2,R_i}$. Furthermore, the path loss exponents is set to four. We assume that the relays are located on a straight line vertical to the distance between the two sources, however, the results and conclusions of this paper extend to any setting. We furthermore assume that the primary system forms a cluster where PU-TXs are closely located to each others and as all PU-RXs. The distance between the transceivers equals one.

We also assume that $\lambda_{s_1,p} = \lambda_{s_2,p} = 1, \lambda_{m,s_1} = \lambda_{m,s_2} = 5$, $\lambda_{s_j,r_i} = 1$,$\lambda_{m,r_i,1} = \lambda_{m,r_i,2} = 1$. We also set $P_r = 5$ dB, the outage threshold as $\gamma_{th} = 1$ dB and $Q_1 = Q_2 = Q$. We compare the two DF relaying strategies with a three time-slot AF relaying strategy proposed in Chapter 4. For a fair comparison, we assume that the total available power at the two transceivers and the relays, i.e., $P_{s_j} + P_r$,$\forall j = 1, 2$, is kept the same for the various relaying strategies. Also, we use $\alpha_1 = \alpha_2 = 0.5$ for a fixed power allocation strategy and we use (5.29) when the optimal power allocation strategy is used. We consider BPSK modulation scheme, however, the derived expressions are general for any higher modulation scheme.

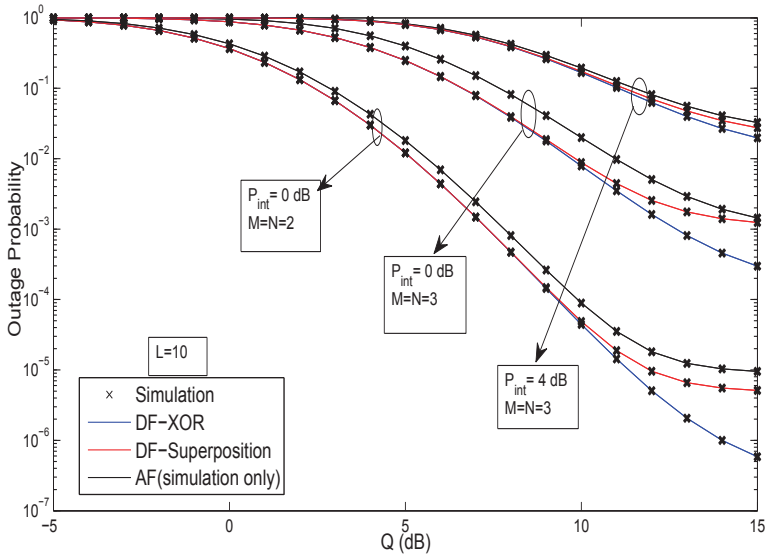

Figure 5.4: Outage probability vs. Q (dB) for $M = N = 2, 3, L = 10$ and different P_{int} values.

5.5.1 Fixed Power Allocation Parameters

Fig. 5.4 shows the outage performance of S_j versus Q for $L = 10$, $M = N = 2, 3$ and different values of $P_{int} = 0, 4$dB. As observed from the figure, as the value of Q increases, the outage performance improves substantially for all curves. Clearly, as the number of existing PU-TX increases from two to three, the outage performance becomes worse as this will increase the sum of the CCIs that severely affects the received signals at the transceivers. Also, the figure shows the impact of CCIs on the outage performance. As P_{int} increases,

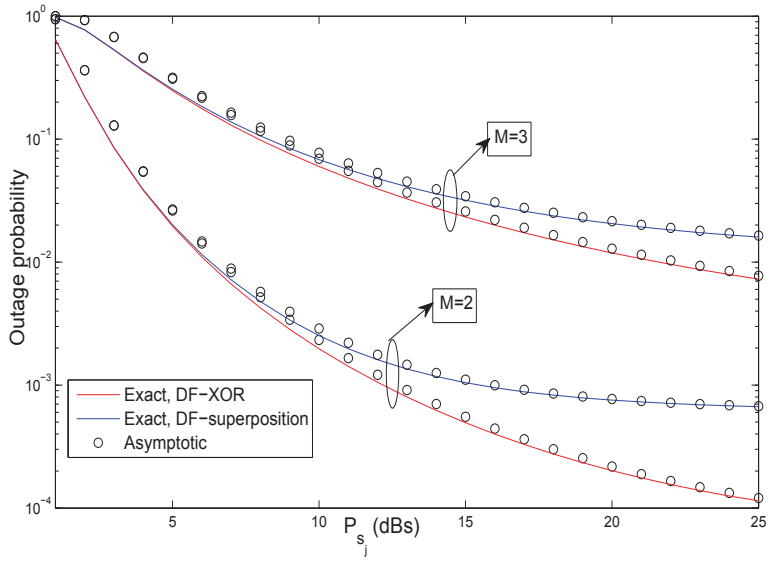

Figure 5.5: Asymptotic outage probability vs. P_{s_j} (dB) for $M = N = 2, 3, L = 6$ and fixed P_{int}.

it degrades the system performance significantly. However, a compensation of this loss in performance is gained by the use of beamforming with cooperative diversity. Comparing between the three strategies, it is seen that the performance of the DF-XOR outperforms the DF-superposition and AF. The reason is that, for the case of the DF-superposition, R_i transmits $\mathbf{x}_{s_{1,2}} = \sqrt{\alpha_1}\mathbf{w_{zf_1}}x_{s_1} + \sqrt{\alpha_2}\mathbf{w_{zf_2}}x_{s_2}$. One of the terms is actually self-interference to S_j, and hence, the power used to transmit this term is wasted. However, when DF-XOR is used, R_i transmits $\mathbf{x}_{s_{1,2}} = \mathbf{W_{zf}b_{s_{1,2}}}$ and no transmission power is wasted to transmit self-interferences. In the case of AF relaying, the relays do not decode the signals and simply amplify both the signal and the noise which leads to the worst performance.

In Fig. 5.5, a plot of the asymptotic outage probability is shown versus P_{s_j} for both relaying strategies. It shows a good agreement between the exact and asymptotic analytical curves at high SNRs. As predicted by the previous analysis, an error floor occurs at high values of P_{s_j} which indicates that the CR networks are only applicable in the low P_{s_j} region.

In Fig. 5.6, a comparison between employing the optimal beamforming vector in (5.16) (simulations only) and ZFB vectors in (5.14) in terms of outage performance is investigated. For the same transmit powers, number of relays and PUs, the results show that there is only

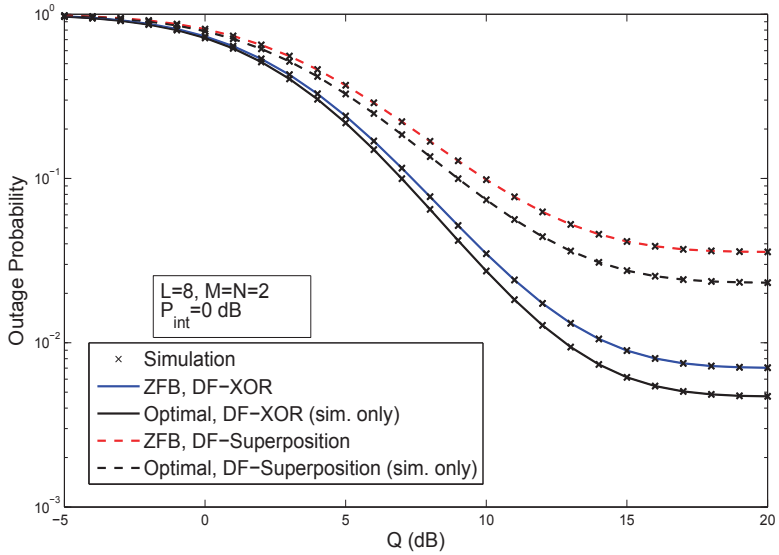

Figure 5.6: Outage performance comparison employing ZFB and optimal beamforming vectors for $M = N = 2, L = 8$ and fixed P_{int}.

a little difference in the system performance when employing the optimal beamformer versus the ZFB as Q becomes higher. However, the complexity of ZFB is less since it involves only projection to the null space of the interference channel matrix without designing the weights parameters α_{v_j} and β_{v_j}.

Fig. 5.7 illustrates the E2E BER performance versus Q for L= 6, 8 and $M = N = 2$. It is obvious that the BER performance improves substantially as the number of relays increases and Q becomes looser. This is attributed to the combined cooperative diversity and beamforming which enhances the total received SNR at the receiver. In addition, it is observed from the BER and outage figures that there is an error floor in the high Q region and the curves result in zero-diversity. This error flooring is due to the limitations on the secondary transmit powers and co-channel interferences. Similar to the outage performance observations, the DF-XOR outperforms both DF-Superposition and AF strategies due to the same reasons mentioned earlier.

Fig. 5.8 shows the E2E BER performance versus L for $M = N = 1, 2$ at fixed $P_{int} = -1.25$ dB. As the number of available relays increases, all relaying strategies' performance improves. This is due to the reason that the probability to get more potential relays that succeed to

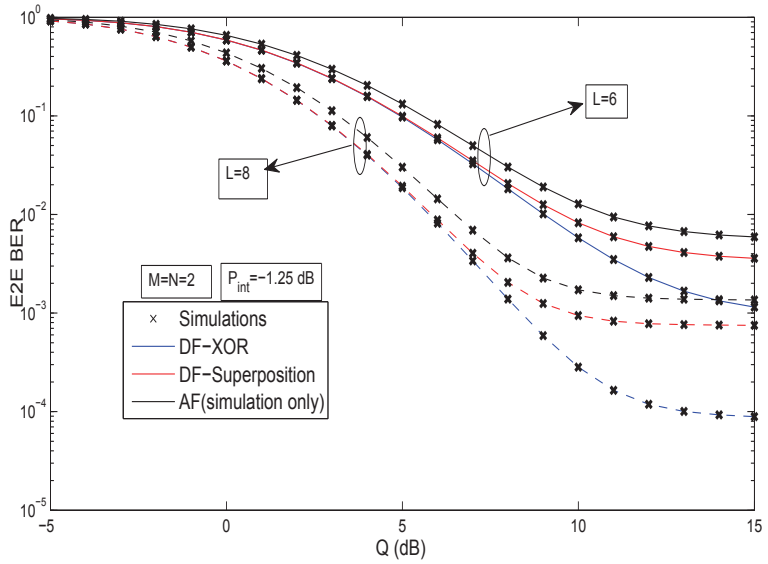

Figure 5.7: E2E BER vs. Q (dB) for $L = 6, M = N = 2$ and different P_{int} values.

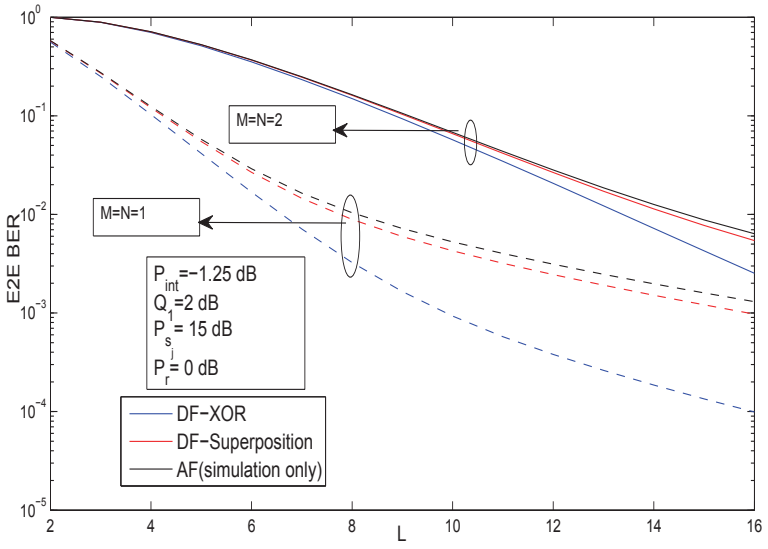

Figure 5.8: E2E BER vs. L for $M = N = 1, 2$ at fixed P_{int}.

decode both signals increases, i.e., L_s becomes higher, hence, more participating relays in the beamforming and relaying process. It is also seen that as the number of PU-RXs increases from one to two, the BER performance degrades. Since increasing the number of PU-RXs makes the probability to avoid the interference on all PU-RXs decreases which forces the secondary transceivers to transmit with lower power.

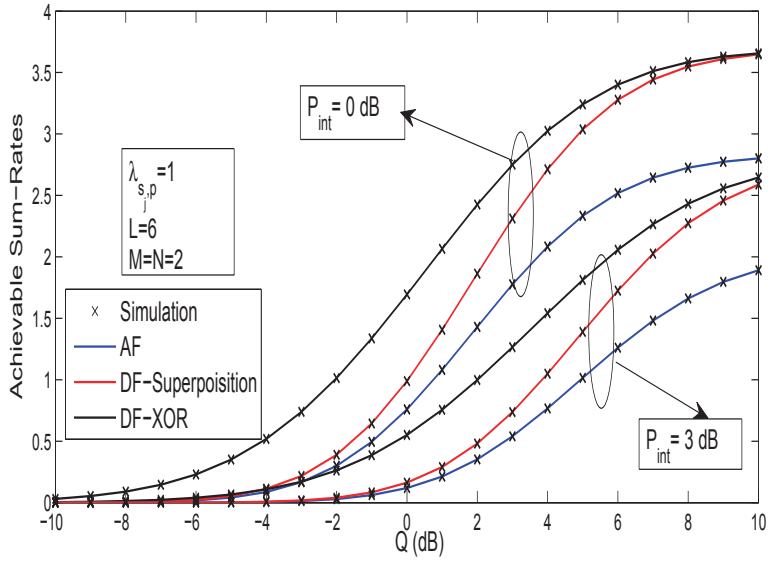

Figure 5.9: Achievable Sum-Rates vs. Q (dB) for $L = 6, M = N = 2$ and different CCI values.

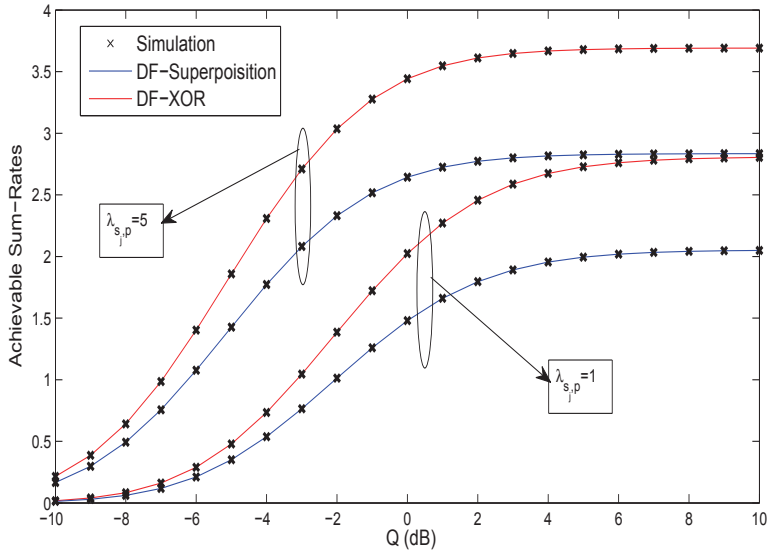

Figure 5.10: Achievable Sum-Rates vs. Q (dB) for $L = 6, M = N = 2$ with fixed P_{int} and different $\lambda_{s_j,p}$ values.

In Fig. 5.9, the achievable sum-rate performance of the secondary system is illustrated for several values of P_{int} at the same values of $L = 6$ and $M = N = 2$. The CCIs effect degrades the performance when it is increased from 0 to 3 dBs for all relaying strategies. It

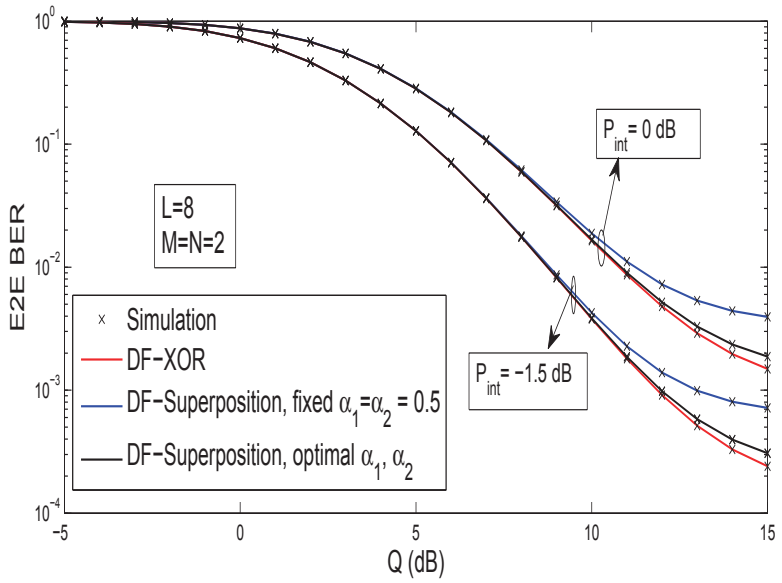

Figure 5.11: E2E BER vs. Q (dB) for $L = 6, 8, M = N = 2$ and different P_{int} values at fixed and optimal α_j values.

can be observed that DF-XOR sum-rates performance is the best meanwhile all of the curves saturate at high values of Q_j due to the interference constraints.

Fig. 5.10 shows the achievable sum-rate performance of the secondary system versus Q for L= 6 and $M = N = 2$ and different values of P_{int} and fixed $\lambda_{s_j,p}$. Again, the same observations as in the previous figures are repeated. Besides, it is clear that the achievable sum-rate increases with $\lambda_{s_j,p}$ increasing from one to five. The reason is that as $\lambda_{s_j,p}$ increases, the quality of the channel between S_j and PU-RX becomes worse, which reduces the co-channel interference between S_j and PU-RX. However, when $\lambda_{s_j,p}$ reaches a certain value, the achievable sum-rate curve saturates due to the constraints on P_{s_j} and Q_j.

5.5.2 Optimal Power Allocation Parameters

Fig. 5.11 compares the E2E BER performance of the DF-XOR and superposition relaying versus Q when the power allocation parameter α_1, α_2 is either fixed or optimized. The power allocation numbers are optimized such that the achievable sum-rates at the transceivers is

maximized. Specifically, α is chosen according to the optimization problem:

$$\begin{aligned} \alpha_{opt} = \arg \max_{\alpha_1,\alpha_2} (R_1(\alpha_1) + R_2(\alpha_2)) \\ \text{subject to } \ 0 < \alpha_1, \alpha_2 < 1 \end{aligned} \tag{5.29}$$

where $R_1(\alpha_1)$ and $R_2(\alpha_2)$ can be obtained from (5.28). Obtaining a closed-form expression for the solution to (5.29) is not easy. As an alternative, it can be solved numerically. As previously mentioned in the performance analysis section, when α_1, α_2 are optimized to maximize the achievable sum-rates, the BER performance becomes better than when $\alpha_1 = \alpha_2 = 0.5$, i.e., fixed. It can be observed that, when the power allocation parameters are optimized, the DF-superposition curve performs closely as in the DF-XOR case. This is due to the reason that the transceiver with the higher transmit power is weighted at the relays more than the one with lower transmit power providing that the two transceivers are transmitting at different power.

5.6 Conclusion

We investigated a cooperative two-way DF selective relaying based distributed ZFB spectrum-sharing system in the presence of multiple PU-RXs. Two different relaying strategies were considered and the corresponding optimal weights vectors were designed. The beamforming weights were optimized to maximize the received SNR at both secondary transceivers while the interference inflicted on the primary users is kept to a predefined threshold. For each relaying strategy, we analyzed the performance of the secondary system by deriving closed form expressions for the outage probability, BER and achievable sum-rates. Our numerical results showed that the combination of the distributed ZFB and the cooperative diversity enhances the secondary link performance by compensating the performance loss due to CCIs. Moreover, the results showed that the DF-XOR outperformed DF-superposition and AF relaying strategies when equal power allocation is assumed at the relays while the DF-superposition performance is closer to the DF-XOR when the weightining at the relays is different.

Chapter 6

Distributed Beamforming with Limited Feedback

6.1 Introduction

In all works mentioned in the previous chapters, we assume perfect CSI availability of the interference channels between the secondary transmitters and primary receivers, which is an ideal assumption. In this chapter, we consider partial CSI knowledge at the secondary transmitters. In particular, we address the availability of partial CSI via a finite rate feedback from the primary receiver to the secondary transmitter, where the primary receiver quantizes its vector channel to one of 2^B codebook size and conveys back the corresponding index for some positive integer B. This feedback is used to get information regarding only the channel direction, known as channel direction information (CDI), and not the channel quality information (CQI).

In general, the optimal beamforming tools require the secondary transmitters to obtain the instantaneous CSI of their interference channels to the PUs, which requires the PU's cooperation. Most of the beamforming designs assumed that the SUs either have prior CSI of the interference channels to the PUs or monitor the PUs continuously, which may be impractical. Assuming perfect CSI of the interference channels, an optimal beamforming design was proposed in [36] for maximizing the SU throughput while respecting a set of interference power constraints at the PUs. The authors in [90] relaxed the perfect CSI assumption, where a SU transmitter estimates the required CSI by making use of channel reciprocity and continuously observing the PU transmission. However, the estimation errors

are unavoidable and cause residual interference to the PU receivers. This problem was tackled in [91] by optimizing the optimal beamformer to cope with the estimation uncertainty. Besides beamforming, power control techniques can be used to mitigate the interference to the PUs by exploiting the primary-links CSI, however, such CSI is even more difficult for SUs to obtain than that of the SUs-to-PUs interference channels [92], [93].

For traditional multi-antenna wireless systems, CSI feedback from the receiver to the transmitter enables the latter to do precoding, which enhances the system throughput [94]. However, CSI feedback can incur heavy overhead. This motivates scientists to work on designing feedback quantization algorithms, called limited feedback [95]. There exists a considerable literature on limited feedback, where CSI quantizers are designed based on different principles such as Lloyd's algorithm [96] and line packing [97]. However, the limited feedback case is rarely studied in the CRNs.

In [98], limited feedback was considered in a multi-antenna downlink CR system. The authors in [98] tried to minimize the outage probability of the SU system while satisfying the QoS requirement of the PU. In [99], the same problem was addressed using a different approach, whereby the objective is to maximize the SU link gain while limiting the interference inflicted to the PU. In the same context, the authors in [100] proposed a framework of limited cooperative ZFB for multiuser multiple-input single-output (MISO) CRNs to cancel the inter-network and intra-network interferences. In particular, the authors investigated the feedback utility function in order to derive the transmission mode and feedback amount.

In this chapter, we focus on a dual-hop DF cooperative spectrum-sharing system with limited feedback from an existing PU. In particular, the secondary relays communicate with the PU using a quantized CSI so that the relays exploit this information to apply the beamforming process. If perfect CSI is assumed, the interference to the PUs using the ZFB will be nullified. However, since the CSI feedback is limited only to the quantized channel direction information, the secondary relays can not transmit with zero interference due to the quantization error of the CDI, and the residual interference increases with the increase of the secondary transmit power. Therefore, the secondary relays transmit power should be adjusted to meet the PU interference constraint. In this regard, we derive an upper bound for the secondary relays transmit power that meets the PU interference constraint. We also

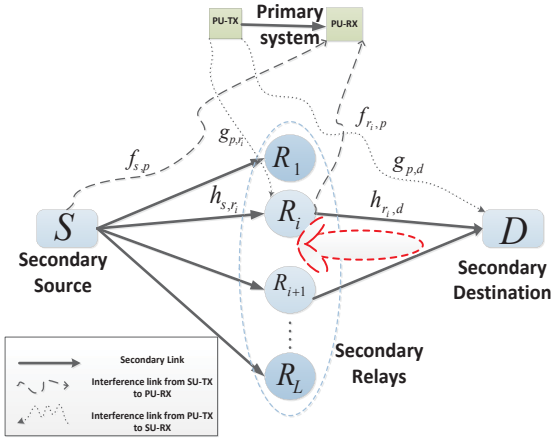

Figure 6.1: Spectrum-Sharing System with Dual-hop Relaying.

derive the statistics of the end-to-end SINR employing the ZFB with limited feedback. To investigate the effect of the quantized CSI on the secondary system performance, we derive closed-form expressions for the outage probability and the BER assuming that the secondary receivers (relays and destination) are affected by the PU's interference power. as expected, our results show that the performance improves as the number of feedback bits increases.

6.2 System and Channel Models

We consider a dual-hop relaying system that is composed of a pair of secondary source S and destination D and a set of L DF secondary relays denoted by R_i for $i = 1, ..., L$ coexisting in the same spectrum band with a primary system which consists of a primary transmitter (PU-TX) and a primary receiver (PU-RX) pair as shown in Fig. 6.1. It is similar to the system model described in Chapter 3, Section 3.2.

All channel coefficients are assumed to be independent Rayleigh flat fading such that $|h_{s,r_i}|^2, |f_{s,p}|^2, |f_{r_i,p}|^2, |g_{p,d}|^2$ and $|g_{p,r_i}|^2$ are exponential distributed random variables with parameters $\lambda_{sr_i}, \lambda_{sp}, \lambda_{r_ip}, \lambda_{pd}$ and λ_{pr_i} respectively. All the noise is assumed to be AWGN with zero-mean and variance σ^2. Let the ZFB vector $\hat{\mathbf{w}}_{\mathbf{zf}}^T = [w_1, w_2, ..., w_{L_s}]$ used to direct the signal to D. Let $\mathbf{h}_{r,d}^T = [h_{r_1,d}, ..., h_{r_{L_s},d}]$ be the channel vector between the potential relays and D. Let $\mathbf{f_{r,p}} = [f_{r_1,p}, ..., f_{r_{L_s},p}]$ be the channel vector between the potential relays and the

PU-RX.

6.2.1 Quantized CSI Feedback Model

At the beginning of the second time-slot, the primary and secondary receivers convey the corresponding CSI to the secondary relays based on quantization codebooks. All the codebooks are designed in advance and stored at the relays and receivers. Let $\mathcal{F}_{r,p} = \{\hat{\mathbf{f}}_{\mathbf{r},\mathbf{p}_1}, \hat{\mathbf{f}}_{\mathbf{r},\mathbf{p}_2}, ..., \hat{\mathbf{f}}_{\mathbf{r},\mathbf{p}_{2^B}}\}$ be a codebook of size 2^B at the primary receiver, which is a collection of unit norm vectors. Then the optimal quantization codeword selection criterion can be expressed as [101]

$$i = \arg \max_{1 \leq j \leq 2^B} |\hat{\mathbf{f}}_{\mathbf{r},\mathbf{p}_j}^H \tilde{\mathbf{f}}_{\mathbf{r},\mathbf{p}}|^2, \tag{6.1}$$

where $\tilde{\mathbf{f}}_{\mathbf{r},\mathbf{p}} = \frac{\mathbf{f}_{\mathbf{r},\mathbf{p}}}{||\mathbf{f}_{\mathbf{r},\mathbf{p}}||}$ is the channel direction vector. Specifically, index i is conveyed by the primary receiver and $\hat{\mathbf{f}}_{\mathbf{r},\mathbf{p}_i}$ is recovered at the secondary relays and is used in lieu of the instantaneous CSI of the interference channel. Similarly, let $\mathcal{H}_{r,d} = \{\hat{\mathbf{h}}_{r,d_1}, \hat{\mathbf{h}}_{r,d_2}, ..., \hat{\mathbf{h}}_{r,d_{2^C}}\}$ be a quantization codebook of size 2^C at the secondary receiver, which is also a collection of unit norm vectors. Same process of codeword selection, index conveyance and CSI recovery is used, where $\hat{\mathbf{h}}_{r,d_i}$ is recovered at the relays in lieu of the instantaneous CSI of the relaying channels between the relays and the receiver.

6.2.2 Transmission Protocol

In this dual-hop system, the communication process occurs over two TSs. In TS_1, S broadcasts its signal to all L relays, then the received signal at the ith relay is given as

$$y_{r_i} = \sqrt{P} h_{s,r_i} x_s + \sqrt{P_{int}}\, g_{p,r_i} \hat{x}_{ip} + n_{i1}, \tag{6.2}$$

where P is the source's transmit power, P_{int} is the interference power from PU-TXs, x_s is the information symbol of S, $\hat{x}_{ip}$ is the PU-TX interfering symbol at the ith relay and n_{i1} denotes the noise at the ith relay in TS_1. We assume that the transmitted symbols are equiprobable with unit energy.

In TS_2, the decoding set $\mathcal{C}$, which consists of the relays that can correctly decode x_s by using cyclic redundancy codes, transmits the decoded signals to the destination simultaneously

by using beamforming. In particular, each relay weights the decoded signal and forwards it to the destination. Thus the received signal at D is given by

$$y_d = \sqrt{P_r}\mathbf{h}_{r,d}^H \hat{\mathbf{x}}_s + \sqrt{P_{int}}\, g_{p,d}\, \hat{x}_{pd} + n_2, \tag{6.3}$$

where $\hat{\mathbf{x}}_s = \mathbf{w_{zf}} x_s$ is the weighted vector, $\hat{x}_{md}$ is the PU-TX interfering symbol at D and n_2 is the noise at D in the second time-slot. Therefore, the corresponding total received SINR at D given $\mathcal{C}$, denoted by $\gamma_{d|\mathcal{C}}$, is given as

$$\gamma_{d|\mathcal{C}} = \frac{P_r |\mathbf{h}_{r,d}^H \hat{\mathbf{w}}_{\mathbf{zf}}|^2}{P_{int}\,|g_{p,d}|^2 + \sigma^2}. \tag{6.4}$$

6.2.3 Mathematical Model and Size of $\mathcal{C}$

In this system model, P is constrained as $P = \min\left\{\frac{Q}{|f_{s,p}|^2}, P_s\right\}$ where P_s is the maximum transmission power of S. So the received SINR, γ_{s,r_i} at the ith relay is given as

$$\gamma_{s,r_i} = \frac{\min\left\{\frac{Q}{|f_{s,p}|^2}, P_s\right\}|h_{s,r_i}|^2}{P_{int}|g_{p,r_i}|^2 + \sigma^2}. \tag{6.5}$$

Next, we derive the CDF of $\gamma_{s,r_i} = \frac{U}{P_{int}V+\sigma^2}$, where $U = \min\left\{\frac{Q}{|f_{s,p}|^2}, P_s\right\}|h_{s,r_i}|^2$ and $V = |g_{p,r_i}|^2$. By using the definition of CDF of γ_{s,r_i}, we find

$$F_{\gamma_{s,r_i}}(x) = \int_0^\infty \Pr(U < (P_{int}\, y + \sigma^2)x) f_V(y) dy. \tag{6.6}$$

The CDF of U is obtained with the help of (3.3) as,

$$F_U(x) = 1 + e^{-\frac{\lambda_{sr_i} x}{P_s}} \left(\frac{e^{-\frac{\lambda_{sp} Q}{P_s}}}{\frac{\lambda_{sp} Q}{\lambda_{sr_i} x} + 1} - 1 \right). \tag{6.7}$$

Substituting (6.7) into (6.6), and after several algebraic manipulations, (6.6) is equivalently expressed as

$$\begin{aligned} F_{\gamma_{s,r_i}}(x) &= 1 + e^{-\frac{\lambda_{sr_i}\sigma^2 x}{P_s}} \int_0^\infty e^{-(\frac{\lambda_{sr_i}\sigma^2 x}{P_s} + \lambda_{mr_i})y} \\ &\times \left[(e^{-\frac{\lambda_{sp}Q}{P_s}} - 1) - \frac{\frac{\lambda_{sp}Q}{\lambda_{sr_i}} e^{-\frac{\lambda_{sp}Q}{P_s}}}{x P_{int}\, y + \sigma^2 x + \frac{\lambda_{sp}Q}{\lambda_{sr_i}}} \right] dy. \end{aligned} \tag{6.8}$$

After easy simplifications, and with the help of [56, Eqs. (3.351.3), (3.353.5)], the CDF of γ_{s,r_i} is derived as

$$F_{\gamma_{s,r_i}}(x) = 1 + e^{-\frac{\lambda_{sr_i}\sigma^2 x}{P_s}} \left[\frac{(e^{-\frac{\lambda_{sp}Q}{P_s}} - 1)}{\frac{\lambda_{sr_i}P_{int}x}{P_s} + \lambda_{pr_i}} - (\frac{\lambda_{sp}Qe^{-\frac{\lambda_{sp}Q}{P_s}}}{\lambda_{sr_i}})(-1)e^{\beta\mu}Ei[-\beta\mu] \right], \quad (6.9)$$

where $\beta = \frac{\sigma^2}{P_{int}} + \frac{\lambda_{sn}Q}{\lambda_{sr_i}P_{int}x}$, $\mu = \lambda_{mr_i} + \frac{\lambda_{sr_i}P_{int}x}{P_s}$ and $Ei[.]$ is the exponential integral defined in [56].

As mentioned in Chapter 3, we define $\mathcal{C}$ to be the set of relays which perfectly decode the signals received in the first time-slot, then, the probability $\Pr[|\mathcal{C}| = L_s]$ becomes

$$\Pr[|\mathcal{C}| = L_s] = \binom{L}{L_s} P_{\text{off}}^{L-L_s}(1 - P_{\text{off}})^{L_s}, \quad (6.10)$$

where P_{off} denotes the probability that the relay does not decode correctly the received signal and keeps silent in the second time-slot. Then P_{off} is computed as

$$P_{\text{off}} = F_{\gamma_{s,r_i}}(\gamma_{th}), \quad (6.11)$$

where $\gamma_{th} = 2^{2R_{min}} - 1$ is the SINR threshold.

6.2.4 ZFB Weights Design

Recalling the optimization problem (3.7) from Chapter 3, the ZFB vector is given as

$$\hat{\mathbf{w}}_{\mathbf{zf}} = \frac{\boldsymbol{\Xi}^{\perp}\hat{\mathbf{h}}_{r,d}}{\left\|\boldsymbol{\Xi}^{\perp}\hat{\mathbf{h}}_{r,d}\right\|}, \quad (6.12)$$

where $\boldsymbol{\Xi}^{\perp} = \left(\mathbf{I} - \hat{\mathbf{f}}_{\mathbf{rp}}(\hat{\mathbf{f}}_{\mathbf{rp}}^H\hat{\mathbf{f}}_{\mathbf{rp}})^{-1}\hat{\mathbf{f}}_{\mathbf{rp}}^H\right)$ is the projection idempotent matrix with rank $(L_s - 1)$. It is worthwhile to mention that, in ZFB, CDI feedback is sufficient for obtaining beamforming vectors and there is no need for the CQI [102].

6.3 Performance Analysis

6.3.1 End-to-End SINR statistics

Because of the quantization error due to the partial CSI, the secondary relays cannot transmit with zero interference. In this case, the relays should reduce the transmit power and meet the

interference constraint. Since the instantaneous interference CSI cannot be exactly estimated because of the partial CSI, we consider the average interference constraint instead of the the peak interference constraint [99], [100]. If $\bar{Q}_{av}$ is the maximum average threshold, the interference constraint is given by

$$\bar{Q} = \mathrm{E}[Q] \leq \bar{Q}_{av}. \tag{6.13}$$

By using ZFB based on limited feedback information from the PU, the relationship between the residual $\bar{Q}$, the transmit power, and the feedback amount is given by the following Lemma.

Lemma 6.3.1. *Given P_r and B, the residual $\bar{Q}$ at the PU after ZFB is tightly upper bounded by $\frac{P_r L_s}{L_s - 1} 2^{-\frac{B}{L_s - 1}}$.*

Proof. Following the theory of random vector quantization (RVQ) [101], the relationship between the true and quantized channel direction vectors can be expressed as

$$\tilde{\mathbf{f}}_{\mathbf{r,p}} = \sqrt{1-a}\hat{\mathbf{f}}_{\mathbf{r,p}} + \sqrt{a}\mathbf{f}_o, \tag{6.14}$$

where $\hat{\mathbf{f}}_{\mathbf{r,p}}$ is the quantization codeword based on (6.1), $a = \sin^2(\angle(\tilde{\mathbf{f}}_{\mathbf{r,p}}, \hat{\mathbf{f}}_{\mathbf{r,p}}))$ is the magnitude of the quantization error, and $\mathbf{f}_o$ is the unit norm vector isotropically distributed in the nullspace of $\hat{\mathbf{f}}_{\mathbf{r,p}}$, and is independent of a.

The interference term $|\tilde{\mathbf{f}}_{\mathbf{r,p}}^H \hat{\mathbf{w}}_{\mathbf{zf}}|^2$ is derived as

$$\begin{aligned} |\tilde{\mathbf{f}}_{\mathbf{r,p}}^H \hat{\mathbf{w}}_{\mathbf{zf}}|^2 &= |\sqrt{1-a}\hat{\mathbf{f}}_{\mathbf{r,p}}^H \hat{\mathbf{w}}_{\mathbf{zf}} + \sqrt{a}\mathbf{f}_o^H \hat{\mathbf{w}}_{\mathbf{zf}}|^2 \\ &= a|\mathbf{f}_o^H \hat{\mathbf{w}}_{\mathbf{zf}}|^2, \end{aligned} \tag{6.15}$$

where (6.15) follows from the fact the $\hat{\mathbf{w}}_{\mathbf{zf}}$ is in the nullspace of $\hat{\mathbf{f}}_{\mathbf{r,p}}$, i.e., $|\hat{\mathbf{f}}_{\mathbf{r,p}}^H \hat{\mathbf{w}}_{\mathbf{zf}}| = 0$. Due to the independence between the channel magnitude and the channel direction, $\bar{Q}$ is reduced to

$$\bar{Q} = \mathrm{E}[||\mathbf{f}_{\mathbf{r,p}}||^2]\mathrm{E}[a]\mathrm{E}[|\mathbf{f}_o^H \hat{\mathbf{w}}_{\mathbf{zf}}|^2]. \tag{6.16}$$

Hence, in order to obtain $\bar{Q}$, we need to compute the three expectation terms.

For the first expectation, since $||\mathbf{f}_{\mathbf{r,p}}||^2$ is a Chi-square distributed χ^2 with $2L_s$ degrees of freedom, we have $\mathrm{E}[||\mathbf{f}_{\mathbf{r,p}}||^2] = L_s$. For the second expectation, for an arbitrary quantization

codeword $\hat{\mathbf{f}}_{\mathbf{r},\mathbf{p}_j}$, $(1-|\tilde{\mathbf{f}}_{\mathbf{r},\mathbf{p}_j}^H \hat{\mathbf{f}}_{\mathbf{r},\mathbf{p}}|^2)$ is a Beta distributed as $\beta(L_s-1,1)$ [101]. So that, $a = 1-|\tilde{\mathbf{f}}_{\mathbf{r},\mathbf{p}}^H \hat{\mathbf{f}}_{\mathbf{r},\mathbf{p}}|^2$ is the minimum of 2^B independent $\beta(L_s-1,1)$ random variable, and thus its expectation is tightly upper bounded as $\mathrm{E}[a] < 2^{-\frac{B}{L_s-1}}$. For the third expectation, since $\mathbf{f}_o$ and $\hat{\mathbf{w}}_{\mathbf{zf}}$ are i.i.d. isotropic vectors in the (L_s-1) dimensional nullspace of $\hat{\mathbf{f}}_{\mathbf{r},\mathbf{p}}$, $\mathrm{E}[|\mathbf{f}_o^H \hat{\mathbf{w}}_{\mathbf{zf}}|^2]$ is $\beta(1, L_s-2)$ distributed [101], with expectation equals to $\frac{1}{L_s-1}$. As a result, we have $\bar{Q} < \frac{P_r L_s}{L_s-1} 2^{-\frac{B}{L_s-1}}$. □

According to Lemma 6.3.1, given $\bar{Q}_{av}$ and feedback B, in order to meet the interference constraint, P_r has an upper bound as

$$P_r \leq \frac{(L_s-1)\bar{Q}_{av}}{L_s} 2^{\frac{B}{L_s-1}} \tag{6.17}$$

Before analyzing the system performance, we need to know the PDF and CDF of the received SINR at the secondary destination, which is upper bounded by

$$\begin{aligned}
\gamma_{d|\mathcal{C}} &\leq \frac{\frac{(L_s-1)\bar{Q}_{av}}{L_s} 2^{\frac{B}{L_s-1}} |\mathbf{h}_{r,d}^H \hat{\mathbf{w}}_{\mathbf{zf}}|^2}{P_{int}\,|g_{p,d}|^2 + \sigma^2} \\
&\leq \frac{\frac{(L_s-1)\bar{Q}_{av}}{L_s} 2^{\frac{B}{L_s-1}} ||\mathbf{h}_{r,d}||^2 |\tilde{\mathbf{h}}_{r,d}^H \hat{\mathbf{w}}_{\mathbf{zf}}|^2}{P_{int}\,|g_{p,d}|^2 + \sigma^2} \\
&\triangleq \frac{\frac{(L_s-1)\bar{Q}_{av}}{L_s} 2^{\frac{B}{L_s-1}} ||\mathbf{h}_{r,d}||^2 \beta(1, L_s-1)}{P_{int}\,|g_{p,d}|^2 + \sigma^2} \qquad (6.18) \\
&\triangleq \frac{\chi_2^2}{\delta P_{int}\,|g_{p,d}|^2 + \delta\sigma^2} \qquad (6.19)
\end{aligned}$$

where $\delta = \frac{L_s}{(L_s-1)\bar{Q}_{av}} 2^{-\frac{B}{L_s-1}}$, and (6.18) and (6.19) hold as analyzed in (6.16).
Next, we derive the CDF of $\gamma_{d|\mathcal{C}} = \frac{U}{\delta P_{int} V + \delta\sigma^2}$, where $U \sim \chi_2^2$ and V is an exponential random variable. By using the definition of CDF, we find

$$\begin{aligned}
F_{\gamma_{d|\mathcal{C}}}(x) &= \int_0^\infty \Pr(U < (P_{int}\,\delta\, y + \delta\,\sigma^2)x) f_V(y) dy \\
&= \int_0^\infty (1 - e^{-\delta\, x(\sigma^2 + P_{int}\, y)}) e^{-\lambda_{pd}\, y} dy \\
&= 1 - e^{-\delta\sigma^2 x} \int_0^\infty e^{-(\delta\, P_{int}\, x + \lambda_{pd}) y} dy \\
&= 1 - \frac{e^{-\delta\sigma^2 x}}{\delta\, P_{int}\, x + \lambda_{pd}} \qquad (6.20)
\end{aligned}$$

which is plotted in Fig. 6.2, where it shows the impact of increasing the feedback amount on enhancing the performance.

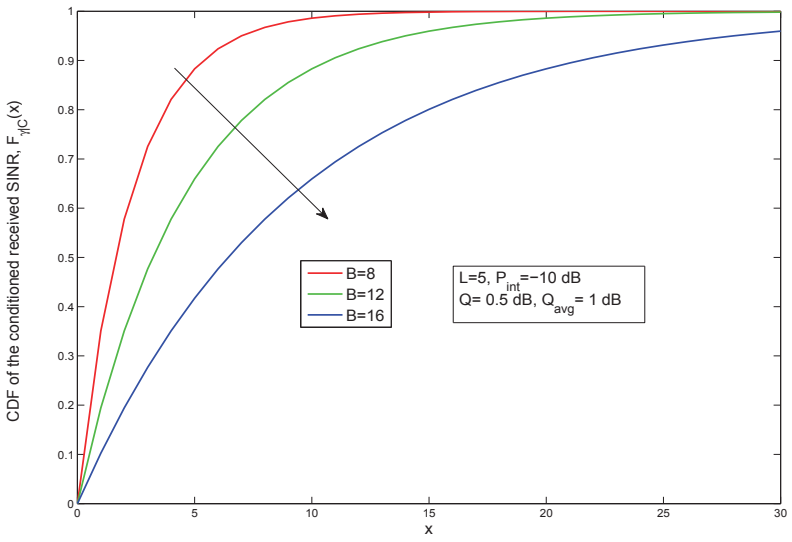

Figure 6.2: $F_{\gamma_{d|\mathcal{C}}}(x)$ vs. x for L=5 and $M = 1$ and different values of B.

To compute the unconditional CDF denoted as $F_{\gamma_d}(\gamma)$, we use the total probability theorem to get

$$F_{\gamma_d}(x) = \sum_{L_s=0}^{1} \binom{L}{L_s} P_{\text{off}}^{L-L_s}(1-P_{\text{off}})^{L_s} + \sum_{L_s=2}^{L} \binom{L}{L_s} P_{\text{off}}^{L-L_s}(1-P_{\text{off}})^{L_s} F_{\gamma_{d|\mathcal{C}}}(x), \quad (6.21)$$

where $F_{\gamma_{d|\mathcal{C}}}(x)$ is substituted from (6.20). In the subsequent section, we make use of $F_{\gamma_d}(x)$ to derive closed-form expressions for the outage and E2E BER performance.

6.3.2 Outage Probability

An outage event occurs when the total received SINR falls below a certain threshold γ_{th} and is expressed as $P_{out} = \Pr(\gamma_d < \gamma_{th})$. By using (6.21), the outage probability of the secondary system in a closed-form can be written as

$$P_{out} = F_{\gamma_d}(\gamma_{th}). \quad (6.22)$$

6.3.3 E2E BER

We analyze the BER performance due to errors occurring at D assuming that all participating relays have accurately decoded and regenerated the message. The BER could be evaluated

using the following identity

$$P_e = \frac{a\sqrt{b}}{2\sqrt{\pi}} \int_0^\infty \frac{e^{-bx}}{\sqrt{x}} F_{\gamma_d}(x) dx \tag{6.23}$$

In this Chapter, we consider BPSK for which $(a, b) = (1, 1)$.

$$P_e = \frac{a\sqrt{b}}{2\sqrt{\pi}} \left(A \underbrace{\int_0^\infty \frac{e^{-bx}}{\sqrt{x}} dx}_{I_1} + B \underbrace{\int_0^\infty \frac{e^{-bx}}{\sqrt{x}} F_{\gamma_{d|\mathcal{C}}}(x) dx}_{I_2} \right) \tag{6.24}$$

where $A = \sum_{L_s=0}^{N} \binom{L}{L_s} P_{\text{off}}^{L-L_s} (1 - P_{\text{off}})^{L_s}$ and $B = \sum_{L_s=N+1}^{L} \binom{L}{L_s} P_{\text{off}}^{L-L_s} (1 - P_{\text{off}})^{L_s}$. I_1 is evaluated with the help of [56, (3.361.2)]. Next, to compute I_2, we represent the integrands of I_2 in terms of Meijer's G-functions using [65, Eq. 10, 11], which are given, respectively, as

$$(\delta\, P_{int}\, x + \lambda_{bd})^{-1} = \eta x^{-1} G_{1,1}^{1,1} \left(\frac{\delta P_{int}\, x}{\lambda_{pd}} \Big|_1^1 \right), \tag{6.25}$$

where $\eta = (\delta P_{int})^{-1}$.

$$e^{-(b+\delta\sigma^2)x} = G_{0,1}^{1,0} \left(\left(b + \delta\sigma^2\right) x \Big|_0^- \right). \tag{6.26}$$

Thus, I_2 can be expressed as

$$I_2 = 0.5 - \eta \int_0^\infty x^{-1.5} G_{1,1}^{1,1} \left(\frac{\delta P_{int}\, x}{\lambda_{pd}} \Big|_1^1 \right) G_{0,1}^{1,0} \left(\left(b + \delta\sigma^2\right) x \Big|_0^- \right) dx. \tag{6.27}$$

Now, I_2 is in the form of a product of a power term and two Meijer's G-function, which can be solved using [65, Eq. 21] as

$$I_2 = 0.5 - \eta \left(b + \delta\sigma^2\right)^{-0.5} G_{2,1}^{1,2} \left(\frac{\delta P_{int}}{b\lambda_{pd} + \lambda_{pd}\sigma^2\delta} \Big|_1^{1,1.5} \right). \tag{6.28}$$

By incorporating the results of I_1 and I_2 into (6.24), a closed-form expression for the unconditional E2E BER at D is given as

$$P_e = 0.5A + B\Big[0.5 - \eta \left(b + \delta\sigma^2\right)^{-0.5} G_{2,1}^{1,2} \left(\frac{\delta P_{int}}{b\lambda_{pd} + \lambda_{pd}\sigma^2\delta} \Big|_1^{1,1.5} \right) \Big]. \tag{6.29}$$

6.4 Numerical Results and Discussion

In this section, we present numerical results to validate our derived expressions in Section 6.3. Without loss of generality, we assume that the relays are located on a straight line vertical to the distance between the source and destination. The distance between them equals one. Unless otherwise stated, we also assume that $\lambda_{sp} = \lambda_{r_ip} = 1$, $\lambda_{sr_i} = \lambda_{r_id} = 1, \forall i$ and $\lambda_{pr_i} = \lambda_{pd} = 1, \forall i$. We use $C = 25$ bits for the relays-destination channels to focus on the effect of the quantized interference CSI channel.

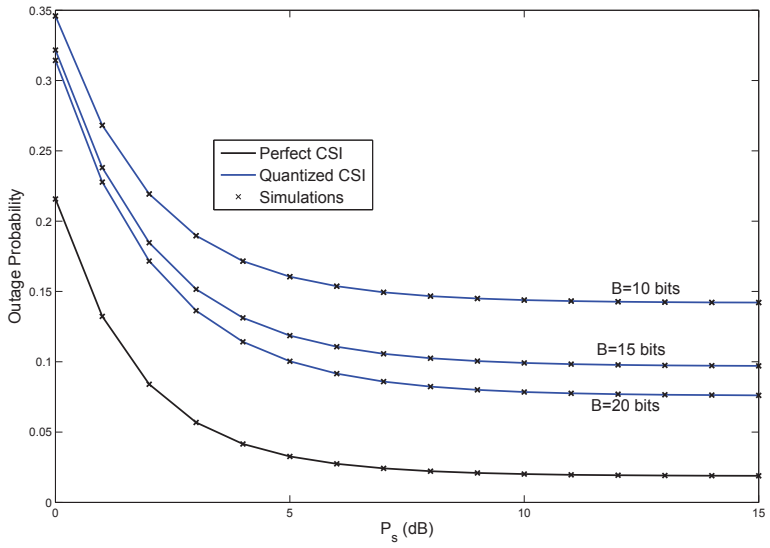

Figure 6.3: Outage probability vs. P_s (dB) for different values of B.

Fig. 6.3 shows the outage performance versus P_s for $L = 8$, $M = 1$ under different values of B for P_{int} =-10 dB. As observed from the figure, as the value of P_s increases, the outage performance improves substantially. Also, the figure shows the impact of the number of the quantized CSI feedback bits on the outage performance. As B increases, the system performance improves. However, a compensation of this loss in performance is gained by the use of beamforming. A floor in the outage performance curve is noticed which is due to the interference level constraint.

Fig. 6.4 illustrates the BER performance versus P_s for L= 8 and $M = 1$. Similar observation is obtained as that in Fig. 6.3. It is seen that as $\bar{Q}_{av}$ and B increase, the BER

performance improves. We also observe the large performance gap between the perfect CSI curve and the quantized CSI curves due to the limited feedback. In addition, it is observed from the figure that BER curves saturate at high P_s region and an error floor occurs which results in zero-diversity.

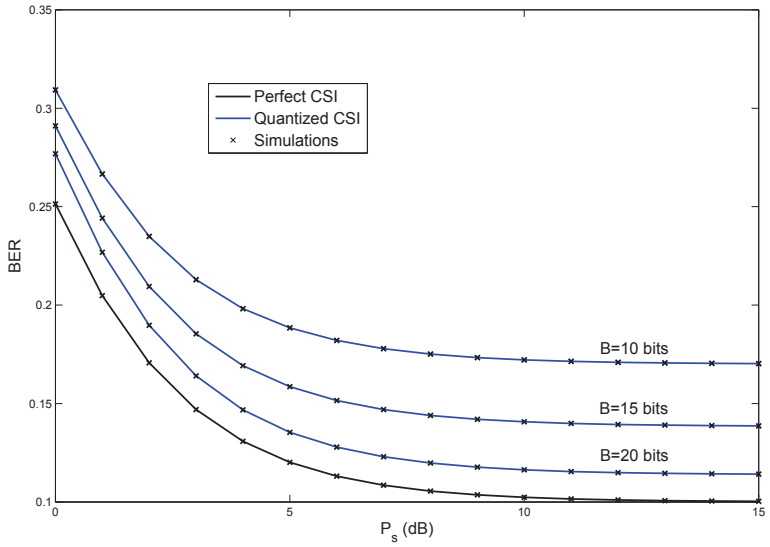

Figure 6.4: BER vs. P_s (dB) for different values of B.

6.5 Conclusion

We investigated in this chapter the system model described in Chapter 3 with a quantized CSI assumption for the interference channel between the secondary relays and the primary receiver. We derived a tight upper bound for the residual interference received at the primary receiver due to the partial CSI at the relays. From this upper bound, we derived the upper bound end-to-end received SINR at the secondary destination. To study the impact of the limited feedback, we analyzed the system performance by deriving the outage and BER performance at different number of feedback bits and compared it with perfect CSI. Obviously, the results show the effect of increasing the number of the feedback bits on enhancing the system performance.

Chapter 7

Conclusions and Future Work

7.1 Conclusions

Spectrum-sharing systems are being investigated to solve the problems resulting from the bandwidth scarcity and the spectrum usage inefficiency by exploiting the existing licensed spectrum opportunistically. Wireless systems, equipped with the substantial capabilities of CR, will provide an ultimate spectrum-aware communication model in wireless networks. In this thesis, we have tackled a major thrust of research in the CR area, namely, distributed beamforming in cooperative spectrum sharing systems. We have made significant contributions, which is evident from the track record of publications that resulted from this research. Below, we briefly summarize those accomplishments.

We investigated the possibility of combining beamforming and cooperative communications for spectrum-sharing systems. The rationale behind this is that beamforming can be very efficient in nulling the interference inflected in the primary system while the secondary system is using the primary spectrum. We examined a network setting in which there are two secondary nodes that wish to communicate with each other through a number of secondary relays. The secondary nodes are assumed to be far away from each other and hence there is no direct link between them. At the same time, both systems share the same spectrum, but the primary system imposes certain restrictions on the amount of interference that the secondary system can cause. In this case, the secondary relay nodes that receive the source signal participate in the cooperation process. These relays form a distributed spatial array, which is used to beamform the signal of interest towards the intended destination, while making sure there is no signal transmitted in the direction of the primary receivers. This

technique has proved very efficient in enabling the secondary system to co-exist with the primary system without causing much harm to the primary system.

In Chapter 3, we considered different relaying schemes, including DF and AF. In both cases, we derived optimal beamforming vectors and sub-optimal ZFB vectors at the relays. Then, we developed an analytical framework for the developed techniques of the secondary system performance. It was shown that coupling distributed beamforming and cooperative communications can be very efficient in sharing the available spectrum with the primary system and enhancing the secondary system performance.

Furthermore, we examined the system performance when there are multiple primary receivers are present in the system. This makes the system requirement much more stringent since all the primary receivers must be accommodated in terms of interference. We were able to incorporate this assumption in our system model. The results we obtained were very favorable.

While we considered in Chapter 3 one-way communications, whereby only one secondary source sends information to the other source, in Chapters 4 and 5, we considered two-way communications, in which the relays will have to either AF or DF the received signals. The challenge in this scenario stems from the fact that there is no obvious way as to how to perform beamforming to the received signals. That is, will beamforming be applied to the two signals individually or combined? Which technique is optimal? In this work, we answered these questions as follows.

First, in Chapter 4, we considered two-way AF relaying scheme over two, three, and four time-slot protocols. Our results showed that when beamforming is applied to each individual signal and then combined in the three time-slot protocol, the performance is better since the received signals are not weighted equally. The signal transmitted with higher power is weighted more than the other one. In particular, our results showed that the three time-slot protocol outperforms the two time-slot protocol and four time-slot protocol in certain scenarios where it offers a good compromise between bandwidth efficiency and system performance.

In Chapter 5, we extended the two-way relaying system to the DF scheme, where two practical two-way relaying strategies are investigated, namely, DF-XORing and DF-superposition.

The former is based on bit-wise level XORing of the detected signals at the relays, whereas the latter is based on symbol-wise level addition at the relays. The numerical results showed that, when the the received signals at the relays are weighted equally, the DF-XOR always outperforms both DF-superposition and AF relaying.

All previous chapters assumed perfect CSI knowledge at the secondary relays to perform beamforming. In Chapter 6, we considered partial CSI of the interference channel between the relays and PUs. We used only CDI to obtain the ZFB weights. Due to the limited feedback, a residual interference occurs at the primary receivers. In this case, we derived an upper bound for the transmit power of the secondary relays. We also investigated the impact of the limited number of feedback bits on the secondary system performance and compared it with the perfect CSI case.

7.2 Future Work

Since beamforming needs perfect CSI between between the secondary and primary systems to fully null the interference inflicted at the primary receivers, more practical CSI knowledge should be assumed, including quantized CSI and statistical CSI. In our research, we focused on perfect CSI. A direct extension to our work is to consider the limited feedback and partial CSI. Complete analytical framework for cooperative spectrum-sharing systems assuming limited feedback is not addressed yet. Also, estimation errors and feedback delay are not considered.

Single antenna nodes are assumed in our system models, however, MIMO systems are of high interest in the nowadays wireless applications. Extension of the precoding methods to MIMO-cognitive systems is a another future direction of research. In addition, multi-user MIMO and massive MIMO systems can be considered as system models for future work.

Beamforming is an alternative technology that can be used in physical-layer secrecy. Recently, some work on cooperative relaying is done as a good means to add artificial noise in order to enhance physical-layer security. Combining beamforming and cooperative relaying in CR as tools to enhance the physical-layer secrecy is a recent branch in nowadays academic research.

We used in this thesis single carrier transmission, another future direction is the multi-carrier OFDM CR systems, where combination of bemforming and relaying in such systems, to our knowledge, are not tackled yet. In addition, other fading models, such as frequency and time selective fading channels can be assumed. We also assumed Rayleigh channels and this can be extended to other general fading channels such as Nakagami channels.

Bibliography

[1] Akyildiz et al., NeXtgeneration dynamic spectrum access/cognitive radio wireless networks: A survey, *Computer Networks* 50 (2006).

[2] X. Kang, Y. Liang, and A. Nallanathan, "Optimal power allocation for fading channels in cognitive radio networks: delay-limited capacity and outage capacity," in *Proc. IEEE Vehicular Technology Conference,* pp. 1544−1548, May 2008.

[3] R. Etkin, A. Parekh, and D. Tse, "Spectrum sharing for unlicensed bands," *IEEE J. Sel. Areas Commun.,* vol. 25, pp. 517−528, Apr. 2007.

[4] L. Zhang, Y. Liang, Y. Xin, and V. Poor, "Robust cognitive beamforming with partial channel state information," *IEEE Trans. on Wireless Commun.*, vol. 8, no. 8, pp. 4143−4153, Aug. 2009.

[5] A. Tajer, N. Prasad, and X. Wang, "Beamforming and rate allocation in MISO cognitive radio networks," *IEEE Trans. on Signal Process.,* vol. 58, no. 1, pp. 362−377, Jan. 2010.

[6] C. Stevenson, G. Chouinard, Z. Lei, W. Hu, S. Shellhammer, and W. Caldwell, "IEEE 802.22: The first cognitive radio wireless regional area network standard," *IEEE Commun. Mag.,* vol. 47, pp. 130 −138, 2009.

[7] J. N. Laneman, D.N.C Tse, and G.W. Wornell, "Cooperative diversity in wireless networks: Efficient protocols and outage behavior," *IEEE Trans. Inf. Theory,* vol. 50, no. 12, pp. 3062−3080, Dec. 2004.

[8] F. Onat, A. Adinoyi, F. Yijia, H. Yanikomeroglu, J. Thompson, and I. Marsland, "Threshold selection for SNR-based selective digital relaying in cooperative wireless networks," *IEEE Trans. Wireless Commun.,* vol. 7, no. 11, pp. 4226−4237, Nov. 2008.

[9] S. Haykin, "Cognitive radio: brain-empowered wireless communications," *IEEE J. Sel. Areas Commun.,* vol. 23, no. 9, pp. 201−220, 2005.

[10] J. Mitola and G. Q. Maguire, "Cognitive radio: Making software radios more personal," *IEEE Pers. Commun.,* vol. 6, pp. 13−18, Aug. 1999.

[11] A. Nosratinia, T.E. Hunter, and A. Hedayat, "Cooperative communication in wireless networks," *IEEE Commun. Mag.,* vol. 42, no. 10, pp. 74− 80, Oct. 2004.

[12] A. Sendonaris, E. Erkip, and B. Aazhang, "User cooperation diversity Part I and Part II," *IEEE Trans. Commun.,* vol. 51, no. 11, pp. 1927−48, Nov. 2003.

[13] Y. Han, A. Pandharipande, and S. Ting, "Cooperative decode-and-forward relaying for secondary spectrum access," *IEEE Trans. Wireless Commun.*, vol. 28, no. 10, pp. 4945−4950, Oct. 2009.

[14] V. Asghari and S. Aissa, "End-to-end performance of cooperative relaying in spectrum-sharing systems with quality of service requirements," *IEEE Trans. Veh. Technol.,* vol. 60, no. 6, pp. 2656−2668, July 2011.

[15] Y. Guo, G. Kang, Q. Sun, M. Zhang, and P. Zhang, "Outage performance of cognitive-radio relay system based on the spectrum-sharing environment," in *Proc. IEEE Globecom 2010,* pp. 1−5, Dec. 2010.

[16] Z. Yan, X. Zhang, and W. Wang, "Exact outage performance of cognitive relay networks with maximum transmit power limits," *IEEE Commun. Lett.,* vol. 15, no. 12, pp. 1317−1319, Dec. 2011.

[17] S. Sanguk, J. Lee, and D. Hong, "Capacity of reactive DF scheme in cognitive relay networks," *IEEE Trans. Wireless Commun.,* vol. 10, no. 10, pp. 3133−3138, Oct. 2011.

[18] V. Asghari, S. Affes and A. Ghrayeb, "Reactive relay selection in cooperative spectrum-sharing systems" in *Proc. IEEE WCNC 2012,* Paris, France, Apr. 2012.

[19] Y. Han, A. Pandharipande, and S. Ting, "Cooperative spectrum sharing via controlled amplify-and-forward relaying," in *Proc. IEEE PIMRC,* Cannes, France, pp.1−5, Sep. 2008.

[20] K.B. Fredj and S. Aissa, "Performance of amplify-and-forward systems with partial relay selection under spectrum-sharing constraints," *IEEE Trans. Wireless Comm.,* vol. 11, no. 2, pp. 500−504, Feb. 2012.

[21] H. L. Van Trees, *Optimum Array Processing*, Hoboken, NJ: Wiley, 2002.

[22] Y. Jing and H. Jafarkhani, "Network beamforming using relays with perfect channel information," in *Proc. IEEE Int. Conf. Acoustics, Speech and Signal Processing (ICASSP07),* Honolulu, HI, pp. 473−476, Apr. 2007.

[23] M. Bengtsson and B. Ottersten, *Handbook of Antennas in Wireless Communications*, Boca Raton, FL: CRC, Aug. 2001, Optimal and Suboptimal Transmit Beamforming.

[24] T. M. Duman and A. Ghrayeb, *Coding for MIMO Communication Systems,* Wiley & Sons, January 2008.

[25] L. Zhang, Y. Liang, and Y. Xin, "Joint beamforming and power allocation for multiple access channels in cognitive radio networks," *IEEE J. Sel. Areas in commun.,* Vol. 26, No. 1, January 2008.

[26] M. Islam, Y. Liang, and A. Hoang, "Joint power control and beamforming for cognitive radio networks," *IEEE Trans. Wireless Commun.,* Vol. 7, No. 7, July 2008.

[27] D. Tse and P. Viswanath, *Fundamentals of Wireless Communication*, Cambridge University Press, 2005.

[28] M. Schubert and H. Boche, "Solution of the multiuser downlink beamforming problem with individual SINR constraints," *IEEE Trans. Vehicular Technol.,* vol. 53, no. 1, pp. 18−28, Jan. 2004.

[29] K. Cumanan, L. Musavian, S. Lambotharan, and A. B. Gershman, "SINR balancing technique for downlink beamforming in cognitive radio networks" *IEEE Signal Process. Lett.,* Vol. 17, No. 2, February 2010.

[30] F. Rashid-Farrokhi, K. Liu, and L. Tassiulas, "Transmit beamforming and power control for cellular wireless systems," *IEEE J. Sel. Areas Commun.,* vol. 16, no. 8, pp. 1437−1450, Oct. 1998.

[31] W. Yang and G. Xu, "Optimal downlink power assignment for smart antenna systems," in *Proc. IEEE ICASSP,* Seattle, WA, May 1998, vol. 6, pp. 3337−3340.

[32] A. Khachan, A. Tenenbaum, and R. S. Adve, "Linear processing for the downlink in multiuser MIMO systems with multiple data streams," in *IEEE International Conf. on Communications,* Jun. 2006.

[33] Y. Jing and H. Jafarkhani, "Network beamforming using relays with perfect channel information," *IEEE Trans. on Info. Theory,* vol. 55, no. 6, pp. 2499−2517, June 2009.

[34] V. Havary-Nassab, S. Shahbazpanahi, A. Grami, and L. Zhi-Quan, "Distributed beamforming for relay networks based on second-order statistics of the channel state information," *IEEE Trans. on Signal Process.,* vol. 56, no. 9, pp. 4306−4316, Sept. 2008.

[35] R.H.Y Louie, Y. Li, and B. Vucetic, "Zero forcing in general two-hop relay networks," *IEEE Trans. Veh. Technol.,* vol. 59, no. 1, pp. 191−201, Jan. 2010.

[36] R. Zhang, Y. Liang, C. Chai, and S. Cui, "Optimal beamforming for two-way multi-antenna relay channel with analogue network coding," *IEEE Journal on Selected Areas in Comm.,* vol. 27, no. 5, pp. 699−712, June 2009.

[37] J. Joung and A. Sayed, "Multiuser two-way amplify-and-forward relay processing and power control methods for beamforming systems," *IEEE Trans. on Signal Process.,* vol. 58, no. 3, pp. 1833−1846, March 2010.

[38] Z. Yi and I. Kim, "Optimum beamforming in the broadcasting phase of bidirectional cooperative communication with multiple decode-and-forward relays," *IEEE Trans. on Wireless Commun.,* vol. 8,no. 12, pp. 5806−5812, Dec. 2009.

[39] R. Zhang and Y. C. Liang, "Exploiting multi-antennas for opportunistic spectrum sharing in cognitive radio networks," *IEEE J. Sel. Topics Signal Process.,* vol. 2, no. 1, pp. 88−102, Feb. 2008.

[40] K. Hamdi, W. Zhang, and K. B. Letaief, "Joint beamforming and scheduling in cognitive radio networks," in *Proc. IEEE Globecom,* Washington, DC, Nov. 2007, pp. 2977−2981.

[41] K. Cumanan, R. Krishna, V. Sharma, and S. Lambotharan, "Robust interference control techniques for multi-user cognitive radios using worst-case performance optimization," in *Proc. Asilomar Conf. Sign., Syst. and Comp.,* Pacific Grove, CA, Oct. 2008, pp. 378−382.

[42] K. Cumanan, R. Krishna, Z. Xiong, and S. Lambotharan, "SINR balancing technique and its comparison to semidefinite programming based QoS provision for cognitive radios," in *Proc. IEEE VTC,* Barcelona, Spain, Apr. 2009, pp. 1−5.

[43] K. Hamdi, K. Zarifi, K. Ben Letaief, and A. Ghrayeb, "Beamforming in relay-assisted cognitive radio systems: A convex optimization approach," in *Proc. IEEE ICC,* Kyoto, Japan, pp.1−5, June 2011.

[44] R. Krishna, K. Cumanan, Z. Xiong, and S. Lambotharan "Cooperative relays for an underlay cognitive radio network", *International Conference on Wireless Communications and Signal Processing WCSP,* 2009.

[45] K. Zarifi, A. Ghrayeb, and S. Affes, "Jointly optimal source power control and relay matrix design in multipoint-to-multipoint cooperative communication networks," *IEEE Trans. Sig. Process.,* vol. 59, no. 9, pp. 4313−4330, Sept. 2011.

[46] R. Manna, R.H.Y Louie, Y. Li, and B. Vucetic, "Cooperative spectrum sharing in cognitive radio networks with multiple antennas," *IEEE Trans. Signal Process.,* vol. 59, no. 11, pp. 5509−5522, Nov. 2011.

[47] S.H. Safavi, M. Ardebilipour, and S. Salari, "Relay beamforming in cognitive two-way networks with imperfect channel state information," *IEEE Wireless Commun. Lett.*, vol. 1, no. 4, pp. 344−347, August 2012.

[48] A. Afana, V. Asghari, A. Ghrayeb, and S. Affes, "On the performance of cooperative relaying spectrum-sharing systems with collaborative distributed beamforming," *IEEE Trans. on Commun.,* vol. 62, no. 3, pp. 857−871, March 2014.

[49] A. Afana, A. Ghrayeb, V. Asghari, and S. Affes, "Distributed beamforming for spectrum-sharing relay networks under mutual primary-secondary interference" in *Prco. IEEE WCNC,* Istanbul, Turkey, April, 2014.

[50] A. Afana, V. Asghari, A. Ghrayeb, and S. Affes, "Cooperative spectrum sharing systems with beamforming and interference constraints," in *Prco. IEEE SPAWC,* Turkey, Jun., 2012.

[51] A. Afana, V. Asghari, A. Ghrayeb, and S. Affes,"Enhancing the performance of spectrum sharing systems via collaborative distributed beamforming and AF relaying," in *Proc. IEEE GlobeCom,* Anehaim, USA, Dec., 2012.

[52] J. M. Peha, "Approaches to spectrum sharing," *IEEE Communications Magazine,* vol. 8, no. 1, pp. 10-11, Feb., 2005.

[53] L. Tong, B.M. Sadler, and M. Dong, "Pilot-assisted wireless transmissions: general model, design criteria, and signal processing," *IEEE Signal Processing Magazine,* vol. 21, no. 6, pp. 12−25, Nov. 2004.

[54] V. Havary-Nassab, S. Shahbazpanahi, and A. Grami, "Optimal distributed beamforming for two-way relay networks," *IEEE Trans. Signal Process.,* vol. 58, no. 3, pp. 1238−1250, March 2010.

[55] A. Goldsmith, S.A. Jafar, I. Maric, and S. Srinivasa, "Breaking spectrum gridlock with cognitive radios: an information theoretic perspective," *Proc. IEEE,* vol. 97, no. 5, pp. 894−914, May 2009.

[56] I. S. Gradshteyn and I. M. Ryzhik, *Table of integrals, series and products*, 7th ed. Elsevier, 2007.

[57] R. J. Pavur, "*Quadratic forms involving the complex Gaussian,*" M.Sc. dissertation, Math. Dept., Texas Tech. Univ., Lubbock, TX, Aug. 1980.

[58] A. Papoulis and S. U. Pillai, *Probability, random variables, and stochastic processes*, 4th ed. Boston: McGraw-Hill, 2002.

[59] V. Asghari and S. Aissa, "Performance of cooperative relaying in spectrum-sharing systems with amplify and forward relaying" *IEEE Trans. Wireless Comm.,* vol. 11, no. 4, pp. 1295−1300, April 2012.

[60] J. Proakis, *Digital Communications*, 4th ed. McGraw-Hill, 2000.

[61] M. Li, M. Lin, Q. Yu, W.-P. Zhu, and L. Dong, "Optimal beamformer design for dual-hop MIMO AF relay networks over Rayleigh fading channels," *IEEE J. Sel. Areas in Commun.,* vol. 30, no. 8, pp. 1402−1414, September 2012.

[62] M. K. Simon and M.-S. Alouini, *Digital Communications over Fading Channels*, 2nd ed. Wiley, 2005.

[63] A. P. Prudnikov, Y. A. Brychkov, and O. I. Marichev, *Integrals and Series, Volume 2: Special Functions,* Second Printing with corrections, Gordon and Breach Science Publishers, 1988.

[64] M. Di Renzo, F. Graziosi, and F. Santucci, "A unified framework for performance analysis of CSI-assisted cooperative communications over fading channels," *IEEE Trans. Commun.,* vol. 57, no. 9, pp. 2251−2257, Sep. 2009.

[65] V. Adamchik and O. Marichev, "The algorithm for calculating integrals of hypergeometric type functions and its realization in reduce systems," in *Proc. Intern. Conf. Symbolic Algebraic Computation,* Tokyo, Japan, 1990.

[66] M. Abramowitz and I. A. Stegun, "*Handbook of Mathematical Functions with Formulas, Graphs, and Mathematical Tables,*" 9th printing. New York: Dover, pp. 890 and 923, 1972.

[67] X. Zeng, A. Ghrayeb, and M. Hasna, "Joint optimal threshold-based relaying and ML detection in network-coded two-way relay," *IEEE Trans. Commun.,* vol. 60, no. 9, pp.2657−2667, September 2012.

[68] X. Zhang, M. Hasna, and A. Ghrayeb, "Performance analysis of relay assignment schemes for cooperative networks with multiple source-destination pairs," *IEEE Trans. Wireless Commun.,* vol. 11, no. 1, pp. 166−177, Jan. 2012.

[69] S. Nguyen, A. Ghrayeb, G. Al-Habian, and M. Hasna, "Mitigating error propagation in two-way relay channels employing network coding," *IEEE Trans. Wireless Commun.,* vol. 9, no. 11, pp. 3380−3390, November 2010.

[70] R.H.Y Louie, Y. Li, and B. Vucetic, "Practical physical layer network coding for two-way relay channels: performance analysis and comparison," *IEEE Trans. on Wireless Commun.,* vol. 9, no. 2, pp. 764−777, Feb. 2010.

[71] B. Rankov and A. Wittneben, "Spectral efficient protocols for half-duplex fading relay channels," *IEEE Journal on Selected Areas in Commun.,* vol.25, no.2, pp.379−389, February 2007

[72] M. Zeng, R. Zhang, and S. Cui, "On design of collaborative beamforming for two-way relay networks," *IEEE Trans. on Signal Process.,* vol. 59, no. 5, pp. 2284−2295, May 2011.

[73] Q. Li, S. H. Ting, A. Pandharipande, and Y. Han, "Cognitive spectrum sharing with two-way relaying systems," *IEEE Trans. Veh. Technol.,* vol. 60, no. 3, pp. 1233−1240, Mar. 2011.

[74] L. Yang, M. S. Alouini, and K. Qaraqe, "On the performance of spectrum sharing systems with two-way relaying and multiuser diversity," *IEEE Commun. Lett.,* vol. 16, no. 8, pp. 1240−1243, August 2012.

[75] K. Jitvanichphaibool, Y.-C. Liang, and R. Zhang, "Beamforming and power control for multi-antenna cognitive two-way relaying," in *Proc. IEEE Wireless Communications and Networking Conf. WCNC,* 2009.

[76] R. Wang, M. Tao, and Y. Liu, "Optimal linear transceiver designs for cognitive two-way relay networks," *IEEE Trans. on Signal Process.,* vol. 61, no. 4, pp. 992−1005, Feb. 15, 2013.

[77] A. Afana, A. Ghrayeb, V. Asghari, and S. Affes, "Distributed beamforming for spectrum-sharing systems with AF cooperative two-way relaying," *accepted to IEEE Transaction on Communications,* May, 2014.

[78] A. Afana, A. Ghrayeb, V. Asghari, and S. Affes,"On the performance of spectrum sharing two-way relay networks with distributed beamforming" in *Prco. IEEE SPAWC,* Darmstadt, Germany, 2013.

[79] L. Musavian, S. Aissa, and S. Lambotharan, "Effective capacity for interference and delay constrained cognitive-radio relay channels," *IEEE Trans. Wireless Commun.,* vol. 9, no. 5, pp. 1698−1707, May 2010.

[80] K. Huang and R. Zhang, "Cooperative feedback for multiantenna cognitive radio networks," *IEEE Trans. Signal Process.,* vol. 59, no. 2, pp. 747−758, Feb. 2011.

[81] Z. Wang and G. B. Giannakis, "A simple and general parameterization quantifying performance in fading channels," *IEEE Trans. Commun.,* vol. 51, no. 8, 2003.

[82] A. Basilevsky, *Applied Matrix Algebra in the Statistical Sciences,* New York, NY: North-Holland, 1983.

[83] I. Trigui, S. Affes, and A. Stephenne, "Closed-form error analysis of variable-gain multi-hop systems in Nakagami-m fading channels," *IEEE Trans. commun.*, vol. 59, no. 8, pp. 2285−2295, August 2011.

[84] E. Mekic, N. Sekulovic, M. Bandjur, M. Stefanovic, and P. Spalevic, *The distribution of ratio of random variable and product of two random variables and its application in performance analysis of multi-hop relaying communications over fading channels,* (Electrical Review), ISSN 0033-2097, R. 88 NR 7a/2012.

[85] A. Afana, A. Ghrayeb, V. Asghari, and S. Affes, "Distributed beamforming for cognitive DF two-way relay networks under mutual secondary-primary interference," *submitted to IEEE Transaction on Vehicular Technology,* Feb. 2014.

[86] A. Afana, A. Ghrayeb, V. Asghari, and S. Affes,"Collaborative beamforming for spectrum-sharing two-way selective relay networks under co-channel interferences" in *Prco. IEEE PIMRC,* London, UK, Sept. 2013.

[87] A. Afana, A. Ghrayeb, V. Asghari, and S. Affes, "Cooperative two-way selective relaying in spectrum-sharing systems with distributed beamforming," in *Prco. IEEE WCNC,* Shangahi, April, 2013.

[88] A. Jovicic and P. Viswanath, "Cognitive radio: An information-theoretic perspective," *IEEE Trans. Infor. Theory,* vol. 55, no. 9, pp. 3945−3958, Sep. 2009.

[89] J. Hong, B. Hong, T. Ban and W. Choi, "On the cooperative diversity gain in underlay cognitive radio systems," *IEEE Trans. on Commun.,* vol. 60, no. 1, pp. 209−219, January 2012.

[90] R. Zhang, F. Gao, and Y. C. Liang, "Cognitive beamforming made practical: Effective interference channel and learning-throughput tradeoff," *IEEE Trans. Commun.,* vol. 58, pp. 706−718, Feb. 2010.

[91] L. Zhang, Y. C. Liang, Y. Xin, and H. V. Poor, "Robust cognitive beam- forming with partial channel state information," *IEEE Trans. Commun.,* vol. 8, pp. 4143−4453, Aug. 2009.

[92] Y. Chen, G. Yu, Z. Zhang, H. Chen, and P. Qiu, "On cognitive radio net-works with opportunistic power control strategies in fading channels," *IEEE Trans. Wireless Commun.,* vol. 7, pp. 2752−2761, Jul. 2008.

[93] R. Zhang, "Optimal power control over fading cognitive radio channels by exploiting primary user CSI," in *Proc. IEEE Globecom,* New Orleans, LA, Nov. 2008

[94] A. Scaglione, P. Stoica, S. Barbarossa, G. B. Giannakis, and H. Sam- path, "Optimal designs for space-time linear precoders and decoders," *IEEE Trans. Signal Process.*, vol. 50, no. 5, pp. 1051−1064, May 2002.

[95] D. J. Love, R. W. Heath, Jr., W. Santipach, and M. L. Honig, "What is the value of limited feedback for MIMO channels?," *IEEE Commun. Mag.,* vol. 42, pp. 54−59, Oct. 2004.

[96] D. J. Love, R. W. Heath, V. K. N. Lau, D. Gesbert, B. D. Rao, and M. Andrews, "An overview of limited feedback in wireless communication systems," *IEEE J. Sel. Areas Commun.,* vol. 26, no. 8, pp. 1341−1365, 2008.

[97] D. J. Love, R. W. Heath, Jr., and T. Strohmer, "Grassmannian beamforming for MIMO wireless systems," *IEEE Trans. Inf. Theory,* vol. 49, pp. 2735−2747, Oct. 2003.

[98] K. Huang and R. Zhang, "Cooperative feedback for multiantenna cognitive radio networks," *IEEE Trans. Signal Process.*, vol. 59, pp. 747−758, Feb. 2011.

[99] J. Noh and S-J. Oh, "Beamforming in a multi-user cognitive radio system with partial channel state information," *IEEE Trans. Wireless Commun.,* vol. 12, no. 2, pp.616−625, February 2013.

[100] X. Chen, Z. Zhang, and C. Yuen, "Adaptive mode selection in multiuser MISO cognitive networks with limited cooperation and feedback," *IEEE Trans Veh. Tech.,* accepted 2014.

[101] N. Jindal, "MIMO Broadcast channels with finite-rate feedback," *IEEE Trans. Inf. Theory,* vol. 52, no. 11, pp. 5045−5060, Nov. 2006.

[102] T. Yoo, N. Jindal, and A. Goldsmith, "Multi-antenna downlink channels with limited feedback and user selection," *IEEE J. Sel. Areas Commun.,* vol. 25, no. 7, pp. 1478−1491, September 2007.

[103] Q. Zhang, J. Jia and J. Zhang, "Cooperative relay to improve diversity in cognitive radio networks," *IEEE Commun. Mag.,* vol. 47, no. 2, pp. 111−117, February 2009.

[104] G. Al-Habian, A. Ghrayeb, M. Hasna, and A. Abu-Dayya, "Threshold-based relaying in coded cooperative networks," *IEEE Trans. on Vehicular Tech.,* vol. 60, no. 1, pp. 123−135, January 2011.

[105] P. Ubaidulla and S. Aissa, "Optimal relay selection and power allocation for cognitive two-way relaying networks," *IEEE Wireless Commun. Lett.,* vol.1, no.3, pp.225−228, June 2012.

[106] H. Chen, S. Shahbazpanahi and A.B. Gershman, "Filter-and-forward distributed beamforming for two-way relay networks with frequency selective channels," *IEEE Trans. on Signal Process.,* vol.60, no.4, pp.1927−1941, April 2012.

[107] K. Hamdi, M. Hasna, A. Ghrayeb and K. Ben Letaief , "Opportunistic spectrum sharing in relay-assisted cognitive systems with imperfect CSI," in *IEEE Trans. Vech. Tech.,* Accepted, Aug. 2013.

Appendix A

Proofs of Chapter 3

A.1 Proof of Lemma 3.2.1

Let $X = |h_{s,r_i}|^2, Y = |f_{s,p}|^2, Z = P_{int}|g_{m,r_i}|^2 + \sigma^2$, then the CDF of γ_{s,r_i} conditioned on Z is given as

$$\begin{aligned} F_{\gamma_{s,r_i}|Z}(\gamma) &= \underbrace{\Pr\left(\frac{QX}{Y} < Z\gamma, Y \geq \frac{Q}{P_s}\right)}_{I_1(Z)} \\ &+ \underbrace{\Pr\left(P_s X < Z\gamma, Y < \frac{Q}{P_s}\right)}_{I_2(Z)}; \end{aligned}$$

$$\begin{aligned} I_1(Z) &= \int_{\vartheta}^{\infty} f_Y(y) \int_0^{\frac{Z\gamma}{Q}y} f_X(x)dxdy \\ &= \int_{\vartheta}^{\infty} f_Y(y) F_X(\frac{Z\gamma}{Q}y)dy, \end{aligned} \tag{A.1}$$

where $\vartheta = \frac{Q}{P_s}$.

Substituting for the PDF of Y and CDF of X, we derive $I_1(Z)$ as

$$I_1(Z) = 1 - F_Y(\vartheta) - \frac{\lambda_y e^{-(\frac{\lambda_x Z\gamma}{Q} + \lambda_y)\vartheta}}{(\frac{\lambda_x Z\gamma}{Q} + \lambda_y)}, \tag{A.2}$$

where $\lambda_x = \lambda_{s,r_i}$ and $\lambda_y = \lambda_{s,p}$. Next, due to the statistical independence between X and Y, the second integral $I_2(Z)$ is evaluated as

$$I_2(Z) = F_Y(\vartheta) F_X(\frac{\gamma}{P_s}Z). \tag{A.3}$$

The unconditional CDF of γ_{s,r_i} is derived by averaging (A.1) and (A.2) over the PDF of Z as follows

$$F_{\gamma_{s,r_i}}(\gamma) = \mathrm{E}_Z\left\{F_{\gamma_{s,r_i}|Z}(\gamma)\right\} = I_3 + I_4,$$

where $I_3 = \mathrm{E}_Z\{I_1(Z)\}$ and $I_4 = \mathrm{E}_Z\{I_2(Z)\}$. To proceed, we need the PDF of Z which is given by

$$f_Z(z) = \frac{\lambda_z e^{\frac{\lambda_z \sigma^2}{P_{int}}}}{P_{int}} e^{-\frac{\lambda_z z}{P_{int}}} u(z-\sigma^2), \tag{A.4}$$

where $\lambda_z = \lambda_{m,r_i}$ and $u(.)$ is the unit-step function. Incorporating (A.4) into (A.1), I_3 is derived as

$$\begin{aligned} I_3 &= 1 - F_Y(\vartheta) - \frac{\lambda_y \lambda_z e^{\frac{\lambda_z \sigma^2}{P_{int}}} e^{-\lambda_y \vartheta}}{P_{int}} \\ &\times \underbrace{\int_{\sigma^2}^{\infty} \left(\frac{\lambda_x \gamma z}{Q} + \lambda_y\right)^{-1} e^{-(\frac{\lambda_x \gamma}{Q} + \frac{\lambda_z}{P_{int}})z} dz}_{I_{31}}. \end{aligned} \tag{A.5}$$

Utilizing [56, Eq. 3.352.2], I_{31} can be computed as follows.

$$\begin{aligned} I_{31} &= \frac{e^{-\lambda_{s,p}\vartheta + \frac{\lambda_{m,r_i}\sigma^2}{P_{int}}}}{\gamma} \left(-e^{\frac{Q\lambda_{s,p}}{\lambda_{s,r_i}\gamma}\left(\frac{\lambda_{m,r_i}}{P_{int}} + \frac{\lambda_{s,r_i}\gamma}{Q}\right)}\right. \\ &\times \left. Ei\left[-\left(\frac{Q\lambda_{s,p}}{\gamma\lambda_{s,r_i}} + \sigma^2\right)\left(\frac{\lambda_{m,r_i}}{P_{int}} + \frac{\lambda_{s,r_i}\gamma}{Q}\right)\right]\right), \end{aligned} \tag{A.6}$$

where $\frac{Q\lambda_{s,p}\lambda_{m,r_i}}{\lambda_{s,r_i}P_{int}}$. Similarly, to evaluate I_4, we average over $I_2(Z)$ with respect to Z which results in

$$\begin{aligned} I_4 &= F_Y(\vartheta)\left(\frac{\lambda_{m,r_i} e^{\frac{\lambda_{m,r_i}\sigma^2}{P_{int}}}}{P_{int}}\right)\left(\frac{e^{-\frac{\lambda_{m,r_i}\sigma^2}{P_{int}}} P_{int}}{\lambda_{m,r_i}}\right. \\ &\left. - \frac{e^{-\sigma^2\left(\frac{\lambda_{m,r_i}}{P_{int}} + \frac{\lambda_{s,p}\gamma}{P_s}\right)} P_s P_{int}}{P_{int}\lambda_{s,p}\gamma + P_s\lambda_{m,r_i}}\right). \end{aligned} \tag{A.7}$$

Substituting (A.6) into (A.5) and adding with (A.7) results in (3.2), which concludes the proof.

A.2 Proof of Theorem 3.4.2

First, we represent the Gauss-hypergeometric function in (3.17) and also the exponential function in (3.30) in terms of Meijer's G-functions using [65, Eq. 10, 11], which are given, respectively, as

$$\begin{aligned} 2F_1\left(\varphi+1,\varphi;\varphi+1;-\frac{P_{int}u}{\lambda_{m,d}P_r}\right) &= \frac{\varphi\, P_{int}\, u}{\Gamma(L_s)P_r} \\ \times G_{2,2}^{1,2}\left(-\frac{P_{int}\,u}{\lambda_{m,d}P_r}\Big|_{-1,-(\varphi+1)}^{-L_s,-\varphi}\right); & \end{aligned}$$

$$e^{-bu} = G_{0,1}^{1,0}\left(bu\big|_{0}^{-}\right). \tag{A.8}$$

Thus, integrating the second term of (3.17) yields

$$\begin{aligned} J_1 &= \varpi\,\epsilon\int_0^{\infty}\left(u^{\varphi+\frac{1}{2}}G_{2,2}^{1,2}\left(-\frac{P_{int}u}{\lambda_{m,d}P_r}\Big|_{-1,-(\varphi+1)}^{-L_s,-\varphi}\right)\right. \\ &\times \left. G_{0,1}^{1,0}\left(bu\big|_{0}^{-}\right)\right)du, \end{aligned} \tag{A.9}$$

where $\varphi = L_s - 1$, $\varpi = \frac{a\sqrt{b}}{2\sqrt{\pi}}\frac{\lambda_{m,d}}{P_{int}\Gamma(\varphi)P_r^{\varphi}}$, $\epsilon = \frac{\varphi P_{int}}{\Gamma(L_s)P_r}$.
By exploiting the integral of the product of a power term and two Meijer's G-function in [65, Eq. 21], (A.9) results in

$$J_1 = \varpi\,\epsilon\left(\frac{\lambda_{m,d}P_r}{P_{int}}\right)^{\nu} G_{2,3}^{3,1}\left(-\frac{\nu\, b\,\lambda_{m,d}P_r}{P_{int}}\Big|_{0,1-\frac{1}{2},-\frac{1}{2}}^{\frac{1}{2}-\varphi,\frac{1}{2}}\right), \tag{A.10}$$

where $\nu = \varphi + \frac{3}{2}$. Therefore, adding (A.10) with the integration of the first term of (3.17), a closed-form expression for the unconditional BER at SD is given as in (3.31). Thus the proof is completed.

A.3 Proof of Lemma 3.5.2

Let $\gamma_1 = (\frac{\gamma_q\|\mathbf{h_{sr}}\|^2}{|h_{s,p}|^2}) = \frac{X}{Y}$. As we mentioned above, $\|\mathbf{h_{sr}}\|^2$ is a chi-square random variable with $2L_s$ degrees of freedom, and $|h_{s,p}|^2$ is an exponential random variable. We use the integral

formula from [58, Eq. 6.60] to find the PDF of $f_{\gamma_1}(\gamma)$ as follows

$$\begin{aligned} f_{\gamma_1}(\gamma) &= \int_{y=0}^{\infty} y f_{\|\mathbf{h_{sr}}\|^2}(y\gamma) f_{|h_{s,p}|^2}(y) dy \\ &= \frac{\lambda_{s,p}(\gamma)^{L_s-1}}{(\gamma_q)^{L_s}(L_s-1)!} \int_{y=0}^{\infty} y^{L_s} e^{(-y\gamma/\gamma_q)} e^{-\lambda_{s,p} y} dy. \end{aligned} \tag{A.11}$$

The last integral can be determined using [56, Eq. 3.326.1], resulting in (3.48).

To find the CDF, we integrate the PDF as follows

$$\begin{aligned} F_{\gamma_1}(\gamma) &= \int_0^{\gamma} f_{\frac{\|\mathbf{h_{sr}}\|^2}{|h_{s,p}|^2}}(x) dx \\ &= \frac{\lambda_{s,p} L_s}{(\gamma_q)^{L_s}} \int_0^{\gamma} \frac{(x)^{L_s-1}}{(\frac{x}{\gamma_q} + \lambda_{s,p})^{L_s+1}} dx. \end{aligned} \tag{A.12}$$

We use [56, Eq. 3.194.1] to solve the above integral which gives (3.49). This completes the proof.

A.4 Proof of Theorem 3.5.3

In the following, we derive the exact form for the CDF of the equivalent SNR in the form $\gamma_{eq} = \frac{\gamma_1\gamma_2}{\gamma_1+\gamma_2}$. By using the definition of CDF $F^{AF}_{\gamma_{eq_1}}(\gamma) = F\left(\frac{\gamma_1\gamma_2}{\gamma_1+\gamma_2} \leq \gamma\right)$, and invoking (3.14), (3.46) and (3.47), $F^{AF}_{\gamma_{eq_1}}(\gamma)$ can be expressed as

$$\begin{aligned} F^{AF}_{\gamma_{eq_1}}(\gamma) &= \int_0^{\infty} \Pr\left[\frac{\gamma_1\gamma_2}{\gamma_1+\gamma_2} \leq \gamma | \gamma_2\right] f_{\gamma_2}(\gamma_2) d\gamma_2 \\ &= \int_0^{\gamma} \Pr\left[\gamma_1 \geq \frac{\gamma\gamma_2}{\gamma_2-\gamma} | \gamma_2\right] f_{\gamma_2}(\gamma_2) d\gamma_2 \\ &+ \int_{\gamma}^{\infty} \Pr\left[\gamma_1 \leq \frac{\gamma\gamma_2}{\gamma_2-\gamma} | \gamma_2\right] f_{\gamma_2}(\gamma_2) d\gamma_2 \\ &= I_1(\gamma) + I_2(\gamma), \end{aligned} \tag{A.13}$$

where

$$\begin{aligned} I_1(\gamma) &= \int_0^{\gamma} f_{\gamma_2}(\gamma_2) d\gamma_2 \\ &= F_{\gamma_2}(\gamma), \end{aligned} \tag{A.14}$$

and

$$I_2(\gamma) = \int_{\gamma}^{\infty} F_{\gamma_1}\left(\frac{\gamma\gamma_2}{\gamma_2-\gamma}\right) f_{\gamma_2}(\gamma_2)d\gamma_2. \tag{A.15}$$

Then, substituting (3.47) and (3.14) into (A.15), $I_2(\gamma)$ becomes

$$\begin{aligned} I_2(\gamma) &= \int_{\gamma}^{\infty}\left(1-\frac{\Gamma(L_s,\frac{\gamma}{\gamma_2-\gamma}\frac{\gamma_2}{\gamma_s})}{(L_s-1)!}\right) f_{\gamma_2}(\gamma_2)d\gamma_2 \\ &= \int_{\gamma}^{\infty} f_{\gamma_2}(\gamma_2)d\gamma_2 - \int_{\gamma}^{\infty}\frac{\Gamma\left(L_s,\frac{\gamma}{\gamma_2-\gamma}\frac{\gamma_2}{\gamma_s}\right)}{(L_s-1)!} \\ &\quad \times f_{\gamma_2}(\gamma_2)d\gamma_2 \\ &= 1-\int_{0}^{\gamma} f_{\gamma_2}(\gamma_2)d\gamma_2 - \\ &\quad \int_{\gamma}^{\infty}\frac{\Gamma\left(L_s,\frac{\gamma}{\gamma_2-\gamma}\frac{\gamma_2}{\gamma_s}\right) f_{\gamma_2}(\gamma_2)}{(L_s-1)!}d\gamma_2. \end{aligned} \tag{A.16}$$

Then substituting (A.14) and (A.16) into (A.13) yields

$$F^{AF}_{\gamma_{eq_1}}(\gamma) = 1-\underbrace{\int_{\gamma}^{\infty}\frac{\Gamma\left(L_s,\frac{\gamma}{\gamma_2-\gamma}\frac{\gamma_2}{\gamma_s}\right)}{(L_s-1)!}f_{\gamma_2}(\gamma_2)d\gamma_2}_{I_3}. \tag{A.17}$$

By using the variable change $u=\gamma_2-\gamma$, the integral I_3 can be written as

$$I_3 = a\int_{0}^{\infty}\Gamma\left(L_s, c_o\gamma+\frac{c_o\gamma^2}{u}\right)\frac{(u+\gamma)^{L_s-2}e^{-\frac{u+\gamma}{\gamma_r}}}{(L_s-2)!(\gamma_r)^{L_s-1}}du, \tag{A.18}$$

where $a=\frac{1}{(L_s-2)!(L_s-1)!\gamma_r^{L_s-1}}$ and $c_o=1/\gamma_s$.

By using [56, Eq. 8.352.2] and [56, Eq. 1.111], the incomplete gamma function of the integral in (A.18) can be expressed as

$$\begin{aligned} \Gamma(L_s-1, c_o\gamma+\frac{c_o\gamma^2}{u}) &= (Ls-2)!e^{\left(-c_o\gamma-\frac{c_o\gamma^2}{u}\right)} \\ &\times \sum_{k=0}^{Ls-2}\sum_{v=0}^{k}\frac{1}{k!}\binom{k}{v}(c_o\gamma)^{k-v} \\ &\times (c_o\gamma^2)^v\frac{1}{(u)^v}. \end{aligned} \tag{A.19}$$

By using [56, Eq. 1.111] again for the term $(u+\gamma)^{L_s-2}$, I_3 can be expressed as

$$\begin{aligned} I_3 &= a\,(Ls-2)!e^{(-\frac{\gamma}{\gamma_s})}\sum_{n=0}^{Ls-2}\sum_{k=0}^{Ls-1}\sum_{v=0}^{k}\frac{1}{k!}\binom{k}{v}\binom{L_s-2}{n} \\ &\times (c_o)^k\int_0^{\infty} e^{\left(-\frac{\gamma^2}{\gamma_s u}\right)}(u)^{n-v}e^{-\frac{u}{\gamma_r}}du \\ &\times (\gamma)^{L_s-2-n}(\gamma)^{k+v}e^{-\frac{\gamma}{\gamma_r}}. \end{aligned} \tag{A.20}$$

The inner integral of I_3 can be solved by exploiting [56, Eq. 3.471.9], resulting in

$$\begin{aligned} I_3 &= a\,(Ls-2)!e^{(-\frac{\gamma}{\gamma_s})}\sum_{n=0}^{Ls-2}\sum_{k=0}^{Ls-1}\sum_{v=0}^{k}\frac{1}{k!}\binom{k}{v}\binom{L_s-2}{n} \\ &\times (\gamma)^{L_s-2-n}(\gamma)^{k+v}e^{-\frac{\gamma}{\gamma_r}}2(\gamma_r)^{\frac{n-v+1}{2}}(\frac{1}{\gamma_s})^{k+\frac{n-v+1}{2}} \\ &\times (\gamma)^{n-v+1}\,K_{n-v+1}\left(2\sqrt{\frac{\gamma^2}{\gamma_s\gamma_r}}\right). \end{aligned} \tag{A.21}$$

With the help of (A.17) and (A.21) and after some mathematical manipulations, we get the exact CDF expression of the equivalent SNR $F^{AF}_{\gamma_{eq_1}}(\gamma)$ as in (3.52).

A.5 Proof of Theorem 3.5.4

Following the same approach as in the *Proof of Theorem 3.5.3* and after some mathematical manipulations, we obtain the exact CDF expression of the equivalent SNR $F^{AF}_{\gamma_{eq_2}}(\gamma)$ as given in (3.53).

Appendix B

Proofs of Chapter 5

B.1 Proof of Lemma 5.2.1

We derive the CDF of $\gamma_{s_j,r_i,k} = \frac{U}{P_{int}V+\sigma^2}$, where $U = \min\left\{\frac{Q_j}{|f_{s_j,p}|^2}, P_s\right\}|h_{s_j,r_i}|^2$ and $V = \sum_{m=1}^{M}|g_{m,r_i}|^2$. By using the definition of CDF of $\gamma_{s_j,r_i,k}$, we find

$$F_{\gamma_{s_j,r_i,k}}(x) = \int_0^\infty \Pr(U < (P_{int}\, y + \sigma^2)x) f_V(y) dy. \tag{B.1}$$

Since V is the sum of M exponential random variables with parameter λ_{m,r_i}, it presents a chi-square random variable with $2M$ degrees of freedom and its PDF is given by

$$f_V(y) \;=\; \frac{\lambda_{m,r_i}^M y^{M-1} e^{-\lambda_{m,r_i} y}}{\Gamma(M)}. \tag{B.2}$$

The CDF of U is given as follows,

$$\begin{aligned} F_U(x) \;&=\; 1 - F_T\left(\frac{Q_j}{P_s}\right) - N\lambda_{s_j,n}\sum_{n=1}^{N-1}\binom{N-1}{n}(-1)^n \frac{e^{-\frac{Q_j}{P_s}\left(\lambda_{s_j,n}(n+1)+\frac{\lambda_{s_j,r_i}x}{Q_j}\right)}}{\left(\lambda_{s_j,n}(n+1)+\frac{\lambda_{s_j,r_i}x}{Q_j}\right)} \\ &+\; F_T\left(\frac{Q_j}{P_s}\right)\left(1 - e^{\frac{\lambda_{s_j,r_i}x}{P_s}}\right), \end{aligned} \tag{B.3}$$

where $F_T\left(\frac{Q_j}{P_s}\right) = F_{\max\limits_{n=1,\ldots,N}|f_{s_j,n}|^2}\left(\frac{Q_j}{P_s}\right) = \left(1 - e^{\frac{\lambda_{s_j,n}Q_j}{P_s}}\right)^N$. Substituting (B.2) and (B.3) into (B.1), and after several algebraic manipulations, (B.1) is equivalently expressed as

$$\begin{aligned} F_{\gamma_{s_j,r_i,k}}(x) \;&=\; 1 - \psi\int_0^\infty \left[\hat{\psi}\frac{1}{xP_{int}\, y + \sigma^2 x + \frac{(n+1)\lambda_{s_j,n}Q_j}{\lambda_{s_j,r_i}}} - F_T\left(\frac{Q_j}{P_s}\right)\right] \\ &\times\; y^{M-1} e^{-(\frac{\lambda_{s_j,r_i}P_{int}x}{P_s}+\lambda_{m,r_i,k})y} dy, \end{aligned} \tag{B.4}$$

where $\psi = e^{-\frac{\lambda_{s_j,r_i}\sigma^2 x}{P_s}} \frac{\lambda^M_{m,r_i,k}}{\Gamma(M)}$ and $\hat{\psi} = \frac{Q_j}{\lambda_{s_j,r_i}} N\lambda_{s_j,n} \sum_{n=1}^{N-1} \binom{N-1}{n} (-1)^n e^{-\frac{Q_j}{P_s}\lambda_{s_j,n}(n+1)}$. After simple manipulations, and with the help of [56, Eqs. (3.351.3), (3.353.5)], $F_{\gamma_{s_j,r_i,k}}(x)$ is derived as (5.7), which concludes the proof.

B.2 Proof of Lemma 5.4.1

To analyze the system performance, we first need to obtain the CDF of $\gamma^*_{s_j|\mathcal{C}}$. Let $U_1 = P_r||\mathbf{\Xi}^{\perp}\mathbf{h}_{\mathbf{r},\mathbf{d}}||^{\mathbf{2}}$ and $V_1 = \sum_{m=1}^{M} |g_{m,s_j}|^2$, by following the same previous approach, we need the CDF of $U_1$and the PDF of V_1 which can be obtained from (3.3) and (B.2), respectively. We find the conditional CDF of $\gamma^*_{s_j|\mathcal{C}}$ as

$$F_{\gamma^*_{s_j|\mathcal{C}}}(x) = \int_0^{\infty} \frac{\psi_1 \gamma\left(\tau, \frac{(P_{int}\, y+\sigma^2)x}{\alpha P_r}\right) y^{\kappa} e^{-\lambda_{m,s_j} y}}{\Gamma(L_s - N - 1)} dy, \tag{B.5}$$

where $\psi_1 = \frac{\lambda^M_{m,s_j}}{\Gamma(M)}$ and $\tau = L_s - N$. By representing the incomplete Gamma function into another form utilizing the identities [56, Eqs. (8.352.1), (1.11)], and after several mathematical manipulations, the integral in (B.5) is expressed as

$$\begin{aligned} F_{\gamma^*_{s_j|\mathcal{C}}}(x) &= 1 - \psi_1 e^{-\frac{\sigma^2 x}{\alpha_j P_r}} \sum_{i=0}^{L_s-N-1} \sum_{k=0}^{i} \binom{k}{i} P^k_{int} (\sigma^2)^{i-k} x^i \\ &\times \int_0^{\infty} y^{M-1+k} e^{-(\lambda_{m,s_j} + \frac{P_{int}x}{\alpha_j P_r})y} dy. \end{aligned} \tag{B.6}$$

With the help of [56, (3.3351.3)], $F_{\gamma^*_{s_j|\mathcal{C}}}(x)$ is given as

$$\begin{aligned} F_{\gamma^*_{s_j|\mathcal{C}}}(x) &= 1 - \psi_1 \sum_{i=0}^{L_s-N-1} \sum_{k=0}^{i} \binom{k}{i} P^k_{int} (\sigma^2)^{i-k} \\ &\times e^{-\frac{\sigma^2 x}{\alpha_j P_r}} \frac{(M-1+k)! x^i}{(\lambda_{m,s_j} + \frac{P_{int}x}{\alpha_j P_r})^{M+k}}. \end{aligned} \tag{B.7}$$

To compute the unconditional CDF denoted as $F_{\gamma^*_{s_j|\mathcal{C}}}(x)$, we use the total probability theorem to get (5.20), which completes the proof.

B.3 Proof of Corollary 5.4.2

From (5.6), let $X = |h_{s_j,r_i}|^2, Y = \max_{n=1,\ldots,N} |f_{s_j,n}|^2, Z = \sum_{m=1}^{M} P_{int}|g_{m,r_i}|^2$, and $\sigma^2 = 0$, then the CDF of $\gamma_{s_j,r_i,k}$ conditioned on Z is given as

$$F_{\gamma_{s_j,r_i,k}|Z}(\gamma) = \underbrace{\Pr\left(\frac{Q_j X}{Y} < Z\gamma, Y \geq \frac{Q_j}{P_{s_j}}\right)}_{I_1(Z)} + \underbrace{\Pr\left(P_{s_j} X < Z\gamma, Y < \frac{Q_j}{P_{s_j}}\right)}_{I_2(Z)}.$$

$$I_1(Z) = \int_{\vartheta}^{\infty} f_Y(y) F_X(\frac{Z\gamma}{Q_j} y) dy, \tag{B.8}$$

where $\vartheta = \frac{Q_j}{P_{s_j}}$ and $f_Y(y) = \lambda_y N \sum_{n=0}^{N-1} \binom{N-1}{n} (-1)^n e^{-(n+1)\lambda_y y}$.

We approximate the CDF of X by applying the Taylor series expansion, i.e., $F_X(x) = 1 - e^{-(\lambda_x x)}$ is approximated as $F_X(x) \overset{x\to 0}{\approx} \lambda_x x$. Using that, we have

$$F_X\left(\frac{Z\gamma}{Q_j} y\right) \overset{P_{s_j}\to\infty}{\approx} \frac{\lambda_x Z\gamma}{Q_j} y. \tag{B.9}$$

Using the variable change of $y = \left(\frac{Q_j}{P_{s_j}} u\right)$, we obtain

$$I_1(Z) \overset{P_{s_j}\to\infty}{\approx} \frac{N\gamma\lambda_x Z}{\lambda_y Q_j} \left(\sum_{n=0}^{N-1} \binom{N-1}{n} \frac{(-1)^n}{(n+1)^2}\right) e^{-\frac{\lambda_y (n+1) Q_j}{P_{s_j}}} \left(\frac{\lambda_y (n+1) Q_j}{P_{s_j}} + 1\right) \tag{B.10}$$

With further simplification of (B.10) as $P_{s_j} \to \infty$, it yields

$$I_1(Z) \overset{P_{s_j}\to\infty}{\approx} \frac{\gamma\lambda_x Z}{\lambda_y Q_j} \left(\sum_{n=0}^{N-1} \binom{N-1}{n} \frac{(-1)^n}{(n+1)^2}\right). \tag{B.11}$$

Next, due to the statistical independency between X and Y, the second integral $I_2(Z)$ is evaluated as

$$I_2(Z) = F_Y(\vartheta) F_X(\frac{\gamma}{P_{s_j}} Z). \tag{B.12}$$

Also, $I_2(Z)$ is approximated as

$$I_2(Z) \overset{P_{s_j}\to\infty}{\approx} F_Y(\vartheta) \left(\frac{\gamma}{P_{s_j}} Z\right). \tag{B.13}$$

The unconditional CDF of $\gamma_{s_j,r_i,k}$ is derived by averaging $I_1(Z)$ and $I_2(Z)$ over the PDF of Z as follows

$$F_{\gamma_{s_j,r_i,k}}(\gamma) = \mathrm{E}_Z\left\{F_{\gamma_{s_j,r_i,k}|Z}(\gamma)\right\} = I_3 + I_4,$$

where $I_3 = \mathrm{E}_Z\{I_1(Z)\}$ and $I_4 = \mathrm{E}_Z\{I_2(Z)\}$. To proceed, we need the PDF of Z. Because Z is the sum of M exponential random variables with parameter P_{int}, it presents a chi-square random variable with PDF given by

$$f_Z(z) = \frac{\lambda_z^M z^{M-1} e^{-\frac{\lambda_z z}{P_{int}}}}{\Gamma(M) P_{int}^M}. \tag{B.14}$$

Next, averaging $I_1(Z)$ and $I_2(Z)$ over the PDF of Z, I_3 and I_4 are approximated, respectively, as

$$I_3 \overset{P_{s_j}\to\infty}{\approx} \left(\frac{\lambda_x M N P_{int}}{\lambda_y \lambda_z Q_j}\right)\gamma \left(\sum_{n=0}^{N-1}\binom{N-1}{n}\frac{(-1)^n}{(n+1)^2}\right). \tag{B.15}$$

$$I_4 \overset{P_{s_j}\to\infty}{\approx} F_Y(\vartheta)\left(\frac{\lambda_x M P_{int}}{\lambda_z P_{s_j}}\right)\gamma. \tag{B.16}$$

Adding (B.15) and (B.16) together, we get the asymptotic expression of the CDF of $\gamma_{s_j,r_i,k}$ as follows

$$F_{\gamma_{s_j,r_i,k}}(\gamma) \overset{P_{s_j}\to\infty}{\approx} \left(\frac{\lambda_x M N P_{int}}{\lambda_y \lambda_z Q_j}\right)\gamma \left(\sum_{n=0}^{N-1}\binom{N-1}{n}\frac{(-1)^n}{(n+1)^2}\right) + F_Y(\vartheta)\left(\frac{\lambda_x M P_{int}}{\lambda_z P_{s_j}}\right)\gamma. \tag{B.17}$$

Computing (B.17) at $\gamma = \gamma_{th}$, we get

$$\tilde{P}_{\text{off}} \overset{P_{s_j}\to\infty}{\approx} \left(\left(\sum_{n=0}^{N-1}\binom{N-1}{n}\frac{(-1)^n}{(n+1)^2}\right)\frac{\lambda_{s_j,r_i} M N P_{int}}{\lambda_{s_j,p}\lambda_{m,r_i,k} Q_j} + \left(1 - e^{-\frac{Q_j}{\lambda_{s_j,p} P_{s_j}}}\right)^N \left(\frac{\lambda_{s_j,r_i} M P_{int}}{\lambda_{m,r_i,k} P_{s_j}}\right)\right)\gamma_{th}. \tag{B.18}$$

By substituting (B.18) into (5.22), we get (5.23). This completes the proof.

B.4 Proof of Theorem 5.4.3

We divide (5.24) into two integrals as follows

$$P_{err_j^*} = \frac{a\sqrt{b}}{2\sqrt{\pi}}\left(A\underbrace{\int_0^\infty \frac{e^{-bx}}{\sqrt{x}}dx}_{I_1} + B\underbrace{\int_0^\infty \frac{e^{-bx}}{\sqrt{x}}F_{\gamma^*_{s_j|c}}(x)dx}_{I_2}\right), \tag{B.19}$$

where $A = \sum_{L_s=0}^{N} \binom{L}{L_s} P_{\text{off}}^{L-L_s}(1-P_{\text{off}})^{L_s}$ and $B = \sum_{L_s=N+1}^{L} \binom{L}{L_s} P_{\text{off}}^{L-L_s}(1-P_{\text{off}})^{L_s}$. I_1 is evaluated with the help of [56, (3.361.2)]. Next, to compute I_2, we represent the integrands of I_2 in terms of Meijer's G-functions using [65, Eq. 10, 11], which are given, respectively, as

$$\left(\lambda_{m,s_j} + \frac{P_{int}x}{\alpha_j P_r}\right)^{-\nu} = \eta x^{-\nu} G_{1,1}^{1,1}\left(\frac{P_{int}\,x}{\lambda_{md}\alpha_j P_r}\Big|_{\nu}^{1}\right), \tag{B.20}$$

where $\eta = \frac{(\frac{P_{int}}{\alpha_j P_r})^{-(M+k)}}{\Gamma(M+k)}$ and $\nu = (M+k)$.

$$e^{-(b+\frac{\sigma^2}{\alpha_j P_r})x} = G_{0,1}^{1,0}\left(\left(b+\frac{\sigma^2}{\alpha_j P_r}\right)x\Big|_{0}^{-}\right). \tag{B.21}$$

Thus, I_2 yields as

$$\begin{aligned} I_2 &= \frac{a}{2} - \eta\,\Phi \int_0^{\infty} x^{-M-k+i-\frac{1}{2}} G_{1,1}^{1,1}\left(\frac{P_{int}\,x}{\lambda_{m,s_j}P_r}\Big|_{M+k}^{1}\right) \\ &\times G_{0,1}^{1,0}\left(\left(b+\frac{\sigma^2}{\alpha_j P_r}\right)x\Big|_{0}^{-}\right)dx, \end{aligned} \tag{B.22}$$

where $\Phi = \frac{a\sqrt{b}}{2\sqrt{\pi}} \frac{\lambda_{m,s_j}^{M}}{\Gamma(M)} \sum_{i=0}^{L_s-N-1} \sum_{k=0}^{i} \binom{k}{i} P_{int}^{k} (\sigma^2)^{i-k} (M-1+k)!$. Exploiting that the integral of the product of a power term and two Meijer's G-function [65, Eq. 21], I_2 results in

$$\begin{aligned} I_2 &= \frac{a}{2} - \frac{\eta\,\Phi}{\Gamma(M+k)} \left(\frac{P_{int}}{\alpha_j P_r}\right)^{-(M+k)} \left(\frac{\sigma^2}{\alpha_j P_r} + b\right)^{-\beta} \\ &\times G_{2,1}^{1,2}\left(\frac{P_{int}}{b\alpha_j P_r + \lambda_{m,s_j}\sigma^2}\Big|_{M+k}^{1,1-\beta}\right), \end{aligned} \tag{B.23}$$

where $\beta = i-M-k+0.5$. By incorporating the results of I_1 and I_2 into (B.19), a closed-form expression for the unconditional E2E BER at S_j is given in (5.25), which completes the proof.

B.5 Proof of Theorem 5.4.5

First, we obtain the conditional achievable rate for S_j by averaging over the conditional PDF in (5.21) which yields in

$$R_{j|\mathcal{C}} = \frac{\zeta\,\Gamma(\varphi+M)}{3} \int_0^{\infty} \frac{x^{\varphi-1}}{\left(\frac{x}{\alpha_j P_r} + \frac{\lambda_{m,s_j}}{P_{int}}\right)^{\varphi+M}} \log_2(1+x)dx, \tag{B.24}$$

where $\varphi = L_s - N$. Again, expressing the integrand terms in terms of Meijer G-functions which are respectively, given as [65, Eqs. 7, 10, 11]

$$\log_2(1+x) = \log_2(e)\; G_{2,2}^{1,2}\left(x\Big|_{1,0}^{1,1}\right). \tag{B.25}$$

and

$$x^{\varphi-1}\left(\frac{x}{\alpha_j P_r}+\frac{\lambda_{m,s_j}}{P_{int}}\right)^{-(\varphi+M)} = x^{\varphi-1}\frac{\left(\frac{x}{\alpha_j P_r}\right)^{-(\varphi+M)}}{\Gamma(\varphi+M)}G_{1,1}^{1,1}\left(\frac{P_{int}\,x}{\lambda_{m,s_j}\alpha_j P_r}\Big|_{(\varphi+M)}^{1}\right). \tag{B.26}$$

Incorporating (B.25) and (B.26) into (B.24), thus yielding

$$R_{j|\mathcal{C}} = \psi\int_0^\infty x^{-M-1}G_{1,1}^{1,1}\left(\frac{P_{int}\,x}{\lambda_{m,s_j}P_r}\Big|_{\varphi+M}^{1}\right)G_{2,2}^{1,2}\left(x\Big|_{1,0}^{1,1}\right)dx, \tag{B.27}$$

where $\psi=\frac{\log_2(e)}{3}\frac{(-1)^{-M-1}(\alpha_j P_r)^M}{\Gamma(\varphi)\Gamma(M)P_{int}^M}$. Again, using [65, Eq. 21], (B.27) results in

$$R_{j|\mathcal{C}} = \psi\,G_{3,3}^{3,2}\left(\frac{P_{int}}{\lambda_{m,s_j}\alpha_j P_r}\Big|_{L_s,M,M}^{1,M,1+M}\right). \tag{B.28}$$

Thus, the unconditional closed-form expression is found as in (5.28), which completes the proof.